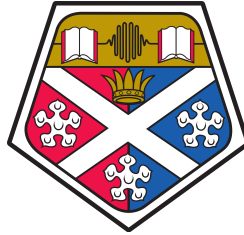


Comparative Study of Drainage in Soils and Foams: Early-time and Late-time Solutions



Yaw Akyampon Boakye-Ansah

Thesis submitted to the University of Strathclyde for the degree of

Doctor of Philosophy

Department of Chemical and Process Engineering

University of Strathclyde

March 2021

Declaration of Authenticity and Author's Rights

'This thesis is the result of the author's original research. It has been composed by the author and has not been previously submitted for examination which has led to the award of a degree.'

'The copyright of this thesis belongs to the author under the terms of the United Kingdom Copyrights Acts as qualified by the University of Strathclyde Regulation 3.50. Due acknowledgement must always be made of the use of any material contained in, or derived from, this thesis.'

Signed: Yaw A. Boakye-Ansah

Date: March, 2021

Dedication

This thesis is dedicated to everyone who loves to discover knowledge, especially Kwasi Akyampon Boakye-Ansah.

Acknowledgements

"If I have seen further, it is by standing on the shoulders of giants"

- Isaac Newton

I would like to express my sincere gratitude to my God for life, intellect and the opportunity to develop myself further as a man, and as an academic. As far as giants go, God created them for the very purpose of making life smoother for such as I. My gratitude to God knows no bounds. This PhD journey has challenged me in ways I could not have imagined, and I hope that I have become a better person.

I would like to acknowledge my principal supervisor, Dr Paul Grassia for supporting me throughout this research; his attention to students and dedication to making the research experience an enriching one is both endearing and a big motivation. I realise that there is so much more I can learn from you. You are a testament to yourself. Thank you. The good advice, support and friendship of my second supervisor, Dr Demosthenes Kivotides has been invaluable both on academic and personal levels, for which I am grateful. By this, I extend my warmest thanks to the Department of Chemical and Process Engineering for their support throughout this research. The good advice and support from all teaching and non-teaching staff have made my study a smooth one.

I am grateful for my colleagues who have shared this PhD journey with me, both friends made and my closer research group. Your cheerful influence, the times we spent motivating each other, dealing with challenges and being there for each other will always be remembered. I would especially like to thank my friend Carlos Alejandro Torres-Ulloa for his immeasurable help with programming many of my problems, and the added insight into some of the principles that I needed to understand for my work. Thank you everyone.

I would also like to thank Ghana National Petroleum Corporation (GNPC) without whose sponsorship and funds I could not have pursued this Doctoral Research. I would like to specially thank Mr Andrew Badoo without whose selfless dedication I would not have had an opportunity for this funding. May God enlarge your territory.

Last but not least, my gratitude goes to my family who have been enormous support for me throughout my life especially through the difficult times I have had to endure from disappointments to successes. Thank you for being the wind in my sail. Your support and interest in my development have helped me come this far.

John 4:37-38 (KJV)

³⁷ *And herein is that saying true, One soweth, and another reapeth.*

³⁸ *I sent you to reap that whereon ye bestowed no labour: other men laboured, and ye are entered into their labours.*

Contents

Declaration	ii
Dedication	iii
Acknowledgements	iv
Nomenclature	xiii
Abstract	xvii
1 Introduction	1
1.1 Background to Research	1
1.2 Motivation for Thesis	3
1.3 Relevance of this Research	4
1.4 Scope of Thesis	5
1.5 Layout of Thesis	7
2 Literature Survey	9
2.1 Introduction	10
2.2 Foams	13
2.2.1 Structure of Foams	14
2.2.2 Drainage in Foams	16
2.3 Derivation of Foam Drainage Equation	17
2.3.1 Channel-dominated Foam Drainage	17
2.3.2 Node-dominated Foam Drainage	20
2.3.3 Boundary conditions at top and bottom of foam	22
2.4 Soils: Fundamental concepts	23
2.4.1 Drainage in Soils	24
2.4.2 Darcy's Law	26

2.4.3	Capillary Properties of Water in Soil	27
2.4.4	Flow in Unsaturated Soil	28
2.5	Soil Material Property Functions	29
2.5.1	Soil-Water Retention Curve	29
2.5.2	Hydraulic Conductivity	34
2.5.3	Relative Diffusivity	40
2.6	Analogies: Richards Equation and Foam Drainage	
	Equations	42
2.6.1	Bridging the Gap	44
2.7	Summary	46
3	Richards Equation: Drainage in Unsaturated Soils	47
3.1	Introduction	48
3.2	Richards Equation	49
3.2.1	Derivation of Richards Equation	50
3.2.2	Nondimensionalisation of Richards Equation	52
3.3	Initial and Boundary Conditions	53
3.3.1	Initial Conditions	54
3.3.2	Boundary Conditions	54
3.4	Early-Time Solution	55
3.4.1	Formulation of Early-time Solutions	56
3.4.2	Setting Up Problem	57
3.4.3	General Similarity Solution	59
3.4.4	Flux-based Solution	60
3.5	Travelling Wave Solution	61
3.5.1	General Form of Travelling Wave	61
3.5.2	Identifying Travelling Wave Propagation Velocity	62
3.5.3	Evaluating the Travelling Wave Propagation Velocity	63
3.5.4	Profile of Travelling Wave	64
3.6	Special Case: Single Travelling Wave	65
3.7	Interaction of Travelling Waves	65
3.7.1	Profile of Two Interacting Travelling Waves	66
3.8	Summary	66

4	Soil Material Property Functions Models	68
4.1	Introduction	69
4.2	Brooks and Corey Models	69
4.2.1	Soil Water Retention Curve	70
4.2.2	Relative Hydraulic Conductivity	71
4.2.3	Relative Diffusivity	72
4.3	Van Genuchten Models	73
4.3.1	Soil Water Retention Curve	73
4.3.2	Relative Hydraulic Conductivity	75
4.3.3	Relative Diffusivity	77
4.3.4	Comparison of Brooks-Corey and van Genuchten functions	78
4.4	Other Models	79
4.4.1	Fredlund-Xing Models	80
4.4.2	Assouline Model	80
4.5	Summary	81
5	Early-time Similarity Solutions in Foams and Soils	82
6	Comparing and Contrasting Travelling Wave Behaviour for Groundwater Flow and Foam Drainage	105
7	Sensitivity of Travelling Wave Solutions	135
8	Conclusions and Future Work	159
8.1	Conclusions	159
8.2	Future Work	163
	Bibliography	165
A	Travelling Wave Solutions: Brooks-Corey Models	A-1
A.1	Overview	A-1
A.2	Richards Equation	A-2
A.3	Soil Material Property Functions	A-2
A.3.1	Capillary Suction Head	A-3
A.3.2	Relative Hydraulic Conductivity	A-4
A.3.3	Relative Diffusivity	A-5

A.4	Richards Equation: Travelling Wave Solution	A-6
A.4.1	Asymptotic Behaviour of Solutions	A-7
A.5	Conclusion	A-9
B	Setting Up an Initial Condition for Richards Equation	B-11
B.1	Overview	B-11
B.2	Introduction	B-11
B.3	Lower Travelling Wave	B-13
B.3.1	Asymptotic Behaviour in Lower Travelling Wave	B-13
B.4	Upper travelling wave	B-15
B.4.1	Asymptotic Analysis in Upper Travelling Wave	B-15
B.5	Interaction of Travelling Waves	B-17
B.6	Setting Up the Crank-Nicolson Scheme	B-18
B.6.1	Generalising Interacting Travelling Wave Profiles	B-19
B.6.2	Travelling Wave Solution	B-21
B.7	Summary	B-23

List of Figures

2.1	Typical figures of liquid foam and a foam bubble	10
2.2	A typical structure of a porous medium	11
2.3	Cross-section of foam Plateau border and node	14
2.4	Schematic showing the direction of foam drainage	23
2.5	Schematic showing the direction of drainage in soils. This sets up the problem that is solved in this thesis.	28
2.6	Capillary suction head profiles	32
2.7	Profile comparing RHC for equations (2.29) and (2.30)	40
2.8	Profiles of relative diffusivity	42
3.1	Diffusivity profile for foam drainage and soil samples	58
3.2	Travelling wave propagation velocity for FDEs and soil samples	64
4.1	Profile of capillary suction head using Brooks and Corey [56] definitions	70
4.2	Relative hydraulic conductivity using Brooks and Corey [56] definitions	71
4.3	Profile of relative diffusivity using Brooks and Corey [56] definitions	72
4.4	Profile of capillary suction head over entire moisture content range	74
4.5	Profile of relative hydraulic conductivity	75
4.6	Asymptotic profiles of relative hydraulic conductivity	76
4.7	Profile of relative diffusivity	77
4.8	Profile of relative diffusivity at varying moisture content limits.	78
4.9	Profile of soil material property functions	79
A.1	Semi-log profile of capillary suction head for three soil samples. The data is largely comparable for each soil over the entire range of moisture content.	A-3
A.2	Profile based on three soil samples	A-4
A.3	RD profile for three soil samples	A-5
A.4	Numerical solution to Richards Equation using (A.8a) & (A.8b).	A-6

A.5	Profile of asymptotic analytical and numerical solution in the limit as $\Theta \rightarrow 0$.	A-8
A.6	Profile of asymptotic analytical and numerical solution in the limit as $\Theta \approx 1$.	A-9
B.1	Asymptotic approximation profiles for lower travelling waves	B-14
B.2	Asymptotic approximation profiles for upper travelling waves	B-16
B.3	Profile of two interacting travelling waves	B-17

List of Tables

- 2.1 Equivalent terminology and differences for describing flow in foams and soils. 45
- 2.2 Analogues of equivalent expressions for relative hydraulic conductivity $K_r(\Theta)$ and relative diffusivity $D_r(\Theta)$ for drainage in foams [14, 36] and soils (via van Genuchten [38] equations). A third property shows $dH_+/d\Theta$ 46
- B.1 Midpoint RHC values for three soil types B-13

Nomenclature

Table of nomenclature follows.

α	reciprocal length scale in expression for head (m^{-1})
α'	fitting parameter
β	constant developed to describe a convex hull
χ	fitting parameter (–)
ζ	fitting parameter (–)
δ	fitting parameter (–)
θ	fractional moisture content (cm^3)
θ_r	residual moisture content (cm^3)
θ_s	saturated moisture content (cm^3)
Θ	rescaled moisture content (–)
η	similarity variable (–)
γ	surface tension (N m^{-1})
γ_s	similarity variable (–)
κ	fitting parameter (–)
λ_f	bubble-size length parameter (mm)
λ_s	pore-size distribution index (–)
π	curve-fitting parameter (–)
λ	Plateau border length per bubble volume (m^{-2})
ρ	density (kg m^{-3})

v	velocity (m s^{-1})
μ	dynamic viscosity ($\text{Pa} \cdot \text{s}$)
$\bar{\omega}$	fitting parameter
a_1	curve-fitting parameter (–)
a_3	curve-fitting parameter (–)
b_1	curve-fitting parameter (–)
b_3	curve-fitting parameter (–)
A	cross-sectional area of a Plateau border (m^2)
C	geomteric shape factor (–)
\hat{C}	constitutive expression (–)
\hat{c}	empirical constant
D	hydraulic diffusivity ($\text{m}^2 \text{ s}^{-1}$)
D_r	relative hydraulic diffusivity (–)
F	flux similarity expression (–)
f	numerical Plateau border cross-section shape factor (–)
$f(r)$	pore-radius distribution function
g	acceleration due to gravity (m/s^2)
$\hat{\mathbf{g}}$	gravity unit vector (–)
h	capillary suction head (m)
h_b	air-entry/bubbling pressure head (m)
H_+	rescaled capillary suction head (–)
p_g	pressure in the gas (Pa)
k	absolute permeability (m^2)
k_e	effective permeability (m^2)
K	hydraulic conductivity (m s^{-1})
K_s	saturated hydraulic conductivity (m s^{-1})
K_r	relative hydraulic conductivity (–)

L	Plateau border length scale (–)
l	scaling interval (–)
m	soil-specific parameter (–)
N	capillary diffusivity power-law exponent (–)
n	soil-specific parameter
q	Darcy flux (–)
\mathbf{q}	vector flux (–)
r	radius of curvature of Plateau border wall (m)
t	time (s)
v	velocity (m/s)
x	distance (m)
z	vertical distance (m)

Abbreviations

BC	Brooks-Corey
BCB	Brooks-Corey-Burdine
BCM	Brooks-Corey-Mualem
CD FDE	Channel-dominated foam drainage equation
FDE	Foam drainage equation
HCF	Hydraulic conductivity function
ND FDE	Node-dominated foam drainage equation
PB	Plateau border
PCM	Predictive conductivity model
RD	Relative diffusivity
RE	Richards equation
RHC	Relative hydraulic conductivity
SWRC	Soil-water retention curve
VGB	Van Genuchten-Burdine
VGM	Van Genuchten-Mualem

Abstract

Richards equation has been known and used to describe unsaturated flow of liquids in porous media since it was proposed by Richards in 1931. This is a highly nonlinear equation with no exact solution in general. There has however been significant research in developing specific solutions of this equation using various analytical and/or numerical approaches. In comparison, the foam drainage equation has been derived to describe flow of water through a complex network of foam channels (Plateau borders). It is a nonlinear equation, again with no solution in general, although a number of analytical solutions are known. Research in the physics and mathematics of foams have produced considerable knowledge that have helped advance the theory of drainage and propagation of liquid through foams. Not much has been done to compare and contrast these equations (Richards equation and the foam drainage equation) although they obey the same governing fundamental laws. Flow situations involving these two governing equations can be designated as either early-time nonlinear diffusion or late-time travelling wave propagation problems. Various complex analytical (and also numerical) mathematical techniques are required to solve such problems. Material properties such as capillary suction head, hydraulic conductivity and capillary diffusivity are also required before these problems can be studied. In order to find material properties for Richards equation, soil material property functions derived by van Genuchten and Brooks & Corey are employed in this thesis. The foam drainage equation (of which various forms exist) has the analogous material properties embedded in its formulation. This research has obtained solutions for Richards equation and for foam drainage comparing them both for early-time diffusion and for late-time travelling wave solutions. The obtained solutions can be used to predict such physical behaviours as the amount of fluid needed to be injected to flood an oil reservoir or alternatively to irrigate a piece of land without flooding it. Knowledge from these solutions will be of immense benefit to many practical situations similar to those mentioned above.

Introduction

This introductory chapter consists of five main sections. Firstly, the background of this thesis is considered in Section 1.1, then the motivation is given in Section 1.2. Subsequently, in Section 1.3, the potential relevance of this research is considered, the scope of the thesis is presented in Section 1.4 and finally, in Section 1.5, the structure of the thesis is described. The background of flow in soils and foams is briefly discussed in this chapter. The important fundamental and governing equations that are used in this thesis are also briefly introduced. In the motivation, the gap in knowledge and impact of this research are considered while possible applications to industry and the environment are also presented. Finally, the layout and content of this thesis are outlined.

1.1 Background to Research

Movement or flow of fluids is a common, and yet, quite fascinating physical phenomenon. Fluid flow, which has been studied extensively, can be observed through simple media such as pipes and ducts [1–3], flowing ordinarily on the floor, or through more complex media without a definite internal arrangement (e.g. through a foam [4–9], or through soil [10–12] among others). Whether through a simple or complex medium, fluid flow requires rigorous mathematics to describe and understand the physics related to it. Fluid at a specified point flows when there is a pressure or potential difference between it and another point. Flow is hence typically from the place of higher to lower pressure or potential. Flow of fluids is predominantly controlled by the following forces: capillary suction, gravity and viscous dissipation acting on the fluid within the medium it can be found, or as an interaction between both the fluid and the medium [4, 10, 12–15].

One of the pioneering works that advanced knowledge in the theory of flow in porous media is work by the French Civil Engineer, Henry Darcy [13] in 1856. His work presented studies on the flow of water through a permeable sand core (porous medium). It was one of the early works that extended the study and principles of classical fluids to flow in porous media. In the next century, many scientists undertook research in this area: transport in porous media; with applications to irrigation, hydrology, geotechnical engineering, petroleum engineering, soil-water transport phenomenon, and soil science. Some notable works in these areas include Buckingham [10], Haines [11], Richards [12], Brooks and Corey [16], Philip [17], Mualem [18]. Capillary action which had previously been only used to describe fluid movement in pipes and cylindrical objects was one of the earliest determined factors that was thought to affect movement of fluid in porous media [10]. Richards published seminal work on the capillary conduction of liquids (water) through porous media which included viscous and gravity forces in addition to the capillary action [12]. This was largely work that presented data and equations for the capillary conduction of water through soil (and clay). The mathematical formulae (and experimental procedure) developed may be used to express capillary flow in other liquids and media [12]. Richards equation has been modified [17, 19, 20], and there have been many other numerical and analytical solutions provided for it [21–26]. Richards [12] proposed this equation to describe capillary flow that has been used since the previous century in all areas of transport in porous media [27, 28]. This equation will be discussed further in Chapter 3, and solutions to this equation presented in Chapter 5 – 7. Appendices A and B present further discussions using Richards equation.

Plateau formulated the basic principles for foam structure (a special type of porous medium) in the 19th century [29]. Research on transport phenomena in foams (drainage, flow properties, dynamics) developed more recently from 1980s to early 2000s years. Drainage in foams has been widely studied [4–6, 30–34]. Structure and drainage are however linked since the regions between three touching bubbles (which are called Plateau borders are the channels for liquid flow or drainage. Four of these channels join in the region between four touching bubbles, which is called a node. Equations have been developed to describe dominant viscous dissipation through the channels [32] or nodes [33].

Foam drainage which is governed by analogous forces to the Richards equation (hereafter RE) was first described with a relevant equation derived by Gol'dfarb et al.

[31]. This was later advanced as a channel-dominated case (channel-dominated drag) by Verbist et al. [32], who developed the so-called foam drainage equation (hereafter FDE). Their work was also based on research done by Princen and Kiss [30] who worked on emulsions. The FDE is based on the assumption of viscous dissipation through the PB as opposed to the nodes (junctions of four PB) via a Poiseuille flow. Dissipation through the foam is sometimes predominantly via the PB [4, 35, 36] but sometimes dominated by the nodes [14, 33, 37], a case advanced by Koehler et al. [14] who also developed another FDE. Both variants of the FDE are of interest in this research. The foam drainage equations have so-called travelling wave solutions which can be used to predict certain behaviours of wave fronts [14, 32, 33, 36].

It has been shown [68] that these two drainage equations for foams and soils have some analogies. Despite the close analogies between these bodies of knowledge and research in foams and soils [68], there is little to date that has been done to exploit the physics of foam drainage to gain a deeper understanding of flow in porous media, and vice versa. This is likely due to the limitation from the terminology used in both the foam and soil communities. This research is aimed at studying these close analogies via Richards equation [12] for flow in porous media and the foam drainage equation variants [14, 36].

Summarily, this thesis seeks to study Richards equation [12] (main equation for describing flow of water in unsaturated soils [20, 38]) in close analogy to foam drainage [32, 33], comparing not only late-time travelling wave solutions but also early-time similarity solutions for these drainage equations. Future work can be considered for the intermediate-time behaviour of these equations.

1.2 Motivation for Thesis

The many daily uses of foams and flow therein, and the uses of recovered fluids from porous media flow (e.g. oil or water flow in soils/rocks) make studying the laws and principles governing their drainage or infiltration economically important. Understanding the flow characteristics within foams and porous media can help predict fluid accumulation to aid fluid recovery in foams and porous media. The modern economy is largely dependent on fossil fuels (petroleum, in its fluid form) and its by-products especially in the areas of transportation [39]. Petroleum is fundamental to many domestic, commercial, and industrial activities and

processes. Hence, a one per-cent (1%) improvement in oil recovery translates to significant produced oil volume increment and huge economic benefits to the global oil industry.

In order to obtain these benefits, laws governing fluid flow must be studied and well understood. The common principle that guides all of these various flow situations in foams and porous media is flow/drainage or infiltration in complex porous media [68]. Certainly, the fundamental law which describes drainage in these porous media formations is Darcy's law [13]. Richards equation was developed to describe drainage in unsaturated porous media [12, 17] but is based on Darcy's law. Likewise, the foam drainage equation was derived based on Darcy's law.

Until now (known to this author), there is no known work that tries to bridge the gap between literature and mathematics of foams and soils. One key reason could be the differences in terminology that are used in these two research communities. Chapter 5 and 6 (also Boakye-Ansah and Grassia [68]) have shown that drainage in foams is analogous to drainage in soils. It is hoped that this precursory work will encourage other researchers to present further research that consider some other similarities and differences in drainage in foams and soils.

The early-time (similarity) and late-time (travelling wave) solutions that will be obtained when applied to oil recovery can be used to improve the overall recovery efficiency of oil reserves. Additionally, the efficient prediction of liquid saturation profiles for different soil types can help in many daily agricultural processes including irrigation while the environmental and civil engineer can also find many applications for these solutions either in contaminant spreading or groundwater flow.

In this section, the motivation for this research and some introductory concepts governing flow in porous media have been considered. The gap in the literature has been identified, and the basis for this research will therefore be explored further.

1.3 Relevance of this Research

Richards equation [12] has been extensively used for describing flow in soils for groundwater hydrology, agricultural and environmental engineering [20, 28]. New insights into solutions of Richards equation compared with drainage in foams are therefore valuable. Modelling

flow in porous media is ultimately important in the process of irrigation, in geotechnical and geo-environmental studies as well as many other areas of science and engineering. Study of these phenomena requires detailed and careful formulation of the governing equations and the relationships involved, which depend on the properties of the porous media in question.

This project therefore seeks to answer the following objectives:

- i. To develop analogous solutions for Richards equation from methods applied to the solution of foam drainage equations.
- ii. To investigate how these solutions vary for the Richards equation (using soil parameters given by so-called van Genuchten conductivity/diffusivity models [38]) compared with foam drainage equation. Using these developed solutions, predictions of behaviour can be made for porous media applications.
- iii. To ascertain the closeness of the analogy between these two governing equations (Richards equation and foam drainage equation).
- iv. To derive a continuum level and/or pore scale level expression that can be used to predict and determine parameters that can be adjusted to help improve irrigation practices and oil recovery.

Some other targets for this research include using the solutions obtained to control fluid recovery processes (e.g. volumes of water that may be injected to recover another fluid) in a porous medium, and possibly, water injection for enhanced oil recovery, or land remediation after an oil (contaminant) spill. This is possible since the solutions here obtained are for equations that describe these physical processes.

1.4 Scope of Thesis

This research seeks to draw a parallel between the mathematics and physics of water movement in porous media, specifically between foams and soil. The key equations describing flow in these two porous media are studied together, comparing similarities and differences in their solutions using specific mathematical techniques.

Much work has been done in the area of foam drainage [6, 32–34, 40]. The principles

that were studied have helped in modelling certain physical and industrial processes in minerals processing, brewing and oil recovery [6, 34, 41, 42]. The foam drainage equation has travelling wave solutions which can be used very elegantly to predict the transport of fluid within the foam over time and distance. Also, the node-dominated variant of the drainage equation [14, 33] has early-time similarity solutions already available in the literature (in the limit where early-time similarity solutions are considered, the node-dominated solution is analogous to the linear heat equation applying the same technique) [43].

Meanwhile, Richards equation has been used to predict position and drainage of moisture in porous media [20, 44, 45]. There has been some work that relates the movement of fluid with respect to time and works that relate depth to moisture content [25, 44]. Some authors [22, 45, 46] also present early-time similarity solutions to Richards equation. These studies are common in the literature [17, 27, 46–54] spanning several decades. Most of the work done on drainage in soils is applied towards agriculture and the soil sciences which focus on irrigation and remediation [28, 55].

The foam drainage equation deduced by Verbist and Weaire [36] and Koehler et al. [14] are here shown to be analogous to Richards equation [12]. The mathematics of flow of liquid in foams can thus be studied in close analogy to flow of water (liquid) through unsaturated soils to gain a clearer understanding of these two phenomena. Early-time similarity solutions and late-time travelling wave solutions are considered in detail in this thesis. In order to obtain these aforementioned solutions, functions equivalent to those components of the governing equations must be known. These are the hydraulic conductivity (driven by gravity) and diffusivity (driven by capillarity) terms. Both of these functions are obtained in terms of a capillary suction head function based on retention of moisture in a soil. The foam drainage equation variants have analogues of these material property functions already embedded within their governing equations. Specifically, for Richards equation, van Genuchten [38] soil material property functions are employed when its solutions are derived. These solutions obtained using van Genuchten material property function are compared with solutions obtained using Brooks and Corey [56] variants of the soil material property functions (see Appendix A).

This research thus seeks to bridge the gap between the physics and mathematics of drainage in dry foams to that in unsaturated soils. The primary focus is on the early-time

diffusion (Chapter 5) and late-time drainage (Chapter 6 and 7) in soils and foams. Appendix B presents foundational work and boundary conditions that may be considered in the setting up of solutions towards interaction of travelling waves. Such a solution methodology can also be used to represent the intermediate-time regime.

1.5 Layout of Thesis

This thesis is presented in an alternative format as allowed by the University of Strathclyde thesis submission guidelines. In this thesis, journal articles which have been submitted or accepted are presented in the place of standard thesis chapters. An introductory summary of these articles is given at the beginning of those chapters that consist of journal articles to elucidate the connection among them.

The literature reviewing the relevant material related with this research is presented in Chapter 2. The governing fundamental equations, namely, Richards equation and foam drainage equations are considered. To facilitate comparison, typically not only the equations are considered but their dimensionless forms also. Thus, this section considers nondimensionalising and rescaling the channel-dominated FDE, and also presents the node-dominated FDE. The dimensionless node-dominated FDE is already available in the literature. Drainage in soils is briefly considered in this chapter as well as analogies between drainage in soils and foams.

Chapter 3 discusses Richards equation in detail. Here, its derivation, nondimensionalisation, and rescaling are presented. The methods that are employed in solving it, referencing standard published research, are introduced. Chapter 4 considers the soil material property functions that are employed in the solution of Richards equation in this thesis. Here, the original derivation of these property functions and their asymptotic approximations under varying limits of soil saturation are reviewed.

In Chapter 5, early-time similarity solution which present nonlinear diffusion equations to both Richards equation and the two foam drainage equations are discussed. This chapter is an article that has been submitted to a journal for publication. Similarity transformation is applied to the nonlinear partial differential equation and solutions for the initial moisture content under the underlying assumptions are discussed.

Chapter 6 presents published results for the travelling wave solutions for both Richards equation and the foam drainage equations. Physical applications of this solution procedure are also discussed. Chapter 7 considers solutions to Richards equation which are obtained when the soil material property functions are modified. The sensitivity of the resulting travelling wave solutions to Richards equation are presented. Varying assumptions and considerations for this approach are discussed and certain behaviours elucidated for further understanding of the hydraulic functions that are used to solve Richards equation.

The thesis is summarised and concluded in Chapter 8, where some recommendations and possible direction of future research are stated. Follow up work on Chapter 6 is presented in Appendix A specifically for another functional form of the soil material properties. Appendix B gives the boundary and initial conditions that are required to set up solutions for the interaction of travelling wave profiles.

In this thesis, unless otherwise stated, the functions have been scaled to be non-dimensional in order to make them universally applicable to any scale or system. Porous media as used in this thesis may represent foams or soils. Also, the so called soil water retention curve SWRC (suitably nondimensionalised) is equivalently used to represent capillary suction head, capillary head or sometimes ordinary head. Hydraulic conductivity and capillary diffusivity are also presented in suitable non-dimensional forms in the interests of making results more universally applicable. Where possible, solutions obtained using non-dimensional formulation are benchmarked to existing solutions in foam literature.

Chapter 2

Literature Survey

This chapter of the thesis pertains to understanding of and comparison between the physics and mathematics of drainage in soils and foams. A better physical understanding and a rigorous mathematical analysis of the equations governing flow in these porous media is expected to help bridge these two hitherto “unrelated” research communities while ensuring the ease of communication between them. Detailed knowledge of drainage in soils and foams is important to help improve recovery processes in oil reservoirs, design separation and remediation processes, plan irrigation activities among many other benefits to science and engineering, and to elucidate comparisons in drainage in foams and soils for improved research collaboration and application between these foam and soil physics communities.

In this chapter, a literature review of foams and soils is presented. Specifically, the structure of foams, the fundamental concepts of drainage in foams, and the derivation of those equations that govern this drainage are considered. A general description of foams is given in Section 2.2. Here, the structure of foams is considered prior to a discussion of drainage in foams for two variants of the foam drainage equation, while Section 2.3 discusses the derivation of these equations.

For soils, fundamental concepts in drainage and soil material hydraulic properties required to study drainage are discussed in Section 2.4. Richards equation (for transport of moisture in soils) is mentioned at this point. However, detailed discussion of drainage in unsaturated soils (i.e. detailed discussion of Richards equation) is presented in Chapter 3. The functions that describe these aforementioned soil material properties are introduced in

Section 2.5. These functions specifically required to obtain solutions to Richards equation in this thesis are discussed in detail in Chapter 4. Finally, the analogy of flow in soils and foams is considered in Section 2.6 and a summary of the chapter is given in Section 2.7.

2.1 Introduction

Foam drainage is a well-studied concept that is based on the idea of movement of the liquid within a foam (usually dry or slightly wet) [6, 37] predominantly along a Plateau border (channels between bubbles) [32, 36] or through the node (the junction between Plateau borders) [14, 33]. This movement is controlled by capillary suction, gravity, and viscous forces. Plateau [29] proposed the fundamental principles that govern the structure, and hence drainage in foams in 1873. An equation governing flow in foams was first derived by Gol'dfarb et al. [31] and later derived independently by Verbist and Weaire [36]. This equation was derived based on the assumption that liquid dissipation occurred predominantly in the Plateau border. Another form of the foam drainage equation was also given by Koehler et al. [14, 33] who suggested that liquid dissipation was dominant within the nodes. The foam drainage equation has thus been derived based on two models: the channel-dominated [32, 36] and node-dominated [14, 33] dissipation. Detailed discussion of the derivation of these equations are given in Section 2.3.1 and 2.3.2.

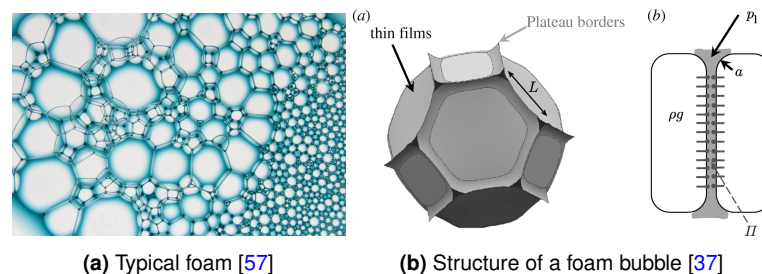


Figure 2.1: Figure describing (a) a typical liquid foam, and (b) a tetrakaidecahedral foam bubble showing the thin films in a foam and the PB. The adjoining image is of a single PB channel Π occupied by liquid as well as the pressure in the liquid (p_l) and the gravity body force (ρg). Here, a is the bubble film, and L is the Plateau border length.

Figure 2.1 shows a typical mass of liquid foam (in 2.1a) and the structure of a tetrakaidecahedral foam bubble with a zoomed in view of a Plateau border (in 2.1b). A detailed view of a Plateau border is shown with the foam bubble. Some liquid flows through the Plateau border. From this diagram shown in Figure 2.1b, a node is identified as where three Plateau borders meet. The significance of L , a length scale showing the Plateau

border length is discussed in the rescaling of the channel-dominated foam drainage equation (see Section 2.3.1).

Drainage in soils is also a very well-studied phenomenon [27, 28] which can be described as either infiltration, imbibition or convection-diffusion [55]. Buckingham [10] determined that capillary action affected movement of fluids in porous media such as soils. Subsequently, Richards [12] derived an equation to describe capillary conduction of liquids in porous media. This equation has been generally accepted and widely used to describe flow of water in unsaturated soils. It is thought that Buckingham was the first to derive this equation [55], although not in the form currently known. Richardson [58] is also known to have derived this equation but it was not widely known until the 1950s, a period where Philip [17] also independently derived this infiltration equation, which is in essence the moisture-based variant of Richards equation (originally given in a head-based form). Philip [55] suggested that Richards equation is a general flow equation composed as a type of nonlinear Fokker-Planck equation. Other authors have described Richards equation as related to the Navier-Stokes or convection-diffusion expression [28, 59].

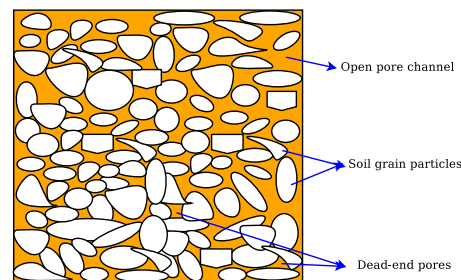


Figure 2.2: A typical structure of a porous medium (soil) showing various kinds of pore space structures present in porous media. The open pore channels may form connected or interconnected pores to allow for movement of water through the porous medium. The grains of soil could either be well-sorted or poorly-sorted which may control the flow of the water through it. The grains could also be oriented in various ways that give preference to the dominant direction of resulting flow.

Figure 2.2 shows an image of a typical porous soil. Here, two major pore types, open and dead-end pores are shown. These open pores are interconnected and hence allow for movement of fluids within the soil while those dead-end pores seal off passages for fluid movement in the porous medium. In a dry soil, at the onset of infiltration and imbibition, capillary forces dominate movement of water within the soil. In already wetted soils, water flows more easily since a combination of capillary and gravity (conductivity) forces control drainage. In addition to the pore connectivity, other factors affect the movement of fluids within the soil structure. These shall be discussed in detail later (see Chapter 3).

Zitha [41] proposed an equation for describing foam drainage in porous media. Based on both drainage equations for soils and foams, he considered an equation to describe the generation of foam in a reservoir for oil recovery as well as its drainage. This equation is essentially a generalised 'foam drainage equation'. Further, Or and Assouline [24] proposed an alternative to Richards equation based on the foam drainage equation. Here, they assumed that the soil pores could be mapped as similar to a foam network. Thus, foam structure is attributed to porous media. These equations are however not discussed further in this thesis. Therefore, foams will be considered as analogous to porous media and may be loosely referred to as porous materials in this thesis.

As stated earlier, one of the key objectives of this research is to make the terminology of both research communities, foam and soils, to be more familiar to encourage collaboration and research between them. Therefore, some key similarities and differences in foams and soils as well as the equations describing their drainage are presented. Key among them are the terms that represent the different parts of the governing equations. In both of these equations, there are terms that describe suction, gravity and diffusion [12, 14, 36]. The suction and diffusion terms are capillary-based forces.

By virtue of its composition, the foam drainage equation incorporates the terms that describe these suction, gravity and diffusion forces earlier mentioned. Conversely, Richards equation does not provide those terms required to solve it, making it necessary at the outset to determine functions that can be used to solve it. These are the soil material property functions which are mathematical expressions arising from those forces earlier mentioned. Many researchers [38, 56, 60–62] have proposed functions that can be used within the solution of Richards equation. As shown in this thesis, depending on the type of functions used, in order to obtain those expressions for the relative hydraulic conductivity (RHC) and relative diffusivity (RD), the suction head must be known. This suction head is used to derive the RHC via a predictive conductivity model (PCM), and these two functions (RHC and first derivative of suction head) are used together to derive the RD expression. Other formulations of these functions are briefly discussed in later sections, but they are not employed in solutions obtained in the thesis.

Richards equation (see chapter 3 for details) is a partial differential equation that does not have an exact solution. Nevertheless, some mathematical techniques have been

employed in its solutions with a degree of success. At early times when capillary diffusion is the dominant force affecting flow of water, similarity transformation expressions are employed to solve Richards equation, e.g., as discussed in [17, 22, 45, 63, 64]. Depending on the type of transformation and diffusivity functions that are employed, analytical [17, 45, 65] or numerical [66] solutions may be obtained, sometimes requiring the *shooting method* [67] to satisfy boundary conditions. For late times, the principle of *travelling waves* is often used to solve Richards equation, e.g., as shown in [17, 22, 25, 26, 44, 68, 69]. These principles have also been applied to the foam drainage equations as shown in Chapters 5, 6 & 7, and Appendices A & B. In this thesis, the solutions obtained via these mathematical principles are compared and contrasted to elicit similarities and differences for drainage in foams and soils, specifically between the functions employed and the profiles of these solutions as well as their physical meaning.

In the following sections, the themes here briefly outlined are considered in detail. Particularly, in the next section, foams are presented with the governing equation that describes dissipation in its network.

2.2 Foams

The study of foams concerns their formation, structure (experimental determination and simulation), stability (coarsening and drainage), and rheology. The primary area of interest for this thesis is the equation describing drainage in foams. This equation was composed primarily to describe drainage in dry or slightly wet foams.

Foams may be described as a random packing of bubbles in a relatively small amount of water containing surface-active impurities. They are formed through agitation of a solution of surfactant and water. Air is trapped in bubbles of this solution which form the foam network. The regions between three touching bubbles are called Plateau borders and are channels for liquid flow. Four channels join and this region formed between the four touching bubbles is referred to as a node. Foams may be monodisperse (having same bubble sizes) or polydisperse (having varied bubble sizes). An exact arrangement of foams is irreproducible. Many materials may form foam structures in nature (e.g., corks, bones, honeycomb) or artificially (e.g., metals, glass and concrete). Other analogous cellular structures may be found in other areas of biology and ecology, as well as spatial distributions of planets, people

and animals among others.

In what follows, the structure of foams and the drainage in foams are discussed in detail.

2.2.1 Structure of Foams

A typical foam can be found in many daily applications including its use in the kitchen (in washing up liquids, and in cake making), in mining processes (separation of products via froth flotation), in metal manufacturing among other many uses [5–7, 32, 34]. Another very important economic application of foam is in the recovery of petroleum [41, 42], and remediation of soils in the event of contamination of the surface or subsoils [70, 71]. As earlier stated, the foams observed herein may be generally classified as mono-dispersed (when the foam bubbles have equal sizes), or polydisperse (when the foam bubbles have varying sizes) [7]. Generally, foams may also be described as dry or wet. All of these foams may be physically different, but they are governed by similar laws [5, 32–34, 72]. Figure 2.3 shows a typical network unit that consists of a node and sections of its four PBs. The significance of PB length L as earlier mentioned is discussed in the next section.

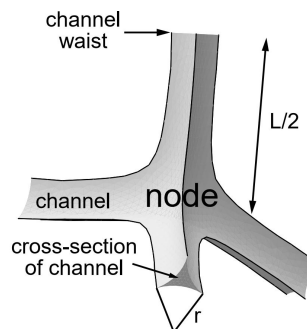


Figure 2.3: Figure showing a cross-section of foam Plateau border and node. [14]

Common to all these kinds of foam are the fundamental concepts that govern their structure, movement, drainage, and overall stability. Structurally, a foam can be described as a multi-scale system, with bubbles, Plateau border channels, nodes and films each having different scales. Plateau [29] proposed some laws that govern the shape and structure of a typical foam, namely [7],

- i. Foam films consist of entirely smooth surfaces.
- ii. The mean curvature of a portion of a film is everywhere constant on any point on the same film.

- iii. These films join each other by threes at equal angles (120°) along an edge called a Plateau border.
- iv. These Plateau borders are distributed such that four of them always meet at the same point (forming a node) making equal angles ($\approx 109.47^\circ$) between them.

These laws can be re-expressed as below as equilibrium laws that guide the geometry, structure and arrangement of the foam bubbles. [7]

- A1 *For a dry foam, the films can intersect only three at a time, and must do so at 120° . In two dimensions, this applies to the lines which define the bubble or cell boundaries.*
- A2 *For dry foams, at the vertices of the structure, no more than four of the intersection lines (or six of the surfaces) may meet, and that this tetrahedral vertex is perfectly symmetric at a value of $\arccos(-1/3)$.*
- B *Where a Plateau border joins an adjacent film, the surface is joined smoothly, that is, the surface normal is the same on both sides of the intersection.*
- D *Any two-dimensional dry foam structure can be decorated by the superposition of a Plateau border at each threefold vertex, to give an equilibrated wet foam structure, provided these Plateau borders do not overlap. In three-dimensions, a dry foam skeleton can be decorated with a finite thickness Plateau border.*

Static foams obey these equilibrium laws proposed by Plateau [29]. Any other configuration that does not obey Plateau's laws are unstable, and the bubbles will rearrange themselves to conform to these laws. These laws were originally presented as empirical only but have now been proven mathematically [73].

As earlier mentioned, the forces that govern drainage in foams include viscous drag, capillary suction (or capillary diffusivity), and gravity forces [4, 5, 32, 33]. Since drainage from wet foam leads to the formation of dry foams, the forces here listed govern the evolution of the structure of foams. Thus, these forces are required to analyse how a foam structure might evolve.

2.2.2 Drainage in Foams

A detailed study on the drainage of foams is required at this stage since its understanding is key to the research objectives. Investigating the details of foam drainage can elucidate its similarities and differences with regards to flow in unsaturated soils, and hence, with regards to Richards equation which describes the latter process. The primary concern here will be flow in either dry or wetter foams up to the point just before they form bubbly liquids (the limit up to which the foam drainage equation is assumed to apply).

Drainage in foams is a flow process that is induced by gravity and capillarity [14]. Foams have a higher liquid content immediately after they are formed [5, 72]. This liquid content reduces over time due to foam drainage, which also occurs as a result of capillary and gravity forces acting on the liquid in the foam [14, 32, 33, 36, 74]. The process of drainage within the foam that eventually leads to a hydrostatic equilibrium of its liquid content is described as free drainage [4, 5, 32]. Such drainage significantly affects the stability and structure of foams. During drainage, dissipation occurs either predominantly through the foam channels [32, 36], hence channel-dominated foam drainage, or via the nodes [14, 33], hence node-dominated foam drainage. These drainage or dissipation have been found to be characteristic of the surfactant solution used to make the foam [7, 40].

After foams have drained for a long time, they form dry foams at the top until just a little way from the bottom where liquid drains. Dry foams describe a state of these foams when the liquid content within the foam network is negligible ($\leq 5\%$ typically). The exact delineation between “wet” and “dry” varies, depending on several factors and the process under discussion. The model for foam drainage equation was formulated for, and therefore applies best within this limit of foam liquid content up until when the foam becomes too opaque for simple experimentation and observation [32].

Three main types of drainage in foams experiments are generally performed. They include forced, free and pulsed drainage [5, 7, 32, 33]. Forced drainage experiments in foams are undertaken by pouring liquid through the top of a foam column once it has been formed [32, 33]. In free drainage as mentioned earlier, the liquid content of the foam is allowed to drain by the action of gravity [32, 33]. Such an experiment is very difficult to undertake with precision since the liquid in the foam begins to drain from the foam as soon as the foam production has been stopped. There is very limited literature describing this

case due to the difficulty of experimentation [5, 72]. For pulsed drainage, the foam is allowed to sit for some time after it is formed. Afterwards, liquid is flowed into the foam from the top through the column of foam for specific time periods after which the liquid from the top is stopped. This step is repeated in pulsed drainage [5, 72].

In the next section, the equations that describe the foam drainage process are presented. The two main variants of this equation that are analysed in this thesis are presented.

2.3 Derivation of Foam Drainage Equation

An equation describing drainage in foam was first derived by Gol'dfarb et al. [31]. It was independently derived by Verbist et al. [32], Verbist and Weaire [36]. The foam drainage equation as described [32, 36] is one of the main equations that are discussed extensively in this thesis. It was derived based on the approximation that liquid dissipation in foams is predominantly via the channels, or Plateau borders. A variant of the foam drainage equation which posits that liquid dissipation is predominantly within the nodes of the foam [14, 33] is also discussed.

2.3.1 Channel-dominated Foam Drainage

Flow through foams neglects liquid flow in the films [5, 32, 72]. Plateau borders are much thicker than these films, thus most of the liquid flow through a foam is through the network of Plateau borders [4, 5, 33, 75]. Representing a foam by a network of Plateau borders is reasonable when very dry foams are considered. The form of the so-called *foam drainage equation* employed in this thesis was given by Verbist and Weaire [36]. The major prevailing assumption for this so-called channel-dominated drainage is that region in which dissipation occurs within the foam is predominantly through the Plateau borders [4–6, 32, 33, 75]. A number of key assumptions [32] were made in order to derive this equation, which include:

1. The contribution to drainage of liquid flow in films is entirely neglected. Hence, only flow along Plateau borders is considered.
2. Flow in the channels is of the Poiseuille type implying zero velocity at the boundaries. This is related to the first assumption.

3. Shearing motion that is associated with flow through the junctions (nodes) do not make a significant contribution to the viscous dissipation.
4. The system assumes a constant surface tension γ and a constant liquid (bulk) viscosity, μ .

The authors [32] admit to the limitations of the assumptions for the derivation of this equation. Other authors [4, 40] have noted these limitations, and yet others [6, 40] have suggested some modifications of this channel-dominated equation. One author [76] has suggested criteria ($\mu_s > 10\mu\theta^{1/2}d$) for the validity of some assumptions in terms of the surface viscosity (μ_s) and bulk viscosity (μ), the liquid fraction (θ), and average bubble diameters (d). Observations of certain systems prompted a variant [14, 33] of the foam drainage equation which was proposed to address some of these limitations observed. This work [14, 33] assumed dissipation is predominantly within the nodes of the foam, and it is presented in Section 2.3.2.

2.3.1.1 Foam Drainage Equation

The formulation of the foam drainage equation as given by [32, 36] is here discussed.

Consider a Plateau border with cross-sectional area $A(x, t)$ changing with vertical coordinate x and time t . Within this Plateau border is a liquid which is assumed to be incompressible. The foam drainage equation is modelled after the continuity equation as

$$\frac{\partial}{\partial t}A(x, t) + \frac{\partial}{\partial x}[A(x, t)v(x, t)] = 0, \quad (2.1)$$

where v is the average velocity over the cross-section of a Plateau border.

The radius of curvature of the Plateau border is a function of the pressure difference between the liquid in the Plateau border and the surrounding gas which follows from the Laplace-Young law,

$$p_l = p_g - \frac{\gamma}{r}, \quad (2.2)$$

where r is radius of curvature of the Plateau border wall, p is pressure either in the gas g or liquid l . Note that $r = \sqrt{A}/C$ and $C = \sqrt{\sqrt{3} - \pi/2}$ i.e. 0.4016 obtained from elementary geometry.

For a volume element of the Plateau border $A(x, t)dx$, the dissipative force due to flow is $-f\mu v/A$, where $f \approx 49$ is a numerical factor representing the shape of the cross-section of a Plateau border, and μ is liquid viscosity. Here, dissipation is balanced by gravity, ρg and capillary pressure gradient $-\partial p_l/\partial x$ to obtain,

$$\rho g - \frac{\partial}{\partial x} p_l - \frac{f\mu v}{A} = 0. \quad (2.3)$$

When p_l from equation (2.2) is substituted into equation (2.3), the velocity v is given as

$$v = \frac{1}{3f\mu} \left(\rho g A - \frac{C\gamma}{2\sqrt{A}} \frac{\partial A}{\partial x} \right), \quad (2.4)$$

which is again substituted into the continuity equation (2.1) to give,

$$\frac{\partial A}{\partial t} + \frac{1}{3f\mu} \frac{\partial}{\partial x} \left(\rho g A^2 - \frac{C\gamma}{2} \sqrt{A} \frac{\partial A}{\partial x} \right) = 0. \quad (2.5)$$

This equation (2.5) is the originally determined channel-dominated foam drainage equation. However, it is re-expressed in terms of foam liquid fraction by including a factor λ (a function of L mentioned in Section 2.1) proposed by Neethling et al. [40] to account for the length of the Plateau border per cell volume. This λ is effectively a measure of the bubble size (λ scales like the inverse square of bubble size) [40]. This is relevant since one could envisage a foam in which bubble size (and hence permeability to liquid flow) could be a function of position. Thus, the effect of a gravity force upon flow (hydraulic conductivity) could be a function of position (even for a uniform liquid saturation). Presumably, capillary suction head would also be a function of position under circumstances like these (again even for a uniform liquid saturation). Volumetric liquid fraction is given as $\theta = A\lambda$, and for dodecahedral bubbles $\lambda = 5\sqrt{3}/(\pi\psi r_b^2)$ [40]. Here, $\psi = (1 + \sqrt{5})/2 \approx 1.618$. The foam drainage equation as used in this thesis is therefore

$$\frac{\partial(\lambda A)}{\partial t} + \frac{1}{\mu} \frac{\partial}{\partial x} \left(\frac{\rho g (\lambda A)^2}{\lambda} - \frac{C\gamma}{2\sqrt{\lambda}} \sqrt{\lambda A} \frac{\partial(\lambda A)}{\partial x} \right) = 0. \quad (2.6)$$

Using the following nondimensionalising scheme $x = \xi x_0$ and $t = \tau t_0$, $x_0 = \sqrt{(C\gamma)/(2\rho g\lambda)}$ and $t_0 = (\mu\sqrt{2\lambda})/(\sqrt{C\gamma\rho g})$, the following is deduced

$$\frac{\partial\theta}{\partial\tau} + \frac{\partial}{\partial\xi} (\theta^2 - \sqrt{\theta} \frac{\partial\theta}{\partial\xi}) = 0. \quad (2.7)$$

This is the dimensionless channel-dominated foam drainage equation that is used in this thesis (see Chapter 5, 6, 7 and B). It differs slightly from a form derived by Verbist et al. [32], Verbist and Weaire [36] (there is a factor of 2 appearing in their equation, but this has been scaled out to permit a fairer comparison with the node-dominated foam drainage equation (see Section 2.3.2)). Here the factor θ^2 is identified as a conductivity term, and $\sqrt{\theta}$ is identified as a diffusivity term. Note (for later comparison with the node-dominated form) that the diffusivity is scaled such that it goes to unity at full saturation.

Strictly speaking, the foam drainage equation is only valid in dry foam limit $\theta \ll 1$, but it is often considered to apply all the way up to some liquid fraction θ_s (saturated liquid content) at which the foam breaks up into bubbly liquid. This notwithstanding, the picture of long straight Plateau borders leading to a simple formula for conductivity θ^2 and diffusivity $\sqrt{\theta}$ does not apply for wet foams. Thus, volumetric liquid content θ is defined as $\Theta = \theta/\theta_s$ with Θ being a rescaled liquid fraction (also moisture content in this thesis), and after suitably rescaling ξ and τ to new variables (setting $\hat{\tau} = \theta_s^{3/2}\tau$ and $\hat{\xi} = \theta_s^{1/2}\xi$), leads to the equation below

$$\frac{\partial \Theta}{\partial \hat{\tau}} - \frac{\partial}{\partial \hat{\xi}} \cdot \sqrt{\Theta} \frac{\partial \Theta}{\partial \hat{\xi}} + \frac{\partial \Theta^2}{\partial \hat{\xi}} = 0. \quad (2.8)$$

The foam drainage equation above is the form that is used throughout this thesis. It has been scaled such that its diffusivity and gravity conduction component are unity at full saturation to ensure an easier comparison with the node-dominated variant of the foam drainage equation, which is discussed in the succeeding section.

2.3.2 Node-dominated Foam Drainage

An experimental study of forced drainage through foam was conducted by Koehler et al. [14, 33]. In this work, a constant liquid flux was maintained at the top of a dry foam. This produced a downward travelling wave with a constant velocity and uniform liquid content. Koehler et al. [14] reported that the results were not consistent with existing models [32, 36], and hence proposed a new model which was based on two further assumptions which varied from those given for the channel-dominated foam drainage. These include,

1. relaxing the condition of wall rigidity throughout the network, and
2. emphasizing the importance of viscous dissipation in the nodes in the network.

Similarities with the channel-dominated foam drainage model include the experimentally measured power-law scaling of the drainage velocity, and hence the gravity component (hydraulic conductivity). It has been observed [7] for this model, as reported in Koehler et al. [14], that the critical micelle concentration may have affected surface rheological properties and thereby dissipation, and hence the derivation of this equation [5, 7, 40]. The node-dominated equation was thus derived based on the surfactant solution used in the experiment, .

2.3.2.1 Node-dominated foam drainage equation

Details of this model, the node-dominated foam drainage model, are discussed herewith. The derivation of this equation, as earlier stated, is similar to that for channel-dominated foam drainage equation, thus it is not presented in detail here.

The node-dominated foam drainage equation proposed by Koehler et al. [14, 33] is

$$\frac{\partial \theta}{\partial t} + \frac{2\delta_a L^2}{\mu \delta_\theta^{1/2} I} \left(\rho g \cdot \frac{\partial}{\partial x} \theta^{3/2} - \frac{\gamma \delta_\theta^{1/2}}{2L} \frac{\partial^2 \theta}{\partial x^2} \right) = 0, \quad (2.9)$$

where θ is liquid fraction, t is time, L is length of a Plateau border, $\delta_a \equiv C^2$ is a geometric shape factor, μ is fluid viscosity, δ_θ is another geometric shape factor, I is a dimensionless number representative of the viscous force in the nodes and is assumed to be independent of θ , ρ is density of liquid, g is gravity, and γ is surface tension. Koehler et al. [14, 33] reported $\delta_a \equiv C^2 \approx 0.1613$, $\delta_\theta \approx 0.1711$, and $I \approx 400$. The value of I was evaluated empirically, although more recent studies [77, 78] indicate a method to compute it.

The dimensionless form of equation (2.9) using time scale $t_0 = (\delta_\theta I \gamma \mu) / (4\delta_a \rho^2 g^2 L^3)$ and length scale $x_0 = (\delta_\theta^{1/2} \gamma) / (2\rho g L)$ as identified in [14, 33] is

$$\frac{\partial \theta}{\partial \tau} - \frac{\partial}{\partial \xi} \cdot \frac{\partial \theta}{\partial \xi} + \frac{\partial \theta^{3/2}}{\partial \xi} = 0. \quad (2.10)$$

As noted for the channel-dominated case in the preceding section, it is possible to rewrite equation (2.10) in terms of a new variable Θ (and setting also $\hat{\tau} = \theta_s \tau$ and $\hat{\xi} = \theta_s^{1/2} \xi$) as done for equation (2.8),

$$\frac{\partial \Theta}{\partial \hat{\tau}} - \frac{\partial}{\partial \hat{\xi}} \cdot \frac{\partial \Theta}{\partial \hat{\xi}} + \frac{\partial \Theta^{3/2}}{\partial \hat{\xi}} = 0. \quad (2.11)$$

It is worthwhile to note that both equations (2.8) and (2.11) are presented in the form of convection-diffusion equations where the convection (gravity) term Θ^2 or $\Theta^{3/2}$ and diffusion coefficient $\Theta^{1/2}$ or 1 is always unity at full saturation. This seems to enable a “fair” comparison between channel-dominated and node-dominated theory (and compared to the formulation of [32, 36], it is the reason for restructuring the channel-dominated foam drainage equation (FDE) and eliminating the factor of 2 that would otherwise appear in the channel-dominated FDE of equation (2.8)).

In the next section, boundary conditions for drainage in foams that are required for solving both channel- and node-dominated foam drainage equations are presented.

2.3.3 Boundary conditions at top and bottom of foam

From the derivation of the foam drainage equation, it is necessary [32] to impose boundary conditions at the top and bottom of a foam sample. Physically this is often quite awkward to do since the bottom section that is in contact with liquid is usually quite wet (Figure 2.4), whereas the foam drainage equation strictly speaking has been simplified to apply in a dry foam. Often this is ignored, and a saturated (wet) foam is assumed to apply at the bottom. Sometimes the awkward boundary condition is actually at the top, e.g., in the case of forced drainage, where a significant flux of liquid is provided at the top.

In foam drainage, a fixed flow rate $\alpha^2 - (\sqrt{\alpha}/2)(\partial\alpha/\partial\xi)$ boundary condition is set at both the top and bottom of the foam sample. This condition is valid at the top whenever liquid is added at a constant rate (forced drainage). However, the constant at the top is zero for free drainage.

For the problems presented in this work,

- Neumann boundary condition is given for the early-time constant rate imbibition problem presented in Chapter 5; and
- Dirichlet boundary conditions are given for the late-time travelling wave problem discussed in Chapter 6 and 7.

Using specific boundary conditions to be presented later, solutions to the foam drainage equations are obtained and compared with solutions to Richards equation. The mathematical

set up for obtaining these solutions are discussed in Chapter 3 (see Sections 3.4–3.7). Based on these formulations, early-time similarity solutions are presented in Chapter 5. Travelling wave solutions to these equations at late times are discussed in Chapter 6 (see Appendix A for solutions using Brooks and Corey [56] soil material property function). These solutions are again presented in Chapter 7 when the soil material property functions are modified to enable a “fairer” comparison with foam drainage equation.

Figure 2.4 shows the general orientation used in the experimental setup for flow in foams. In forced or pulse drainage, liquid is injected at the top of the foam sample whereas in free drainage, the liquid in the foam drains immediately after the foam is formed. In foam literature, direction is always measured positive downwards. This will be maintained in this thesis.

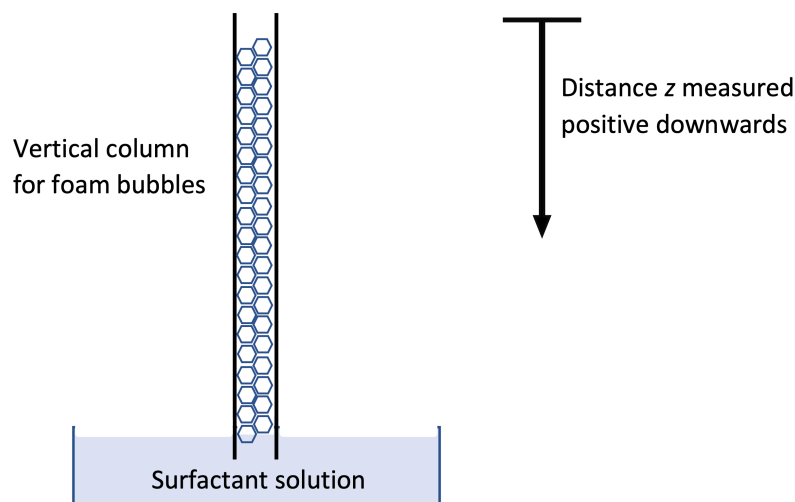


Figure 2.4: Schematic showing the direction of foam drainage

2.4 Soils: Fundamental concepts

Soil is an aggregate of rock minerals with the capacity to retain water or fluids. It is made up of solid (granular) material, water, and air. The portion of the soil that retains these fluids make up the pore spaces. It is these pores that contain the water and air. Figure 2.2 shows a diagram for typical soil detailing its pores and grains.

Depending on the degree of saturation, various flow regimes apply. Generally there are two main classes of flow in soils, namely saturated and unsaturated flow. The forces

that affect flow vary for these flow regimes. Quite conveniently, some of the laws derived for saturated flow have been adequately applied to unsaturated flow. Key among them is the flow rate derived by Darcy [13]. Here, the primary concern is with infiltration in unsaturated soils. Philip [55] defined infiltration as the process of entry into the soil, water being made available at its surface.

In this section, the general theme of drainage in soils is discussed (see section below) in addition to the capillary behaviour of soils and soil water, and how these interact to influence flow in soils, as discussed in the sections that follow. In particular, Darcy law is presented, and the physical basis underpinning Richards equation is given. Here, as mentioned, flow in unsaturated soil is considered rather than flow in saturated soils.

Flow of water in soils is a common concept which has been thoroughly investigated since the turn of the last century [10, 12, 38, 55, 79]. The equation most commonly used to describe flow in soils [20, 25, 59, 80] is Richards equation [12]. A brief discussion of this equation is presented in Section 2.4.4 (see Chapter 3 for a more detailed discussion). The succeeding sections describe those properties of the soil that are essential to understanding the physical basis, derivation and formulation of Richards equation.

2.4.1 Drainage in Soils

Transient-state (unsaturated) flow processes generally involve changes in the water content in a specific volume of soil. Most theoretical treatments of water flow in unsaturated soil ignore the presence of an air phase, or at least imply that soil air does not impede water movement. For a given bulk of soil, a net inflow of water implies expulsion of air, and an outflow of water implies entry of air. In a continuous air-phase, resistance to water flow is limited. Conversely, in a restricted or confined environment, the air phase is not continuous and hence, the water flow is necessarily affected dependent on the air pressure. Kutílek and Nielsen [81] suggested that under such conditions, the simultaneous flow of the two fluids should be jointly considered. In this thesis however, it is assumed that the air movement does not necessarily affect water flow, and hence the air phase is not treated explicitly. Under those circumstances, the factors that contribute to movement of water through the soil are discussed below.

The volume filling factor of water (or moisture content) of the soil or rock structure is

denoted as θ . At the surface of the porous medium, depth $x = 0$, moisture content θ can be set at time $t = t_1$ to some value $\theta(0, t_1)$, where the moisture content there is at a maximum. As one progresses downwards, a wetting front develops which conducts the fluid through the soil system until it reaches the bottom $x \rightarrow -\infty$ at time $t \rightarrow \infty$. The duration it takes to reach a certain depth is dependent on the soil type.

For fluids to move within a porous media system, there must be a pore structure which is able to conduct the fluid from one point to another. The ability and capacity of a porous system to conduct fluid through it is its *permeability*. There are two types, effective and absolute permeability, represented by k_e and k respectively. Absolute permeability is an intrinsic property of the porous medium, while effective permeability is that permeability to a fluid in the presence of another fluid. Two or more fluids in a porous medium will exert forces on each other thereby affecting each other's movement. The wetting or non-wetting phase and the volume of each fluid present contribute to this effective permeability. The units for permeability in dimensional form is L^2 . For ease of representation, a dimensionless quantity, the relative permeability $k_r = k_e/k$ is often adopted.

In unsaturated flow, a related quantity hydraulic conductivity is often described [55] following the concept of permeability, although permeability and hydraulic conductivity are not the same. Soil water transport is usually modelled and described using the concept of hydraulic conductivity. Hydraulic conductivity K describes the ease with which water flows in porous media. Hence, it is dependent on the permeability of the porous medium. It is given mathematically as

$$K = K_r K_s \quad (2.12)$$

where K_r is relative hydraulic conductivity for unsaturated soil, and $K_s = kg/\nu$ is saturated hydraulic conductivity. Here, k is absolute permeability of the porous medium, g is acceleration due to gravity and ν is liquid kinematic viscosity. Hydraulic conductivity in dimensional form is L/T which in S.I. units is m/s . Its value is often given in other units by different systems of measurement. Note that it scales equivalent to velocity.

At early times, or for an infiltration front in previously dry soils, drainage within the soil is dominated by capillary action [17] rather than by gravity-based conduction. Water movement in horizontal profiles is also dominated by capillary action. This capillary action is referred

to as suction, pressure head or capillary suction head. It describes the ability of a wetting phase (soil water in this thesis) to fill narrow channels without the effect of, or even against gravity, and it is also sometimes described as a soil-water retention curve (SWRC). Capillary suction can also be expressed in terms of a potential due to the capillarity of a porous medium in the presence of a wetting phase.

There are drainage scenarios in soils that are equivalent to the three drainage types for foams described in Section 2.2.2. In particular, forced drainage is the same as the so-called travelling wave solutions that have been studied for soils (see Chapter 6 & 7). Here, irrigation is long-duration and continuous until the system reaches full saturation. For foams, that would indicate forced drainage evolution from dry foams to just before a bubbly liquid structure is formed. All of this is presented in detail in Chapter 6.

Free drainage as discussed in foam literature may be likened to a situation where one irrigates the soil for a long time and then stops the irrigation allowing water to drain away (this is not a case that is discussed in this thesis). For instance, water from an irrigation process or rainfall immediately starts to drain away when the source of the water is stopped. Unlike foams, the soil may have a higher retention of the water before any drainage occurs at all: a residual water saturation may exist for instance. Pulsed drainage meanwhile describes a situation whereby one irrigates for a short time, stops irrigating, and then irrigates again, in a controlled and repeated process.

2.4.2 Capillary Properties of Soil

This section considers the derivation and formulation of Darcy [13] equation used to describe flow in soils. Darcy [13] derived an equation for describing flow of water in reservoir rocks [15, 82]. Although in such an environment, the system is typically fully saturated, the equation can be adequately used to describe flow of water in unsaturated soils. Hence, it is a widely used standard tool for petroleum engineers and soil scientists alike.

Consider horizontal linear flow of an incompressible fluid, superficial velocity $v_s = q/A$ where q is flow rate and A is cross-sectional area across which flow occurs. Depending on the orientation of flow, there are conventions to convert from linear to radial flow, and to polar coordinates. These conversions are not discussed in this thesis. In terms of flow rate,

Darcy's law can be expressed as

$$q = -K\nabla\psi, \quad (2.13)$$

where ψ is total potential and K is hydraulic conductivity of the medium. Here, potential is defined by the equation,

$$\psi = (P/\rho g) + \omega \quad (2.14)$$

where P is pressure (resultant stress due to the hydrostatic and adsorptive force fields), ρ is density of water (fluid), g is acceleration due to gravity and ω is potential of the external forces per unit weight of water. Here ω is equal to the capillary head.

2.4.3 Capillary Properties of Water in Soil

Water has many properties that affect its flow. Key among them are its viscosity (determined by pressure and dissolved solids), surface tension, and density. Water moves from a position of high to low pressure or potential. The flow of water in porous media is thereby described by Darcy's law [13].

Within the pores of a porous medium, water forms a concave or convex surface depending on whether or not it wets the surface of the porous medium [15, 82]. For a curved interface, the pressure is known to be greater on the concave side [15]. The following equation (similarly given in (2.2)) describes the force balance of the pressure difference,

$$\Delta p = 2\gamma/r, \quad (2.15)$$

where p is pressure, γ is surface tension and r is radius of curvature of the water surface. This equation can be applied to other fluid interfaces (as shown in the derivation of the channel-dominated foam drainage equation) [14, 36]. The general Laplace equation is derived based on this principle.

For water in a soil, the major forces that act on it are the capillary and adsorptive forces [12, 17]. Together, these forces contribute to soil matrix potential. Gravitational forces and drag forces also affect the movement of water in soils.

2.4.4 Flow in Unsaturated Soil

Flow in unsaturated soils (a transient flow regime) is adequately described using Richards equation. Richards equation [12] (to be discussed in detail in Chapter 3) was derived as a continuity equation from Darcy's law [13], and Buckingham's work [10] on capillary application in soils. Richards equation has been derived under varying assumptions by other authors [17, 19], and has been identified as being of the same form as the Fokker-Planck equation [17, 55]. Richards equation was first discovered following from some experimental work, the results of which were published in 1931 [12]. Richards equation describes a general, macroscopic theory for the flow of water in unsaturated soils. It was derived as a mixed-form, involving both moisture and capillary head dependent functions. Since this original formulation, Philip [17, 55] has proposed a modified moisture-based variant while Whitaker [19] has also derived the same using the method of volume averaging [28].

Figure 2.5 shows the general orientation for flow in soils. Unlike flow in foams, here flow is measured positive upwards.

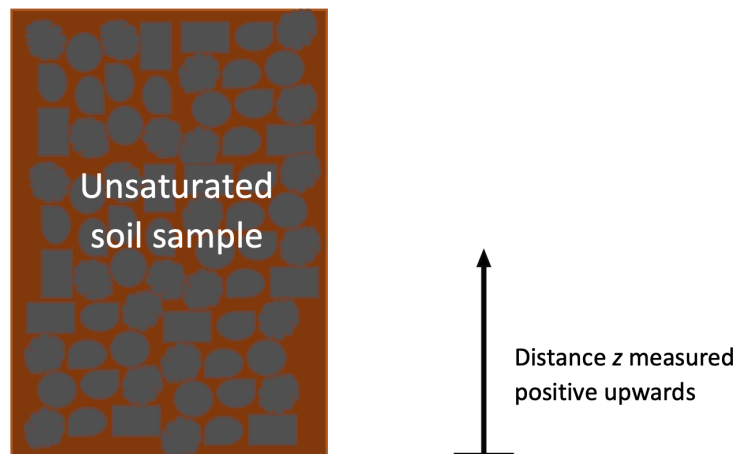


Figure 2.5: Schematic showing the direction of drainage in soils. This sets up the problem that is solved in this thesis.

By virtue of its formulation, which involves gradient-induced transport, Richards equation is analogous to some other known equations (e.g., heat transfer, electricity, and foam drainage equation). Of particular interest to this research is its analogy to the foam drainage equation. Richards equation was originally obtained as a mixed-form, mixing head (or potential) and moisture content. Two other forms, namely head-based and moisture-based

forms can be obtained via the chain rule of differentiation. As alluded to above, details on the derivation and formulation as well as application and solution of Richards equation are discussed further in Chapter 3.

2.5 Soil Material Property Functions

The so-called mixed-form of Richards equation contains two constitutive relationships, the soil-water retention curve (SWRC) and the unsaturated hydraulic conductivity function (HCF) which are strongly nonlinear functions dependent on suction head. Functional forms of these relationships are required in the solution of Richards equation. These constitutive equations are discussed below in detail. Those constitutive equations employed in solving Richards equation in this thesis are discussed in detail in Chapter 4.

As mentioned, in order to solve Richards equation, functions for these constitutive equations describing the hydraulic properties of soils (soil material property functions) are required [17, 20, 68, 80]. Among these are the SWRC which when inserted in a predictive conductivity model (PCM) produces the relative hydraulic conductivity (RHC). Using the first derivative of the SWRC with the RHC, it is possible to determine an expression for relative diffusivity (RD). Many equations describing these material properties have been proposed in literature [38, 56, 60, 83, 84].

Moreover, these hydraulic properties indicate the ability of the soil to either retain or transmit water, and the rate at which these occur. As an illustration, they may specify the amount of water that either infiltrates or runs-off at the soil surface in the event of rainfall [46], the rate and amount of water redistribution in a soil profile [22], among many other such processes in the unsaturated (vadose) zone in soils or the groundwater table [45]. When these hydraulic properties are modelled, they can also be used to design water irrigation schemes, study, and minimise water and soil pollution.

2.5.1 Soil-Water Retention Curve

The soil-water retention characteristic (SWRC) curve is the relationship between the amount of water held in the soil and the forces (suction) holding the water [60]. SWRC has also been described in literature as soil moisture characteristic curve, capillary suction-saturation

relation, or the pF curve (these abound in literature, e.g., [38, 56, 60, 62, 83]). The two forces that hold water in the soil are adsorptive and capillary forces. The former governs wetting on the immediate attachment to the soil surface while the latter governs water within the pores of the soil [85]. The SWRC is used to predict the water content of the soil at a given water tension, or suction head.

The SWRC relates the capillary suction head to the moisture content specific to each soil type. This suction head has been referred also as moisture potential or pressure head. A number of empirical functions have been proposed to simulate the SWRC. These SWRC functions have been classified as 3-parameter (e.g., Tani [86]), 4-parameter (e.g., [38, 56, 87]) and 5-parameter (e.g., Fredlund and Xing [60]) models [85]. A two-parameter model [83] is also available with reliable solutions [61]. Based on their presentation, many of the proposed SWRC functions are 4-parameter models. Some 4-parameter models can be suitably scaled as 3-parameter models, e.g. van Genuchten's [38] model. The choice of a specific SWRC model may be based on certain factors which are not limited to the number of parameters previously available, the zone of interest (wet or dry region), and even mathematical convenience [85].

There are two models of the SWRC commonly used in literature with similar degrees of success. These are the SWRC proposed by Brooks and Corey [56] and van Genuchten [38]. Among the earliest SWRC relationships, the Brooks and Corey [56] is a power-law relationship. The SWRC expressions for Brooks and Corey [56] and van Genuchten [38] are respectively given as

$$\Theta = \left(\frac{h}{h_b} \right)^{-\lambda_s} = H_+^{-\lambda_s}; \quad H_+ = \Theta^{-1/\lambda_s}, \quad (2.16a)$$

$$\Theta = \left[\frac{1}{1 + H_+^n} \right]^m; \quad H_+ = \left(\Theta^{-1/m} - 1 \right)^{1/n}, \quad (2.16b)$$

where

$$\Theta = \frac{\theta - \theta_r}{\theta_s - \theta_r}, \quad (2.17)$$

where θ , θ_s and θ_r are the actual, saturated and residual water contents, h is capillary suction head, h_b is air-entry value (which is the suction, if any, at full saturation). Likewise for Brooks-Corey $H_+ = h/h_b$ (albeit with h and h_b both negative, as they are suctions, so H_+ is positive). For van Genuchten SWRC though, the suction vanishes at full saturation, so

H_+ is just a suitably nondimensionalised version of suction head, and λ_s and m represent pore-size distribution index. Here, $\lambda_s = n - 1$, $m = 1 - 1/n$ (using Mualem [18] definitions) for the profiles plotted in Figure 2.6. Equation (2.16a) has been applied with much success in several studies (e.g., [54, 60] and the references therein). Although the Brooks-Corey SWRC (2.16a) has been found to be valid for suction values greater than the air-entry value of the soil, this equation has been reported to be invalid under fully saturated conditions [60]. This is because the SWRC does not fall to zero at full saturation as expected, but rather unity. Nevertheless, the Brooks-Corey model has been widely used in literature.

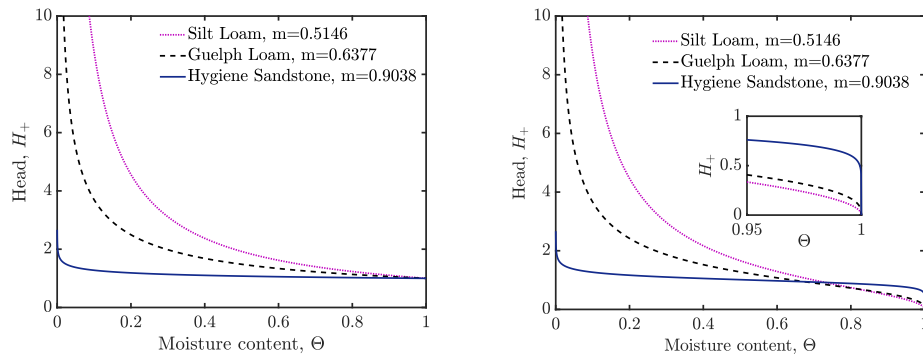
Equation (2.16b) was derived by van Genuchten [38], and it is the most widely used SWRC function [22, 45, 62, 83, 85, 88]. Its popularity can be attributed to two main reasons, its simplicity when seeking exact solutions for unsaturated flow problems, and its more accurate representation of behaviour in the near saturated limit. This near saturation behaviour is aided by an inflection leading the capillary suction head to fall abruptly to zero at full saturation, i.e. $H_+ = 0$ when $\Theta = 1$ but with $dH_+/d\Theta$ diverging there. However, it is equivalent to the Brooks-Corey model in the dry region [69].

The Brooks and Corey [56] SWRC is limited by the absence of an inflection point which might cause discrepancies with field-measured data in addition to a sharp discontinuity at h_b (air-entry or bubbling pressure). Meanwhile because of the inflection point and fitting parameters (m and n) in the van Genuchten [38] SWRC, it performs better near full saturation [83]. Assouline et al. [83] proposed another SWRC that reportedly fits data better than both Brooks-Corey and van Genuchten and is suitable for a wider range of water contents than those proposed by [38, 56], but it is not used in this thesis since it is more complex. It is possible to develop solutions from this equation, albeit using more robust computing methods and even more complex numerical solutions. It is expected that the results will not be qualitatively different from those obtained using the van Genuchten material property functions. Hence, solutions via the latter set of functions are presented and discussed in this thesis.

Subsequently, van Genuchten and Nielsen [89] have proposed that the parameters m and n given in equation (2.16b) could be left as free-fitting for better fitting to data in more cases. They however identified that this makes the equation more complex to solve analytically. For the purposes of this research however, m and n will be treated as related

($m = 1 - 1/n$) as given in van Genuchten [38], and this makes the system more tractable.

From Figure 2.6, observe that the head goes to a finite value (unity) at full saturation in Figure 2.6a as opposed to going to zero, albeit in a singular fashion (the inset gives a more detailed view) in Figure 2.6b. These are behaviours of interest which shall be explored further in Chapter 4. The data presented is for three soil samples. The parameter m represents the pore size distribution, with clayey soils given by $m \ll 1$ and sandstones given by $m \approx 1$. In literature, another relation between m and n is introduced after the Burdine [79] model for which $m = 1 - 2/n$.



(a) Capillary suction head using equation (2.16a). (b) Capillary suction head using equation (2.16b).

Figure 2.6: Capillary suction head profiles for (a) Brooks and Corey [56] and (b) van Genuchten [38] functions for three different soil types. In both cases, Mualem [18] definitions ($m = 1 - 1/n$) are used for the models. Inset in (b) shows behaviour near full saturation. The parameter m represents pore size distribution for these soil types.

Fredlund and Xing [60] report that some authors (McKee and Bumb), based on some of the challenges for adequately describing the SWRC earlier mentioned, suggested the following relationship:

$$\Theta = \frac{1}{1 + \exp((|h| - a_3)/b_3)}, \quad (2.18)$$

where a_3 and b_3 are curve-fitting parameters. This equation reportedly gives a better approximation in the low-suction (near saturated) region, but it is not very suitable in the high-suction (dry) region since the curve for Θ drops exponentially to zero at high suction values [60]. Therefore, Fredlund and Xing [60] proposed the following SWRC relationship:

$$\Theta = \frac{1}{[\ln(e + |h/a^n|)]^m}. \quad (2.19)$$

All the parameters are as previously defined (and e is the base of the natural logarithm),

and a , n and m can be systematically identified through a best-fit analysis on experimental data. The authors report that their model fits data reasonably well over the entire suction range, although it predicts logarithmic not power law behaviour of Θ at high suctions. In order to use this equation, the pore-size distribution of the soil must be known since the SWRC can be related to the pore size distribution and the suction (equation (2.15)) that each pore exerts.

The following linear relationship between the logarithm of Θ and the logarithm of suction have also been used to describe SWRC of many soils in Australia [90]:

$$\ln |h| = a_1 + b_1 \ln \Theta, \quad (2.20)$$

where a_1 and b_1 are curve-fitting parameters. Other authors have proposed equations that are suited to local soils in their research.

As earlier mentioned, models for material property functions are essential to be able to solve Richards equation. Although there are many available models in literature, and many more are being developed, for ease of analysis and the purposes of the research objectives, the Brooks and Corey model [56] and the van Genuchten model [38] are those discussed in detail in this thesis.

2.5.1.1 Theoretical basis for shape of soil-water retention Curve

As alluded to earlier, in establishing the theoretical basis for the SWRC, the soil pore-size distribution must be considered. The soil may be regarded as a set of connected and interconnected pores that are randomly distributed. These pores are characterized by a pore-radius r the distribution of which is described by a function $f(r)$, where $f(r)dr$ is the relative volume of pores of radius r to $r + dr$. Hence, an increment dr in pore radius implies an increment $d\Theta = f(r)dr$ in saturation, which is integrated to give a relation between Θ and r . Meanwhile capillary suction pressure is related to r via equation (2.15), and capillary suction head is just pressure divided by ρg , so obtaining a relation between h and r is straightforward. The relation between Θ and h then follows.

This forms the basis of all the predictive conductivity functions (e.g., [18, 79]). This is discussed in detail in the Appendix of Chapter 7.

2.5.1.2 Modifications of SWRC

As earlier stated, there are many versions of the SWRC available in literature (see [60, 83] and references therein). Some of those SWRC functions most commonly used are modifications of previously existing ones. Popular among these is the van Genuchten [38] SWRC given in equation (2.16b) which in effect is a modification of equation (2.16a) given by Brooks and Corey [56]. As previously stated, the Brooks and Corey [56] SWRC does not go to zero suction at full saturation, instead, H_+ goes to unity for all soil types. However, van Genuchten [38] introduced an inflection in the profile that causes this function to go to zero (albeit in a singular fashion) as is expected in the behaviour of suction head in this limit. Nevertheless, from residual saturation (maximum suction head) until a behaviour referred to in this thesis as Θ_{inf} (see Chapter 7), the two SWRC functions are almost equal to each other. Mathematically, up to about 30% moisture content, the SWRC given by van Genuchten [38] can be approximated using the Brooks and Corey [56] SWRC function (a behaviour shown in Chapter 6).

This section has considered just one of those material property functions that are required to characterise flow and retention of water in unsaturated soils. In the next section, another one of these material properties and its function, namely hydraulic conductivity, is considered.

2.5.2 Hydraulic Conductivity

Hydraulic conductivity relates the ease with which fluid moves through porous media. Mathematically, this is given by the hydraulic conductivity function (hereafter HCF) which describes the relationship between the unsaturated hydraulic conductivity function K and the water content Θ or alternatively the capillary suction head h , and it generally has the dimensions $[L][T]^{-1}$. This HCF is given as

$$K = k\rho g/\mu, \quad (2.21)$$

where μ is dynamic viscosity, ρ is density of the fluid, g is gravity and k is intrinsic (absolute) permeability of the medium. Hence, HCF depends on the permeability of the porous material, the degree of saturation, the density and viscosity of the fluid. In contrast, absolute permeability (with dimensions $[L]^2$) relates specifically to the innate properties of the porous

material itself (which depends solely on the internal geometry of the medium), excluding the specific effects of the type of fluid. Thus, to estimate permeability from hydraulic conductivity, the viscosity and density of the fluid must be accounted for.

It is easier to relate this HCF value relative to its saturated value K_s since $K(\Theta)$ is not always easy to determine, and there are numerous units of measurement of K (e.g., m/s, ft/day, etc.). Hence, the relative hydraulic conductivity, $K_r(\Theta)$ (also RHC) is used and it relates both the hydraulic conductivity K and hydraulic conductivity at full saturation K_s . Mathematically, RHC is given as

$$K_r = K/K_s. \quad (2.22)$$

These measurements vary for every soil type, and arrangement. RHC may be given as a function of either moisture content or hydraulic head.

There are two broad categories for obtaining hydraulic conductivity values. These are

1. empirical approach whereby the hydraulic conductivity is correlated to soil properties like pore size and particle size (grain size) distributions, and soil texture, and
2. experimental approach by which the hydraulic conductivity is determined from hydraulic experiments using Darcy's law.

Data from the experimental approach can be expensive and time consuming to obtain [61, 62, 89, 91], hence the need for correlations and mathematical expressions. In this thesis, the empirical approach is employed to obtain values for hydraulic conductivity.

Typical expressions from this empirical approach may be classified as either data-matching, macroscopic or statistical [84], given respectively in general as

$$K_r(h) = [(h^k/a^k) + 1]^{-1}, \quad (2.23a)$$

$$K_r(\Theta) = \Theta^{\bar{\omega}}, \quad (2.23b)$$

$$K_r(\Theta) = \Theta^{\kappa} \left[\int_0^{\Theta} \frac{1}{H_+^{\delta}} d\Theta \Big/ \int_0^1 \frac{1}{H_+^{\delta}} d\Theta \right]^{\eta}, \quad (2.23c)$$

where k , a and $\bar{\omega}$ are fitting parameters for equations (2.23a) and (2.23b); κ , δ , η are model parameters in equation (2.23c). It is known for equation (2.23c) that $\kappa = 2$, $\delta = 2$, and $\eta = 1$ from the so-called Burdine model [79], and $\kappa = 1/2$, $\delta = 1$, and $\eta = 2$ from the so-called

Mualem model [18]. The assumptions, mathematical derivation and analysis of the Mualem [18] model is presented in the appendix of Chapter 7.

The data-matching approach involves fitting specified mathematical formulae to available hydraulic conductivity data [84]. A typical example is equation (2.23a). This approach is limited since no single formula is valid for all soil types. Thus, new equations must be obtained for every different soil type. Hysteresis may be observed in these functions (typically more pronounced in those dependent on h than in those which are moisture content Θ dependent). Assouline [84] remarks that these data-matching equations are valid for continuous wetting or drying processes. This set of functions is not however used in the analysis and derivation of solutions in this thesis, and hence they are not discussed any further.

The macroscopic approach gives a simple analytical formula for RHC based on some physical considerations for the soil type. Equation (2.23b) is such an example. For instance, Irmay [92] derived $\bar{\omega} = 3.0$ whereas Mualem [93] determined $2.5 < \bar{\omega} < 24.5$ based on experimental data for 50 soils. This is essentially a power law relationship for the soil which determines how quickly the RHC reaches unity at full saturation. Power law relationships like these will be used in some instances in this thesis, but as they also turn out to arise in the statistical approach (discussed below), at least assuming special cases for the SWRC, the macroscopic approach is not considered specifically any further.

The statistical approach relates RHC of soils to its measured retention curve data. It is the basis on which Burdine [79] and Mualem [18] derived their conductivity models. The RHC model presented by Mualem [18] is based on this general model, and it is discussed in the next section. Its mathematical basis is presented in detail in Appendix A of Chapter 7. Since this approach gives the most widely used RHC functions (e.g., van Genuchten [38], Brooks and Corey [56]) applied in most solutions to unsaturated flow in soils, it is adopted in this thesis. Other recent authors [62, 84, 88] employ this approach in obtaining RHC functions.

2.5.2.1 Predictive Conductivity Models

So-called predictive conductivity models (PCM) are based on the statistical approach. Using information about pore size distributions (which feed into SWRCs) and assumptions about

pore connectivity, such models attempt to estimate conductivity.

According to some authors [89, 94], the simplifying assumptions for determining the hydraulic conductivity relationship do not reflect the real soil. This leads to a mathematically simplified but erroneous assumption based on which the RHC is also obtained. They argue that the functional form of the RHC is based on a capillary model which does not accurately describe a soil. Recently, other authors [62, 88] have presented models to address the limitations of assumptions used in those RHC functions obtained from the capillary models.

In particular, Peters and Durner [62] suggest the need to account for film flow near pore walls. A further assumption is made in Peters [88] for vapour flow in the soils. In both instances, the equations are able to model these additions. Most of these modifications are limited to high suction or the onset of infiltration in dry soils. However, Assouline [84] derived an equation for predicting behaviour in the saturation limit. He reports that his equation performs better than the van Genuchten [38] model. However, this equation is complex to solve analytically.

Another assumption accounts for adsorptive moisture content in the retention function which is captured in the statistical pore bundle method that tends to be employed (e.g., using either Burdine [79] or Mualem [18] models). Profiles obtained using this proposed model are reported to more adequately describe behaviour in the very dry region and near-saturated region (e.g., [84, 88]).

Recent research has shown the general importance of accounting for the vapour phase in flow in soils [61, 84]. Hence, with improving research and the abundance of high performing computers, behaviour in the very low or near saturated regions can be modelled more easily. Most of these equations cannot be solved analytically though and hence require numerical simulation.

Note that RHC is obtained from HCF which in turn is determined using the relationship

$$K(\Theta) = \hat{c}(\theta_s - \theta_r) \int_0^\Theta \frac{d\Theta}{h^2}, \quad (2.24)$$

where \hat{c} is an empirical constant that cannot be determined experimentally. Thus, the equation above tends to be used to determine the RHC, a process which scales out the

constants \hat{c} and $\theta_s - \theta_r$.

2.5.2.2 Commonly employed conductivity models

To summarise, among the class of equations used to describe RHC, Mualem [18] proposed to distinguish between two main groups: the first group is based on a generalisation of Kozeny's [95] approach for saturated and unsaturated porous media. Here, the RHC is determined to be a power-law function of effective saturation or rescaled moisture content (Θ),

$$K_r(\Theta) = \Theta^{\alpha'}. \quad (2.25)$$

Brooks and Corey [56] proposed a value of $\alpha' = 3.5$ which agrees with observations much better than $\alpha' = 3.0$ derived by Irmay [92].

The second group of solutions generally called predictive hydraulic models include those by Mualem [18], Burdine [79]. Using an SWRC function, the RHC is obtained via these predictive models. From equation (2.23c), the Burdine [79] equation, commonly used in petroleum engineering [84], is given as

$$K_r(\Theta) = \Theta^2 \int_0^\Theta \frac{1}{h^2(x)} dx \Big/ \int_0^1 \frac{1}{h^2(x)} dx. \quad (2.26)$$

It has been used to develop RHC functions as was done by Brooks and Corey [16], van Genuchten [38]. The Mualem [18] predictive model is also given as

$$K_r(\Theta) = \Theta^{1/2} \left[\int_0^\Theta \frac{1}{h(x)} dx \Big/ \int_0^1 \frac{1}{h(x)} dx \right]^2, \quad (2.27)$$

which has been used to derive RHC functions in literature [16, 38, 61]. This model is the most widely used format of the predictive conductivity model. It has been reported [38] that data obtained using the Mualem model matches field data better than the Burdine model.

Soil scientists refer to a generally modified form of Childs and Collis-George [96] RHC equation [18], also given (in discretised form) as

$$K_r(\Theta) = \Theta^\pi \sum_{i=1}^l \frac{[2(l-i)+1]}{h_i^2} \Big/ \sum_{i=1}^b \frac{[2(b-i)+1]}{h_i^2}, \quad (2.28)$$

where b represents the total number of intervals into which the Θ domain is divided, and

l is the number of intervals up to a prescribed value of Θ . Childs and Collis-George [96], Millington and Quirk [97], and Kunze et al. [98] suggest $\pi = 0, \frac{1}{2}$ & 1, respectively. The Millington and Quirk value has been reported [18] to more closely match experimental data.

2.5.2.3 Special cases of Relative Hydraulic Conductivity

Those RHC equations derived using the PCM (based on the statistical approach) have been commonly used in literature [56, 62, 84, 88]. Among those most widely used is that derived by van Genuchten [38]. Its use is helped by its mathematical simplicity and the ease of its manipulation in models as shown in Chapter 6 and 7 of this thesis. It is given based on (2.16b) with (2.27) as

$$K_r(\Theta) = \Theta^{1/2} (1 - (1 - \Theta^{1/m})^m)^2. \quad (2.29)$$

This equation was also given dependent on head h [38] but as earlier noted, K_r functions dependent on h can have significant hysteresis, and since those are not used in this thesis, they will therefore not be discussed any further here. This function as written is a closed-form expression [38] which was obtained from an SWRC which was made to “artificially” go to zero at full saturation via a mild singularity. The implications following from this are discussed further in Chapter 6 (see also Appendix A) and Chapter 7.

The equation derived using the SWRC of Brooks and Corey [56] (as opposed to that of van Genuchten [38]) is also given as

$$K_r(\Theta) = \Theta^{1/2+2/m}. \quad (2.30)$$

In theory, although the RHC in equation (2.25) is also a power-law, it is not identical to this expression (2.30) here given since the value of α' (in equation (2.25)) was a fitting parameter that varies when considering different soil types. Instead, the Brooks-Corey RHC in equation (2.30) is obtained via a predictive conductivity model using the Brooks-Corey SWRC. Both equations (2.29) and (2.30) have been given using the PCM of Mualem [18] (albeit with different SWRC formulae) and assuming a particular relationship between the soil specific parameters m and n (i.e. $m = 1 - 1/n$). These are plotted together here in Figure 2.7. Profiles of these equations are shown again in Figure 4.2a & 4.5.

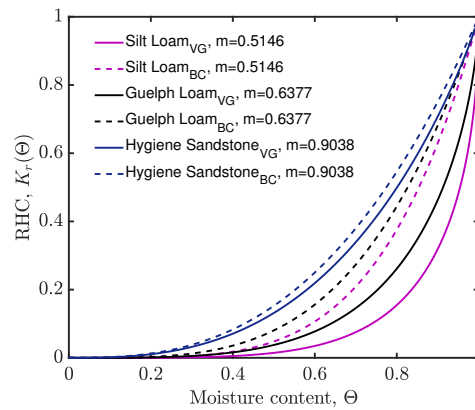


Figure 2.7: Profile comparing RHC for equations (2.29) (van Genuchten) and (2.30) (Brooks-Corey).

2.5.3 Relative Diffusivity

It has been shown that the mixed form of Richards equation has better properties with respect to numerical solutions [20] than a purely pressure-based or equivalently head-based form since mass balance errors persistent in the pressure-based form are minimised. Richards equation can also be solved with all the pressure head terms replaced by a moisture content relationship. The moisture-based form of Richards equation is easier to solve numerically, and it was also derived independently by Philip [17]. It is from this reformulation of Richards equation that a hydraulic diffusivity function arises: it is not a “new” soil material property per se, but rather a way of re-expressing information contained in soil material properties previously mentioned that just happens to be more convenient to deal with when treating a moisture-based form. This diffusivity function is essentially the product of hydraulic conductivity and the first derivative of the SWRC. It is thereby a capillary based function.

The interaction of soil with water and air phases determines the movement of water in unsaturated soil. Moisture content affects not only the SWRC, but also the hydraulic conductivity. Thus, the value of K_s (saturated hydraulic conductivity) cannot be used to define water flow in general since it is solely the value of K at full saturation. In nature, the soil is never really fully saturated since some pores cannot be reached. However, ponding and water run-off are indicative that a maximum possible saturation has been reached. Unsaturated soil is then any soil with moisture content below this maximum saturation.

The term hydraulic diffusivity (D) is now introduced recognising that all parameters

such as capillary suction (water potential), and permeability (or hydraulic conductivity) that would be constant in saturated soil become a function of water content in the case of unsaturated soil [99, 100]. Unsaturated soil behaviour is dependent on the basic relationship between suction head and water content (either, gravimetric or volumetric) or saturation (the graphical representation of this relationship is called the soil moisture characteristic curve or equivalently the SWRC). Hydraulic diffusivity is the product of hydraulic conductivity and the gradient of the SWRC. Relative diffusivity D_r (a normalised version of D , albeit not necessarily normalised at full saturation since the gradient of the SWRC might diverge there [38]) is hence a hydraulic property of soils that describes the capillary diffusion of water in unsaturated soils.

As alluded to above, the general mathematical expression [99] for deriving RD (which will itself appear in Richards equation later on, see chapter 3) is thus

$$D_r(\Theta) = K_r(\Theta) \left| \frac{dH_+}{d\Theta} \right|. \quad (2.31)$$

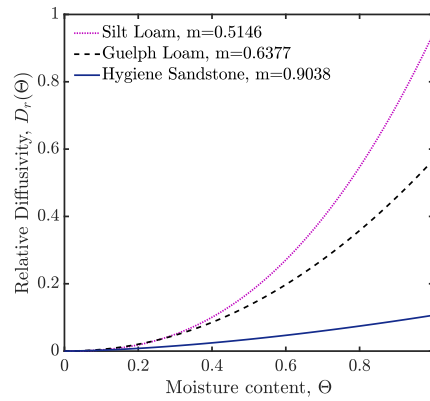
Therefore, having obtained a head function, and using the desired PCM to obtain an RHC function, a function that describes the RD of any porous medium can be obtained. This form of the RD function makes the moisture-based form of Richards equation (see chapter 3) easier to treat since it is cast in a particular way (convection-diffusion) that can be tackled relatively easily using a solution procedure proposed by Philip [17].

Among those capillary diffusivity functions commonly used are those obtained using SWRC functions proposed by Brooks and Corey [56] and van Genuchten [38]. They are given as,

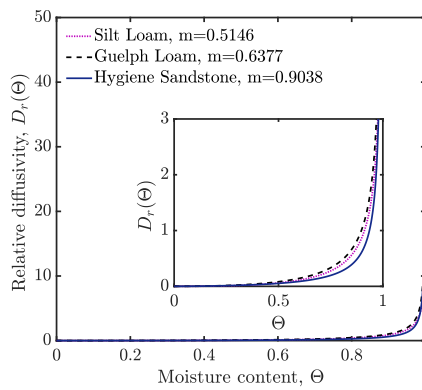
$$D_r(\Theta) = \frac{(1-m)}{m} \Theta^{1/2+1/m}, \quad (2.32a)$$

$$D_r(\Theta) = \frac{(1-m)}{m} \frac{(\Theta^{-1/m-1/2})}{(\Theta^{-1/m}-1)^m} [1 - (1 - \Theta^{1/m})^m]^2. \quad (2.32b)$$

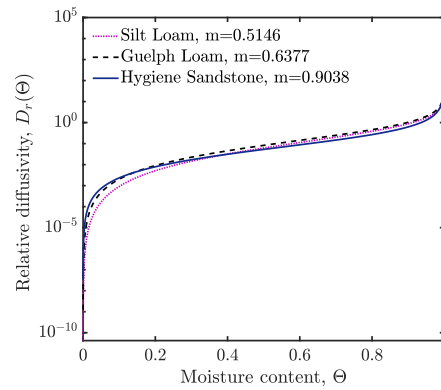
The parameter m and the variable Θ are as previously defined. The functions here given are based on RHC obtained using Mualem [18] PCM definitions. The head or SWRC part of the expressions were supplied by equations (2.16a) and (2.16b), respectively from Brooks and Corey [56] and van Genuchten [38]. The resulting RD functions are shown as profiles in Figure 2.8.



(a) Brooks-Corey model



(b) van Genuchten model



(c) semi-log van Genuchten model

Figure 2.8: Profiles of relative diffusivity based on equations (2.32a) (shown in (a)) and (2.32b) (shown in (b) and (c)). The figure (c) highlights the upper and lower limits using van Genuchten [38] model.

To summarise, the functions describing soil material properties described in this section and preceding sections are those that will be used to obtain solutions for drainage in soils, specifically for Richards equation. The methods for solving Richards equation are discussed in latter sections of Chapter 3.

2.6 Analogies: Richards Equation and Foam Drainage Equations

Up to this point, foams and soils have been considered separately with no explicit similarities between them presented. In this section, these similarities or differences relevant to this thesis are considered. In particular, these discussions are based on the phenomena that drive drainage in both of these porous media.

There is a close analogy between the physics behind Richards equation for soils and

the physics behind foam drainage. Primarily, they are both continuity and mass conservation equations that describe flow (in complex porous media). The forces that control fluid flow are the same in both equations (capillary, gravity and viscous forces). Equations (2.8) and (2.11) (both FDEs) and Richards equation (see Chapter 3) based on their format have their first term (which involves a derivative with respect to time t) as an accumulation term. The other parts of the equation involve derivatives with respect to depth or distance and are represented by capillary diffusivity and hydraulic conductivity (gravity) functions.

Some authors have formulated alternative equations that either describe “foam drainage-like” effects within soil [24, 101] or flow of a mass of foam within porous media [41]. Particularly, Or and Assouline [24, 101] have formulated an alternate approach to drainage in porous media using a variant of the foam drainage equation (FDE) which they call the “soil FDE”. They proposed that due to the complexity of obtaining accurate values for the hydraulic functions (conductivity and diffusivity) in Richards equation (RE), a variant of the FDE could be considered if the capillary network in soils were viewed as foam channels (PBs). This is admittedly a simplified view considering that unlike soils, the channels within foams expand with increasing moisture content until the foam breaks into a bubbly liquid state, which is not the case with soils. Additionally, soils have very large local variations in their pore sizes unlike the typical situation with foams where capillary suction limits the local variation of Plateau border (PB) cross-sectional area.

Despite these differences structurally, foams and soils still have many similarities. In both porous media, the capillary suction effects are strongest when the system is dry but fall to zero at full saturation. Similarities like these can be exploited when comparing foam and soil systems. It is possible then that the solutions which have been determined for the FDE may be extended to the RE to gain insights into flow behaviours in soils or other porous media. As mentioned earlier, the FDEs have those functions needed to solve them embedded in their equations. Material properties for the soils are however required to solve these flow problems. These have been briefly discussed in this chapter. A more detailed discussion of those material property functions that are used in this thesis are discussed in detail in Chapter 4.

In both foams and soils, hydraulic conductivity (gravity) effects are negligible at very low moisture contents, becoming more significant as the moisture content increases. As shown

in Chapter 6, when water is added to an already wetted foam or soil, its velocity increases. This is another similarity for foams and soils that will be exploited in this research.

As in all cases of drainage, in the early-time limit, the fluid moves solely under the effect of capillary diffusion rather than with gravity [55]. In this regime, the effect from gravity can be neglected, and hence, the resulting equation for transport of moisture can be given as

$$\frac{\partial \Theta}{\partial t} = \frac{\partial}{\partial x} \left(D_r \frac{\partial \Theta}{\partial x} \right). \quad (2.33)$$

The resulting equation can either be a linear or nonlinear partial differential equation dependent on the nature of the diffusivity function. This is considered in detail in Chapter 5. Hence, whether at early times (when equation (2.33) applies) or late times (when the full expressions apply, see chapter 3), Richards equation and the two variants of the foam drainage equation are equivalent in form and can be solved using the same mathematical approach. In more cases, the foam drainage equations may yield analytical solutions, but this is harder to achieve with Richards equation since the material property functions used tend to be more complicated. In this thesis, for the most part numerical solutions are obtained for Richards equation.

2.6.1 Bridging the Gap

While soils are generally formed from natural processes and some foams may occur naturally, those foams studied experimentally are formed using surfactant solutions. It is from these latter category foams that the foam drainage equations are obtained. In this section, some definitions that are used in the literature of unsaturated flow in porous media (Richards equation) are compared with equivalent definitions from the literature of foam drainage (channel- and node-dominated equations). In Table 2.1 terms that are used in general flow in foams and soils communities are presented. The descriptor term as used in porous media flow community is given in the first column with the equivalent terms for flow in foams and soils presented in their respective columns. These may help to distinguish between the terminology used to describe certain parameters in the foam drainage equation and the Richards equation respectively. The terminology that are used in describing flow in soils and foams differ even for similar processes. Drainage in foams describe the movement of liquid through the foam network whereas in soils, drainage usually refers to expulsion of water out

of the soil usually into the water table. Infiltration as used in soil literature is the equivalent term for drainage in foams. However, both early-time foams and soils may be similarly described by capillary imbibition. It is quite common to find capillarity used in foam literature for the same process as capillary suction. Early-time imbibition is dependent on capillary diffusivity whereas late time drainage/infiltration is a mixture between capillary forces and gravity (hydraulic conductivity). Gravity and hydraulic conductivity are the equivalent terms in foams and soils respectively.

Table 2.1: Equivalent terminology and differences for describing flow in foams and soils.

Term	Foam	Soil
Flow channels	Plateau border or nodes	Pore space
Fluid saturation	Liquid content	Water content
Fluid suction	Capillarity	Capillary suction head
Fluid drawdown	Gravity	Hydraulic conductivity
Percolation	Drainage	Drainage
Influx	Drainage	Infiltration
Early-time flow	Imbibition	Imbibition
Flow direction	Positive downward	Positive upward

Table 2.2 also presents the equivalent material property functions (relative hydraulic conductivity and relative diffusivity) and their foam drainage analogues that are employed in this thesis to derive solutions to Richards equation and the two variants of the foam drainage equation. Of more interesting physical significance, is the relationship function, $dH_+/d\Theta$. This relates how a change in moisture content affects the pressure head. Observe that this relationship is equivalent for both variants of the foam drainage equation, indicating overall capillarity or suction within the foam network is equivalent. The equivalent expression for soils is the absolute form of the derivative of suction head (2.16b). Whereas for the foam drainage equations this property goes to unity at full saturation, it goes to infinity in Richards equation. The significance of this property is discussed further in Chapter 6.

Table 2.2: Analogues of equivalent expressions for relative hydraulic conductivity $K_r(\Theta)$ and relative diffusivity $D_r(\Theta)$ for drainage in foams [14, 36] and soils (via van Genuchten [38] equations). A third property shows $dH_+/d\Theta$.

Property	CD FDE	ND FDE	RE (VGM)
$K_r(\Theta)$	Θ^2	$\Theta^{3/2}$	$\Theta^{1/2}[1 - (1 - \Theta^{1/m})^m]^2$
$D_r(\Theta)$	$\sqrt{\Theta}$	1	$\frac{(1-m)}{m} \frac{(\Theta^{-1/m-1/2})}{(\Theta^{-1/m} - 1)^m} [1 - (1 - \Theta^{1/m})^m]^2$
$\frac{dH_+}{d\Theta} = \frac{D_r(\Theta)}{K_r(\Theta)}$	$\Theta^{-3/2}$	$\Theta^{-3/2}$	$\frac{(1-m)}{m} \frac{\Theta^{-1/m-1}}{(\Theta^{-1/m} - 1)^m}$

2.7 Summary

This chapter has considered the concepts of drainage in foams and soils, the governing equations describing this drainage, and the fundamental material properties and their functions that are used in solving moisture propagation in both porous media. An important feature in foam drainage equation is that these material property functions are already supplied in the composition of the equation itself. For soils, specially derived material property functions are required to solve Richards equation. These equations abound in literature, and a few of them are presented in this chapter.

In the next chapter, Richards equation is considered in detail. Its derivation, nondimensionalisation, and rescaling are discussed. Additionally, the concepts that have been employed to solve Richards equation in this thesis, namely similarity solutions and travelling wave solutions are discussed.

Richards Equation: Drainage in Unsaturated Soils

Abstract

Drainage (infiltration) of water in soils describes saturated or unsaturated flow driven by a combination of gravity and capillary forces, or with one of these forces dominating flow. This work is primarily concerned with flow in unsaturated soil. In order to describe flow in unsaturated soils, Richards [12] derived an equation based on Darcy [13] flow and the Buckingham [10] continuity requirement for which the dominant forces were found to be gravity (given by hydraulic conductivity) and capillary suction head (potential). This equation was determined to be analogous to the heat equation. Recently, it has been shown to be similar/analogous to the equation describing drainage in foams [68]. Richards equation is a nonlinear partial differential equation with, in general, no exact analytical solutions. It is therefore difficult to tackle having no closed-form solution (except in simplified cases). Despite these difficulties, since its formulation, Richards equation has been applied in many areas of soil science, agriculture, hydrology, petroleum engineering among others. As such this chapter focuses on Richards equation, its derivation and formulation of its solutions. The boundary conditions fundamental to the various flow regimes and their solutions thereof are also discussed. In order to solve Richards equation, certain soil material properties must be known. The functions for these properties are input in Richards equation and using certain mathematical or numerical techniques, solutions are then found. These soil material property functions themselves are discussed in the next chapter.

3.1 Introduction

As expressed in the previous chapter, the problem of flow in unsaturated soils is important in many fields of engineering including drainage, irrigation, geotechnical, environmental, soil and petroleum engineering [28, 80, 102]. Flow in unsaturated soils is a two-phase flow of immiscible fluids such as air and water. For the purposes of this research, contribution of the air to flow is neglected, and focus is instead on the movement of water.

Richards [12] derived an equation for flow of water in unsaturated porous media based on the flux laws derived by Darcy [13] and Buckingham [10]. The equation is a non-linear partial differential equation originally presented in a mixed form (dependent both on moisture content θ and suction head h). A constitutive relationship between h and θ allows the equation to be transformed between forms. It may be written in several other forms with either the head, h (units of length) or the moisture content θ (volume of moisture per volume of pore space) as the dependent variable [20]. Based on how the equation is composed, the key components are an accumulation term, a capillary diffusivity term, and a hydraulic conductivity term. These are reflection of the soil type, and whether or not it was previously dry or wet (there is a hysteresis effect between suction head and moisture content). These parameters or terms can either be determined experimentally or using mathematical functions to model them. Several expressions have been proposed in order to have those terms that are required to solve Richards equation. These functions have been introduced in the previous chapter, and are discussed in detail in the next chapter.

A flow regime characterises drainage in soils. Based on the flow regime (early or late times), either one of or both of gravity (hydraulic conductivity) and capillary suction are dominant in the infiltration of water in the soil. In the early-time regime, capillary effects (mainly diffusivity) dominates movement of water in soils. At late times, both capillary suction and hydraulic conductivity influence flow, and at full saturation, effects of suction may be ignored with hydraulic conductivity dominating flow. Therefore, two main cases of Richards equation are solved: the nonlinear diffusion equation (a special case) and the original formulation of Richards equation.

In this chapter, the derivation of Richards equation and a brief discussion of some of the techniques applied to solve it in this thesis are presented. A general description of how

these techniques may be applied are also presented. The solutions to Richards equation which are obtained using these methods are presented in later chapters, namely Chapter 5, 6, 7 and B. As those chapters indicate, some of the results presented have been submitted for publication. Hereafter, the derivation, nondimensionalisation and rescaling of Richards equation are presented.

3.2 Richards Equation

This section considers the derivation and forms of Richards equation in Sections 3.2.1 and its nondimensionalising in 3.2.2. Composing Richards equation in dimensionless form allows for a consistent comparison with the foam drainage equation, allowing us to compare drainage phenomena in soils and foams directly. It also allows for a universal interpretation irrespective of the dimensions or scales of measurement for the soil material properties.

Richards equation describes drainage of liquids in unsaturated porous media [12]. Its existence was implied by Buckingham [10] after which it was experimentally derived by Richards [12]. Philip [17] has shown that Richards equation is a type of Fokker-Planck convective-diffusive equation. Philip has extensively discussed solutions to Richards equation [17, 47–52] with a summary of his work also presented in Philip [55]. Richards [12] identified similarities/analogies between flow in soils and heat conduction. The experimental methods developed by Richards and the mathematical formulations may be used to express capillary flow for other liquids and media [12].

Various authors have solved Richards equation applying different techniques to the equation in various forms, either to the original mixed form, the head based form or the moisture based form. Some of the techniques applied include travelling wave solutions [17, 26, 44, 45, 68], Picard iteration methods [20, 103] usually used with the mixed form, and mass-conservative numerical solutions [104, 105]. It is reported that numerical solutions based on the standard head-based form of Richards equation generally yields poor results which is characterised by large mass balance errors and erroneous estimates of infiltration depths [20]. Literature is replete with works on solutions to Richards equation partly because it is interesting mathematically, but especially since it has many physical applications. Some authors [46, 53] have found exact solutions to general soil-water flow based on Burgers' equation.

Generally, in deriving Richards equation, soil water properties are assumed to be constant for the purposes of simplifying the mathematics. Therefore, viscosity, density and surface tension are assumed not to change for the entire duration of the flow process.

3.2.1 Derivation of Richards Equation

Richards equation can be deduced using the continuity and Darcy equations,

$$\frac{\partial \theta}{\partial t} = \nabla \cdot \mathbf{q} = \frac{\partial q}{\partial z}, \quad (3.1)$$

where q is the Darcy flux which is measured downwards and distance z is measured *upwards*. This is a common sign convention for Richards equation (and hence flow in unsaturated soils) but differs from the usual convention employed for foam drainage. Equation (3.1) is the continuity equation for describing fluid flow in porous media. Meanwhile, the vector flux \mathbf{q} is given as

$$\mathbf{q} = K(\hat{\mathbf{g}} - \nabla h), \quad (3.2)$$

where K is hydraulic conductivity, $\hat{\mathbf{g}}$ is a unit vector in the direction of gravity, and h is the capillary suction head. One key component of equation (3.2) is the capillary suction head factor which is related with the soil water retention. It is analogous to a capillary suction term in the foam drainage equation. The capillary suction head and the hydraulic conductivity are given as nonlinear functions of either the head h or moisture content θ , and these functions govern and predict the movement and storage of water in the soil. The relationship $h(\theta)$ is reportedly hysteretic [20, 38]. Likewise, $K(h)$ is hysteretic since it is dependent on h . It is this behaviour that reportedly causes the observed mass balance errors [20, 80].

Flow rate following the sign convention chosen is given as,

$$q = K \left[\frac{\partial h}{\partial z} + 1 \right]. \quad (3.3)$$

This is the Darcy equation for describing fluid flow in porous media for any orientation and it is based on a potential or pressure differential. Substituting the expression for q in (3.3) into (3.1) gives the originally determined Richards equation [12] in one-dimension that describes fluid flow in porous media,

$$\frac{\partial \theta}{\partial t} = \frac{\partial}{\partial z} \left[K \left(\frac{\partial h}{\partial z} + 1 \right) \right]. \quad (3.4)$$

The capillary head is strictly speaking negative (i.e. it is a suction), but here a positive value via $h_+ = -h$ can be defined. If the system becomes drier, i.e. h becomes more negative (or h_+ a much bigger positive value) as one moves downwards (i.e. as z decreases), then $\partial h/\partial z$ makes a positive contribution to the downward flux. Hence, an area of low moisture content sucks in more moisture primarily through capillary suction effects.

Richards equation (3.4) as determined above has been given in a “mixed-form” involving two dependent variables, θ and h . It is more convenient to give the equation in terms of a single variable, either as a moisture-based (θ) form or a head-based (h) form. In particular, the moisture based form is obtained via the chain rule. Richards equation may thus be given as,

$$\frac{\partial \theta}{\partial t} - \nabla \cdot K(h) \nabla h - \frac{\partial K(h)}{\partial z} = 0, \quad (3.5a)$$

$$\frac{\partial \theta}{\partial t} - \nabla \cdot D(\theta) \nabla \theta - \frac{\partial K(\theta)}{\partial z} = 0, \quad (3.5b)$$

$$\hat{C}(h) \frac{\partial h}{\partial t} - \nabla \cdot K(h) \nabla h - \frac{\partial K(h)}{\partial z} = 0, \quad (3.5c)$$

where (3.5a), (3.5b) and (3.5c) represent the mixed, moisture-based and head-based forms of Richards equation respectively; t is time (s), z is vertical displacement measured positive upwards (m), $D(\theta)$ is soil water diffusivity (m^2/s), $\hat{C}(h)$ is the derivative $|d\theta/dh|$ (m^{-1}) and $K(\theta)$ is hydraulic conductivity (m/s).

In order to obtain relevant practical solutions, these two other forms of the equation have been derived in a form which can be more readily solved than the mixed form. Regardless of how the equation is written, the first term ($\partial\theta/\partial t$ or $\hat{C}(h)\frac{\partial h}{\partial t}$) in Richards equation can be described as the accumulation term. The second term is representative of capillary diffusivity and the final term given is the gravity term.

As alluded to above, here $\hat{C}(h)$ is a constitutive expression $\hat{C}(h) = d\theta/dh_+$ (remembering $h_+ = -h$) and $D \equiv K/\hat{C}(h) = K|dh_+/d\theta|$. As θ decreases, h_+ becomes increasingly positive, i.e. h becomes more negative. Hence, $dh_+/d\theta$ is negative but an absolute value is taken to return a positive quantity. Equation (3.5a) and (3.5c) can be used to solve both saturated and unsaturated flow problems, but are not equivalent. Equation (3.5b) may not apply at full saturation, since in that case, within the gradient of the gravity-driven flux (hydraulic conductivity) term, the moisture gradient at full saturation is non-existent (i.e. $d\theta/dz = 0$)

[55]. The gradient of the suction head (potential/pressure differential) is however on the other hand not limited in this fashion at full saturation or even ponding.

Equation (3.5b) is described as a *nonlinear Fokker-Planck equation* [55]. Linear forms analogous to the Fokker-Planck equation arise in physical phenomena such as heat conduction from sources moving relative to the medium and diffusion under an external force field. This equation is of the diffusion or heat-conduction form, but with complications that add very greatly to the difficulty of its solutions. The right hand side of the equation contains a diffusivity term the formulation of which is also dependent upon or influenced by gravity. Additionally, as noted in Chapter 2, both D and $dK/d\theta$ (following on from the chain rule) are dependent on θ . Indeed this dependence is very strong given that D and $dK/d\theta$ are both infinite on the approach to full saturation [38].

Nonlinear forms of Fokker-Planck equations for diffusion (without convection)

$$\partial\theta/\partial t = \nabla \cdot (D\nabla\theta), \quad (3.6)$$

are obtained for horizontal flow and systems, or in instances where gravity may be neglected (i.e. early-time imbibition, as presented in Chapter 5). This nonlinear diffusion equation arises in numerous important areas of science and physical processes e.g. heat transfer [43], mass transfer [106, 107], and soil science [22, 45], among others.

To summarise, this section has considered the derivation and forms of Richards equation. In the next section, the nondimensionalisation and rescaling of Richards equation is presented. The non-dimensional form is considered for its wide applicability irrespective of the units of measurement for the physical quantities used.

3.2.2 Nondimensionalisation of Richards Equation

The moisture-based form of Richards equation eliminates the head h which has units of length from the original mixed-form derivation. There is a characteristic length scale in the SWRC function (for h vs θ) which is typically denoted $1/\alpha$ (α having units of reciprocal length). Meanwhile, considering the moisture-based form of the RE, hydraulic conductivity is $K = K_s K_r(\theta)$. The function $K_r(\theta)$ (relative hydraulic conductivity hereafter RHC) is a dimensionless variable while K_s has the same units as K , namely $L T^{-1}$ in dimensional form

and it represents the hydraulic conductivity at saturation. The length scale is expressed as $z = \xi/\alpha$ (ξ is measured positive upwards), $t = \tau/(\alpha K_s)$ for the time scale, and $D(\theta) = K_s D_r^*(\theta)/\alpha$ for diffusivity. Here $D_r^*(\theta)$ is relative diffusivity (hereafter denoted RD) and it is $D_r^* = K_r |dH_+/d\theta|$. Inserting these in equation (3.5b) gives

$$\frac{\partial \theta}{\partial \tau} - \frac{\partial}{\partial \xi} \cdot D_r^*(\theta) \frac{\partial \theta}{\partial \xi} - \frac{\partial K_r}{\partial \xi} = 0. \quad (3.7)$$

The equation above has been expressed in a dimensionless form which is equivalent to the original Richards equation. To describe the moisture content of a porous medium, a relative or rescaled moisture content is given as

$$\Theta = (\theta - \theta_r)/(\theta_s - \theta_r), \quad (3.8)$$

where θ_s and θ_r indicate saturated and residual moisture content values respectively. Relative diffusivity D_r^* can be rescaled as $D_r = K_r |dH_+/d\Theta|$ where $D_r = (\theta_s - \theta_r) D_r^*$. From equations (3.7) and (3.8), choosing $\hat{\tau} = \tau/(\theta_s - \theta_r)$ and $\hat{\xi} = \xi$, and inserting them in equation (3.7), it is possible to obtain

$$\frac{\partial \Theta}{\partial \hat{\tau}} - \frac{\partial}{\partial \hat{\xi}} \cdot D_r(\Theta) \frac{\partial \Theta}{\partial \hat{\xi}} - \frac{\partial K_r(\Theta)}{\partial \hat{\xi}} = 0, \quad (3.9)$$

which is the dimensionless Richards equation employed in this thesis. Moreover, $\hat{\tau}$ and $\hat{\xi}$ are rescaled time and distance, respectively. The similarity between equations (3.9), and (2.8) & (2.11) is clear, modulo a sign change in the final term due to measuring $\hat{\xi}$ in different directions.

3.3 Initial and Boundary Conditions

Generally, given a set of initial and boundary conditions, there is no known general solution to Richards equation (3.9). Mathematically, there may even be a question about the existence of a solution [21]. The conditions necessary for having a well-posed solution for equation (3.9) are discussed in the following sections.

In choosing initial and boundary conditions, the nature of a problem is specified. For instance, Witelski [22] specifies a boundary condition that determines a travelling wave problem inherently different from Zlotnik et al. [44], and hence finds a different solution.

Also, in the choice of the boundary conditions, Caputo and Stepanyants [45] solve for a pulsed-drainage system for early-time problem different from the constant infiltration problem that is set up in Boakye-Ansah and Grassia [66] which is presented in Chapter 5.

Additionally, the choice of boundary conditions can contribute to whether or not a problem may have analytical solutions or whether numerical ones must be sought instead, e.g. [22, 45, 47, 55].

3.3.1 Initial Conditions

In this thesis, the porous medium under study is limited to a homogeneous system initially. Hence, for Richards equation, only the spatially uniform, initial value of the moisture content needs to be specified.

3.3.2 Boundary Conditions

Boundary conditions describe the behaviour of the solution to the governing equations at the physical boundaries of the domain. Three types of the boundary conditions are generally provided in literature for solutions to flow in soils, e.g. [108]:

1. Dirichlet boundary conditions which give the specific values of the solution at a given boundary;
2. Neumann boundary conditions which also specify the value of the spatial derivative of the solution. In the case of flow in porous media, this type of condition is usually written in terms of the fluid flux in the direction normal to the boundary; *and*
3. Robin boundary conditions specify a relationship between the value of solution and its derivative, and can be viewed as a generalization of both Dirichlet and Neumann boundary conditions

In this thesis, either Dirichlet or Neumann boundary conditions are used. However, Cauchy boundary conditions [109] are used as shown in Chapter 5, where the flux (involving a derivative) is given as one of the boundary conditions. A shooting method is then applied until a Dirichlet condition is met at the opposite boundary. In that solution, the initial condition for the early-time problem is used as the Dirichlet condition.

3.4 Early-Time Solution

Time-dependent partial differential equations (PDEs) can be used to describe such phenomena as the propagation of heat or sound, fluid flow, and such laws as the conservation of mass, energy and momentum [43, 109]. Their solutions give an insight into the physical processes they model, with some initial information provided on a given domain. Although there are methods for solving the underlying model equations, sometimes the solution (either general or particular) is difficult, if not impossible, to find. Certain limiting cases of the PDEs are often studied as they are more tractable than the originals PDEs. This is the approach followed here.

When moisture begins to accumulate in a porous medium, or for horizontal systems, the infiltration in the early period is dominated by capillary suction and moisture gradients [17, 55]. This is also the case in fine-textured soils (at least over realistic distance and time scale). This implies that for the early-time drainage in porous media, infiltration is a gravity-free suction into the porous medium, i.e. it is independent of hydraulic conductivity [32, 46]. In this state, the equation describing flow of water in soils (Richards equation) reduces to a closely related nonlinear diffusion equation,

$$\partial\theta/\partial t = \nabla \cdot (D\nabla\theta). \quad (3.10)$$

This equation has a complication in its solution. Although it is known that gravity does not influence moisture movement in this limit, the functional form of D is dependent on K which is the gravity term, and also dependent on the capillary suction head h , with both K and h varying with moisture content. In some special cases, D is a constant. This thesis considers these two distinct cases, namely both a constant diffusivity and a variable functional form of diffusivity. This leads in particular to a linear equation for node-dominated foam drainage (with constant diffusivity), and nonlinear equations for channel-dominated foam drainage and drainage in unsaturated soils (both with variable functional form of diffusivity). Details of this are presented in Chapter 5.

In the formulation of solutions in this flow regime, it is important to note that moisture gradients are more important than gravity. As earlier mentioned, these gradients are controlled by capillary effects leading to diffusivity. Generally, a power law diffusivity

relationship (e.g. Brooks and Corey [56] which adequately describes drainage in the relatively dry soils encountered during the early stages of infiltration) is used to solve this problem.

In solving such a problem, boundary and initial conditions are required. In addition, a similarity substitution (e.g. Boltzmann substitution [43, 109]) is employed to reduce equation (3.10) from a partial differential equation to a form that can be composed as an ordinary differential equation.

Hence, similarity transformation (used to convert the equations from a PDE to an ODE) is applied to the nonlinear diffusion expression obtained. It is important to identify the transformation function or similarity variable based on the nature of the diffusivity function that is used to solve this obtained diffusion equation. In considering the transformation function, the boundary conditions must be identified as they effectively define the nature of the function to be used.

Various techniques are employed in solving for these diffusion problems depending on whether the equations are linear or nonlinear. As the expression obtained therefrom is second order in nature, if it cannot be solved analytically, the *shooting method* [67] can be used to solve it. Solutions to Richards equation and the foam drainage equations detailing these procedures are presented later in Chapter 5.

3.4.1 Formulation of Early-time Solutions

The following nonlinear diffusion equation arises for early-time infiltration in soils and foams,

$$\Theta_t = (D_r \Theta_x)_x, \quad (3.11)$$

subject to the conditions

$$\Theta(x, t) \rightarrow 0, \text{ as } x, t \rightarrow \infty, \quad D_r \Theta_x = -1, \text{ when } x, t = 0. \quad (3.12)$$

where Θ is rescaled moisture content, t is time derivate and x is spatial derivative which is measured positive *downwards*. $D_r = D_r(\Theta)$ represents the relative hydraulic diffusivity (RD) function which is a function of the rescaled non-dimensional moisture content. Generally,

the diffusivity can either be a function of moisture content or a constant. The flux for this problem is $-D_r\Theta_x$.

As earlier noted, when moisture begins to accumulate in a porous medium, the infiltration in the early period is dominated by capillary suction. This implies that for the early time solution, infiltration is independent of hydraulic conductivity, i.e. gravity-free suction into the porous medium [32, 46]. The diffusion equation given in (3.11) can now be expressed as

$$\Theta_t = (a\Theta^N\Theta_x)_x, \quad (3.13)$$

where most of the parameters are as previously defined. Note here that $a\Theta^N$ represents the relative diffusivity function which is a power law function of Θ , raised to some power N . This power N is either 0 and $1/2$ for node- and channel-dominated foam drainage respectively, and some function in terms of a soil specific parameter m for Richards equation using van Genuchten's functions [38] in a small Θ limit. This m is a parameter that determines the soil type (whether sandstone $m \rightarrow 1$ or loam $m \rightarrow 0$) and it affects the value of a (being $m - m^2$) and N (being $1/2 + 1/m$). Using Brooks and Corey [56] functions in lieu of van Genuchten, $a = (1 - m)/m$ and $N = 1/2 + 1/m$. The solutions obtained using van Genuchten [38] functions can be simply rescaled for Brooks and Corey [56] solutions. This is however not pursued in this thesis. For both node- and channel-dominated foam drainage, $a = 1$.

Figure 3.1 shows the relative diffusivity profiles for channel-dominated foam drainage and three soil types. The profile for node-dominated foam drainage is not shown since it is unity at all times (constant diffusivity). As shown in the plot, at $\Theta = 1$, relative diffusivity for foam drainage is also unity, but for the van Genuchten functions, the soils go to finite values equal to $a = m - m^2$.

3.4.2 Setting Up Problem

Having identified the functions that will be solved, it is important to consider the domain of the solution. The flow profile is assumed to be in a semi-infinite domain since there is moisture infiltration at one boundary whereas the moisture content Θ approaches zero (dry limit) far from the boundary. In order to obtain solutions of equation (3.13), the following

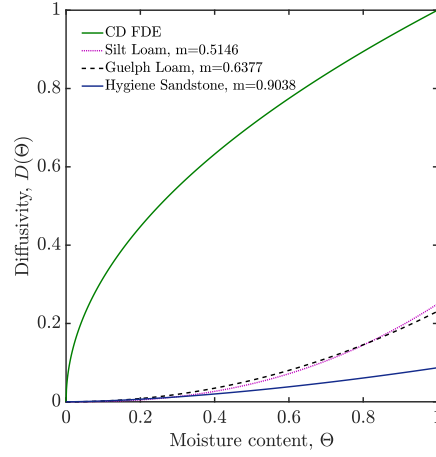


Figure 3.1: Diffusivity profile for channel-dominated foams and three soil samples. The diffusivity profile for node-dominated foam is not shown since it is unity at all times.

relationship is assumed

$$\Theta(x, t) = t^\beta \Phi\left(\frac{x}{t^\gamma}\right); \quad \eta = \frac{x}{t^\gamma}, \quad (3.14)$$

where the moisture content Θ is represented by a similarity variable Φ . Here, η is a non-dimensional independent variable (a function of both x and t , both of which are already made non-dimensional here) that fulfils the similarity requirement. Imposing a unit flux,

$$(a\Theta^N \Theta'_x)|_{\eta=0} = -1. \quad (3.15)$$

Differentiating the similarity expression (3.14) with respect to x , it is possible to deduce

$$\Theta_x = t^{\beta-\gamma} \Phi'; \quad \Theta^N = t^{\beta N} \Phi^N. \quad (3.16)$$

Hence, substituting the above equation in (3.15), the following is obtained

$$a\Phi^N \Phi' t^{\beta(N+1)-\gamma} |_{\eta=0} \approx -1. \quad (3.17)$$

Considering the exponents of t above, it can be deduced that $\beta = \gamma/(N+1)$. Thus, from (3.14), the following is obtained,

$$\Theta(x, t) = t^{\gamma/(N+1)} \Phi\left(\frac{x}{t^\gamma}\right). \quad (3.18)$$

This similarity expression is the correct definition precisely because it is independent of t when the flux definition is applied to it. Additionally, at $\eta = 0$, flux is equal to unity. This is shown as,

$$-D_r \Theta_x \approx -a \Theta^N \Theta_x \quad (3.19a)$$

$$\approx -a t^{\gamma N/(N+1)} \Phi^N t^{\gamma/(N+1)} / t^\gamma, \quad (3.19b)$$

$$\approx -a \Phi^N \Phi' \Big|_{\eta \rightarrow 0}, \quad (3.19c)$$

$$= 1. \quad (3.19d)$$

So far only the boundary condition in similarity form have been considered, but not the differential equation itself. In order to solve the diffusion equation, it is transformed from a partial differential equation into an ordinary differential equation. This is achieved by transforming equation (3.13) using terms of the similarity expression given in equation (3.18). This transformation process is presented in the next section.

3.4.3 General Similarity Solution

In this section, the transformation of the partial differential equation (3.13) to an ordinary differential equation using the similarity definition deduced in (3.18) is presented.

Expressions for the temporal, spatial and diffusivity derivatives from equation (3.13) in terms of the similarity expression obtained in (3.18) are given as

$$\Theta_t = \frac{t^{\gamma/(N+1)}}{t} \left(\frac{\gamma}{N+1} \Phi - \gamma \eta \Phi' \right), \quad (3.20a)$$

$$\Theta_x = \frac{t^{\gamma/(N+1)}}{t^\gamma} \Phi', \quad (3.20b)$$

$$a \Theta^N = a t^{\gamma N/(N+1)} \Phi^N. \quad (3.20c)$$

Thus, the right hand side of equation (3.13) given in terms of the similarity variable is $a \Theta^N \Theta_x = a \Phi^N \Phi'$. This is then differentiated (already given in (3.20b) & (3.20c)) to obtain

$$(a \Theta^N \Theta_x)_x = a t^{-\gamma} (\Phi^N \Phi')'. \quad (3.21)$$

Considering the exponents of t in equations (3.20a) & (3.21),

$$\gamma = (N + 1)/(N + 2). \quad (3.22)$$

Therefore, the similarity definition that is employed in the solution of the nonlinear diffusion problem is,

$$\Theta(x, t) = t^{1/(N+2)}\Phi(\eta), \quad (3.23)$$

noting however that $\eta = x/t^{(N+1)/(N+2)}$.

Consequently, expressing (3.13) in terms of the similarity variables, the following second order ordinary differential equation is obtained,

$$(N + 2)(a\Phi^N\Phi')' = \Phi - (N + 1)\eta\Phi'. \quad (3.24)$$

The boundary conditions in terms of the similarity variable are also given as

$$\Phi \rightarrow 0 \text{ as } \eta \rightarrow \infty; \quad a\Phi^N\Phi' = -1 \text{ as } \eta \rightarrow 0, \quad (3.25)$$

This presents a two-point value boundary problem, and in general can only be solved via the *shooting method* since the expression is a nonlinear differential equation. In the following section, a more elegant technique that can be used to tackle the ordinary differential equation derived in this section are presented.

3.4.4 Flux-based Solution

One of the challenges with equation (3.24) is that as $\Phi \rightarrow 0$ the value of Φ' might diverge, even though the flux $-a\Phi^N\Phi'$ might be small. This issue can be avoided by a change of variables, replacing expressions for Φ' by expressions for flux. The flux, denoted F , represented in terms of similarity variables, in these systems can be expressed as

$$F = -a\Phi^N\Phi', \quad \Phi' = -F/(a\Phi^N), \quad (3.26)$$

where $F = 1$. Note F is positive, since $\Phi' < 0$.

Equation (3.24) can be rewritten in terms of F as

$$F' = -\frac{\Phi}{N+2} - \frac{(N+1)}{(N+2)} \frac{\eta F}{a\Phi^N}. \quad (3.27)$$

Thus, these two equations (3.26)–(3.27) are used to represent infiltration in the porous media system. The boundary conditions that shall be used are given in (3.25). The flux in the porous system is given as the latter expression in that boundary condition, and becomes $F = 1$. Employing the fourth order Runge-Kutta method to solve this system of equations, with a guess for $\Phi(0) \equiv \Phi|_{\eta=0}$ it is possible to obtain the integral estimates for $\Phi(0)$, that satisfy the remaining boundary condition at $\eta \rightarrow \infty$. This can be implemented in applications such as MATLAB, which has inbuilt solvers for such problems.

Having thus presented the scheme for the solution of a nonlinear diffusion problem, details of its implementation to solve for node-dominated and channel-dominated foam drainage and Richards equation are presented in Chapter 5. A discussion and analysis of the solutions obtained are also presented.

3.5 Travelling Wave Solution

This section focuses on the formulation of a travelling wave solution for Richards equation and for the two variants of the foam drainage equation. Travelling waves arise at late times (not at the early times considered hitherto). The formulation is achieved by considering a general expression for the travelling wave obtained from Richards equation in Section 3.5.1, and subsequently identifying the integration constants in the travelling wave equation itself, as well as the velocity of the travelling wave in Sections 3.5.2 and 3.5.3. Finally, an expression is determined that can be used to describe the profile or shape of the travelling wave.

3.5.1 General Form of Travelling Wave

A popular technique that has been used with much success to solve Richards equation is the travelling wave solution, e.g. [17, 22, 44–46]. This technique has also been applied in the solution of foam drainage equation [4, 5, 33].

From the general form of a travelling wave, supposing distance (depth) $\hat{\xi}$ is positive

upwards and velocity v is positive downwards, a solution of the form below is sought:

$$\Theta = \Theta(\hat{\xi} + v\hat{\tau}). \quad (3.28)$$

As length and time only appear in the combination of $\hat{\xi} + v\hat{\tau}$, it is possible to express the solution of Richards equation as a function of position rather than time. The derivatives are related as

$$\frac{\partial \Theta}{\partial \hat{\tau}} = v \frac{\partial \Theta}{\partial \hat{\xi}}. \quad (3.29)$$

Inserting equation (3.29) in (3.9) yields

$$v \frac{\partial \Theta}{\partial \hat{\xi}} - \frac{\partial}{\partial \hat{\xi}} \cdot D_r(\Theta) \frac{\partial \Theta}{\partial \hat{\xi}} - \frac{\partial K_r(\Theta)}{\partial \hat{\xi}} = 0, \quad (3.30)$$

which integrates with respect to $\hat{\xi}$ to obtain

$$v\Theta - D_r(\Theta) \frac{\partial \Theta}{\partial \hat{\xi}} - K_r(\Theta) = \text{constant}. \quad (3.31)$$

The integration constant on the right hand side of equation (3.31) will be determined in Section 3.5.2 below.

3.5.2 Identifying Wave Propagation Velocity and Integration Constant

In order to solve the travelling wave problem, the wave velocity must be identified under the given assumptions and boundary conditions. It is important to identify this in the first instance since *it gives insight into the displacement of the travelling wave*, and also affects the shape of the wave profile.

An objective is to identify the constant on the right hand side of equation (3.31) assuming that a long way upstream $\Theta \rightarrow \Theta_1$ or downstream $\Theta \rightarrow \Theta_2$. The value of Θ_1 and Θ_2 are as yet unspecified boundary conditions but it is anticipated that $\Theta_1 > \Theta_2$ (i.e. there is high saturation at the top and low saturation at the bottom). In both these limits, the change in moisture content with position is zero. Thus,

$$v\Theta_1 - K_r(\Theta_1) = v\Theta_2 - K_r(\Theta_2), \quad (3.32)$$

where Θ_1 , $K_r(\Theta_1)$ and Θ_2 , $K_r(\Theta_2)$ represent the upstream and downstream rescaled moisture content and the relative hydraulic conductivity respectively. An expression for the travelling wave velocity v (first presented by [17]), which obeys the Rankine-Hugoniot condition [110], is derived as

$$v = \frac{K_r(\Theta_1) - K_r(\Theta_2)}{(\Theta_1 - \Theta_2)}. \quad (3.33)$$

Inserting equation (3.33) into (3.31) and evaluating far upstream, or far downstream, expressions for the integration constant are deduced as

$$\frac{K_r(\Theta_1) - K_r(\Theta_2)}{\Theta_1 - \Theta_2} \Theta_1 - K_r(\Theta_1) = \frac{K_r(\Theta_1) - K_r(\Theta_2)}{\Theta_1 - \Theta_2} \Theta_2 - K_r(\Theta_2) = \text{constant}. \quad (3.34)$$

After some algebra, these reduce to

$$\frac{K_r(\Theta_1)\Theta_2 - K_r(\Theta_2)\Theta_1}{\Theta_1 - \Theta_2} = \text{constant}. \quad (3.35)$$

thereby, determining the right hand side of (3.31). Note that in the limit of a dry system at the bottom $\Theta_2 \rightarrow 0$, equation (3.35) vanishes.

3.5.3 Evaluating the Travelling Wave Propagation Velocity

According to literature [5, 32], the velocity at which moisture propagates into (initially dry) foams is directly proportional to the square root of the flux, assuming a channel-dominated case. This can also be deduced if RHC is equated to flux. Unlike foams however, soils do not obey the square root relation, following instead equation (3.33) (for whatever $K_r(\Theta)$ pertains to the soil) as their velocity-flux relation.

Equation (3.33) is plotted for various moisture contents in order to study the travelling wave propagation velocity for different soil types, and the two foam drainage equations. Using the van Genuchten-Mualem relative hydraulic conductivity relationships, the profiles are shown in Figure 3.2 and Chapter 6 at various initial moisture content values where $\Theta_2 < \Theta_1 \leq 1$ ($\Theta_2 = 0, 0.25, 0.5$). In each case, data for Richards equation are plotted against Θ_1 and compared with foam drainage velocities. It can be noted that in the special case where $\Theta_2 = 0$, equation (3.33) reduces to $K_r(\Theta_1)/\Theta_1$ (as shown in Figure 3.2(a)).

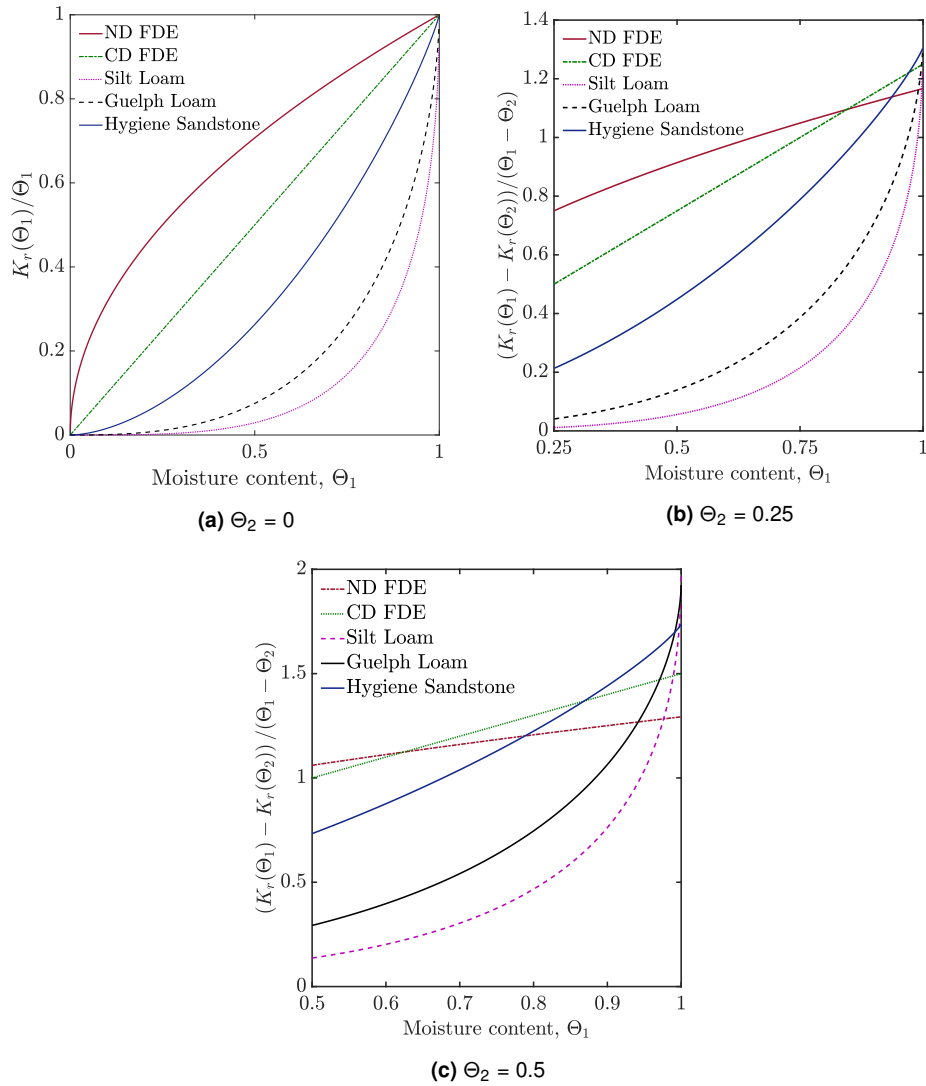


Figure 3.2: Travelling wave propagation velocity for FDEs and three soil samples for various values of Θ . In (b) moisture content $\Theta = 0.25$ and (c) moisture content $\Theta = 0.5$, an already wet system is considered. Observe here that the system has an overall higher velocity as one progresses from a dry to relatively wet system.

3.5.4 Profile of $\hat{\xi}$ versus Θ

Travelling wave solutions satisfying these derived equations can only exist if $\Theta_1 > \Theta_2$.

Inserting equations (3.33) & (3.35) in (3.31), and making $d\hat{\xi}/d\Theta$ the subject gives

$$\frac{d\hat{\xi}}{d\Theta} = \frac{(\Theta_1 - \Theta_2)D_r(\Theta)}{(\Theta - \Theta_2)K_r(\Theta_1) - (\Theta - \Theta_1)K_r(\Theta_2) - (\Theta_1 - \Theta_2)K_r(\Theta)}. \quad (3.36)$$

This is the general expression for a travelling wave profile from one initial moisture content to another. It may be applied as a single profile, or multiple profiles within the same

system or subsystems. The multiple profile case would correspond say to adding liquid to the top of a dry foam or dry soil for a period of time, and then at some point in time increasing the liquid flux. The application of equation (3.36) will be studied further in the next sections.

3.6 Special Case: Single Travelling Wave

Considering a special case where $\Theta_1 = 1$ and $\Theta_2 = 0$ at the upper and lower limits of a travelling wave profile, it is possible to obtain a simplified solution to equation (3.36) above. In this case, $K_r(\Theta_1) = 1$, $K_r(\Theta_2) = 0$ and hence, $\nu = 1$, and the constant on the right hand side of equation (3.31) vanishes. With this information, it is possible to rewrite equation (3.36) as,

$$\frac{d\hat{\xi}}{d\Theta} = \frac{D_r(\Theta)}{\Theta - K_r(\Theta)}. \quad (3.37)$$

Note the term $\Theta - K_r(\Theta)$ in the denominator: its relevance is stated in Section 4.3.2.1 and will be discussed further in Chapter 6.

The key equation (3.37) deduced in this section is analysed to elucidate travelling wave behaviour in Chapter 6. The equations have been derived in the context of Richards equation but the foam drainage equations can be cast in the same form, thus making these equations equally applicable to the latter set of equations.

3.7 Interaction of Travelling Waves

Having established confidence in the general reliability of the travelling wave solution approach of a single travelling wave in an infinite medium, it is worthwhile to develop further solutions under other sets of assumptions. This section considers the behaviour of two travelling waves when they start to interact while moving from one elevated position to another. These two travelling waves will thus be analysed as they move from (a) $\Theta_{1l} = \Theta_m$ to $\Theta_{2l} = 0$, which are referred to as the lower travelling wave, and (b) $\Theta_{1u} = 1$ to $\Theta_{2u} = \Theta_m$, which is the upper travelling wave. Here Θ_m is an intermediate or mid-range value of Θ .

3.7.1 Profile of Two Interacting Travelling Waves

As mentioned earlier, it is worthwhile to consider the interaction of two different travelling waves. In an already wet system or one where a flux already exists, the addition of moisture to the system creates another profile which at some point will interact with the already existing profile. An upper and a lower travelling wave aptly describe such two travelling waves from an upper region to a lower one. It is expected that these two travelling waves will start to interact at a common middle point value of Θ_m that connects them.

The expressions for these two travelling waves may then be given as,

1. **Lower travelling wave** $\Theta_{1l} = \Theta_m$ to $\Theta_{2l} = 0$

$$d\hat{\xi} = \frac{\Theta_m D_r(\Theta)}{\Theta K_r(\Theta_m) - \Theta_m K_r(\Theta)} d\Theta. \quad (3.38)$$

2. **Upper travelling wave** $\Theta_{1u} = 1$ to $\Theta_{2u} = \Theta_m$

$$\frac{d\hat{\xi}}{d\Theta} = \frac{(1 - \Theta_m) D_r(\Theta)}{(\Theta - \Theta_m) - (\Theta - 1) K_r(\Theta_m) - (1 - \Theta_m) K_r(\Theta)}. \quad (3.39)$$

Hence, depending on the middle point Θ_m chosen, e.g. 0.25, 0.5 or 0.75, an expression for the upper or lower travelling wave can be obtained.

As long as the two waves are well separated in space, equations (3.38)–(3.39) give a good representation of the shape of the front. However, the speed of the upper wave $(1 - K_r(\Theta_m))/(1 - \Theta_m)$ tends to exceed the speed of the lower wave $K_r(\Theta_m)/\Theta_m$. Hence, over time, the upper wave tends to catch up with and merge with the lower wave. After the waves merge, a single wave covers the Θ domain from $\Theta_{1u} = 1$ to $\Theta_{2l} = 0$. The velocity of this is unity in all cases. Exactly how to set up the problem in this special case is considered in Appendix B.

3.8 Summary

This chapter has considered Richards equation in detail. Its derivation, various forms (mixed form, head-based, moisture-based), non-dimensional rescaling and various types of solutions have been discussed. The flow problems that can be solved include a nonlinear

diffusion problem, and a travelling wave solution for the full nonlinear partial differential equation. Equivalent analyses for the two variants of the foam drainage equation were also presented.

In considering solutions for the early-time formulations of the diffusion equation, a similarity transformation is applied, and the solution to the resulting ordinary differential equation obtained via numerical schemes. In solving the full nonlinear Richards equation at long times, the principle of travelling wave propagation is applied for its simplicity. The methods for deriving velocity of the travelling wave and its vertical profile (depth vs moisture content) have also been discussed. Furthermore, the special cases of travelling waves interacting within the domain of interest is considered, one wave invading a completely dry zone, and the other invading an already wetted system.

In the following chapter, the soil material property functions that are required as input in Richards equation are presented in detail. In particular those that are employed in this thesis are discussed, namely van Genuchten [38] and Brooks and Corey [56] soil material property models. Some similarities and differences between these material property models are elucidated.

Soil Material Property Functions Models

Abstract

Soil material property functions are required to solve Richards equation and other related flow problems. These soil material properties are namely capillary suction head which is used (via a predictive conductivity model (PCM)) to solve for the relative hydraulic conductivity function, and these two together are used to derive the relative diffusivity function.

This chapter discusses these soil material properties introduced in Section 2.5 in detail for the two models (van Genuchten [38], Brooks and Corey [56]) which have been used predominantly in this thesis. These were chosen due to their general ease of utilisation to develop the material property function required for solving Richards equation. Additionally, they are generally considered reliable and produce results that are widely encountered in literature. Comparing behaviour in the dry to slightly wet regions ($\Theta \ll 1$), these two models present equivalent results. It is close to fully saturation that these two models present marked differences. The Brooks-Corey model terminates at a finite suction head value (unity), while the van Genuchten suction head model goes to zero at full saturation. This latter behaviour observed in the van Genuchten model is expected for soils since capillary action is thought to be negligible in a fully saturated porous medium. Another highlight is that the van Genuchten model has an inflection point which helps it to go to zero near full saturation via a singularity.

4.1 Introduction

In order to characterise flow in unsaturated soil via Richards equation, certain soil material property functions must be known. These are the soil water retention curve (also describes the capillary suction head), hydraulic conductivity and diffusivity functions. These soil material properties are sometimes referred to as hydraulic properties. These characteristic properties of the soil may be obtained experimentally, or using functions that adequately describe them. As earlier mentioned, it is tedious, expensive and time consuming to obtain these functions experimentally [84]. Hence, material function models for predicting and characterising flow in soils have been proposed in literature. Among these, the two most popular models are the van Genuchten (VG) [38], and Brooks & Corey (BC) [56] models. Some other models include those proposed by Fredlund and Xing [60], Assouline et al. [83]. Additionally, some authors [61, 62, 83, 84] have proposed specific formulations for just one of these hydraulic properties, i.e. the formulations are not tied to the other properties.

In the following sections, the models proposed by van Genuchten [38] and Brooks and Corey [56] are discussed in detail. These are the models that are used in this thesis for the solution of Richards equation. The models are especially used in the results presented in Chapters 5, 6 & 7 (see Appendix A also).

4.2 Brooks and Corey Models

Brooks and Corey [56] proposed a model for predicting soil water retention based on experimental data. They proposed a four-parameter model (although the number of parameters can be reduced by suitable rescaling) which has been applied with much success in the field [85]. Like the van Genuchten (VG) model, the Brooks and Corey model (BC) has also been very widely used in soil sciences and engineering problems to much success [85]. In the succeeding sections, the soil water retention curve, relative hydraulic conductivity and relative diffusivity functions for this model are presented.

4.2.1 Soil Water Retention Curve

The Brooks and Corey [56] soil water retention curve (SWRC) function is given as

$$\theta = \theta_r + (\theta_s - \theta_r)(\alpha|h|)^{-\lambda_s}; \quad \Theta = (\alpha|h|)^{-\lambda_s} = H_+^{-\lambda_s}, \quad (4.1)$$

where θ_r is residual water content (m^3 moisture/ m^3 soil), θ_s is saturated water content (m^3/m^3), $\Theta = (\theta - \theta_r)/(\theta_s - \theta_r)$ is rescaled moisture content, h is matrix potential or suction head or simply head (m), λ_s is an exponent (also given as $n - 1$ or $n - 2$ in models by Mualem [18] or Burdine [79] respectively, with yet another parameter m given as $m = 1 - 1/n$ and $m = 1 - 2/n$ respectively, so that in both cases $\lambda_s = mn$) and α is an empirical scale parameter (with units of reciprocal length m^{-1}), and $H_+ = \alpha|h|$. The sign convention here is that h is negative (it is a suction), so for the most part $|h|$ is employed to have a positive quantity. The profile for this relationship is given in Fig 4.1.

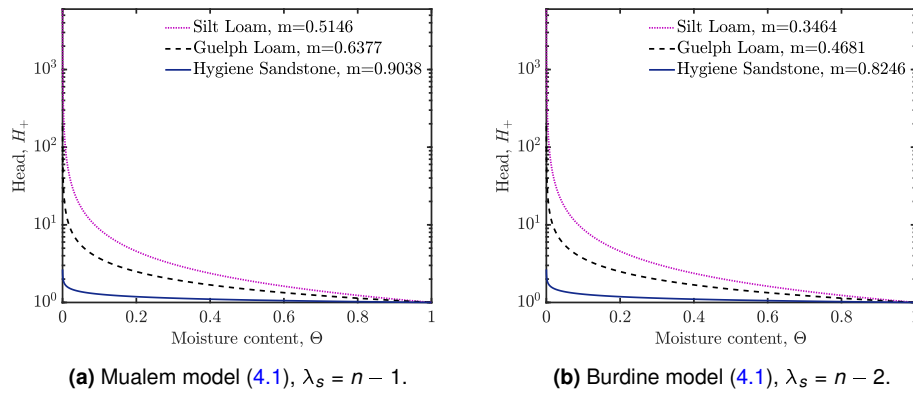


Figure 4.1: Profile of capillary suction head using Brooks and Corey [56] definitions. In the Mualem case (a), $\lambda_s = 1.06$, $n = 2.06$, $m = 0.5146$ for Silt Loam, $\lambda_s = 1.76$, $n = 2.76$, $m = 0.6377$ for Guelph Loam, and $\lambda_s = 9.4$, $n = 10.4$, $m = 0.9038$ for Hygiene Sandstone. In the Burdine case (b), the λ_s values remain the same but $n = 3.06$, $m = 0.3464$ for Silt Loam, $n = 3.76$, $m = 0.4681$ for Guelph Loam, $n = 11.4$, $m = 0.8246$ for Hygiene Sandstone.

Equation (4.1) is frequently used in unsaturated flow studies because of its simple form [89]. The equation is also noted to produce “acceptable results” for comparatively “coarse-textured, often disturbed soils with relatively narrow pore-size distributions” [38], especially when the system is dry or outside the wet range (i.e. $H_+ \gg 1$).

To summarise the Brooks-Corey SWRC corresponds to $\Theta = H_+^{-\lambda_s}$ or equivalently to $H_+ = \Theta^{-1/\lambda_s}$ which can also be written $H_+ = \Theta^{1-1/m}$ (Mualem case) or $H_+ = \Theta^{1/2-1/(2m)}$ (Burdine case).

4.2.2 Relative Hydraulic Conductivity

Relative hydraulic conductivity (RHC) can be obtained using either the Mualem [18] or Burdine [79] PCM (see section 2.5.2.2) respectively as

$$K_r(\Theta) = \Theta^{1/2+2/m}, \quad (4.2a)$$

$$K_r(\Theta) = \Theta^{2+1/m}, \quad (4.2b)$$

where (4.2a) is the function that is obtained using the Mualem [18] PCM, where $m = 1 - 1/n$, and (4.2b) is the function using the Burdine PCM [79], where $m = 1 - 2/n$. It is worth remembering that $\lambda_s = mn$ and hence these formulae can be written in terms of λ_s also [38]. The relations are $m = \lambda_s/(\lambda_s + 1)$ (Mualem) and $m = \lambda_s/(\lambda_s + 2)$ (Burdine), hence $2/m = 2 + 2/\lambda_s$ (Mualem) and $1/m = 1 + 2/\lambda_s$ (Burdine). Substituting these into (4.2a)–(4.2b) is then consistent with (2.27) and (2.26) respectively, whereby the exponents for K_r become $5/2 + 2/\lambda_s$ for Mualem and $3 + 2/\lambda_s$ for Burdine [38].

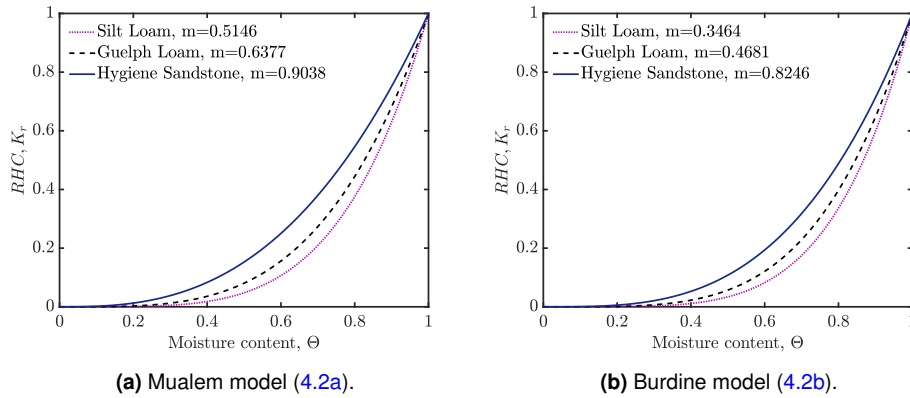


Figure 4.2: Relative hydraulic conductivity using Brooks and Corey [56] definitions.

From their format, these models have been classified as *macroscopic* soil property functions [93], although they can be obtained using the Burdine [79] and Mualem [18] conductivity models. Figure 4.2 shows the profiles of three soil samples using the two proposed forms of RHC. Observe that $K_r(\Theta)$ values are greater in the Mualem (4.2a) than in the Burdine (4.2b) model. Hence, $(\Theta - K_r(\Theta))$ (a term which appears in (3.37)) is greater in (4.2b) than (4.2a).

Note also that relative hydraulic conductivity (RHC) at a given Θ increases as $m \rightarrow 1$. Thus, sandstones (which have m close to unity) have higher RHC than clayey soils ($m \ll 1$).

4.2.3 Relative Diffusivity

Based on the general definition for relative diffusivity (2.31), it is possible to obtain,

$$D_r(\Theta) = \frac{(1-m)}{m} \Theta^{1/2+1/m}, \quad (4.3a)$$

$$D_r(\Theta) = \frac{(1-m)}{2m} \Theta^{3/2+1/(2m)}, \quad (4.3b)$$

where (4.3a) and (4.3b) follow from using equation (4.1) with (4.2a) & (4.2b) respectively.

Remembering that $m = \lambda_s/(\lambda_s + 1)$ (Mualem) and $m = \lambda_s/(\lambda_s + 2)$ (Burdine) and hence $1/m = 1 + 1/\lambda_s$ (Mualem) and $1/(2m) = 1/2 + 1/\lambda_s$ (Burdine), it is clear that the exponents here are $3/2 + 1/\lambda_s$ and $2 + 1/\lambda_s$ respectively. In each case these are smaller than the corresponding exponents in K_r by an amount $1 + 1/\lambda_s$. Meanwhile, $\lambda_s = m/(1-m)$ (Mualem) and $\lambda_s = 2m/(1-m)$ (Burdine). The prefactors in (4.3a)–(4.3b) are therefore $1/\lambda_s$ in each case.

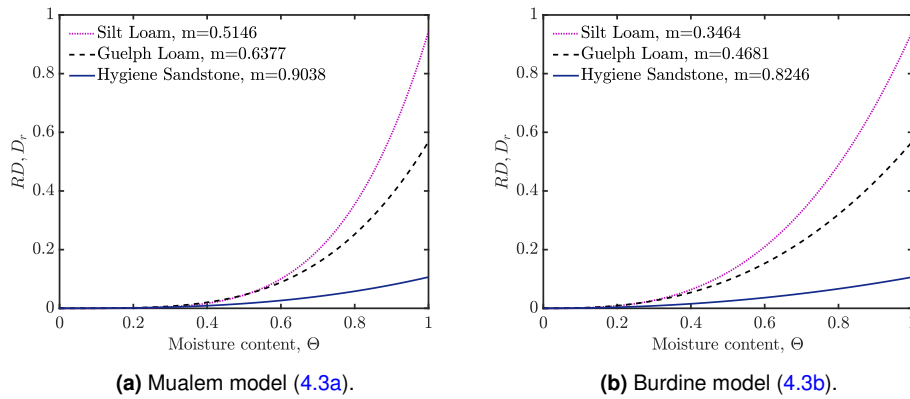


Figure 4.3: Profile of relative diffusivity using Brooks and Corey [56] definitions. As earlier shown, the two variants are equivalent.

Figure 4.3 plots equations (4.3a) and (4.3b) for Mualem and Burdine relative diffusivity definitions respectively. From the scaling of the prefactor in both equations, the profiles in Figure 4.3 do not reach unity as $\Theta \rightarrow 1$. Meanwhile when m is small, D_r goes to larger values for $\Theta \rightarrow 1$ compared with bigger m values. The D_r value for Silt Loam at $\Theta \rightarrow 1$ is closer to unity than for Hygiene Sandstone.

To summarise, the Brooks-Corey model admits power law expression for the SWRC, RHC and RD over the full domain $0 \leq \Theta \leq 1$. As will be seen in what follows however, a more general model, that of van Genuchten [38], does not admit simple power law expressions

over that full domain, but does reduce back to power laws for small Θ values.

4.3 Van Genuchten Models

Van Genuchten proposed a SWRC (to describe capillary suction head) which he then used to derive a relative hydraulic conductivity and diffusivity functions via the Mualem and Burdine PCMs [38]. The SWRC here predicted is equal to the Brooks and Corey [56] in the lower saturation (moisture content) regime but unlike that model, goes to zero capillary suction head at full saturation.

4.3.1 Soil Water Retention Curve

Van Genuchten [38] proposed the following SWRC which relates the moisture content and capillary suction head as

$$\Theta = [1 + H_+^n]^{-m}; \quad H_+ = (\Theta^{-1/m} - 1)^{1/n}, \quad (4.4)$$

where Θ is rescaled water (moisture) content, $H_+ = \alpha h_+$ is dimensionless head ($1/\alpha$ is a length scale parameter, and $h_+ = -h$ noting that by convention head $h < 0$ as it is a suction), n, m are material parameters, and $m = 1 - 1/n$ has reportedly been used to much success in literature [38]. More generally, the material parameters m and n are related via $m = 1 - 1/n$ for the Mualem PCM [38]. Clayey soils are represented by low n values (slightly bigger than unity) while higher n values (much bigger than unity) represent non-clayey soils [59]. Likewise, low m values (much smaller than unity) represent clayey soils while higher m (close to unity) values represent non-clayey soils.

4.3.1.1 Asymptotic Behaviour of Head

As previously stated, SWRC can be recast as capillary suction head in terms of moisture content (as opposed to moisture content in terms of capillary suction head). From Figure 4.4a, observe that changes in head values are very abrupt in the soils for small changes in saturation both near residual and fully saturated moisture content limits (i.e. in small and

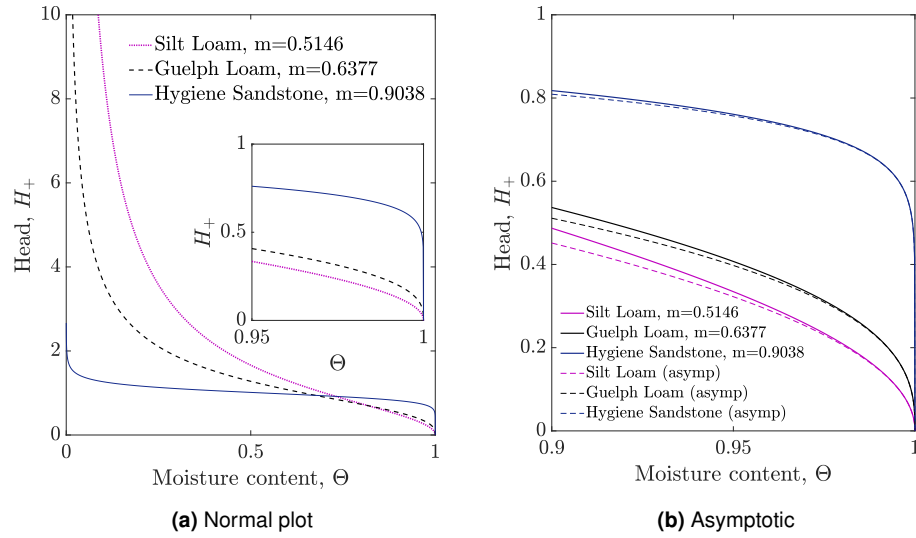


Figure 4.4: (a) The behaviour of dimensionless suction head ($H_+ = \alpha h_+ \equiv -\alpha h$) versus moisture content based on equation (4.4) for three soil types, i.e. three different values of the parameter m . The inset gives a closer view of the behaviour near full saturation. (b) Plot of comparison of behaviour of head equation (4.4) and asymptotic behaviour (4.5b) of head near saturation ($\Theta \approx 1$) [38].

large Θ regions).

$$\Theta|_{\Theta \ll 1} \approx H_+^{-nm}, \quad H_+|_{\Theta \ll 1} \approx \Theta^{-1/nm} = \Theta^{-(1-m)/m}, \quad (4.5a)$$

$$\Theta|_{\Theta \approx 1} \approx (1 - mH_+^{1/1-m}), \quad H_+|_{\Theta \approx 1} \approx \left(\frac{1 - \Theta}{m} \right)^{1-m}. \quad (4.5b)$$

When (dimensionless) head H_+ is significantly bigger than 1 ($H_+ \gg 1$ i.e. in a very dry soil) where $\Theta \ll 1$, equation (4.5a) is obtained, the profile of which can be observed in Figure 4.4a. Observe also that for a system near full saturation ($\Theta \approx 1$), the head H_+ is much less than unity, i.e. $H_+ \ll 1$ as given in equation (4.5b). Figure 4.4b shows this profile (in the wet limit) as a solid line (for the original van Genuchten SWRC), with the asymptotic form (4.5b) shown as a dashed line. Observe here that soils with $m \rightarrow 0$ go to zero less abruptly than those with $m \rightarrow 1$ which go to zero very abruptly indeed (in a singular fashion). The importance of this observation is discussed in Chapter 6.

Note that H_+ for $\Theta \ll 1$ (i.e. equation (4.5a)) is approximately equation (4.2a) as previously given by Brooks and Corey [56] and as shown in Section 4.2.1.

4.3.2 Relative Hydraulic Conductivity

As earlier mentioned, relative hydraulic conductivity can either be determined experimentally (which is rather expensive and time-consuming [24, 89, 101]) or predicted mathematically [18, 38, 79]. There are a number of mathematical models proposed that have been used to derive useful relations for predicting soil behaviour to an appreciable degree of success. The more widely used function derived by van Genuchten [38] which has been used in numerous solutions [20, 25, 45] is employed in this thesis. It is given as

$$K_r(\Theta) = \Theta^{1/2} [1 - (1 - \Theta^{1/m})^m]^2. \quad (4.6)$$

Equation (4.6) is based on the Mualem [18] PCM. Another PCM proposed by Burdine [79] from which van Genuchten [38] derived another equation is less commonly used, and hence it is not discussed here.

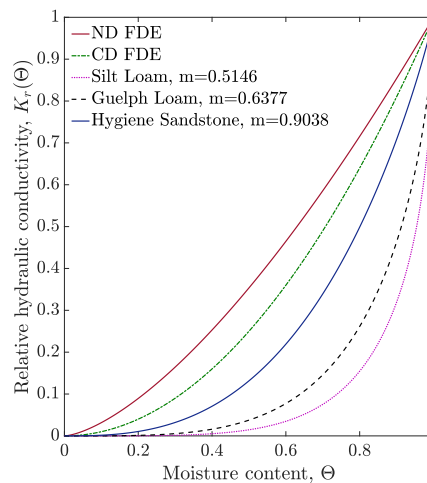


Figure 4.5: Plot of relative hydraulic conductivity against moisture content for the two variants of the FDEs (see Sections 2.3.1 & 2.3.2) and three soil samples. The profiles for the soils are obtained from equation (2.29).

The profiles plotted in Figure 4.5 are based on the van Genuchten solution (2.29) of the Mualem PCM shown in equation (4.6). The values of the three soil samples are based on their individual m values. The two variant FDEs are also shown.

4.3.2.1 Asymptotic Behaviour of RHC

It is constructive to examine the behaviour of the relative hydraulic conductivity function in small and large Θ . Observe that for the limits $\Theta \ll 1$ & $\Theta \rightarrow 1$, equation (4.6) reduces to,

$$K_r(\Theta)|_{\Theta \ll 1} \approx m^2 \Theta^{1/2+2/m}, \quad (4.7a)$$

$$K_r(\Theta)|_{\Theta \approx 1} \approx \left(1 - \frac{2}{m^m} (1 - \Theta)^m\right). \quad (4.7b)$$

Comparing equation (4.7a) with (2.6) & (2.10) (for RHC terms) one may estimate that the channel-dominated FDE is analogous to $m = 4/3$, and $m = 2$ for the node-dominated case.

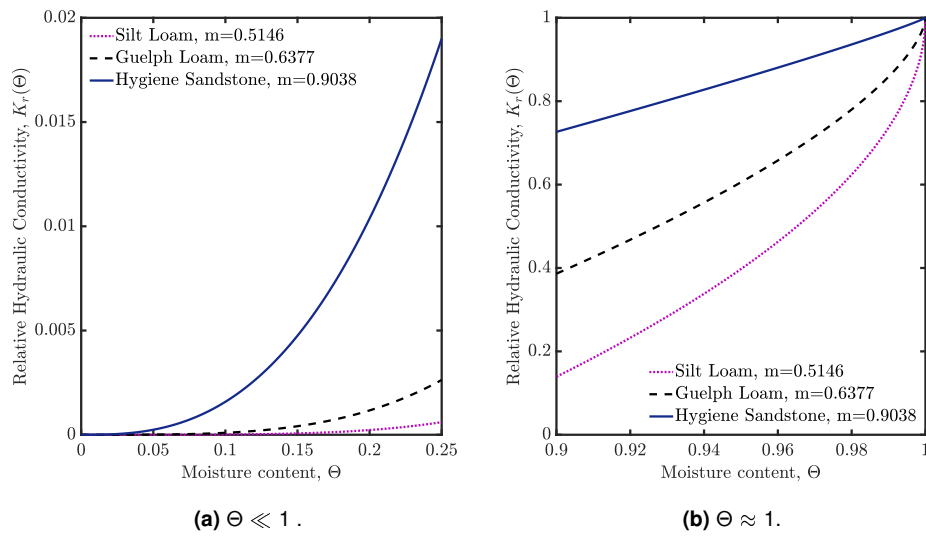


Figure 4.6: Behaviour of the three soil samples based on RHC function in 4.6a $\Theta \ll 1$ region based on equation (4.7a) ; and 4.6b $\Theta \approx 1$ region for equation (4.7b).

Equations (4.7a) & (4.7b) are shown in Figure 4.6a and 4.6b respectively. Observe how profiles for $m \rightarrow 1$ behave in Figure 4.6a. The prefactor given in (4.7a) for such m is significant, and moreover Θ is raised to a slightly smaller power for larger m . Conversely, the prefactor m^2 is an insignificant value as $m \rightarrow 0$ thus significantly reducing the value of RHC in this limit. Additionally, Θ is raised to a bigger power for smaller m .

Using equation (4.5a) & (4.7a), it is also possible to obtain a special limiting $\Theta \ll 1$ case for the relative diffusivity function (cf. section 4.3.3 below) which is equivalent to that given by Brooks and Corey [56]. These two profiles (RHC and RD) are used in the solution of the early-time diffusion problem in Chapter 5. Moreover the RHC solutions presented here are applied to solution of moisture content profiles in Chapter 6 & 7.

4.3.3 Relative Diffusivity

From the expression given in equation (2.31) (also $D_r(\Theta) = K_r(\Theta) |dH_+/d\Theta|$), van Genuchten [38] also proposed a diffusivity equation based on the relationship for suction head (4.4) and relative hydraulic conductivity (4.6) which are used to derive the expression below,

$$D_r(\Theta) = \frac{(1-m)}{m} \frac{(\Theta^{-1/m-1/2})}{(\Theta^{-1/m} - 1)^m} [1 - (1 - \Theta^{1/m})^m]^2. \quad (4.8)$$

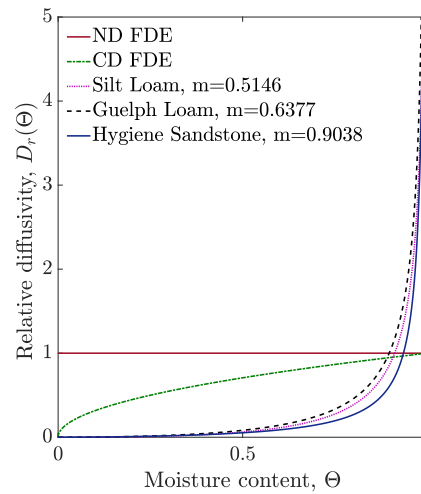


Figure 4.7: Relative diffusivity against moisture content profile for the FDEs (2.8) and (2.11) and some soil samples based on equation (4.8). The relative (capillary) diffusivity term for the FDEs in (2.8) and (2.11) are equivalent to $\sqrt{\Theta}$ and 1 respectively. The function for the soil samples are dependent on m for each soil sample.

Equation (4.8) is plotted in Figure 4.7. Observe here that as $\Theta \rightarrow 1$, $D_r(\Theta) \rightarrow \infty$ (due to the behaviour of $|dH_+/d\Theta|$ in that limit). Relative diffusivity approaches unity when the medium is fully saturated for the FDE variants (i.e. $D_r(\Theta) = 1$ at $\Theta = 1$), observing that $D_r(\Theta) = 1$ at all times for node-dominated case.

4.3.3.1 Asymptotic Behaviour of Relative Diffusivity

The behaviour of the diffusivity function is examined here for small and large Θ values. As already mentioned, $D_r(\Theta) = K_r(\Theta) |dH_+/d\Theta|$. From equation (4.5a) and (4.7a), for the limits

when $\Theta \ll 1$ and $\Theta \rightarrow 1$, it is deduced that,

$$D_r(\Theta)|_{\Theta \ll 1} \approx (m - m^2)\Theta^{1/2+1/m}, \quad (4.9a)$$

$$D_r(\Theta)|_{\Theta \approx 1} \approx \frac{(1 - m)}{m^{(1-m)}}(1 - \Theta)^{-m}. \quad (4.9b)$$

The profiles of equations (4.9a) & (4.9b) are shown in Figure 4.8a & Figure 4.8b respectively. In the $\Theta \rightarrow 1$ limit, relative hydraulic conductivity function goes to 1. This result can be inferred from Figure 4.5. It follows that in this limit, D_r goes to $|dH_+/d\Theta|$.

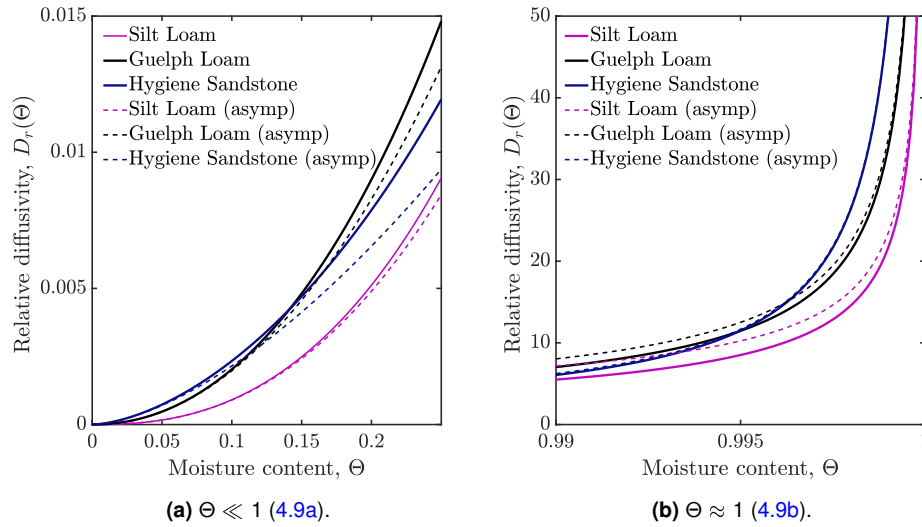


Figure 4.8: Profile of relative diffusivity at varying moisture content limits.

4.3.4 Comparison of Brooks-Corey and van Genuchten functions

In Figure 4.9, plots of the various soil material property functions are shown for Hygiene Sandstone, $m = 0.9038$ from the Mualem [18] model for both Brooks-Corey and the van Genuchten-Mualem models. The two variants of Brooks-Corey SWRC and RHC are plotted alongside same for van Genuchten. Observe that for RHC, the Brooks-Corey-Mualem (BCM) model and van Genuchten's model (also using Mualem definitions) are very closely matched. This is consistent with the mathematics applied in their various expressions. Figure 4.9c shows the profiles for both variants of Brooks-Corey only since the van Genuchten model goes to infinity at full saturation. The BCM values are lower than the BCB values.

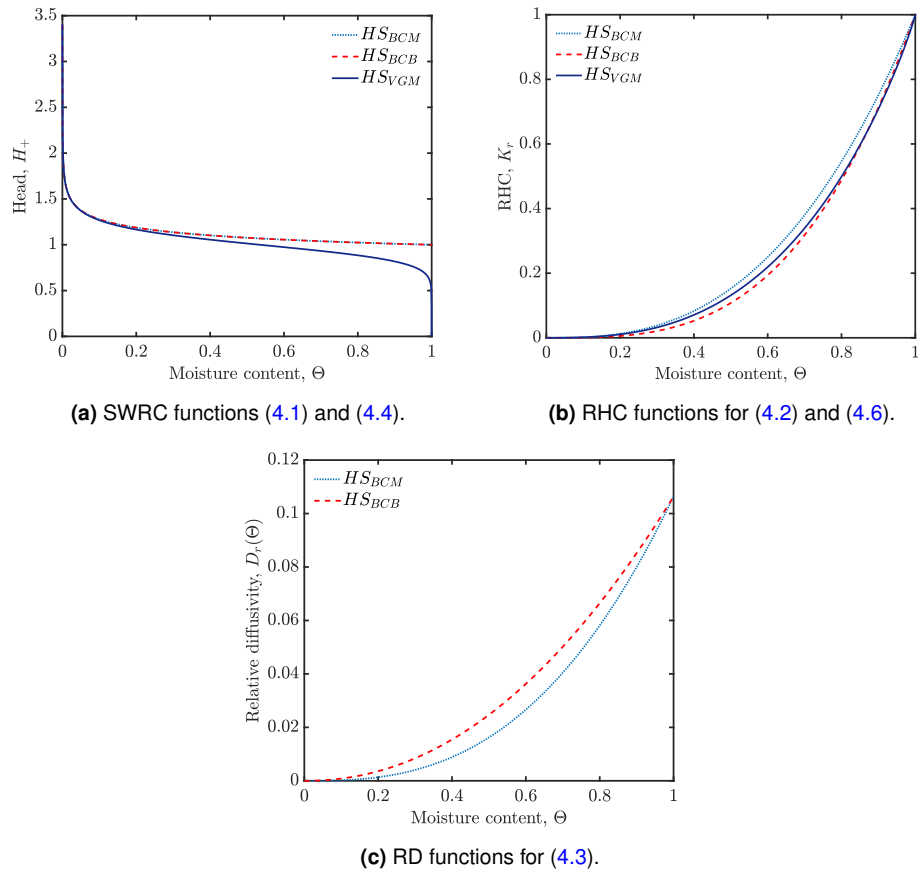


Figure 4.9: Profile of soil material property functions comparing van Genuchten [38], Brooks and Corey [56] definitions for Hygiene Sandstone. For subscripts, VGM and BCM, $m = 0.9038$ and for BCB, $m = 0.8246$.

4.4 Other Models

There are other mathematical models developed for SWRC for which numerous expressions for the RHC and RD may be obtained. In order to obtain closed-form expressions using the Mualem PCM, some of these models may require the use of table of integrals e.g. from [111]. Some of these models include those proposed by Assouline et al. [83] and Assouline [84].

In spite of the proliferation of SWRC models describing flow in soils, it is ideal to identify those that can be solved without expensive computation and which can be utilised to provide reliable analytical solutions based on the existing theories. Numerically expensive models may more accurately describe the solutions but may not necessarily give deeper insight into the problem than closed-form analytical equations.

Some models that are available in literature are discussed in the following sections.

4.4.1 Fredlund-Xing Models

Fredlund and Xing [60] proposed a five-parameter SWRC which gives reliable values [85]. Leong and Rahardjo [112] have presented a three-parameter version of Fredlund and Xing [60] which they compare with functions from van Genuchten [38], Brooks and Corey [56], Fredlund and Xing [60], Gardner [87].

Soil Water Retention Curve

The Fredlund and Xing [60] model for describing soil water retention curve is given as

$$\theta = \theta_r + \frac{\theta_s - \theta_r}{[\ln(e + (h/a)^n)]^m}; \quad \Theta = [\ln(e + (h/a)^n)]^{-m}, \quad (4.10)$$

where all the parameters are as previously defined. Capillary head goes to unity at full saturation which is similar to the function proposed by Brooks and Corey [56]. This is a problem that has previously been addressed by van Genuchten [38].

Using the PCMs, the relative hydraulic conductivity and diffusivity functions can be obtained as defined in literature [60]. These solutions require the use of integral definitions. These are not shown in this thesis document since they are not used in the solution of the problems herein described.

4.4.2 Assouline Model

The soil water retention curve function of Assouline et al. [83] and its constitutive RHC function based on the Mualem [18] PCM are given below.

Soil Water Retention Curve

Another SWRC model quite popular in literature is that proposed by Assouline et al. [83]. It is a complex expression which is given as,

$$\Theta = 1 - \exp \left[-\chi \left(\frac{1}{|H|} - \frac{1}{|H_L|} \right)^\zeta \right], \quad (4.11)$$

where $0 \leq |H| \leq |H_L|$, H_L is the capillary head at the wilting point (the value of H at which $\Theta \rightarrow 0$), and χ & ζ are fitting parameters. From the results presented in Assouline et al. [83], this SWRC fits data better and is suitable for a wider range of water contents than those

SWRC proposed by Brooks and Corey [56] or van Genuchten [38]. However, a complex RHC function is obtained using this SWRC (see Section below), and hence it is not used in this thesis.

Relative Hydraulic Conductivity

Assouline and Tartakovsky [61] later proposed a relative hydraulic conductivity function based on the Mualem [18] predictive model. This is a closed-form analytical expression for RHC. They showed that relative hydraulic conductivity increases monotonically with moisture content. It is here given as,

$$K_r(\Theta) = \sqrt{\Theta} \left[\frac{\chi^{-1/\zeta} \zeta^{-1} \gamma(\zeta^{-1}, \chi a) - |H^{-1}| e^{-\chi a} + |H_L^{-1}|}{\chi^{-1/\zeta} \zeta^{-1} \Gamma(\zeta^{-1}) + |H_L^{-1}|} \right]^2, \quad (4.12)$$

where $\gamma(\beta, u)$ and $\Gamma(u)$ are the incomplete and complete Gamma functions respectively, and $a = (|H^{-1}| - |H_L^{-1}|)^\eta$. Although in closed form, equation (4.12) is rather more complicated than equation (4.6), so it is not pursued further here.

4.5 Summary

This chapter has considered the soil material property (hydraulic) functions that shall be employed in solving Richards equation. In particular, the Brooks-Corey and van Genuchten hydraulic functions were studied in detail, with asymptotic solutions presented and discussed for the latter. Some other models that describe these soil material properties were discussed but they shall not be used further in this work.

In the next chapters (5–7), these soil material property functions are employed to solve Richards equation in comparison with foam drainage equations.

Similarity solution for early-time constant boundary flux imbibition in foams and soil

This chapter is a copy of a manuscript that has been submitted [TIPM-D-21-00060] to the Transport in Porous Media journal for publication. The authors are Yaw A. Boakye-Ansah and Paul Grassia. In this manuscript, the solutions to the diffusion equations obtained for early-time imbibition in foams and soils are discussed. In this study, similarity variables are invoked to enable the solution of diffusion functions for foam and soil drainage. Since the node-dominated foam drainage equation yields analytical solutions, the numerical schemes used to determine solutions for channel-dominated foam drainage and the soil diffusion functions are benchmarked to the numerical solution of the node-dominated foam drainage.

Overview

The general nonlinear diffusion equation arises for early-time infiltration in porous media. In this work, the behaviour of the solution to the diffusion equations for foams and soils are discussed. Node-dominated [14] foam drainage yield linear diffusion equations because the diffusivity function is a constant. The solution of the resulting equation is available in literature since the form obtained is comparable with the heat equation [43]. Channel-dominated [36] foam drainage however yield nonlinear equations likewise Richards equation [12]. The forms

of their diffusivity functions are complex. Hence, only numerical solutions are available for these nonlinear cases.

Nonlinear diffusion arises at early-times in porous media since the imbibition (infiltration is referred to as such in this limit [45]) at these times is dominated by capillary-diffusion. Hence, it is important to study this behaviour in soils and foams since in the case of remediation or irrigation, the dominant process for accumulation and spreading is the capillary diffusion. Nonlinear diffusion can also be used to describe horizontal drainage or infiltration.

This study also develops a benchmark for other systems (channel-dominated foams and imbibition into soils) where the diffusivity functions are variable. The boundary conditions that are considered indicate that there is a constant flux over the duration of the infiltration process. Here a constant infiltration problem is considered, and the interest is in finding how liquid saturation profile evolves into the soils (and foams), and how liquid saturation at the top varies over time.

The early-time similarity solution profiles obtained for both soils and foams have close analogies to their “dry” limit region in their respective travelling wave solutions (travelling wave solutions apply at later times). From the profiles of both the channel-dominated foam drainage and the soils, it can be observed that there is an abrupt change in the water content right at the leading edge of the front (as also observed at the leading edge in Chapter 6). Hence, there is a singularity in the spatial gradient $d\Theta/dx$ as moisture content Θ goes to zero for these nonlinear cases.

In this current work, the diffusion equation that results is solved numerically unlike what happens with an alternative diffusivity model (the Storm-Fujita model, see [45]) which lends an exact analytical solvability to the nonlinear form of Richards equation. Unlike the cases considered here however this has non-zero relative diffusivity when $\Theta = 0$, so Storm-Fujita is not considered here. The focus remains on these other functions where $\Theta = 0$ yields zero relative diffusivity.

The study concluded that in soils, the time evolution of the moisture content at the top boundary denoted $\Theta(0, t)$ is equal to the product of $t^{2m/(5+2m)}$ (where m is a soil specific parameter close to unity for sandstones, but smaller for loams) and a parameter $\Phi(0)$ (that

is an increasing function of m . When t is small, the term $t^{2m/(5+2m)}$ tends to be smaller for larger m (sandstones as opposed to loams) but this is partly offset by the larger $\Phi(0)$.

In obtaining the early-time similarity solutions for foam drainage, the node-dominated drainage equation has a higher power law exponent $t^{1/2}$ (as opposed to $t^{2/5}$ for channel-dominated drainage, the former is smaller in the limit of small t), and also a smaller $\Phi(0)$ value compared with channel-dominated drainage, but the node-dominated solutions tend to extend over a larger spatial distance.

Publication A

Similarity solution for early-time infiltration in foams & soils

Similarity solutions for early-time constant boundary flux imbibition in foams and soils

***Y. A. Boakye-Ansah · P. Grassia**

Received: date / Accepted: date

Abstract The foam drainage equation and Richards equation are transport equations for foams and soils respectively. Each reduces to a nonlinear diffusion equation in the early stage of infiltration during which time, flow is predominantly capillary driven, hence is effectively capillary imbibition. Indeed such equations arise quite generally during imbibition processes in porous media. New early-time solutions based on the van Genuchten relative diffusivity function for soils are found and compared with the same for drainage in foams. The moisture profiles which develop when delivering a known flux into these various porous materials are sought. Solutions are found using the principle of self-similarity. Singular profiles that terminate abruptly are obtained for soils, a contrast with solutions obtained for node-dominated foam drainage which are known from literature (the governing equation being now linear is analogous to the linear equation for heat transfer). As time evolves, the moisture that develops at the top boundary when a known flux is delivered is greater in soils than in foams and is greater still in loamy soils than in sandstones. Similarities and differences between the various solutions for nonlinear and linear diffusion are highlighted.

Keywords Nonlinear diffusion equation · Capillary diffusion · Similarity solution · Drainage · Imbibition

Article Highlights

- Early-time self-similar solutions for nonlinear diffusion in soils via Richards equation are compared with foam drainage

*Y. A. Boakye-Ansah

Present address: Department of Chemical and Process Engineering, University of Strathclyde, James Weir Building, 75 Montrose Street, Glasgow, G1 1XJ, UK, E-mail: yaw.boakye-ansah@strath.ac.uk

Department of Energy and Petroleum Engineering, University of Energy and Natural Resources, P. O. Box 214, Sunyani, Ghana, E-mail: yaw.boakye-ansah@uenr.edu.gh

P. Grassia

Department of Chemical and Process Engineering, University of Strathclyde, James Weir Building, 75 Montrose Street, Glasgow, G1 1XJ, UK, E-mail: paul.grassia@strath.ac.uk

- Moisture that develops at the top boundary for a given imbibition flux is greater in soils than in foams
- Systems with faster growing moisture at the top boundary have a moisture profile terminating at lower depths

1 Introduction

Infiltration in soils is an important problem that arises in multiple applications in agriculture, hydrology, soil sciences, and environmental engineering, among others (Broadbridge et al., 1988; Broadbridge and White, 1988). In work published previously (Boakye-Ansah and Grassia, 2021), we presented solutions for the long-time propagation of moisture into porous media (soils or foams) which yields travelling waves as solutions of a convection-diffusion transport equation. In this present work, we focus instead on (nonlinear) diffusion equations as given for early-time or short-time infiltration (also called imbibition) processes. Early-time imbibition presents a rather different problem from general infiltration problems since the dominant driving force is a diffusive capillary force, instead of a balance between gravity and capillary diffusivity as happens subsequently, up to the point where the system is nearly fully saturated (Philip, 1969; Boakye-Ansah and Grassia, 2021). Similarly for horizontal flow, the dominant force affecting flow is capillary diffusivity (Philip, 1969), and hence solutions obtained for early-time problems can describe this phenomenon as well. Meanwhile much later on, once full saturation is attained, the dominant force affecting flow of moisture in the soil is gravity. Thus, moisture evolution in porous media exhibits several different stages of behaviour during infiltration, but the early-time behaviour invariably involves (capillary) imbibition as we have said.

To summarise, at short times, diffusivity (due to capillary action) must dominate flow in soils since gravity-driven conduction of moisture is weak in dry systems. Indeed, gravity is negligible not only because the system is comparatively dry, but also because the gradients are realised over short distances at short time (strengthening the role of diffusivity). Hence the governing equation for flow of moisture in soils, the so-called Richards equation (Richards, 1931), reduces to a porous medium nonlinear diffusion equation. Moreover as alluded to earlier, in horizontal flow, the gravity term vanishes and reduces Richards equation to the same nonlinear diffusion equation (Philip, 1969; Witeliski, 1997). Thus, in either case we obtain a nonlinear diffusion problem. Self-similar forms of the moisture content Θ in terms of position x and time t are then admitted. Various self-similar solutions have been obtained for this nonlinear problem for soils (Philip, 1969; Witeliski, 1997; Caputo and Stepanyants, 2008) and analogous systems (Cannon, 1984). All these various solutions, recognise that the initial stage of moisture evolution into porous media describes entry from a source for very short times. The solutions therefore necessarily exhibit a large spatial gradient in moisture content over a small interval close to the source (Witeliski, 2003). This structure is what is exploited to describe the infiltration process during early times, even though it gives way eventually to travelling waves at long times.

Soil material properties are required before any of the above mentioned solutions can be obtained. Specifically, the properties required are the soil-water retention

curve (SWRC), along with the relative hydraulic conductivity (RHC) and the relative diffusivity (RD) which derive from it. In literature, the [van Genuchten \(1980\)](#) soil-water retention curve (SWRC) is commonly used, but since in the present work we will focus on the dry limit, it turns out to reduce to the simpler [Brooks and Corey \(1964\)](#) SWRC (a power law). As a result, the SWRC, relative hydraulic conductivity (RHC) and relative diffusivity (RD) all reduce to power laws. Even with these simple material properties, the governing equation for evolution of moisture content remains nonlinear, and solutions of it (even self-similar ones) can usually only be obtained numerically.

Mathematically speaking, the foam drainage equation can be regarded as a special case of Richards equation, just with very particular forms of the SWRC, RHC and RD ([Boakye-Ansah and Grassia, 2021](#)). Unlike other situations that we consider here, for foam drainage in the so-called node-dominated case ([Koehler et al., 1999, 2000](#)), relative diffusivity is unity at all times. This presents a special case for the early-time self-similar solution which can be solved analytically. Indeed, a linear diffusion equation results which is analogous to the linear equation for heat transfer. An alternative foam drainage case, the so-called channel-dominated case ([Verbist and Weaire, 1994; Verbist et al., 1996](#)) still however presents a diffusivity function which varies with moisture content, leading to a nonlinear diffusion equation.

The question that we address in this paper is, what is the evolving moisture content at the boundary of a system that is required to deliver a known imbibition flux into the system? Thus, we solve for a constant rate infiltration process. This changes the structure of the similarity solution relative to previous studies ([Shampine, 1973b; Witelski, 2003; Caputo and Stepanyants, 2008](#)) which imposed a constant moisture content on a boundary. Finding the solutions involves a two-point boundary value problem. We show that in foams, the moisture content on the boundary evolves more slowly with time than in soils. Moreover, as distance from the boundary increases, the moisture content of foam drainage variants go smoothly to zero whereas for the soils, this is abrupt, leading to a singularity at a location where the moisture content reaches zero. Thus we manage to compare and contrast the behaviour of soils and foams, but focussing now on the early-time limit, unlike [Boakye-Ansah and Grassia \(2021\)](#) which treated only long times.

The rest of this work is structured as follows. We consider the formulation of similarity solutions to the diffusion equation in the next section (Section 2). We consider two approaches to the solution, one using a “traditional” shooting method ([Press et al., 2007](#)) and the other, still employing shooting, but using a flux as one of the solution variables. Novel features are introduced to the algorithm in order to deal with possible singularities. Section 3 meanwhile reviews the linear equations that derive from the diffusion equation with unit diffusivity, and Section 4 considers the nonlinear equations resulting from the presence of a variable (power law) diffusivity function. We discuss the solutions obtained in Section 5, and conclude the paper in Section 6.

2 Formulation of Early-time Solutions

Richards equation (Richards, 1931) can be written in the form

$$(\theta_s - \theta_r)\Theta_t = -(K(\Theta))_x + (\theta_s - \theta_r)(D(\Theta)\Theta_x)_x. \quad (1)$$

Here Θ is a rescaled moisture content, defined as $\Theta = (\theta - \theta_r)/(\theta_s - \theta_r)$, with θ being moisture content (i.e. fraction of local pore space filled with liquid), θ_r being a residual moisture content, and θ_s being a saturation moisture content. Moreover, x is distance measured down from the top boundary, and t is time. Meanwhile $K(\Theta)$ is a hydraulic conductivity due to gravity, with $K(\Theta)$ being a continuous function with the property that $K \rightarrow 0$ as $\Theta \rightarrow 0$ and $K \rightarrow K_s$ (a saturation hydraulic conductivity) as $\Theta \rightarrow 1$. In addition, $D(\Theta)$ is a capillary diffusivity. This can be defined in terms of $K(\Theta)$ and a capillary suction head $H(\Theta)$ (also called a soil-water retention curve SWRC), such that $D(\Theta) = K(\Theta)|dH/d\Theta|(\theta_s - \theta_r)^{-1}$.

The capillary suction head necessarily has some characteristic length scale (denoted H_c say) associated with it. If we define relative hydraulic conductivity (RHC) as $K_r = K/K_s$ and relative diffusivity (RD) as $D_r = (\theta_s - \theta_r)D/(K_s H_c)$ and if we make lengths dimensionless on the scale H_c and times dimensionless on the scale $(\theta_s - \theta_r)H_c/K_s$, the above equation reduces to

$$\Theta_t = -(K_r(\Theta))_x + (D_r(\Theta)\Theta_x)_x, \quad (2)$$

where for compactness of notation we now use x and t to denote dimensionless (rather than dimensional) distance and time respectively.

In the early-time infiltration (or imbibition) limit, starting with a dry soil (or a dry foam), we expect values of Θ to be small. Given that $K_r \rightarrow 0$ in the limit as $\Theta \rightarrow 0$ (van Genuchten, 1980), the following nonlinear diffusion equation then arises (it also arises in the case of horizontal flow without gravity)

$$\Theta_t = (D_r\Theta_x)_x. \quad (3)$$

This is subject to the following conditions of the Dirichlet type at the end of the infiltration front, and of Neumann type at top surface boundary imposing a unit dimensionless flux at the top in all cases,

$$\Theta(x, t) \rightarrow 0, \text{ as } x \rightarrow \infty, \quad D_r\Theta_x = -1, \text{ at } x = 0. \quad (4)$$

Moreover $\Theta(x, t) \rightarrow 0$, as $t \rightarrow 0$.

As is evident from the form of equation (3), when moisture begins to accumulate in a porous medium, the infiltration in the early period is dominated by capillary suction. Hence for the early-time solution, infiltration is independent of whatever the hydraulic conductivity might be, i.e. gravity-free suction into the porous medium occurs (Broadbridge et al., 1988; Verbist et al., 1996). As even more moisture accumulates over time however, the infiltration flux is partly due to capillary suction and partly due to hydraulic conductivity with the balance shifting from the former to the latter as time proceeds. We can still use the early-time solution to estimate when the hydraulic conductivity might start to matter, a point we will return to later. In the first instance however, we focus on the capillary-dominated regime.

The diffusion equation can now be expressed as

$$\Theta_t = (a\Theta^N \Theta_x)_x, \quad (5)$$

where $a\Theta^N$ represents the relative diffusivity function which in the dry limit is a power law function of Θ , raised to some power $N \geq 0$. Clearly for N strictly greater than zero, approaching the dry limit is challenging since diffusivity vanishes in that limit, and as we will see, the system responds by limiting the available domain for x .

It turns out that this power N has the value 0 and $1/2$ for node-dominated and channel-dominated foam drainage respectively (Verbist et al., 1996; Koehler et al., 2000). Meanwhile for both node-dominated and channel-dominated foam drainage, the prefactor a is unity.

For soils, the values of N and a can be related to a soil specific parameter m (van Genuchten, 1980). The value of m (with $0 < m < 1$) turns out to be a measure of what proportion of the volume tends to reside in very large pores, i.e. those that are much larger than the average for the specified medium. Values of m close to unity (as is typical for sandstones) have very little volume in pores much larger than average. Smaller values of m (typical for loams) means it is less uncommon to find pores much larger than average, notwithstanding the fact that the average pore size in a loam tends to be smaller than in a sandstone. General formulae for $D_r(\Theta)$ over a range of moisture contents have been given by van Genuchten (1980) and taking these in the limit $\Theta \ll 1$ gives $a = m - m^2$ and $N = 1/2 + 1/m$ (see Boakye-Ansah and Grassia (2021) for details).

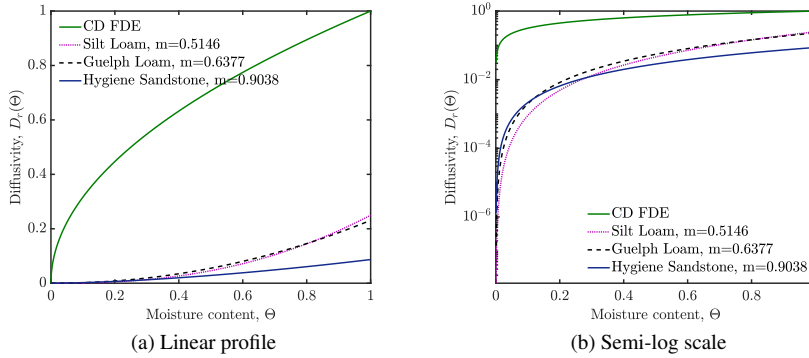


Fig. 1 Diffusivity profile $D_r = a\Theta^N$ for the channel-dominated foam drainage equation ($a = 1$, $N = 1/2$) and three soil samples ($a = m - m^2$, $N = 1/2 + 1/m$, various m). The profile for node-dominated foam drainage is not shown since it is unity at all moisture contents. Profile in (a) shows a linear plot while (b) is the same figure showing D_r on semilog scale to make it easier to see what is happening at small Θ .

Fig. 1 shows the relative diffusivity profiles for channel-dominated foam drainage and three soil types. These are plotted here on the domain $0 \leq \Theta \leq 1$, although in the case of the soils what we have plotted are $\Theta \ll 1$ limiting cases of van Genuchten (1980) formulae which are then extrapolated towards Θ values beyond their limit of applicability. Such extrapolation is not problematic however since ultimately we will

focus on small Θ solutions. The D_r profile for node-dominated foam drainage is not shown since it is unity at all times for all Θ . As shown in the plot, at $\Theta = 1$, relative diffusivity for foam drainage is also unity, but for the extrapolated [van Genuchten \(1980\)](#) functions, the soils go to finite D_r values dependent on the prefactor which is $a = m - m^2$. We again observe that diffusivity at larger saturations are greater in loams than in sandstones, although the opposite is true when saturation is smaller: loams tend to have a higher value of $N = 1/2 + 1/m$ and hence smaller D_r . For early-time infiltration, primarily we are interested in small Θ values.

The origin of the factor $a = m - m^2$ can be traced back ([van Genuchten, 1980](#); [Boakye-Ansah and Grassia, 2021](#)) to the definition of $D_r = K_r |dH_+/d\Theta|$ with $H_+ \equiv H/H_c$ being a dimensionless suction head. The K_r term contributes a factor m^2 to a , and the $|dH_+/d\Theta|$ contributing the remaining factor $m^{-1}(1 - m)$. The latter factor comes from H_+ being relatively insensitive to Θ when m is close to unity, but much more sensitive when $m \ll 1$. The former factor (i.e. the m^2 factor) arises from systems with smaller m having a high proportion of their flux at full saturation coming from large pores. When we look at partial saturations in which only small pores tend to be filled, the flux in relative terms then becomes smaller.

The origin of the exponent $N = 1/2 + 1/m$ meanwhile comes from summing two separate exponents ([van Genuchten, 1980](#); [Boakye-Ansah and Grassia, 2021](#)). The first is an exponent $1/2 + 2/m$ appearing in K_r , representing again that at small m , comparatively little conduction occurs through the small pores. The second is an exponent $-1/m$ appearing in $|dH_+/d\Theta|$ (representing that H_+ increases rapidly as Θ decreases when m is small).

This completes the setting up of the early-time Richards equation, or analogously the early-time foam drainage equation. In the subsections to follow, we explain how to solve it in the particular constant rate infiltration (or imbibition) process that is considered here.

2.1 Similarity Equations

We consider that in the first instance the solution applies on a semi-infinite domain, since there is moisture infiltration or more specifically imbibition at one boundary whereas the moisture content Θ approaches zero (dry limit) arbitrarily far from the boundary. In order to obtain solutions of equation (5) in a semi-infinite domain, we transform the independent variables in the equation into a self-similar form assuming the relationship

$$\Theta(x, t) = t^{1/(N+2)} \Phi \left(\frac{x}{t^{(N+1)/(N+2)}} \right); \quad \eta = \frac{x}{t^{(N+1)/(N+2)}}, \quad (6)$$

where the moisture content Θ is represented by a similarity variable $\Phi(\eta)$. Note the difference here from other literature ([Philip, 1969](#); [Shampine, 1973b](#); [Witelski, 2003](#); [Caputo and Stepanyants, 2008](#)), which impose a fixed moisture content (as opposed to a fixed infiltration rate) on a boundary. Such solutions require a different similarity variable $x/t^{1/2}$ instead of $x/t^{(N+1)/(N+2)}$ as we have here. They also do not have the $t^{1/(N+2)}$ prefactor. However in our case, it is this very prefactor which ensures that $\Theta \ll 1$ in the early-time limit.

The variable η chosen here (a function of both x and t) fulfils the similarity requirement. Imposing a unit flux at the boundary,

$$a\Theta^N \Theta_x \Big|_{x=0} = -1, \quad (7)$$

then leads to

$$a\Phi^N \Phi' \Big|_{\eta=0} = -1. \quad (8)$$

So far we have discussed just the boundary condition expressed in terms of the similarity coordinates. In order to solve the problem however, we need to transform the governing differential equation from a partial differential equation to an ordinary differential equation. This is achieved by expressing equation (5) in terms of the similarity expression deduced in (6), and leads to

$$(a\Phi^N \Phi')' = \frac{\Phi}{(N+2)} - \frac{(N+1)}{(N+2)} \eta \Phi'. \quad (9)$$

Equation (9) is a second order equation, but typically we re-express it in terms of two first order equations, one for the variation of Φ and the other for the variation of Φ' . Even so, we require two boundary conditions. The boundary conditions in terms of the similarity variable are given as

$$\Phi \rightarrow 0 \text{ as } \eta \rightarrow \infty; \quad a\Phi^N \Phi' = -1 \text{ as } \eta \rightarrow 0. \quad (10)$$

This presents a two-point value boundary problem which we solve via the *shooting method*. Since equation (9) is a nonlinear equation, generally speaking a numerical method (such as shooting) is the only way of solving it (Press et al., 2007). Here, it is the initial value $\Phi(0)$ that we seek via shooting, as the initial slope $\Phi'(0)$ is then specified in terms of $\Phi(0)$, as implied by the boundary conditions.

However, challenges still remain with solving the equations in their current form. Provided we have the correct $\Phi(0)$ value, then as η increases, we expect that both Φ and the flux $-a\Phi^N \Phi'$ will tend to zero. Depending on the parameter N however, it need not be the case that Φ' approaches zero even though Φ does. As we will see, it might be the case that $|\Phi'|$ actually becomes infinite as $\Phi \rightarrow 0$, but in such a way that the flux $-a\Phi^N \Phi'$ still tends to zero. This then corresponds to moisture content falling to zero at a *finite* η with an exceedingly abrupt approach of moisture content towards zero. This is a behaviour that is also seen in long-time travelling wave solutions of Richards equation (Boakye-Ansah and Grassia, 2021). Although those long-time travelling wave solutions are by no means the same as the diffusive, early-time similarity solutions considered here, analogies still apply. Sufficiently close to the front of a travelling wave, any flux that is present can be shown to be dominated by a capillary diffusivity (even though, further back the flux in the travelling wave is gravity dominated).

Returning now to consider the early-time case which is to be tackled via a shooting method, if we choose a too large value of $\Phi(0)$, the value of Φ typically fails to fall to zero at all. Instead Φ reaches a minimum and starts to increase again, at large η becoming proportional to $\eta^{1/(N+1)}$. It is easy to check that this functional form $\Phi \sim \eta^{1/(N+1)}$ is a solution of equation (9), albeit not the solution we seek. On the other

hand, if we choose a too small value of $\Phi(0)$, then Φ typically falls to zero abruptly, but now with $|\Phi'|$ becoming infinite very rapidly, such that $-a\Phi^N\Phi'$ remains finite: again this is not the solution we seek. As we will see however for the correctly chosen $\Phi(0)$, whereas Φ still falls to zero abruptly and whereas $|\Phi'|$ still can become infinite, the divergence of Φ' is sufficiently slow that $-a\Phi^N\Phi'$ still manages to approach zero.

We are faced then with the challenge of needing to distinguish between two solutions for which $|\Phi'|$ diverges, i.e. a rapid divergence (an incorrectly chosen $\Phi(0)$) and a slower divergence ($\Phi(0)$ chosen correctly). Dealing with these divergent quantities in a numerical scheme is not straightforward. A simpler approach however is to replace the unknown Φ' by a flux variable which turns out to better behaved in the limit as $\Phi \rightarrow 0$. This approach is explained next.

2.2 Flux-based Solution

The flux, F (represented in terms of similarity variables), can be expressed as

$$F = -a\Phi^N\Phi'. \quad (11)$$

Here flux is positive in general since $\Phi' < 0$ in solutions of interest.

Equation (9) can therefore be rewritten in terms of F as

$$F' = -\frac{\Phi}{N+2} - \frac{(N+1)}{(N+2)} \frac{\eta F}{a\Phi^N}. \quad (12)$$

These two equations (11) (rearranged into the form $\Phi' = -F/(a\Phi^N)$) & (12) now provide two first order differential equations in two unknowns Φ and F .

The boundary conditions for this problem are given in equation (10), although the second boundary condition can now be expressed more elegantly as $F(0) = 1$. We now seek, via the shooting method, a $\Phi(0)$ value such that Φ and F vanish simultaneously, either at $\eta \rightarrow \infty$ or else for some finite but as yet unspecified maximum η value, denoted η_{\max} .

In the case where Φ and F vanish simultaneously at some finite $\eta = \eta_{\max}$, they will both remain identically zero for all $\eta > \eta_{\max}$ (Shampine, 1973b). This means in particular that $\Theta(x, t)$ will be identically zero for any x greater than some value x_{\max} , where we define $x_{\max} \equiv \eta_{\max} t^{(N+1)/(N+2)}$.

The code implementing the shooting solution was written in-house using MATLAB. We employed the fourth order Runge-Kutta method to solve the system of equations, using a step-size for η of 0.001, and thereby determined whether a selected $\Phi(0)$ needed to be increased or decreased to satisfy boundary conditions, the correct $\Phi(0)$ being found via a bisection approach. The obtained Runge-Kutta solutions were compared with the inbuilt routine ode45. The solutions ultimately obtained for $\Phi(0)$ agreed within four significant figures or better, regardless of whether we considered variables Φ and Φ' or variables Φ and F .

In order to benchmark our numerical scheme, we carried out additional tests. Firstly, we solved the node-dominated equation (see equation (21) given in Section 3.1) via the numerical scheme but using the value of $\Phi(0)$ obtained from an analytical

solution (equation (21), being linear, admits an analytical solution (22)). Having obtained a satisfactory solution for Φ vs η via this benchmark, we then applied the numerical scheme to nonlinear systems, obtaining the results shown in Section 4. Before any of that though, we describe in the subsections to follow, how the algorithm we used overcame some of the challenges presented by possibly singular solutions.

2.3 Behaviour of flux when $\Phi \rightarrow 0$ at a finite $\eta = \eta_{\max}$

The equations written in flux form enable us to distinguish between the cases in which $\Phi(0)$ is selected too small within the shooting algorithm, meaning that Φ approaches zero at some finite η_{\max} still with a finite flux F there, and the case in which $\Phi(0)$ is selected correctly, meaning both Φ and F vanish at η_{\max} . Cases in which $\Phi(0)$ is selected too large do not need special consideration, since Φ never reaches zero anywhere in the solution domain in that case, so bespoke techniques to analyse the limiting behaviour as $\Phi \rightarrow 0$ are not needed.

Close to $\Phi \rightarrow 0$, it is clear that the second term on the right hand side of (12) dominates the first term on the right. Hence F' is approximated close to η_{\max} by

$$F' \approx -\frac{(N+1)F\eta_{\max}}{(N+2)a\Phi^N} = \frac{(N+1)}{(N+2)}\Phi'\eta_{\max}, \quad (13)$$

from which it follows (using F_m to denote the value of F at $\eta = \eta_{\max}$),

$$F - F_m \approx \frac{(N+1)}{(N+2)}\Phi\eta_{\max}. \quad (14)$$

The generic case we consider is that close to η_{\max} ,

$$\Phi \sim \varepsilon(\eta_{\max} - \eta)^{1/(N+1)}, \quad \Phi' \sim -\varepsilon(\eta_{\max} - \eta)^{-N/(N+1)}/(N+1), \quad (15)$$

where ε is some a priori unknown value. The value of $F = -a\Phi^N\Phi'$ close to $\eta = \eta_{\max}$ becomes

$$F \rightarrow F_m = \frac{a\varepsilon^{N+1}}{(N+1)}, \quad (16)$$

which indicates that power law relations in (15) are exactly the ones required to admit finite flux even though $\Phi \rightarrow 0$.

In practice, we use the above equations as follows. Suppose using a numerical Runge-Kutta scheme we know values of both Φ and F at some value of η , and also that $\Phi \ll 1$ at this point. Then we can use equation (15) to eliminate ε in favour of Φ and $\eta_{\max} - \eta$. We substitute that expression in (16) to determine a formula for F_m ,

$$F_m \approx \frac{a}{(N+1)} \frac{\Phi^{N+1}}{(\eta_{\max} - \eta)}, \quad (17)$$

and finally substitute this into (14). This then leads to an expression for η_{\max} given the values of Φ and F at some nearby η . In other words, we have estimated the point at which Φ is exactly zero, starting from a point at which Φ is nearly zero. The value of F_m then follows, but generally is nonzero, indicating an incorrectly chosen $\Phi(0)$, meaning a different $\Phi(0)$ value must be sought. How this scheme changes when $\Phi(0)$ is eventually chosen correctly is what we discuss next.

2.4 Behaviour when $\Phi \rightarrow 0$ & $F \rightarrow 0$ at $\eta = \eta_{\max}$

For a correctly chosen $\Phi(0)$, we anticipate that F_m should approach zero. In that case we anticipate a power law behaviour,

$$\Phi \sim \varepsilon(\eta_{\max} - \eta)^{1/N}, \quad \Phi' \sim -\varepsilon(\eta_{\max} - \eta)^{(-1+1/N)}/N. \quad (18)$$

Note that if $N > 1$, this corresponds to an abrupt approach of Φ to zero, in the sense that $|\Phi'| \rightarrow \infty$. Even so, $|\Phi'|$ does not diverge as rapidly as what we saw previously in equation (15).

Assuming equation (18) applies, it then follows via equation (11) that,

$$F \approx a\varepsilon^{N+1}(\eta_{\max} - \eta)^{1/N}/N. \quad (19)$$

Note that the ratio F/Φ is therefore $a\varepsilon^N/N$, i.e. it is insensitive to exactly how close η is to η_{\max} . However, equation (14) with $F_m \rightarrow 0$ suggests this ratio F/Φ is nothing more than $(N+1)\eta_{\max}/(N+2)$. If we equate these quantities and now eliminate ε in favour of Φ and $\eta_{\max} - \eta$ we obtain

$$\frac{a\Phi^N}{(\eta_{\max} - \eta)N} \approx \frac{(N+1)\eta_{\max}}{(N+2)}. \quad (20)$$

We use this equation as follows. Suppose for a certain η , the values of Φ and F are finite, but both are small, such that $\Phi \ll 1$ and $F \ll 1$. Equation (20) is solved for η_{\max} . We then verify a posteriori that the flux evaluated at η_{\max} , which is estimated via (14) as $F - (N+1)\Phi\eta_{\max}/(N+2)$, is much smaller than F itself.

A number of observations follow. Recall N is the exponent of the power law relating capillary diffusivity to moisture content, in the case of soils taking the value $N = 1/2 + 1/m$ for a soil specific parameter $0 < m < 1$. For any $N > 1$, equation (18) indicates an abrupt approach of moisture content towards zero. Specifically moisture content scales like distance from the leading edge of the front raised to the power $1/N$. Equation (18) was derived here in the context of early-time similarity solutions, but (as already alluded to previously) the exact same power law relating moisture content and distance was found (Boakye-Ansah and Grassia, 2021) for long-time travelling waves.

Returning to the early-time case, the situation we solve for channel-dominated foam drainage is different from soils, since the former has $N = 1/2$. Equation (18) still predicts a Φ value that tends to zero at a finite η_{\max} but the approach is not abrupt, since equation (18) now gives moisture content varying like the square of distance from the leading edge (again the same behaviour is observed close to zero moisture content in the long-time channel-dominated case (Boakye-Ansah and Grassia, 2021)).

The node-dominated foam drainage case has $N = 0$, and equation (18) then ceases to apply. In fact, in the node-dominated case there is no finite η_{\max} at which moisture content vanishes. Instead we only ever have $\Phi \rightarrow 0$ when $\eta \rightarrow \infty$. As a matter of fact, the $N = 0$ case is simple to solve since it has constant diffusivity and so the governing differential equation now becomes linear. This situation is discussed next.

3 Linear Equation: Constant Diffusivity

As earlier noted, based on the diffusivity function for node-dominated foam drainage, a linear differential equation for moisture content is obtained. We discuss this situation below.

3.1 Node-dominated Foam Drainage

In the node-dominated case ($N = 0$ and $a = 1$) equation (5) reduces to $\Theta_t = \Theta_{xx}$. Equation (6) now suggests looking for a solution of the form $\Theta = t^{1/2}\Phi(\eta)$ with $\eta = x/t^{1/2}$. Here Φ must satisfy (as follows from equation (9) with $N = 0$)

$$2\Phi'' + \eta\Phi' - \Phi = 0. \quad (21)$$

The solution of this turns out to be (Cannon, 1984)

$$\Phi(\eta) = -\eta \operatorname{erfc}(\eta/2) + \frac{2}{\sqrt{\pi}} \exp(-\eta^2/4). \quad (22)$$

The flux F is now simply $-\Phi'$ with $\Phi' = -\operatorname{erfc}(\eta/2)$, so it is easy to check that the correct boundary condition $F = 1$ at $\eta \rightarrow 0$ is obtained. It follows that the correct value of $\Phi(0)$ we seek is $2/\sqrt{\pi} \approx 1.128$. Knowing this $\Phi(0)$ value in advance in this case $N = 0$ allows us to benchmark the numerical shooting method mentioned in section 2.2. In Figure 2(a), we compare the analytical solution for Φ with the numerical one to verify they match. Meanwhile in Figure 2(b) we plot Φ and F computed analytically.

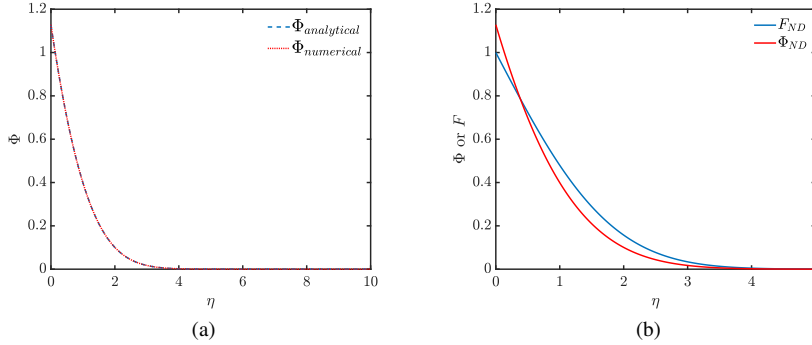


Fig. 2 Profiles for node-dominated foam drainage showing (a) comparison of Φ computed by numerical method and analytical solution, and (b) values of Φ and F .

Note in Figure 2(b) at large η , that Φ itself decays much more quickly than F does. For large η , there is an approximate asymptotic formula for erfc (Cannon, 1984), from which it follows,

$$F = \operatorname{erfc}\left(\frac{\eta}{2}\right) \sim \exp\left(\frac{-\eta^2}{4}\right) \frac{2}{\eta\sqrt{\pi}} \left(1 - \frac{2}{\eta^2}\right), \quad (23)$$

which via (22) leads in turn to, still in the large η limit

$$\Phi \sim \exp\left(-\frac{\eta^2}{4}\right) \times \frac{4}{\sqrt{\pi}\eta^2}, \quad (24)$$

which is order $2/\eta$ times smaller than F . It follows from this that Φ decays much more quickly at large η than either term $\eta \operatorname{erfc}(\eta/2)$ or $(2/\sqrt{\pi})\exp(-\eta^2/4)$ that contributes to Φ decays, i.e. at large η , the two terms contributing to Φ almost (but not quite) cancel one another out.

This completes our analysis of the linear equation that arises when $N = 0$, this analysis being known from literature (Cannon, 1984). In the following section we present results from nonlinear equations with nonzero N , the results to be presented now being obtained via the methods already outlined in sections 2.1–2.4.

4 Nonlinear Equations: Variable Diffusivity

As stated earlier, by the nature of their diffusivity functions, the diffusion equation for the channel-dominated foam drainage and Richards equations are nonlinear. The diffusivity functions are $\Theta^{1/2}$ and $(m - m^2)\Theta^{1/2+1/m}$ respectively for channel-dominated (Verbist and Weaire, 1994) foam drainage and Richards (Richards, 1931) equation, in the latter case diffusivities having been obtained via the van Genuchten (1980) expressions. As already mentioned, we write these diffusivities generically as $D_r = a\Theta^N$.

4.1 Channel-dominated Foam Drainage

Data obtained from the shooting method in the channel-dominated case ($N = \frac{1}{2}$) are presented in Fig. 3. We consider data both for Φ and F .

Notice that (as discussed in section 2.4) Φ and F both go to zero at a finite η_{\max} , but the approach is gradual rather than abrupt. The value of Φ' also tends to zero as $\eta \rightarrow \eta_{\max}$ but the approach (albeit not plotted here) is less gradual than that of either Φ or F .

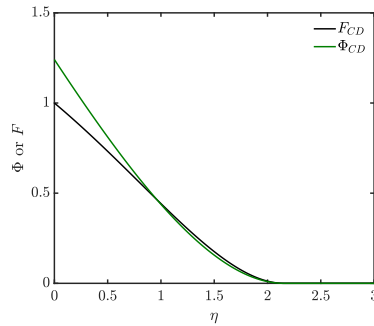


Fig. 3 Profile of channel-dominated foam drainage Φ and F via shooting-method.

Table 1 gives the estimated $\Phi(0)$ that satisfies the boundary conditions above. This value is greater than the node-dominated $\Phi(0)$ value. This is as expected because it is possible to show that $\int_0^{\eta_{\max}^*} \Phi d\eta = 1$ where η_{\max}^* either equals η_{\max} (if there is a finite η_{\max} value at which $\Phi = F = 0$) or else is infinity (if Φ and F only decay to zero as $\eta \rightarrow \infty$). Hence a smaller value of η_{\max}^* tends to be compensated by a larger value of $\Phi(0)$ to keep the value of the integral fixed. This integral relation follows from the notion that if a unit flux enters the system at the top boundary and is accumulated over a time t , then $\int_0^\infty \Theta dx = t$, as indeed follows from integrating equation (5) over x and t . The same relation also follows by writing (9) in the form,

$$(a\Phi^N \Phi')' = \Phi - \frac{(N+1)}{(N+2)}(\eta\Phi)', \quad (25)$$

and then integrating from 0 to η_{\max}^* .

The data obtained from the solution are given in Table 1. The method formulating the equations in terms of Φ and F (section 2.2) has been checked against the method formulating them in terms of Φ and Φ' (section 2.1), and both methods give the same data to at least 4 significant figures. Here $\Phi(0) \approx 1.2410$ for the channel-dominated foam drainage equation, and this exceeds the corresponding node-dominated value of $2/\sqrt{\pi} \approx 1.128$.

4.2 Richards Equation: van Genuchten Diffusivity Function

We focus on the solution of the early-time diffusion problem for soils using the [van Genuchten \(1980\)](#) relative diffusivity functions in the small Θ limit recognising here that at early-times one only ever accesses small Θ . As was the case in section 4.1, there is no general closed-form solution for this problem, so we solve it numerically as a two-parameter shooting problem using the approach discussed in section 2.2. In what follows, we show the numerical solution for $\Phi(\eta)$. Note that Φ now approaches zero (abruptly) as $\eta \rightarrow \eta_{\max}$ (for a finite η_{\max}), and it stays zero for all $\eta > \eta_{\max}$.

The solutions vary for different soil types according to the value of m , since each soil type has its own form of $D_r(\Theta)$ which dictates early-time spreading. These different D_r functions affect how much moisture accumulates near the top of the soil and how far into the soil it propagates at early times. Each soil type thereby has a different $\Phi(0)$ and different η_{\max} . The value of $\Theta(0, t)$ and the maximum penetration distance in x (denoted x_{\max} say) then obey $\Phi(0)t^{1/(N+2)}$ and $\eta_{\max}t^{(N+1)/(N+2)}$, where recall $N = 1/2 + 1/m$.

The solutions for $\Phi(\eta)$ and $F(\eta)$ are shown in Fig. 4–6 for three different soil types, and the $\Phi(\eta)$ profiles are combined together for easy comparison in Fig. 7. Considering equation (9) in the case of Hygiene Sandstone ($m = 0.9038$) and using the boundary conditions given in (10), we obtain $\Phi(0) = 2.6065$ as shown in Table 1. The data for the other soils (Silt Loam $m = 0.5146$ and Guelph Loam $m = 0.6377$) have smaller $\Phi(0)$, namely 1.8183 and 1.9074 respectively. What is striking in Table 1 is that the two loams have nearly the same η_{\max} despite having different $\Phi(0)$. The areas under the Φ vs η curves are all the same however regardless of how $\Phi(0)$ and η_{\max} vary.

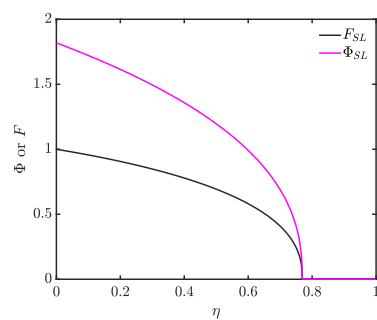


Fig. 4 Profiles of Φ and F for Silt Loam, $m = 0.5146$.

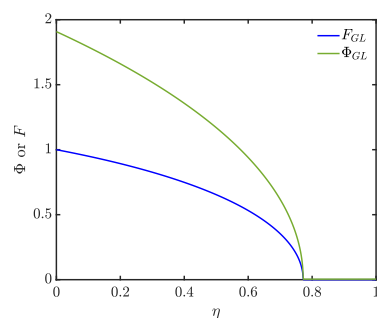


Fig. 5 Profiles of Φ and F for Guelph Loam, $m = 0.6377$.

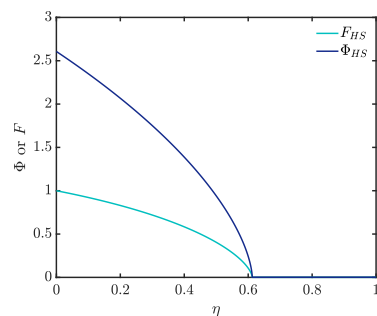


Fig. 6 Profiles of Φ and F for Hygiene Sandstone, $m = 0.9038$.

5 Discussion

We have thus far solved for various nonlinear cases in channel-dominated foam drainage and in soils, the solutions of which are shown in Fig. 3–6, and Table 1. We expect these solutions are unique, since [Shampine \(1973a,b\)](#) showed that nonlinear diffusion problems with singularities typically have only one solution. Additionally, in [Shampine \(1973b\)](#), it was postulated that if $D_r(\Theta) > 0$ for $\Theta > 0$ but $D_r(0) = 0$,

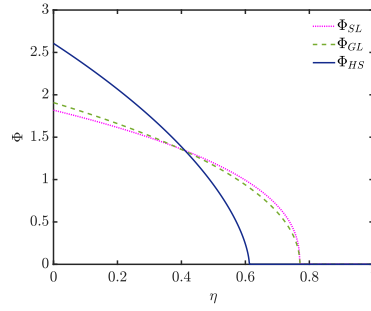


Fig. 7 Profile showing flux method for the three soil types.

Table 1 Values of $\Phi(0)$ and η_{\max} for various porous media (namely node-dominated (ND) foam, channel-dominated (CD) foam and three types of soil). Values of $\Phi(0)$ subscripted ‘SM’ are from the original “traditional” shooting method in terms of Φ and Φ' (rather than in terms of Φ and F which is the preferred method here). The value for the ND foam is an exact analytical solution.

Porous Medium	m	a	N	$\Phi(0)$	$\Phi(0)_{SM}$	η_{\max}
ND foam	–	1	0	$2/\sqrt{\pi}$	–	–
CD foam	–	1	1/2	1.2410	1.2410	2.1587
Silt Loam	0.5146	0.2498	2.4433	1.8183	1.8186	0.7695
Guelph Loam	0.6377	0.2310	2.0681	1.9074	1.9077	0.7698
Hygiene Sandstone	0.9038	0.0869	1.6064	2.6065	2.6066	0.6119

singular behaviour consisting of $\Theta(\eta)$ vanishing at some finite point η_{\max} and then $\Theta(\eta)$ vanishing identically $\eta \geq \eta_{\max}$ is possible: this is indeed the behaviour that we see. Although the similarity expression used in that publication is not what we employ due to the different problem we solve (i.e. a constant boundary flux rather than a constant boundary moisture content), the principle still follows.

In what follows, we use our results to look specifically at the temporal evolution of the system.

5.1 Estimating Moisture Content at the Top Boundary at Early Times

We know that $\Theta(x, t) = t^{1/(N+2)} \Phi(\eta)$ and hence $\Theta(0, t) = \Phi(0)t^{1/(N+2)}$. When we substitute in for the soil specific parameter m in lieu of $N = 1/2 + 1/m$, we find $\Theta(0, t) = \Phi(0)t^{2m/(2+5m)}$. The power law exponent tends to indicate that at early times ($t \ll 1$), $\Theta(0, t)$ for loams (smaller m) grows faster than for sandstones (or indeed for foams which have an even higher exponent still). Offsetting this is the fact that the prefactor $\Phi(0)$ tends to be smaller in loams than in sandstones.

This tells us how moisture content grows at the top boundary, assuming constant unit flux there, and assuming also the flux is entirely diffusive. In reality though, any imposed flux will be comprised of both a conductive and diffusive part, i.e. $F =$

$K_r(\Theta) - D_r(\Theta)\Theta_x$. If the value of Θ at the boundary is estimated as $\Phi(0)t^{2m/(2+5m)}$, it is possible to estimate how the conductive flux which is $K_r \approx m^2\Theta^{1/2+2/m}$ in the small Θ limit (Boakye-Ansah and Grassia, 2021) evolves at the top boundary. If the estimated $K_r(\Theta)$ becomes too large, then the assumption we have made that flux is dominated by diffusion ceases to be valid. In the early-time limit though, we end up with $K_r(0,t) \approx m^2(\Phi(0))^{1/2+2/m}t^{(4+m)/(2+5m)}$. The power law now indicates that for $t \ll 1$, K_r grows more slowly for loams (small m) than for sandstones (larger m), even though $\Theta(0,t)$ is faster growing in the case of loams. This is compounded by the factor $m^2(\Phi(0))^{1/2+2/m}$ which is smaller in loams.

We provide an estimate of three particular times $t_{\Theta(0,t) \sim 0.1}$, $t_{K_r(0,t) \sim 0.1}$, $t_{\Theta(0,t) \sim 1}$, for soils and for foam drainage, and present this in Table 2. The first quantity is the time at which moisture content at the top boundary starts to become significant (reaching an estimated value $\Theta \approx 0.1$). The second is the estimated time at which conductive flux at the top (which is neglected from our purely diffusive model) would start to become significant i.e. $K_r \approx 0.1$ compared with the total flux $F = 1$ at the top. The Θ value at the top attained at this time we denote $\Theta_{K_r(0,t) \sim 0.1}$. The third time that we identify is the time at which moisture content at the top boundary would be predicted via the purely diffusive model to be so large $\Theta \approx 1$, that the model has certainly broken down. Indeed, if we ever obtain $\Theta \approx 1$ at the top boundary then since the relative hydraulic conductivity K_r approaches unity (by construction) in the $\Theta \rightarrow 1$ limit, the flux will definitely be dominated by conduction not diffusion (this is the long-time limit identified by Boakye-Ansah and Grassia (2021)). Note that the soil material property functions we have employed $K_r \approx m^2\Theta^{1/2+2/m}$ and $D_r \approx m^{-1}(1-m)\Theta^{1/2+1/m}$ are unreliable in this limit (we used $\Theta \ll 1$ approximations to the material functions of van Genuchten (1980) here). In particular if we extrapolate the $\Theta \ll 1$ formula, $K_r \approx m^2\Theta^{1/2+2/m}$ all the way to $\Theta \rightarrow 1$, we do not obtain $K_r \rightarrow 1$. Nevertheless, the original van Genuchten (1980) material functions do actually give $K_r \rightarrow 1$ in this limit. In any case, as already mentioned, the early-time similarity solution for Θ vs x and t is replaced by a long-time travelling wave in this case.

Table 2 reveals that loams attain $\Theta(0,t) \approx 0.1$ very quickly indeed, followed by sandstones, with foams requiring more time still. The estimated time to approach $\Theta(0,t) \approx 1$ is also much less in soils than in foams, but sandstones now approach this quicker than loams. Meanwhile the value of $\Theta(0,t)$ required to attain $K_r(0,t) \approx 0.1$ at the top boundary is surprisingly high in loams, a little smaller in sandstone and smaller still in foams. Correspondingly the time at which $K_r(0,t) \approx 0.1$ is much larger than the time at which $\Theta(0,t) \approx 0.1$ in soils. On the other hand, for loams, the time at which $K_r(0,t) \approx 0.1$ is of similar order magnitude to the time (at least as predicted via the purely diffusive model) at which $\Theta(0,t) \approx 1$, but somewhat smaller than that for sandstones. Meanwhile for foams, the time at which $K_r(0,t) \approx 0.1$ is well over an order of magnitude smaller than the time at which $\Theta(0,t)$ becomes close to unity.

5.2 Estimating x_{\max}

We know that for the soils using van Genuchten (1980) or channel-dominated foam drainage (Verbist et al., 1996), the early-time solution terminates at some point η_{\max} ,

Table 2 Table showing time for moisture accumulation.

Porous Medium	$t_{\Theta(0,t)\sim 0.1}$	$\Theta_{K_r(0,t)\sim 0.1}$	$t_{K_r(0,t)\sim 0.1}$	$t_{\Theta(0,t)\sim 1}$
ND foam	0.0079	0.2154	0.0365	0.7854
CD foam	0.0018	0.3162	0.0328	0.5829
Silt Loam	2.5292×10^{-6}	0.8009	0.0262	0.0702
Guelph Loam	6.1800×10^{-6}	0.6799	0.0150	0.0723
Hygiene Sandstone	7.8176×10^{-6}	0.4611	0.0019	0.0316

beyond which $\Phi = 0$. We can estimate at which depth x_{\max} this occurs (or equivalently given the depth to which moisture penetrates, we can estimate the time for which infiltration or imbibition has been ongoing).

We know $x_{\max} = \eta_{\max} t^{(N+1)/(N+2)}$ which in the case of soils now becomes $x_{\max} = \eta_{\max} t^{(2+3m)/(2+5m)}$. Based on the power law, for $t \ll 1$, loams (smaller m) show slower growth in x_{\max} than sandstones (larger m), which are then slower in turn for channel-dominated foam drainage ($x_{\max} = \eta_{\max} t^{3/5}$). These effects are offset by loams having a larger η_{\max} than sandstones do (see Table 1).

Note that the node-dominated foam drainage case is a little different from the others in that there is no finite η_{\max} and hence no finite x_{\max} at which Θ is exactly zero. Fig. 2 however makes it clear that Φ is negligibly small for any η greater than about 4, hence any x greater than about $4t^{1/2}$.

6 Conclusion

The early-time diffusion equations obtained for moisture propagation in foams and soils may be either linear or nonlinear equations based on whether we have constant or variable diffusivity functions describing the dominant capillary-driven transport of moisture. Either way, solutions are available in similarity form. We have given the analytical solution for the node-dominated foam drainage, and the numerical solution for drainage in channel-dominated foams and imbibition in soils, the latter based on the diffusivity function of van Genuchten (1980). The numerical similarity solutions were obtained via the shooting method.

The foam drainage similarity solutions have been compared with those obtained for soils. Even though these are early-time solutions, in all cases it was found that the profiles are similar in some regards to the long-time solutions, in particular the soils approaching the “dry region” (the limit as $\Theta \rightarrow 0$) abruptly, just as was obtained for long-time travelling wave solutions. In fact, the nonlinear cases (channel-dominated foam drainage and drainage in soils) fall to zero moisture content at finite distances $x_{\max}(t)$, but it is only the soils that exhibit abrupt singularities in the profile shape as $\Theta \rightarrow 0$. This behaviour follows from the diffusivity function decaying to zero rapidly with falling Θ in the case of soils.

We examined how evolving moisture content at the boundary of a system $\Theta(0, t)$ develops as we deliver a known imbibition flux. In foams, we found that this boundary

moisture content value is greater in channel-dominated foams (growing like $t^{2/5}$ for $t \ll 1$) than in node-dominated foams (growing like $t^{1/2}$). In soils, the top boundary moisture content depends on a soil specific parameter m which is close to unity for sandstones, but smaller than that for loams. The moisture content required at the boundary to deliver a known flux grows like $t^{2m/(2+5m)}$ for small t . This quantity increases as the value of m decreases, indicating that $\Theta(0,t)$ is faster growing for loams than for sandstones. Overall though, the $\Theta(0,t)$ value tends to be greater in soils than in foams.

Systems that have faster growing $\Theta(0,t)$ at the top tend to terminate at lower x_{\max} values (i.e. at lesser depth). For soils x_{\max} scales like $t^{(2+3m)/(2+5m)}$ for $t \ll 1$. This corresponds to comparatively slow growth in x_{\max} for loams (smaller m) but faster growth for sandstones (m close to unity), albeit still not as fast as channel- or node-dominated foams, for which the respective scalings are $t^{3/5}$ and $t^{1/2}$.

We emphasise that the various solutions described here are only early-time ones and we have provided estimates of dimensionless times at which significant hydraulic conduction flux (i.e. significant effect of gravity) will start to develop, indicating that infiltration is no longer a pure capillary-driven imbibition process. Significant hydraulic conduction tends to happen sooner in soils than in foams, and sooner still in sandstones than in loams. Despite the faster early-time growth in $\Theta(0,t)$ for loams compared to sandstones, in the case of sandstones, the hydraulic conduction contribution to the flux tends to grow faster. This is because hydraulic conduction flux is a more rapidly increasing function of moisture content in sandstones than in loams, meaning that significant hydraulic conduction flux can be realised for sandstones at a more modest moisture content. Of course at even longer times, the early-time solutions obtained here break down altogether and we recover the long-time travelling wave solutions already considered by [Boakye-Ansah and Grassia \(2021\)](#), which for the unit infiltration flux considered here, turn out to give $\Theta(0,t) \approx 1$ at long times. How the system transitions between the early-time and late-time behaviours is a question which in general would need to be addressed numerically, by a methodology like that already developed by [Broadbridge et al. \(1988\)](#).

We declare that we have no conflict of interest.

References

- Boakye-Ansah YA, Grassia P (2021) Comparing and contrasting travelling wave behaviour for groundwater flow and foam drainage. *Transport in Porous Media* 137(1):255–280
- Broadbridge P, White I (1988) Constant rate rainfall infiltration: A versatile nonlinear model: 1. Analytic solution. *Water Resources Research* 24(1):145–154
- Broadbridge P, Knight JH, Rogers C (1988) Constant rate rainfall infiltration in a bounded profile: Solutions of a nonlinear model. *Soil Science Society of America Journal* 52(6):1526–1533
- Brooks R, Corey T (1964) Hydraulic properties of porous media. *Hydrology Papers*, Colorado State University 24:37–48

- Cannon JR (1984) The one-dimensional heat equation. No. 23 in *Encyclopaedia of Mathematics and its Applications*, Addison-Wesley, Menlo Park, London
- Caputo JG, Stepanyants YA (2008) Front solutions of Richards' equation. *Transport in Porous Media* 74(1):1–20
- van Genuchten MT (1980) A closed-form equation for predicting the hydraulic conductivity of unsaturated soils 1. *Soil Science Society of America Journal* 44(5):892–898
- Koehler SA, Hilgenfeldt S, Stone HA (1999) Liquid flow through aqueous foams: The node-dominated foam drainage equation. *Physical Review Letters* 82(21):4232–4235
- Koehler SA, Hilgenfeldt S, Stone HA (2000) A generalized view of foam drainage: Experiment and theory. *Langmuir* 16(15):6327–6341
- Philip JR (1969) Theory of infiltration. In: *Advances in Hydrosience*, vol 5, Elsevier, pp 215–296
- Press WH, Teukolsky SA, Vetterling WT, Flannery BP (2007) *Numerical Recipes: The Art of Scientific Computing*, 3rd edn. Cambridge University Press, Cambridge
- Richards LA (1931) Capillary conduction of liquids through porous mediums. *Physics* 1(5):318–333
- Shampine LF (1973a) Concentration-dependent diffusion. *Quarterly of Applied Mathematics* 30(4):441–452
- Shampine LF (1973b) Concentration-dependent diffusion. II. Singular problems. *Quarterly of Applied Mathematics* 31(3):287–293
- Verbist G, Weaire D (1994) A soluble model for foam drainage. *EPL (Europhysics Letters)* 26(8):631–634
- Verbist G, Weaire D, Kraynik AM (1996) The foam drainage equation. *Journal of Physics: Condensed Matter* 8(21):3715–3731
- Witelski TP (1997) Perturbation analysis for wetting fronts in Richards' equation. *Transport in Porous Media* 27(2):121–134
- Witelski TP (2003) Intermediate asymptotics for Richards' equation in a finite layer. *Journal of Engineering Mathematics* 45(3-4):379–399

Comparing and Contrasting Travelling Wave Behaviour for Groundwater Flow and Foam Drainage

This chapter presents a copy of an article that has been published online in *Transport in Porous Media* (2021), 137:255–280 DOI: 10.1007/s11242-021-01562-w. The authors are Yaw A. Boakye-Ansah and Paul Grassia. This paper focuses on the similarities and differences in travelling wave solutions to flow in foams and flow in soils. Physical applications of the travelling wave solutions are also discussed.

Overview

In this work, Richards equation [12] which was formulated to describe drainage in unsaturated soils, and two variants of the foam drainage equation [14, 36] are compared and shown to be analogous. Richards equation may be expressed in three main forms: the mixed form, the head-based form or the moisture-based form. The moisture-based form is used here. Two forms of the foam drainage equation have been derived, the channel-dominated [36] and node-dominated [14] foam drainage equations.

Here, the close analogy between Richards equation and foam drainage is discussed. Their similarities, including both being continuity and mass conservation equations that describe flow in complex porous media, are established. Consequently, the forces that

control fluid flow in these equations are the same. Conversely, there are some distinguishing differences between foams and soils. Unlike the pores in soils, the channels (Plateau borders) within foams expand with increasing moisture content until the foam breaks into a bubbly liquid state. Soils do not generally exhibit these characteristics since they are usually compact (i.e. those pores do not change shape except when a large deformation force is applied).

In order to achieve the research objectives for this work, the foam drainage equation derived by Verbist and Weaire [36] was rescaled such that its diffusivity became equal to unity at full saturation in order for it to be comparable with the diffusivity of the *so-called* node-dominated foam drainage equation [14], which scales to unity at all times. The foam drainage equations have embedded in their form the functions that are required to solve for their travelling waves, namely the relative hydraulic conductivity (gravity) and diffusivity functions. Having rescaled the channel-dominated foam drainage equation to incorporate this form of the diffusivity function, attention was focused on Richards equation.

In the case of Richards equation, it was initially nondimensionalised and then rescaled according to the physical properties of the functions that enter the equation. As mentioned, the moisture-based form of the equation was used in this research. The diffusivity and hydraulic conductivity functions were rescaled as well as the time and length factors in the equation. Contrasting with the foam drainage equations, in the construction of Richards equation, the functions required to solve it are not given a priori. Hence, soil material property functions that can be used to solve Richards equation were proposed. In this work, those functions derived by van Genuchten [38] were used.

The principle of travelling wave solutions was employed in the current solution as it can elucidate behaviours straightforwardly, particularly at late times for infiltration problems, e.g., when the uppermost part of the soil is close to full saturation. When solving for the travelling wave profiles, Richards equation was transformed from a partial differential equation to an ordinary differential equation dependent on depth only. Additionally, the travelling wave propagation velocity profile and an integration constant were determined which together were used to determine the profile of the travelling wave (i.e. height $\hat{\xi}$ against moisture content Θ).

The following conclusions were offered for the analysis done on comparison of travelling wave solution profiles of height ξ against moisture content Θ for foam drainage and Richards equation. Rise in moisture content with height is very abrupt for low moisture content in the case of Richards equation. This is in contrast with foam drainage where moisture content rises gradually with height in this same limit. Then again, if moisture content at a certain depth is found to be relatively large, the rate still at which full saturation can be reached in soils is very slow: a lot slower than in the case of foams.

For a physical application, during an irrigation process, in the case of soils, these findings suggest how long an irrigation system may need to remain switched on once a predetermined saturation can be achieved at a certain depth. Hence, this solution suggests that once the front reached a certain depth, the amount of missing moisture needed to achieve full saturation down to that depth was greater in the case of foam than soil. This is detailed further prior to concluding the paper with some suggestions on how to achieve the solutions at various moisture content limits.

Publication B

**Comparing and Contrasting Travelling Wave Behaviour for Groundwater
Flow and Foam Drainage**



Comparing and Contrasting Travelling Wave Behaviour for Groundwater Flow and Foam Drainage

Y. A. Boakye-Ansah¹ · P. Grassia¹

Received: 26 August 2020 / Accepted: 28 January 2021 / Published online: 18 February 2021
© The Author(s) 2021

Abstract

Liquid drainage within foam is generally described by the foam drainage equation which admits travelling wave solutions. Meanwhile, Richards' equation has been used to describe liquid flow in unsaturated soil. Travelling wave solutions for Richards equation are also available using soil material property functions which have been developed by Van Genuchten. In order to compare and contrast these solutions, the travelling waves are expressed as dimensionless height, $\hat{\xi}$, versus moisture content, Θ . For low moisture content, $\hat{\xi}$ exhibits an abrupt change away from the dry state in Richards equation compared to a much more gradual change in foam drainage. When moisture content nears saturation, $\hat{\xi}$ reaches large values (i.e. $\hat{\xi} \gg 1$) for both Richards equation and foam drainage, implying a gradual approach of Θ towards the saturated state. The $\hat{\xi}$ values in Richards equation tend, however, to be larger than those in the foam drainage equation, implying an even more gradual approach towards saturation. The reasons for the difference between foam drainage and Richards equation solutions are traced back to soil material properties and in particular a soil specific parameter “ m ” which is determined from the soil-water retention curve.

Article Highlights

- Travelling waves for groundwater flow via Richards equation are compared with node- and channel-dominated foam drainage.
- In dry systems, liquid saturation varies abruptly with spatial location in soils (Richards equation) compared to foam.
- By contrast, in wet systems, full saturation is achieved more gradually with position in soils than in foams.

Keywords Richards equation · Foam drainage · Groundwater flow · Unsaturated flow · Travelling wave

✉ Y. A. Boakye-Ansah
yaw.boakye-ansah@strath.ac.uk; yaw.boakye-ansah@uenr.edu.gh

P. Grassia
paul.grassia@strath.ac.uk

¹ Chemical and Process Engineering, University of Strathclyde, 75 Montrose Street, Glasgow G1 1XJ, UK

1 Introduction

Flow in soils (and foams) involves displacing air with water (or vice versa in fluid recovery processes) in the domain in which flow occurs. The laws governing fluid flow are analogous in both systems but may be expressed differently using different terminology depending on the medium considered. Despite similar physical laws (Celia et al. 1990; Richards 1931; Verbist and Weaire 1994; Verbist et al. 1996), unfamiliarity in terminology has limited exchange of ideas between the flow in soil and flow in foam research fields.

Based on work of Buckingham (1907) on capillary action in soils, Richards (1931) showed that capillary, viscous and gravity forces affected movement of water in porous media. He presented data and a general equation commonly referred to as Richards equation (hereafter RE) to describe capillary conduction of water through soil (and clay). This equation has been used extensively in groundwater hydrology, soil science, agricultural and environmental engineering (Broadbridge and White 1988; Celia et al. 1990; Patel and Pradhan 2015; Philip 1974; Parlange 1971; Raats and Van Genuchten 2006; Zlotnik et al. 2007).

Foam drainage which is governed by forces analogous to those in Richards equation was first described with an equation derived by Gol'dfarb et al. (1988). This was later advanced by Verbist and Weaire (1994; Verbist et al. (1996), who developed the so-called foam drainage equation (hereafter FDE). Their work was also based on research done by Princen and Kiss (1987) who worked on an analogous system (emulsions). The FDE as originally formulated was based on the assumption of viscous dissipation through the Plateau border channels (hereafter PB), which are channels in a foam along which three bubbles meet (Verbist and Weaire 1994; Verbist et al. 1996). Depending on surfactant type, dissipation through the foam may be predominantly via the PB (Verbist and Weaire 1994; Verbist et al. 1996), or through the nodes where PBs meet, a case treated by Koehler et al. (1999, 2000) leading to the formulation of another variant drainage equation. Both variants of the FDE are of interest in this research and both have been analysed extensively mathematically (Koehler et al. 2000; Verbist et al. 1996).

The FDE has been studied so extensively (Grassia et al. 2001; Koehler et al. 1999, 2000; Neethling et al. 2000; Verbist et al. 1996) in fact that, analysis done on it can now be used to gain insights into the behaviour of RE. Thus, the mathematics of flow of liquid in foams can be analysed alongside the flow of liquids through porous media. In particular, it is known that the FDEs have travelling wave solutions (sometimes loosely referred to as solitons (Weaire and Phelan 1996)) which can be used to predict the spatial and temporal transport of fluid within the foam (Koehler et al. 1999; Grassia et al. 2001). In the context of RE, such solutions have been deployed extensively in hydrology (Ahuja and Swartzen-druber 1973; Broadbridge and White 1988; Caputo and Stepanyants 2008; Raats and Van Genuchten 2006; van Duijn et al. 2018).

As we will explain later on, the travelling wave solutions for foams and/or soils are relevant for systems with a constant liquid influx, but at sufficiently long times such that the liquid fraction at the top boundary has ceased to vary with time. They can be used to predict how much water is needed to irrigate a piece of land down to a certain depth, how rapidly water advances into the soil, as well as how rapidly an irrigation system might need to be switched off once a certain saturation is achieved at a specific depth.

A key novel contribution here will be to compare and contrast travelling wave solutions for foams and/or soils obtained over the full range of liquid contents (found numerically in the case of soils) with simpler asymptotic behaviours of those travelling waves, both for

very dry systems and for systems close to saturation. In both asymptotic limits, analytical approximations for the shape of the travelling wave are available and having the analytical formula is convenient in that limit given the numerical solutions diverge there. These analytical approximations for foams and soils and for both dry and wet systems, are particularly appealing, being simple enough in their form to make it straightforward to interpret them physically. This paper thus seeks to bridge the gap between not only the mathematics, but also the physics of drainage in foams compared to that in unsaturated soils.

Some of the physical insights we will gain are that liquid content in soils can change very abruptly with position and/or time when soils are comparatively dry (contrasted with much more gradual changes of liquid content in foams). On the other hand, when soils become wetter, reaching the limit of full saturation is achieved very slowly indeed (more so than in foams). How abruptly or how gradually liquid content within soil changes in space and/or time may affect decisions on how to control a system used to irrigate that soil as we will explain.

This work is laid out as follows. In Sect. 2, we review concepts of liquid transport in soils and foams, and the underlying governing equations, namely Richards equation and the foam drainage equation variants. We look at the non-dimensional rescaling of the channel-dominated and node-dominated FDE variants, and the derivation and dimensionless rescaling of RE. Section 3 considers material properties of the porous media that are required within RE. Section 4 deals with equations that govern travelling wave solutions for RE. Sections 5–6 present results and discussion, and Sect. 7 concludes the paper.

2 Foam Drainage Equation and Richards Equation

As mentioned above, there is a close analogy between RE and the two FDEs. They are both continuity and mass conservation equations describing flow (in complex porous media). The forces controlling fluid flow are the same (capillary, gravity and viscous forces). In Or and Assouline (2013), an alternate approach to drainage in porous media was formulated using a variant of the FDE called the soil foam drainage equation (SFDE). Due to the complexity of obtaining accurate values for the hydraulic functions, namely the so-called hydraulic conductivity and diffusivity (Van Genuchten 1980; Van Genuchten and Nielsen 1985; Vogel and Cislerova 1988) in Richards equation, a variant of the FDE was considered treating the capillary network in soils as a network of foam Plateau borders (PBs). This is an appealing view even though unlike soils, the channels within foams expand with increasing moisture content until the foam breaks up into a bubbly liquid state, which is not the case with soils. Additionally, soils can have large local variations in their pore sizes unlike the typical situation with foams where capillary suction limits local variation of PB cross-sectional area.

Despite these structural differences, foams and soils have many similarities. In both cases, the capillary suction effects are strongest when the system is dry, but fall towards zero at full saturation. Likewise in both cases, hydraulic conduction is weakest when the system is dry, and strongest when the system is wet. Similarities like these can be exploited when comparing foam and soil systems. Solutions that have been determined for FDE (Koehler et al. 1999, 2000; Verbist and Weaire 1994; Verbist et al. 1996; Weaire and Phelan 1996) may therefore be extended to RE to gain insights into flow behaviours in soils or other porous media. This paper seeks to consider RE (Richards 1931) in close analogy to existing studies on the FDEs (Koehler et al. 1999, 2000; Verbist and Weaire 1994;

Verbist et al. 1996), present travelling wave solutions for RE based on those for the FDE, and compare and contrast travelling wave solutions from RE and FDE.

We discuss the FDEs in Sects. 2.1 and 2.2 below, and RE in Sect. 2.3. To facilitate comparison, typically we consider not only the original equations, but also their dimensionless forms. We therefore consider non-dimensionalisation of the channel-dominated FDE and RE. The dimensionless node-dominated FDE is already available in literature (Koehler et al. 1999, 2000). The key dimensionless equations we obtain are Eqs. (4), (7) and (13). Readers familiar with derivations of these equations may wish to skip directly to Sect. 3.

2.1 Channel-Dominated FDE

The general form of the channel-dominated FDE proposed by Verbist and Weaire (1994); Verbist et al. (1996) is given as

$$\frac{\partial A}{\partial t} + \frac{1}{\eta} \frac{\partial}{\partial x} \left(\rho g A^2 - \frac{C\gamma}{2} \sqrt{A} \frac{\partial A}{\partial x} \right) = 0, \quad (1)$$

where A is area of the PB, t is time, x is position (measured downwards), $\eta = f\eta_l$ (f is a dissipation shape factor, and η_l is the liquid viscosity), ρ is density of liquid, g is gravity, C is a geometric shape factor and γ is surface tension. It was found by Verbist et al. (1996) that $C \approx 0.4016$ and $f \approx 49$ (this value being an upper limit for η/η_l based on the assumption of completely immobile film surfaces Leonard and Lemlich 1965).

In non-dimensionalising the channel-dominated FDE, a characteristic length-scale $x_0 = \sqrt{C\gamma/\rho g}$ and time-scale $t_0 = \eta/\sqrt{C\gamma\rho g}$ were chosen (Verbist et al. 1996). Although these scales can be used to non-dimensionalise the channel-dominated FDE, the dimensionless analogue of A (namely A/x_0^2) would not be identical to the moisture content of the foam, making it less straightforward to compare with RE. However, moisture content can be obtained from $\theta = \lambda A$ where λ is the length of PB per unit volume (Brito-Parada et al. 2013; Neethling et al. 2001). Here, λ is sensitive to bubble size (scaling as inverse square of bubble size), whereas $1/x_0^2$ is a continuum quantity (depending on γ and ρ). When we introduce this factor λ , the channel-dominated FDE (1) becomes

$$\frac{\partial(\lambda A)}{\partial t} + \frac{1}{\eta} \frac{\partial}{\partial x} \left(\frac{\rho g (\lambda A)^2}{\lambda} - \frac{C\gamma}{2\sqrt{\lambda}} \sqrt{\lambda A} \frac{\partial(\lambda A)}{\partial x} \right) = 0. \quad (2)$$

This form of the FDE given in Eq. (2) is the more useful form for our problem. Choosing to make the equation dimensionless using $x = x_0\xi$ and $t = t_0\tau$, but now with $x_0 = (C\gamma\sqrt{\lambda})/(2\rho g)$ and $t_0 = (C\gamma\eta\lambda^{3/2})/(2\rho^2g^2)$, we deduce

$$\frac{\partial\theta}{\partial\tau} - \frac{\partial}{\partial\xi} \cdot \sqrt{\theta} \frac{\partial\theta}{\partial\xi} + \frac{\partial\theta^2}{\partial\xi} = 0. \quad (3)$$

This is the dimensionless channel-dominated FDE used here. It differs slightly from a form derived by Verbist et al. (1996) (there is a factor of 2 appearing in their equation, but we have chosen x_0 and t_0 in such a fashion to scale this out to permit a fairer comparison with the node-dominated FDE (see Sect. 2.2 below)). Strictly speaking, the FDE is only valid in dry foam limit $\theta \ll 1$, but it is often considered to apply all the way up to some liquid fraction θ_s (saturated moisture content) at which foam breaks up into a bubbly liquid, although the geometric picture of long straight PBs leading (in the terminology of RE, see Sect. 2.3

below) to simple formulae for hydraulic conductivity and diffusivity, scaling like θ^2 and $\sqrt{\theta}$, respectively, does not apply for wet foams. If we assume these simple formulae apply, at least approximately up to $\theta = \theta_s$, we can define $\Theta \equiv \theta/\theta_s$ as a rescaled liquid fraction, and after rescaling ξ and τ to new variables ($\hat{\xi} = \theta_s^{1/2} \xi$ and $\hat{\tau} = \theta_s^{3/2} \tau$), we obtain

$$\frac{\partial \Theta}{\partial \hat{\tau}} - \frac{\partial}{\partial \hat{\xi}} \cdot \sqrt{\Theta} \frac{\partial \Theta}{\partial \hat{\xi}} + \frac{\partial \Theta^2}{\partial \hat{\xi}} = 0. \quad (4)$$

In literature, this equation is often considered up to Θ values as large as $\Theta = 1$, even though formally (relying as it does upon there being a clear network of Plateau borders through which drainage can occur) the equation should be restricted to rather smaller Θ (Weaire and Phelan 1996; Weaire and Hutzler 2001).

2.2 Node-Dominated FDE

The node-dominated FDE proposed by Koehler et al. (1999, 2000) is given as

$$\frac{\partial \theta}{\partial t} + \frac{2\delta_a L^2}{\eta_l \delta_\theta^{1/2} I} \left(\rho g \cdot \frac{\partial}{\partial x} \theta^{3/2} - \frac{\gamma \delta_\theta^{1/2}}{2L} \frac{\partial^2 \theta}{\partial x^2} \right) = 0, \quad (5)$$

where θ is liquid fraction, t is time, L is length of a PB, $\delta_a \equiv C^2$ is a geometric shape factor, η_l is fluid viscosity, δ_θ is another geometric shape factor, I is a dimensionless number representative of the viscous force in the nodes and is assumed to be independent of θ , ρ is density of liquid, g is gravity, and γ is surface tension. Koehler et al. (1999, 2000) reported that $\delta_a \equiv C^2 \approx 0.1613$, $\delta_\theta \approx 0.1711$ and $I \approx 400$, the value of I having been evaluated empirically, although more recent studies (Anazadehsayed et al. 2017, 2018) indicate a method to compute it.

The dimensionless form of the equation using length and time scales that are identified in Koehler et al. (1999, 2000) ($x_0 = (\gamma/\rho g)\delta_\theta^{1/2}/(2L)$, $t_0 = (\eta_l \delta_\theta I/(4\delta_a L^3))\gamma/(\rho g)^2$) which necessarily differ from the analogous channel-dominated scales, as the parameters in the dimensional equations (2) and (5) also differ is

$$\frac{\partial \theta}{\partial \tau} - \frac{\partial}{\partial \xi} \cdot \frac{\partial \theta}{\partial \xi} + \frac{\partial \theta^{3/2}}{\partial \xi} = 0. \quad (6)$$

As noted for the channel-dominated case, it is possible to rewrite this in terms of a new variable $\Theta \equiv \theta/\theta_s$ setting now $\hat{\xi} = \theta_s^{1/2} \xi$ and $\hat{\tau} = \theta_s \tau$ to obtain

$$\frac{\partial \Theta}{\partial \hat{\tau}} - \frac{\partial}{\partial \hat{\xi}} \cdot \frac{\partial \Theta}{\partial \hat{\xi}} + \frac{\partial \Theta^{3/2}}{\partial \hat{\xi}} = 0. \quad (7)$$

Both Eqs. (4) and (7) are cast in the form of convection-diffusion equations where the convection term Θ^2 or $\Theta^{3/2}$ and diffusivity term $\Theta^{1/2}$ or 1 is always unity when $\Theta = 1$. This seems to enable a “fair” comparison between channel- and node-dominated theory (and compared to the formulation of Verbist and Weaire (1994); Verbist et al. (1996) is the reason for eliminating the factor of 2 that would otherwise appear in the channel-dominated FDE (4)).

2.3 Richards Equation

In Sects. 2.3.1–2.3.2, we review the derivation of Richards equation (RE) and its non-dimensionalisation, the dimensionless form facilitating comparison between RE and FDE.

2.3.1 Derivation of Richards Equation

Richards Eq. (Richards 1931) is deduced via the continuity and Darcy equations. Here,

$$\partial\theta/\partial t = \partial q/\partial z \quad (8)$$

gives the continuity equation, where q is the Darcy flux which is measured downwards and distance z is measured *upwards*. This is a common sign convention for RE but differs from the usual convention for FDE.

Moreover, the vector flux is given as

$$\mathbf{q} = K(\hat{\mathbf{g}} - \nabla h) \quad (9)$$

where K is hydraulic conductivity, $\hat{\mathbf{g}}$ is the unit vector in the gravity direction and h is the capillary suction head (hereafter referred to as head). With our sign convention, $q = K((\partial h/\partial z) + 1)$. This is the Darcy equation for describing fluid flow in porous media and it is based on a potential or pressure differential. One key component is the capillary head factor which is analogous to a capillary suction term in the FDE. Substituting the expression for q into (8) gives the originally determined RE that describes fluid flow in porous media:

$$\frac{\partial\theta}{\partial t} = \frac{\partial}{\partial z} \left[K \left(\frac{\partial h}{\partial z} + 1 \right) \right]. \quad (10)$$

The capillary head is strictly speaking negative (i.e. it is a suction), but we can define a positive value via $h_+ = -h$. If h becomes more negative as we move downwards (i.e. as z decreases), then $\partial h/\partial z$ makes a positive contribution to the downward flux.

Richards equation as in Eq. (10) as determined above is given in a “mixed form” involving two variables, θ and h . It is more convenient to give the equation in terms of a single variable (Celia et al. 1990). Here, we opt for a so called “moisture-based form”

$$\text{Moisture-based form } \partial\theta/\partial t - \nabla \cdot D(\theta)\nabla\theta - \partial K(\theta)/\partial z = 0 \quad (11)$$

where $K(\theta)$ is hydraulic conductivity, while $D(\theta)$ is soil-water diffusivity satisfying $D \equiv K |dh_+/d\theta|$. As θ decreases, h_+ becomes increasingly positive, i.e. h becomes more negative. Hence, $dh_+/d\theta$ is negative, an absolute value being taken to return a positive quantity.

Equation (11) is in a form that is more readily solved than the mixed form. Regardless of the form in which the equation is written, the first term in RE represents accumulation. The second term represents capillary diffusivity, and the final term is the gravity conduction term.

Thus far, we have reviewed how to derive RE. We now consider its non-dimensionalisation.

2.3.2 Non-dimensionalisation of Richards' Equation

The moisture-based form of the RE eliminates the head h which has units of length. There is a characteristic length scale in the soil-water retention curve relation (for h vs θ) which is typically denoted as α^{-1} for some parameter α (Van Genuchten 1980). Meanwhile, the hydraulic conductivity is $K \equiv K_s K_r(\theta)$. The multiplier $K_r(\theta)$ (relative hydraulic conductivity, hereafter RHC) is a dimensionless variable, whereas K_s has the same units as K , namely LT^{-1} in dimensional form and represents the hydraulic conductivity at saturation. We express $z = \xi/\alpha$ for the length scale (ξ is measured positive upwards), $t = \tau/(\alpha K_s)$ for the time scale and $D(\theta) = K_s D_{r^*}(\theta)/\alpha$ for diffusivity. Here, $D_{r^*}(\theta)$ is relative diffusivity (hereafter RD).

Table 1 gives some physical properties of the soil types used in this work, helping to relate the dimensionless variables back to dimensional ones. As just mentioned, the length scale is given by α^{-1} , whereas K_s gives a velocity scale and hence the time scale is $(\alpha K_s)^{-1}$.

Inserting these in Eq. (11), we obtain

$$\frac{\partial \theta}{\partial \tau} - \frac{\partial}{\partial \xi} \cdot D_{r^*}(\theta) \frac{\partial \theta}{\partial \xi} - \frac{\partial K_r(\theta)}{\partial \xi} = 0. \tag{12}$$

Here relative diffusivity D_r (hereafter RD) is defined such that $D = K_s D_r / (\alpha (\theta_s - \theta_r))$, so that $D_r = (\theta_s - \theta_r) D_{r^*}$. We may also recast this equation in the form

$$\frac{\partial \Theta}{\partial \hat{\tau}} - \frac{\partial}{\partial \hat{\xi}} \cdot D_r(\Theta) \frac{\partial \Theta}{\partial \hat{\xi}} - \frac{\partial K_r(\Theta)}{\partial \hat{\xi}} = 0, \tag{13}$$

with Θ indicating the rescaled moisture content

$$\Theta = (\theta - \theta_r) / (\theta_s - \theta_r),$$

where θ_s and θ_r are saturated and residual moisture contents. Note that $D_{r^*}(\theta) = K_r |dH_+ / d\theta|$ where as $D_r(\Theta) = K_r |dH_+ / d\Theta|$. Moreover, rescaled distance and time are $\hat{\tau} = \tau(\theta_s - \theta_r)$ and $\hat{\xi} = \xi$.

The similarity between Eq. (13) and Eqs. (4) and (7) is clear, modulo a sign change in the final term due to measuring $\hat{\xi}$ in different directions. Comparing the above-mentioned equations, it is apparent that foam drainage analogue of diffusivity D_r is $\Theta^{1/2}$ (channel-dominated FDE) or unity (node-dominated). The analogue of hydraulic conductivity K_r is Θ^2 (channel-dominated) or $\Theta^{3/2}$ (node-dominated).

Table 1 Soil-specific properties of the three example soils, with values as reported in Van Genuchten (1980). The parameter m will be discussed further in Sect. 3.1

Soil	m	K_s (cm/day)	α (cm ⁻¹)	αK_s (day ⁻¹)
Silt loam	0.5146	4.96	0.00423	0.0210
Guelph loam	0.6377	31.6	0.0200	0.6320
Hygiene Sandstone	0.9038	108	0.0079	0.8532

3 Properties of Porous Media Within Richards Equation

To solve Richards Eq. (13), we need the functions $K_r(\Theta)$ and $D_r(\Theta)$ which are porous media properties. A number of these functions are available in literature (Brooks and Corey 1964; Van Genuchten 1980). In particular, Van Genuchten (1980) derived hydraulic functions, namely conductivity and diffusivity from predictive conductivity models (hereafter PCM) given by Burdine (1953) and Mualem (1976) using a soil-water retention curve (which describes the suction head). Van Genuchten's analytical expressions via the Mualem PCM (VGM) are generally considered to be the more accurate and more widely known versions (Van Genuchten 1980; Kim et al. 2008; Patel and Pradhan 2015). The PCM relates capillary suction head with water content and unsaturated hydraulic conductivity, eventually leading to capillary diffusivity. The equations that are derived (Van Genuchten 1980) depend on a parameter m which depends on the specific soil type. This model matches experimental data (Van Genuchten 1980), but the functional forms it predicts for RHC and RD turn out to be complicated, making it difficult to solve RE analytically. We deal with that issue in Sect. 4: first, however, we discuss the VGM porous media properties.

3.1 Head Function

The soil-water retention curve (SWRC) relates the rescaled water (moisture) content Θ to the suction head h (in the soil-water retention curve) expressed below

$$\Theta = [1 + H_+^n]^{-m}; \quad H_+ = (\Theta^{-1/m} - 1)^{1/n}, \quad (14)$$

where $H_+ = \alpha h_+$ is dimensionless head (α^{-1} is a length scale and $h_+ = -h$), n and m are material parameters. Although fixed $m = 1$ with variable n has been used in literature (Van Genuchten 1980), usually m and n are related via $m = 1 - 1/n$ by Van Genuchten (1980) (using the predictive conductivity model (PCM) given by Mualem (1976)). Here, $n > 1$, and hence, $0 < m < 1$. Clayey soils are represented by comparatively low n values (m significantly less than 1), while higher n values (m close to 1) represent non-clayey soils (Stankovich and Lockington 1995). A plot of H_+ against Θ for three soil samples with three different m values as determined by Van Genuchten (1980) is presented in Fig. 1.

3.1.1 Behaviour of Head Function in Small and Large Θ Limits

From Fig. 1, we observe that changes in head values are very abrupt for small changes in Θ in the limits of near residual and fully saturated moisture content limits. When head is significantly bigger than unity ($H_+ \gg 1$ or $\Theta \ll 1$, i.e. in a very dry soil), we obtain analogously to the capillary suction head used by Brooks and Corey (1964)

$$\Theta|_{H_+ \gg 1} \approx H_+^{-nm}; \quad H_+|_{\Theta \ll 1} \approx \Theta^{-1/(nm)} \approx \Theta^{-(1-m)/m}. \quad (15)$$

Thus, H_+ is large when Θ becomes small, but the growth in H_+ is modest if $m \rightarrow 1$.

We observe also that for a near-saturated system ($\Theta \approx 1$), the head would be much less than unity, i.e. $H_+ \ll 1$. This implies that Eq. (14) would approximate to

$$\Theta|_{H_+ \ll 1} \approx (1 - mH_+^{1/(1-m)}); \quad H_+|_{\Theta \approx 1} \approx ((1 - \Theta)/m)^{1-m}. \quad (16)$$

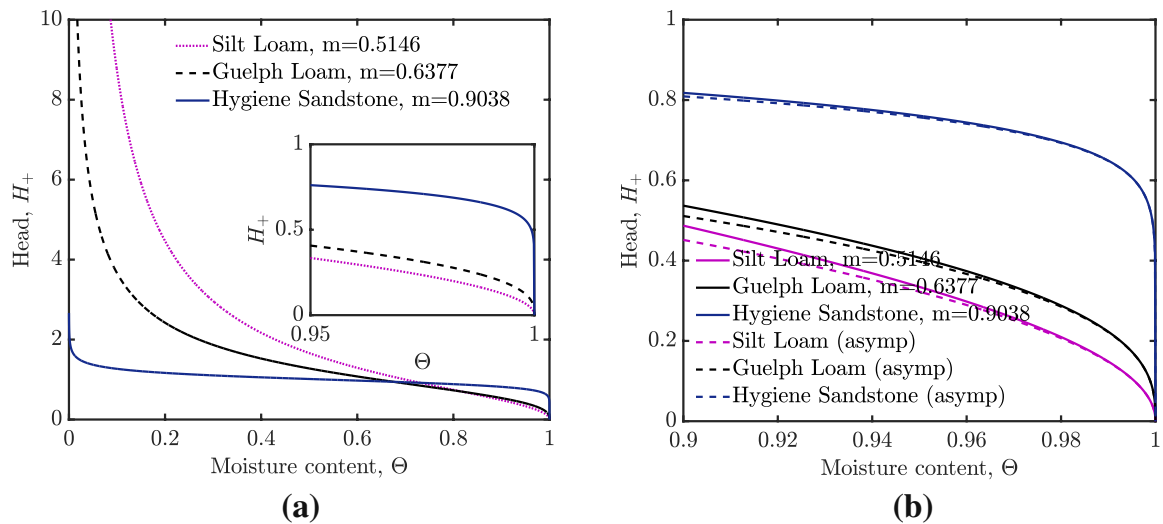


Fig. 1 **a** The behaviour of dimensionless suction head ($H_+ = ah_+ \equiv -ah$) versus moisture content based on Eq. (14) for three soil types (Van Genuchten 1980), i.e. three different values of the parameter m . The inset gives a closer view of the behaviour near full saturation. **b** Plot of comparison of behaviour of head Eq. (14) and asymptotic behaviour (16) of head near saturation ($\Theta \approx 1$)

Figure 1b shows a comparison of original head (14) given by Van Genuchten (1980) and its asymptotic approximation (16) for $\Theta \approx 1$. The two profiles match quite closely, and the approximation is more accurate as $m \rightarrow 1$. Note also that although $H_+ \rightarrow 0$ as $\Theta \rightarrow 1$ as we expect, the approach is not smooth: in fact, the derivative of (14) goes to infinity in that limit

$$|dH_+/d\Theta| \approx (1 - m)m^{-(1-m)}(1 - \Theta)^{-m}. \tag{17}$$

Note that for $m \rightarrow 1$, this predicts a large $|dH_+/d\Theta|$ only at $\Theta \rightarrow 1$ but much smaller $|dH_+/d\Theta|$ elsewhere, i.e. a near step change in H_+ as Fig. 1b shows.

3.2 Relative Hydraulic Conductivity

Several relative hydraulic conductivity (RHC) functions have been proposed in literature (Brooks and Corey 1964; Van Genuchten 1980; Assouline and Tartakovsky 2001). Here, the more commonly used Van Genuchten–Mualem (VGM) function (Van Genuchten 1980) is employed, as has been done by Celia et al. (1990); Caputo and Stepanyants (2008); Patel and Pradhan (2015). It is given as

$$K_r(\Theta) = \Theta^{1/2}[1 - (1 - \Theta^{1/m})^m]^2. \tag{18}$$

This is based on the aforementioned predictive conductivity model (PCM) given by Mualem (1976). Another PCM (Burdine 1953) for which Van Genuchten (1980) derived another hydraulic conductivity equation is available albeit less commonly used. For low moisture contents (considered in Sects. 3.2.1 and 5.2.1), the models developed by Van Genuchten (1980) using both the Burdine and Mualem models become equivalent to RHC models given by Brooks and Corey (1964), although differences appear as Θ grows. The Burdine case will not be discussed further here.

RHC values for different soils are plotted in Fig. 2a and compared against the FDE analogues read off from Eqs. (4) and (7).

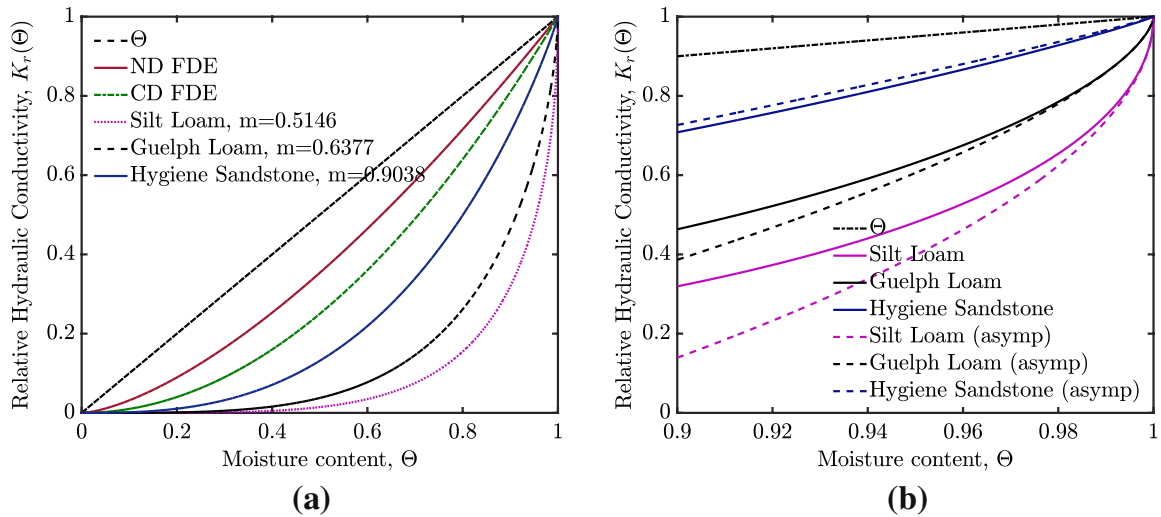


Fig. 2 **a** Plot of relative hydraulic conductivity (RHC) against moisture content for the two variants of the foam drainage equation (FDE) and three soil samples. The analogous RHC values for channel-dominated FDE (4) and node-dominated FDE (7) are Θ^2 and $\Theta^{3/2}$, respectively. The dashed straight line plots the value of Θ , which helps to visualise the amount $K_r(\Theta)$ falls below Θ . **b** Comparison of the true RHC Eq. (18) and its asymptotic form Eq. (20) in the $\Theta \approx 1$ region for three soil samples. The dashed straight line at the top plots Θ , so the value of $\Theta - K_r(\Theta)$ is the difference between this line and the value on each curve

Note that $K_r(\Theta) = 1$ when $\Theta = 1$ in all cases. However, RHC values for soils are less than those for foams, when $\Theta < 1$. Also, the lower the m value, the lower is the RHC at any Θ .

3.2.1 Behaviour of $K_r(\Theta)$ in Small and Large Θ Limits

We examine the behaviour of the RHC function for small and large Θ values. From Eq. (18), when $\Theta \ll 1$, we determine

$$K_r(\Theta) \Big|_{\Theta \ll 1} \approx m^2 \Theta^{(1/2+2/m)}. \tag{19}$$

Consulting Eq. (19), matching power laws and neglecting prefactors, we deduce that the node-dominated and channel-dominated FDE cases are akin to $m = 2$ and $m = 4/3$, respectively. Comparing these m values to those for soils (which have $0 < m < 1$), it leads to differences in drainage behaviour between foams and soils, at least in the small Θ limit.

We also find the behaviour of Eq. (18) for large moisture content $\Theta \approx 1$ values is

$$K_r(\Theta) \Big|_{\Theta \approx 1} \approx (1 - 2m^{-m}(1 - \Theta)^m). \tag{20}$$

The smaller the m value, the faster $K_r(\Theta)$ falls as Θ decreases.

Figure 2b compares true RHC Eq. (18) and its asymptotic form (20) for three different soils, i.e. three different m values (see Table 1). We observe that for all three m values, the asymptotic formula is a reasonable approximation. However, later on (see Sects. 4.3 and 5.2.4), we will be interested not only in values of $K_r(\Theta)$, but also in values of $\Theta - K_r(\Theta)$. The values of $K_r(\Theta)$ tend to be larger, and hence the values of $\Theta - K_r(\Theta)$ are smaller for the Hygiene Sandstone (and generally for cases with $m \approx 1$) than for the other soils, i.e. silt loam and Guelph loam. For $m \approx 1$ then, small errors in the $K_r(\Theta)$ values can lead to large relative errors in $\Theta - K_r(\Theta)$. The implications of this will be explored further later (see Sect. 5.2.4 and the ‘‘Appendix’’).

3.3 Relative Diffusivity

The general equation for determining relative diffusivity (RD) is based on the relationship for relative hydraulic conductivity (RHC) and head (soil-water retention curve, SWRC),

$$D_r(\Theta) = K_r(\Theta) |dH_+/d\Theta|. \quad (21)$$

We use Eq. (21) with Eqs. (14) and (18) to obtain the expression,

$$D_r(\Theta) = \frac{(1-m)(\Theta^{-1/m}-1)^{-m}}{m} \frac{1}{\Theta^{(1/2+1/m)}} [1 - (1 - \Theta^{1/m})^m]^2. \quad (22)$$

Equation (22) is plotted in Fig. 3 for three soil samples where it is compared with the analogous terms from the FDEs. We observe here that as $\Theta \rightarrow 1$, $D_r(\Theta) \rightarrow \infty$ for the three soil samples (due to the behaviour of $|dH_+/d\Theta|$ in that limit). By contrast, diffusivity is unity when the medium is fully saturated for the FDE variants (i.e. $D_r(\Theta) = 1$ at $\Theta = 1$).

3.3.1 Behaviour of $D_r(\Theta)$ in Small and Large Θ Limits

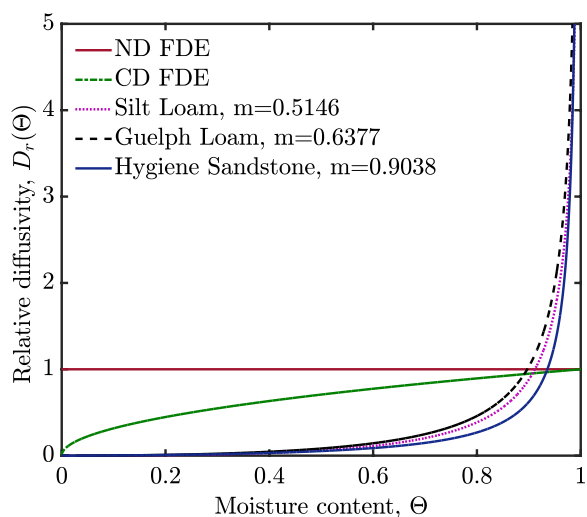
We examine the behaviour of the diffusivity function for small and large Θ values. We deduce from Eqs. (15) and (19) that when $\Theta \ll 1$

$$D_r(\Theta) |_{\Theta \ll 1} \approx m(1-m)\Theta^{(1/2+1/m)}. \quad (23)$$

This Eq. (23) is plotted in Fig. 4a alongside the original Eq. (22). Hygiene Sandstone with higher m not only has a lower exponent, but also a lower prefactor. Thus, $D_r(\Theta)$ for Hygiene Sandstone starts off larger than for Guelph loam or silt loam, but eventually it is overtaken by the two loams as Θ increases. Note also that if we match the power law of Eq. (23) neglecting prefactors to the foam drainage relative diffusivities, the node- and channel-dominated cases now become akin to $m = -2$ (a value that would certainly not appear in the case of soils) and $m \rightarrow \infty$.

We can also find a relationship for $\Theta \approx 1$ given Eq. (22). The RHC function approaches unity in this limit. Hence, via Eq. (17)

Fig. 3 Profile of relative diffusivity against moisture content for the FDEs (4) and (7) and three soil samples based on Eq. (22). The relative (capillary) diffusivity terms in (4) and (7) are equivalent to $\sqrt{\Theta}$ and 1, respectively. The functions for the soil samples are dependent on m for each soil sample



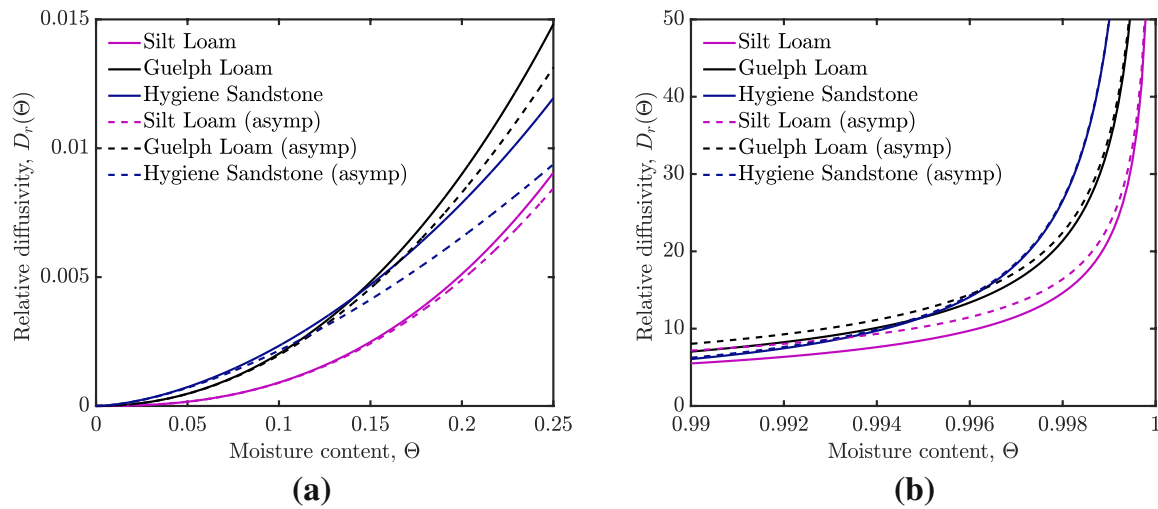


Fig. 4 Plot of relative diffusivity against moisture content for the three soil samples using Eq. (22) and asymptotic Eq. (23) in **a**, and (22) and asymptotic Eq. (24) in **b**. The solid lines are the true functions and the dashed lines are the asymptotic forms. In **b**, we use a zoomed view $0.99 \leq \Theta \leq 1$ to facilitate comparison between (22) and (24)

$$D_r(\Theta)|_{\Theta \approx 1} \approx |dH_+/d\Theta|_{\Theta \approx 1} \approx (1 - m)m^{m-1}(1 - \Theta)^{-m}. \tag{24}$$

Here, $D_r(\Theta) \rightarrow \infty$ as $\Theta \rightarrow 1$ as shown in Fig. 4b (a significant change from FDE for which $D_r(\Theta) \rightarrow 1$ as $\Theta \rightarrow 1$). Here, Hygiene Sandstone has the larger (negative) exponent but the smaller prefactor. Thus, it has the largest $D_r(\Theta)$ as $\Theta \rightarrow 1$, but not as Θ starts to fall. This implies (Fig. 4) that $D_r(\Theta)$ is non-monotonic in m , depending on the Θ value.

This completes our presentation of soil sample material properties.

Good estimates of the SWRC are essential (Van Genuchten 1980; Vogel and Cislserova 1988; Assouline et al. 1998), since the SWRC is used in the Mualem (1976) predictive model to obtain the RHC, and then both the retention curve and RHC are used to obtain the RD. In what follows, this information is used to obtain moisture content profiles.

4 Travelling Wave Solution

Various different types of solution have been studied for foam drainage, among them the so-called free drainage (in which an initially comparatively wet foam loses water from its bottom boundary) and forced drainage (in which water is added to the top of what is initially a comparatively dry foam) (Verbist et al. 1996; Koehler et al. 2000; Neethling et al. 2001).

Given the close analogy between foam drainage and Richards equation, similar scenarios are expected in soils: e.g. rainwater almost saturating soil and then draining down to the water table and/or irrigating an initially almost dry soil. Here we focus on travelling wave solutions that are relevant to the forced drainage case, as these are rather simpler to handle mathematically than free drainage is (Verbist et al. 1996; Cox et al. 2000).

Travelling wave solutions for RE have previously been proposed (Philip 1957a; Gilding 1991; Witelski 1997). In this section, we consider one such travelling wave solution for RE, analysing it specifically in the context of mathematical models for soil material properties (Burdine 1953; Mualem 1976; Van Genuchten 1980) described in Sect. 3. We consider

a general expression in Sect. 4.1 for the travelling wave obtained from RE. We then deduce the velocity of the travelling wave in Sect. 4.2. Finally, we determine the equation that describes the shape of the travelling wave in Sect. 4.3.

4.1 General Form of Travelling Wave

From the general form of a travelling wave, supposing distance (depth) $\hat{\xi}$ is positive upwards and velocity v is positive downwards, we search for a solution of the form

$$\Theta = \Theta(\hat{\xi} + v\hat{t}). \quad (25)$$

As length and time only appear in the combination of $\hat{\xi} + v\hat{t}$, we can express the solution of RE as a function of position rather than time, derivatives being related via $\partial/\partial\hat{t} = v \cdot \partial/\partial\hat{\xi}$. Integrating (13) with respect to $\hat{\xi}$ yields

$$v\Theta - D_r(\Theta) \cdot \partial\Theta/\partial\hat{\xi} - K_r(\Theta) = \text{constant}. \quad (26)$$

We impose boundary conditions that a long way upstream $\Theta \rightarrow \Theta_1$, and a long way downstream $\Theta \rightarrow \Theta_2$, with $\Theta_1 > \Theta_2$ (i.e. high saturation at the top and low saturation at the bottom).

The wave velocity v now obeys the Rankine–Hugoniot condition (Philip 1957b),

$$v = (K_r(\Theta_1) - K_r(\Theta_2))/(\Theta_1 - \Theta_2). \quad (27)$$

After some algebra, we obtain the constant on the right hand side of (26) as

$$\text{constant} = (K_r(\Theta_1)\Theta_2 - K_r(\Theta_2)\Theta_1)/(\Theta_1 - \Theta_2). \quad (28)$$

Note that in the limit of a dry system at the bottom $\Theta_2 \rightarrow 0$, and Eq. (28) vanishes.

4.2 Evaluating the Travelling Wave Propagation Velocity

To study the travelling wave propagation velocity, we plot Eq. (27) for various moisture contents. We use the Van Genuchten–Mualem RHC relationships in Fig. 5 and plot v vs Θ_1 at different initial moisture contents Θ_2 where $\Theta_2 < \Theta_1 \leq 1$ ($\Theta_2 = 0, 0.5$).

In the special case $\Theta_2 = 0$, Eq. (27) reduces to $K_r(\Theta_1)/\Theta_1$ (as in Fig. 5a).

We see in Fig. 5 that v increases with increasing Θ_1 (and does so abruptly near $\Theta_1 = 1$ in the case of soils). Additionally, we observe that v increases with increasing Θ_2 . When Θ_2 is non-zero (i.e. in an already wet system with $\Theta_2 = 0.5$), the soil samples tend to have lower velocity than the foam drainage cases for most Θ_1 values, but it actually have higher velocity when $\Theta_1 \rightarrow 1$.

4.3 Profile of $\hat{\xi}$ Versus Θ

It turns out that travelling wave solutions satisfying Eqs. (26) and (27) only exist if $\Theta_1 > \Theta_2$. Inserting Eqs. (27) and (28) in (26), and rearranging, we obtain

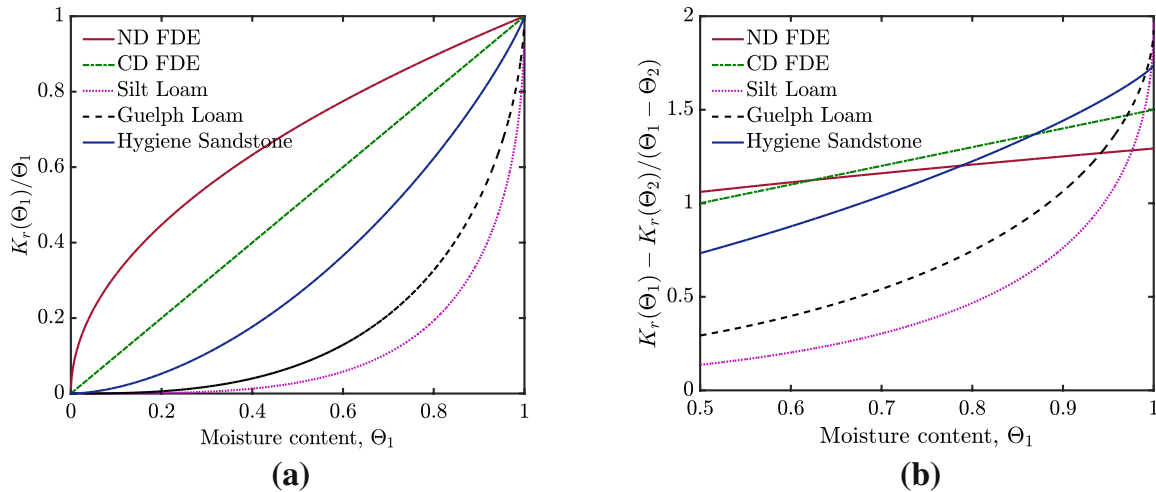


Fig. 5 Travelling wave propagation velocity for foam drainage equations (FDE) and three soil samples from Eq. (27) for a case where **a** moisture content at the bottom $\Theta_2 = 0$ and **b** moisture content at the bottom $\Theta_2 = 0.5$, i.e. in an already wet system

$$\frac{d\hat{\xi}}{d\Theta} = \frac{D_r(\Theta)(\Theta_1 - \Theta_2)}{K_r(\Theta_1)(\Theta - \Theta_2) - K_r(\Theta_2)(\Theta - \Theta_1) - K_r(\Theta)(\Theta_1 - \Theta_2)}. \tag{29}$$

In a special case $\Theta_1 = 1$ and $\Theta_2 = 0$ (the upper and lower limits possible for a travelling wave), Eq. (29) simplifies. In this case, $K_r(\Theta_1) = 1$, $K_r(\Theta_2) = 0$, $v = 1$, and the constant on the right hand side of Eq. (26) vanishes as presented by Parlange (1971); Witelski (1997). We deduce

$$d\hat{\xi}/d\Theta = D_r(\Theta)/(\Theta - K_r(\Theta)). \tag{30}$$

Note $\Theta - K_r(\Theta)$ in the denominator: the relevance of this term was stated in Sect. 3.2.1.

The special case (30) is analysed further in Sect. 5. Equation (30) applies equally well in the case of RE and FDE. It is only the form of the RHC and RD functions that varies. For certain forms of RHC and RD, analytical solutions to (30) are obtained (Verbist et al. 1996; Koehler et al. 2000; Cox et al. 2000). In cases for which choices of RHC and RD do not allow analytical solution of (30), we compute $\hat{\xi}$ against Θ via Simpson’s rule, implemented in MATLAB using a Θ step size of 0.0001.

5 Results for Travelling Wave Profiles

In what follows, we focus on numerical and asymptotic analytical solutions obtained from Eq. (30). Specifically, we compare and contrast solutions to this equation using the parameters from the FDEs and also using soil material properties derived by Van Genuchten (1980) for porous soils in RE. In Sect. 5.1, we review travelling wave solutions to the two variants of the FDE (Verbist et al. 1996; Koehler et al. 1999, 2000) and their asymptotic behaviours in the limit of small and large moisture content (Θ). These FDE solutions are known from literature (Verbist et al. 1996; Koehler et al. 1999, 2000; Cox et al. 2000; Weaire and Hutzler 2001) allowing us to benchmark our approach. Subsequently, we

consider the travelling wave solution to RE in Sect. 5.2, comparing back to the FDE. After that, Sect. 5.3 then considers an integrated quantity that we call “missing moisture”.

5.1 Foam Drainage Equations Solutions

In solving for FDE travelling wave solutions analogously to Eq. (30), we use the parameters describing hydraulic conductivity and capillary diffusivity for the two FDEs from Eqs. (4) and (7). The solutions correspond to travelling waves previously determined in literature (Verbist et al. 1996; Koehler et al. 2000), remembering however from Sect. 2.1 that there is a factor of 2 difference scaled out of Eqs. (3)–(4). Scaling out this factor gives a fairer comparison between the two FDEs as they have the same diffusivity and conductivity at full saturation.

The equation obtained in the case of channel-dominated FDE is given as

$$d\hat{\xi}/d\Theta = 1/(\sqrt{\Theta}(1-\Theta)), \quad (31)$$

the solution of which is given as

$$\hat{\xi} = 2 \operatorname{arctanh} \sqrt{\Theta} + c_{CD} \quad (32)$$

where c_{CD} is an integration constant and can be set to zero. Likewise, we obtain for the node-dominated case

$$d\hat{\xi}/d\Theta = 1/(\Theta(1-\sqrt{\Theta})). \quad (33)$$

Integrating (33), we obtain

$$\hat{\xi} = 2 \log(\sqrt{\Theta}/(1-\sqrt{\Theta})) + c_{ND} \quad (34)$$

where c_{ND} is an integration constant that again we set equal to zero.

Equations (32) and (34) are plotted in Fig. 6a assuming $c_{CD} = c_{ND} = 0$. In the case of the node-dominated FDE, we observed solutions exhibiting inflection points with $\hat{\xi}$ extending to both positive and negative infinity. The channel-dominated solution also exhibits an inflection point, but the moisture content Θ goes to zero at finite depth unlike the node-dominated case where Θ only vanishes as $\hat{\xi} \rightarrow \infty$.

As $\Theta \rightarrow 1$, Fig. 6a shows that ND FDE has larger $\hat{\xi}$ than CD FDE does. This follows because $d\hat{\xi}/d\Theta$ is larger according to Eq. (30). Both ND FDE and CD FDE have a common RD value as $\Theta \rightarrow 1$ but their $\Theta - K_r(\Theta)$ value in Eq. (30) can be approximated by $(1-\Theta)(K_r'(1)-1)$, where K_r' denotes $dK_r/d\Theta$. Figure 2a shows that ND FDE has smaller $K_r'(1)$ than CD FDE hence larger $d\hat{\xi}/d\Theta$, leading in turn to larger $\hat{\xi}$ values.

5.1.1 Asymptotic Behaviour of the CD FDE

We analyse the FDEs in the limits of either $\Theta \rightarrow 0$ or $\Theta \rightarrow 1$ since that will form an interesting contrast from RE. Considering Eq. (31) when $\Theta \ll 1$, and integrating (following an approach of Witelski (1997)) we deduce

$$\hat{\xi} \approx 2\sqrt{\Theta} + c_{CD}, \quad (35)$$

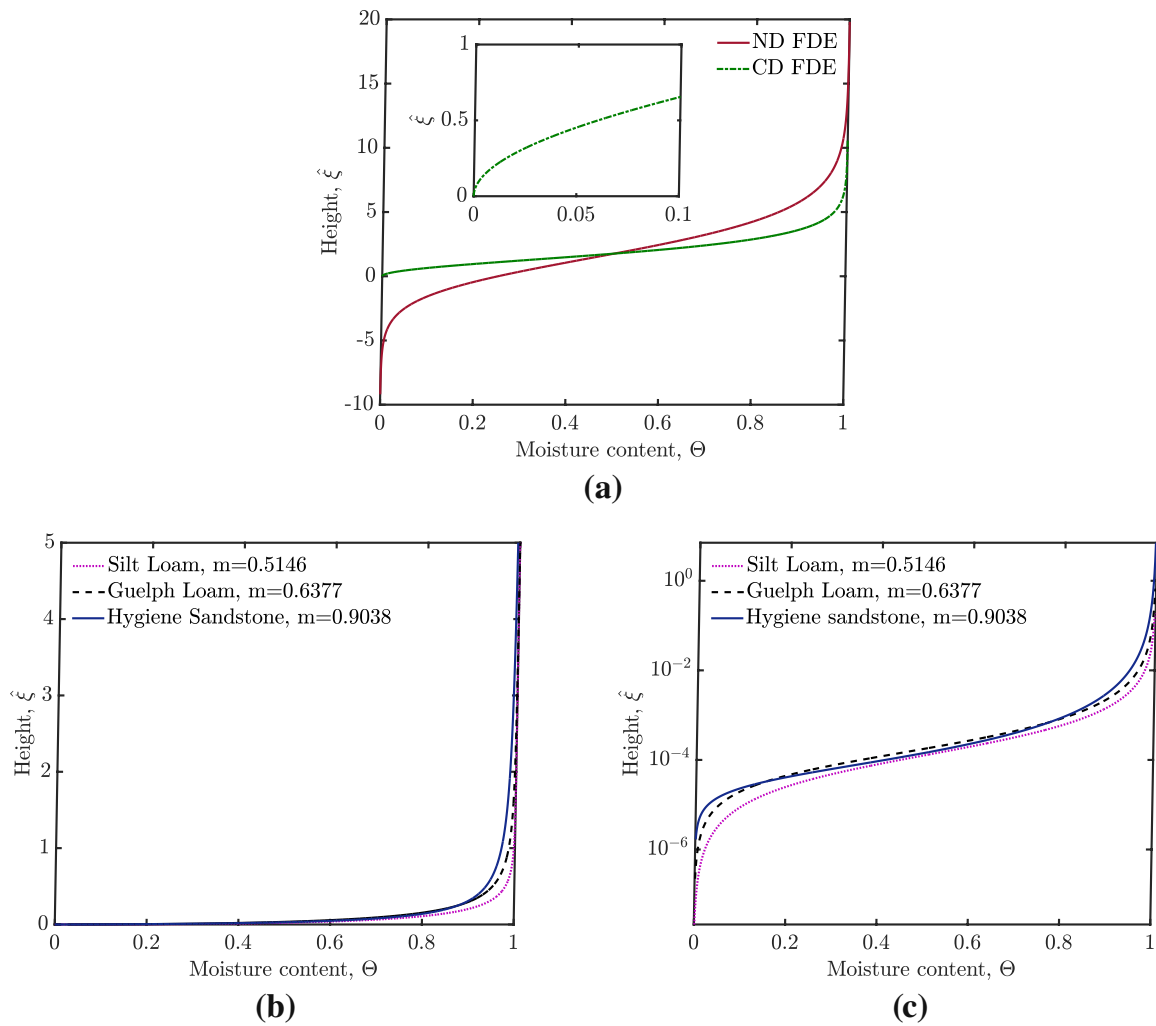


Fig. 6 **a** Profile of travelling wave solution for node-dominated and channel-dominated solutions. The inset shows a zoomed view of the channel-dominated case. **b** Profile of travelling wave solution (using Simpson’s rule) for Richards Eq. (39) using the Van Genuchten soil material functions (18) and (22) for three soil types. **c** The same solution (as **b**) on semi-log axes

where we set the integration constant $c_{CD} = 0$. We note that $\Theta \rightarrow 0$ at finite $\hat{\xi}$ but nonetheless $d\hat{\xi}/d\Theta$ is infinite as $\Theta \rightarrow 0$ (so Θ changes only slowly as $\hat{\xi}$ changes).

We can also consider the case when $\Theta \approx 1$. Taking Eq. (31) in this limit and integrating (again using the approach of Witelski (1997)) we find

$$\hat{\xi} \approx \log(1/(1 - \Theta)) + c_{CD1} \equiv \log(1/(1 - \Theta)) + \log 4, \tag{36}$$

where the integration constant c_{CD1} is set to $c_{CD1} = \log 4$ to match with (32). This follows because $2 \operatorname{arctanh}(\sqrt{\Theta})$ within (32) asymptotes to $\log(4/(1 - \Theta))$ as Θ approaches 1.

5.1.2 Asymptotic Behaviour of the ND FDE

We estimate the behaviour of the node-dominated FDE when the moisture content is very small ($\Theta \ll 1$). Taking (33) in this limit and integrating gives

$$\hat{\xi} \approx \log(\Theta) + c_{ND} \tag{37}$$

where we can set $c_{ND} = 0$. We can likewise obtain an expression for the node-dominated FDE in the limit $\Theta \approx 1$, taking Eq. (33) for $\Theta \approx 1$ and integrating gives

$$\hat{\xi} \approx 2 \log (1/(1 - \Theta)) + c_{ND1} \equiv 2 \log (1/(1 - \Theta)) + \log 4 \tag{38}$$

where the value of the constant $c_{ND1} = \log 4$ is set to match with (34). This follows because $2 \log(\sqrt{\Theta}/(1 - \sqrt{\Theta}))$ within (34) asymptotes to $2 \log(2/(1 - \Theta))$ as Θ approaches 1.

Comparing Eq. (38) with (36) confirms the deduction that compared to the channel-dominated system, the moisture content in the node-dominated system makes a slower approach as $\Theta \rightarrow 1$, i.e. it requires a larger $\hat{\xi}$ to achieve a given Θ . Having now reviewed the FDE solutions from Verbist et al. (1996); Koehler et al. (2000), in what follows, we contrast them with solutions of RE.

5.2 Van Genuchten Solution to Richards Equation

We seek travelling wave solutions for Richards equation (30) using soil functions derived by Van Genuchten (1980) (see Sect. 3). Substituting Eqs. (18) and (22) into (30) gives

$$\frac{d\hat{\xi}}{d\Theta} = \frac{(1 - m) \cdot \Theta^{-1/m-3/2} [1 - (1 - \Theta^{1/m})^m]^2}{m \cdot (\Theta^{-1/m} - 1)^m (1 - \Theta^{-1/2} [1 - (1 - \Theta^{1/m})^m]^2)}, \tag{39}$$

which we integrate by Simpson’s rule. The solution for $\hat{\xi}$ is shown in Fig. 6b. For low Θ , there is a very sharp change in Θ for a small change in $\hat{\xi}$ (a contrast from the FDE solutions). Figure 6c shows a semi-log profile of the solution to (39), making it easier to visualise behaviour at small $\hat{\xi}$ in particular. Looking towards larger Θ values ($\Theta \rightarrow 1$), however, there are very large values of $\hat{\xi}$. How these behaviours come about is considered below.

5.2.1 Asymptotic Behaviour of the Van Genuchten Solution

When $\Theta \ll 1$, the dominant material function affecting the profile shape is diffusivity. Equation (30) reduces to

$$d\hat{\xi}/d\Theta \Big|_{\Theta \ll 1} \approx D_r(\Theta)/\Theta, \tag{40}$$

where the denominator is estimated as being approximately Θ , neglecting $K_r(\Theta)$ relative to Θ in small moisture content limits. Substituting from Eq. (23) and integrating gives (as found by Witelski (1997))

$$\hat{\xi} \Big|_{\Theta \ll 1} \approx \frac{2m^2 (1 - m)}{(2 + m)} \Theta^{(1/2+1/m)} + c_{VGM}, \tag{41}$$

where the constant c_{VGM} is set to zero to ensure $\hat{\xi} = 0$ as $\Theta \rightarrow 0$. This solution is shown in Fig. 7 via dashed lines for each soil type (m value). Noting the scale on the vertical axis, we observe that Θ changes very abruptly with $\hat{\xi}$, or equivalently $\hat{\xi}$ changes only very slowly with Θ . Changes in $\hat{\xi}$ are slowest when m is small (owing to the power law in $\Theta^{(1/2+1/m)}$ in (41)), but are also surprisingly slow for Hygiene Sandstone ($m = 0.9038$) compared to Guelph loam, owing to the prefactor $(1 - m)$ in Eq. (41) which vanishes as $m \rightarrow 1$. As was the case in Fig. 4 for $D_r(\Theta)$, the behaviour here for $\hat{\xi}$ is non-monotonic in m .

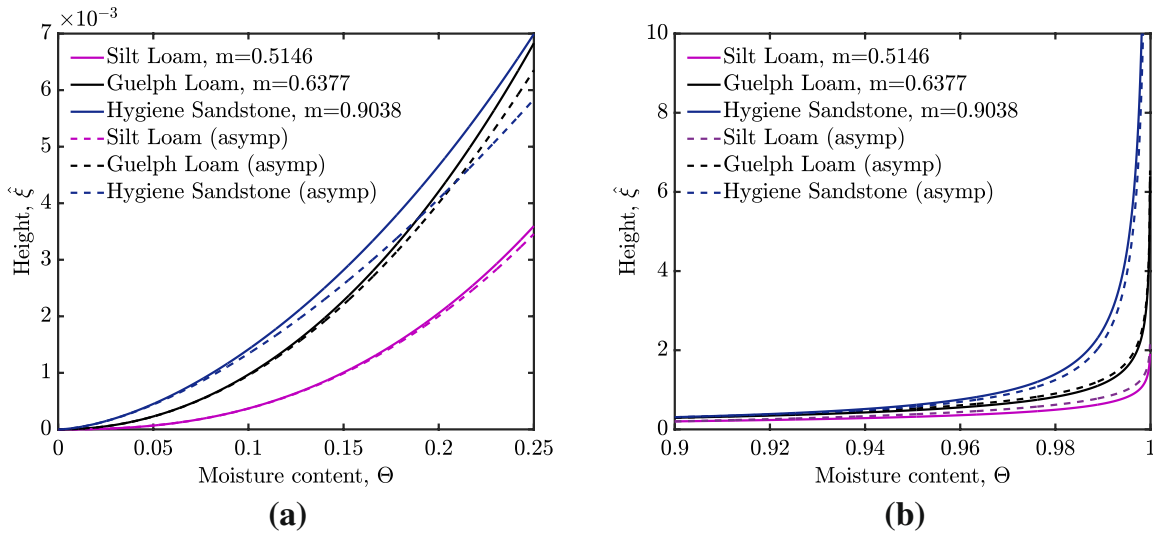


Fig. 7 Comparison of profiles for true or numerical function (39) and the asymptotic function (41) in **a**; and between (39) and the asymptotic function (43) in **b**

These slow changes in $\hat{\xi}$ (or equivalently abrupt changes in Θ) predicted by (41) differ from what is seen in the two FDEs in the $\Theta \ll 1$ limit. The implication for a case in which a sensor had been set to stop irrigating a soil when Θ reached some initial value, e.g. $\Theta = 0.1$, is that substantially higher Θ values $\Theta = 0.2$, $\Theta = 0.3$, etc., will follow just shortly thereafter.

5.2.2 Comparison of True and Asymptotic Solution ($\Theta \ll 1$)

In Fig. 7, we compare solutions from the true (i.e. numerical) solution in Eq. (39) and its asymptotic version Eq. (41) to verify the accuracy of our analysis in Sect. 5.2.1. We observe that the asymptotic solution can barely be distinguished on the scale of the graph for silt loam ($m = 0.5146$) at least up to $\Theta \approx 0.2$, the ratio of the true to asymptotic solution at $\Theta = 0.2$ being 1.0256. The accuracy of the asymptotic solution reduces as m increases. For $m = 0.6377$ (Guelph loam) the ratio of the true to asymptotic solution at $\Theta = 0.2$ becomes 1.0510, whereas for $m = 0.9038$ (Hygiene Sandstone) it is 1.1463. Nonetheless, the scale of the graph (up to less than $\hat{\xi} \approx 10^{-3}$) shows we are dealing with tiny $\hat{\xi}$ values throughout.

5.2.3 Asymptotic Behaviour when $\Theta \approx 1$

When we consider the case $\Theta \approx 1$, we can approximate the behaviour of Eq. (30) as

$$\left. \frac{d\hat{\xi}}{d\Theta} \right|_{\Theta \approx 1} \approx \frac{|dH_+/d\Theta|}{1 - K_r(\Theta)}, \tag{42}$$

where the numerator of (30) has been approximated by $|dH_+/d\Theta|$ (since $K_r(\Theta) \rightarrow 1$) and where the denominator $\Theta - K_r(\Theta)$ is expressed as $(1 - K_r(\Theta)) - (1 - \Theta)$, with $(1 - \Theta) \ll (1 - K_r(\Theta))$ (see Eq. (20) with $m < 1$ here). It follows from (20) that $dK_r(\Theta)/d\Theta$

diverges at $\Theta \rightarrow 1$, explaining the rapid decrease in $K_r(\Theta)$ with decreasing Θ for soils in Fig. 2a–b. Inserting equations (16), (20) and (24) in (42), and integrating

$$\hat{\xi} \Big|_{\Theta \approx 1} \approx \frac{(1 - m)m^{(2m-1)}}{2(2m - 1)}(1 - \Theta)^{1-2m} + c_{VGM1}, \tag{43}$$

where c_{VGM1} can only be obtained by matching to the solution of Eq. (39) via Simpson’s rule. We have arbitrarily chosen to match at $\Theta = 0.9$. The dashed lines in Fig. 7b are the asymptotic solutions given in (43). Out of the soils considered, Hygiene Sandstone (with the largest m) has the biggest $\hat{\xi}$ scaling as $(1 - \Theta)^{1-2m}$, and this is also bigger as $\Theta \rightarrow 1$ than the $\log(1/(1 - \Theta))$ terms obtained in the FDEs (see Eqs. (36) and (38)).

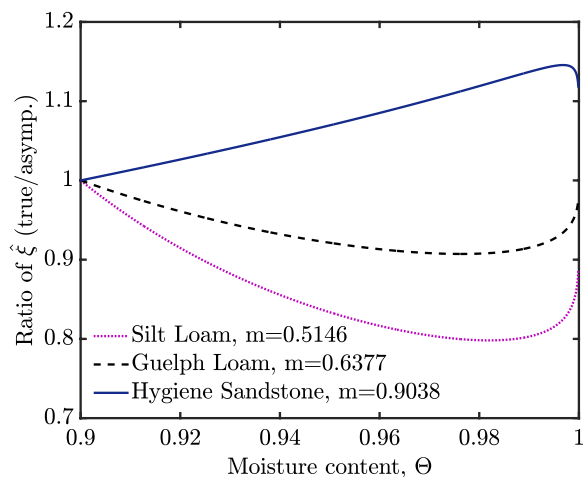
It is interesting to understand how these differences between FDE and RE come about. In Eq. (30), the denominator $\Theta - K_r(\Theta)$ vanishes in both the FDE case and the RE case but does so more slowly for RE. On the other hand, the numerator $D_r(\Theta)$ is finite as $\Theta \rightarrow 1$ for FDE but divergent for RE, and this more than compensates the more slowly vanishing numerator. The net result is that $\hat{\xi}$ grows more rapidly for soils than for foams.

The implication of (43) for an irrigation system is that if a sensor were to detect when the saturation at a certain location reached a certain critical level (e.g. say $\Theta = 0.9$), it might be quite some time in the case of Hygiene Sandstone before substantially higher saturations, e.g. $\Theta = 0.99$ or $\Theta = 0.999$ arrive at the sensor. If the sensor reaching $\Theta = 0.9$ is a signal that an irrigation system might eventually need to be switched off, and the higher level $\Theta = 0.99$ or $\Theta = 0.999$ is the level at which switch off is actually required, there could in the case of Hygiene Sandstone be a delay between the original signal and the eventual switch off.

5.2.4 Comparison of True and Asymptotic Solution ($\Theta \approx 1$)

We again compare solutions from the numerical solution of RE and its asymptotic approximation but now for $\Theta \rightarrow 1$. Specifically, Fig. 7b shows a comparison of the true solution from (39) (obtained via Simpson’s rule) and the asymptotic solution (43) (with a value matched to the numerical solution at $\Theta = 0.9$). For each m , the two profiles (true profile vs asymptotic) show slight differences. For $m = 0.9038$ (Hygiene Sandstone), the asymptotic profile is an underestimate, whereas for $m = 0.5146$ (silt loam) and $m = 0.6377$ (Guelph

Fig. 8 Profile of ratio of solution to equation for true $\hat{\xi}$ (Eq. (39)) to approximate $\hat{\xi}$ (Eq. (43))



loam) it is an overestimate. To highlight this, we take a ratio of $\hat{\xi}$ between the true (numerical) and asymptotic solutions as shown in Fig. 8.

On the domain of Θ plotted, the ratio reaches a maximum value of 1.1456 in the case of Hygiene Sandstone and reaches minimum values of 0.7981 & 0.9072 in the case of silt loam and Guelph loam, respectively.

We now examine the different behaviour in Fig. 8 for different m , identifying terms which lead to such behaviour by decomposing the governing equations (30) and (42). Differences could arise from the numerator ($D_r(\Theta)$) itself broken down into two components, i.e. the product of $|dH_+/d\Theta|$ and $K_r(\Theta)$. Alternately, differences could arise from the denominators, respectively $(\Theta - K_r(\Theta))$ and $(1 - K_r(\Theta))$ as shown in (30) and (42).

Figure 9 shows considerable variation between the original and the asymptotic $|dH_+/d\Theta|$ functions. The true $|dH_+/d\Theta|$ obtained via (14) exceeds the asymptotic one given by (17), by up to 25% at some points in the domain $0.9 < \Theta < 1$ in the case of silt loam. The ratio of true $K_r(\Theta)$ in the original Eq. (18) to the asymptotic $K_r(\Theta)$ (which can be taken equal to 1 when $\Theta \rightarrow 1$) is the same as the solid lines shown in Fig. 2b. Whereas, the original $dH_+/d\Theta$ is bigger than the asymptotic one, the original $K_r(\Theta)$ is smaller to compensate, falling to less than half the asymptotic value in the case of silt loam at $\Theta = 0.9$. As $|dH_+/d\Theta|$ and $K_r(\Theta)$ are multiplied together to form $D_r(\Theta)$, the dominant effect is the original $K_r(\Theta)$ being less than the asymptotic one (crudely approximated by unity here) and this is reflected in the $\hat{\xi}$ versus Θ profiles for silt loam and Guelph loam in Fig. 7b and also in the ratios in Fig. 8. The effect is less pertinent for Hygiene Sandstone since its $K_r(\Theta)$ does not decrease as sharply with decreasing Θ as happens for the other soils.

We now consider the denominators of (30) and (42). Figure 9b shows that using the asymptotic expression for $1 - K_r(\Theta)$ in lieu of $\Theta - K_r(\Theta)$ gives some deviation (about 30%) for the soils over the domain $0.9 < \Theta < 1$. It is accurate (to within 10%) at $\Theta \approx 0.99$ for both loams. For Hygiene Sandstone however, the asymptotic $1 - K_r(\Theta)$ exceeds the true $\Theta - K_r(\Theta)$ significantly even for $\Theta \approx 0.99$. When m is close to 1, it appears that the assumption employed in (42) that $1 - \Theta \ll 1 - K_r(\Theta)$ is no longer applicable, for reasons that are explained in the ‘‘Appendix’’.

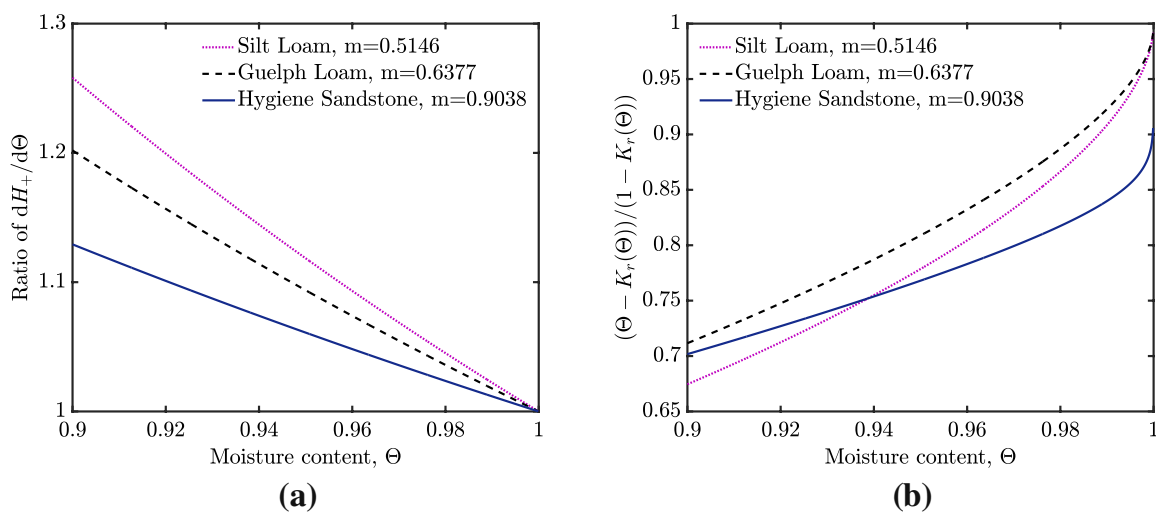


Fig. 9 Ratio of **a** true $dH_+/d\Theta$ used in Eq. 30 (via Eq. (21)) to the approximate $dH_+/d\Theta$ in equation (42) (via Eq. 17), and **b** the denominator in Eq. (30) to the asymptotic version in Eq. (42) (via Eq. 20)

The result is that for Hygiene Sandstone in particular, equation (30) has a smaller denominator than the asymptotic prediction even for Θ really close to 1, hence the predicted $\hat{\xi}$ via Eq. (30) is larger as Figs. 7b and 8 show.

To summarise, numerical (i.e. Simpson's rule) solutions generated for Richards equation have been examined. Analytical asymptotic approximations for $\Theta \ll 1$ & $\Theta \approx 1$ captured the true solution behaviour reasonably well within $0 < \Theta < 0.25$ and $0.9 < \Theta < 1$, respectively, although the level of agreement is sensitive to a parameter m . This parameter m reflects the pore structure (capillary model) for each soil type (Van Genuchten 1980). Due to variability of pore structure and how it affects soil-water retention, the value of m can vary from one soil type to another (clayey soils have smaller m), and this is reflected in the moisture content profile.

5.3 Integral of $\hat{\xi}$

There is one final quantity we consider, namely $\int_0^1 \hat{\xi} d\Theta$. For a front that has reached a given location, setting $\hat{\xi} = 0$ at the point where $\Theta = 0$, the value $\int_0^1 \hat{\xi} d\Theta$ is a measure of the amount of additional liquid that would be needed above the front to saturate fully the liquid above. In other words, it is the "missing" moisture that is required to saturate fully or flood the soil down to the current depth of the front. The integral is easily computed by dividing up the domain $0 \leq \Theta \leq 1$ into three subdomains: $\Theta'_1 \leq \Theta \leq 1$ (for some Θ'_1 close to unity), $\Theta'_2 \leq \Theta \leq \Theta'_1$ (for some $\Theta'_2 \ll 1$), and $0 \leq \Theta \leq \Theta'_2$. Integration is done analytically using asymptotic formulae for $\hat{\xi}$ in the first and third subdomain and numerically via Simpson's rule in the second subdomain. We chose $\Theta'_1 = 0.1$ and $\Theta'_2 = 0.9$. The missing moisture evaluates to 0.2243 for Hygiene Sandstone ($m = 0.9038$), 0.1204 for Guelph loam ($m = 0.6377$) and 0.0808 for silt loam ($m = 0.5146$). Based on this, loam is more readily flooded than sandstone. By comparison for the channel-dominated FDE, the value of $\int_0^1 \hat{\xi} d\Theta$ is 2. Hence, the amount of missing moisture is larger for foam than for the soil.

Even though the $\hat{\xi}$ values for soils approach $\hat{\xi} \rightarrow \infty$ more rapidly as $\Theta \rightarrow 1$ than the CD FDE does (i.e. a power law Eq. (43) rather than a logarithm Eq. (36)), the integral $\int_0^1 \hat{\xi} d\Theta$ is greater for foam. This is because the channel-dominated case has significant $\hat{\xi}$ values even for smaller Θ , away from the neighbourhood of $\Theta = 1$.

It is meaningless to compute $\int_0^1 \hat{\xi} d\Theta$ for the node-dominated FDE as there is no finite $\hat{\xi}$ location at which Θ falls to zero so there is a degree of arbitrariness in how much $\hat{\xi}$ is shifted up or down.

6 Discussion

In the previous section, we studied in detail the travelling wave solutions of Richards equation and foam drainage, focussing on asymptotic behaviour in various ranges of liquid saturation. We have not, however, discussed whether and if so when these solutions are relevant in real world infiltration problems.

The travelling wave solutions presented in this paper are long time solutions and thus are by themselves insufficient to describe real infiltration problems, since travelling waves take some time to develop under standard boundary conditions (Broadbridge and White 1988). In order to approach close to a travelling wave solution, depths of at least several dimensionless units have to be reached, or converting to dimensional lengths, several times α^{-1} (see Table 1). Additionally, infiltration needs to proceed long enough for that to

happen, i.e. several units of dimensionless time, which is easily related to dimensional time ($(\alpha K_s)^{-1}$ being the typical time scale in Table 1). An unsteady state simulation of liquid infiltration into soils could be safely ceased as soon as the simulated front shape matched the travelling wave, and it would continue to follow the travelling wave thereafter.

Whereas, long time solutions assume a given liquid saturation moving arbitrarily far up from the travelling wave front, in nature, what is set is the infiltration rate (rate at which liquid enters the soil (Parlange 1972; Broadbridge and White 1988), or analogously (for the FDE) enters the foam (Brito-Parada et al. 2013)) rather than setting liquid saturation at the top. In the long time limit, where the gradient of liquid saturation is negligible near the top, all infiltration at the top is due to gravity. Hence, setting the infiltration rate at the top defines the liquid saturation and vice versa (in the long time limit).

For shorter times, however, when there are still significant gradients of liquid saturation near the top, it is not necessary to have a high liquid saturation right at the top to achieve the same infiltration rate, since only part of the infiltration is contributed by gravity, the rest being contributed by capillarity. It is possible to consider early-time solutions to Richards equation, in which liquid saturation at the top grows with time, rather than being fixed. There turns out to be a similarity solution (Broadbridge and White 1988; Witelski 1997; Caputo and Stepanyants 2008) in which liquid saturation is mostly uniform with height but shows a slight increase near the top localised over a small height.

The amount of the slight increase in liquid saturation gradually increases over time, as does the height over which it is registered. However, solutions at one time can be overlain with solutions at a different time by a suitable rescaling. In other words, the solutions at different times are self-similar provided we remain within the early-time limit. Note that because we are dealing with just slight increases over an initial liquid saturation in this limit, we should not need to know soil material properties over the entire range of liquid saturations, just the local behaviour near the initial saturation. We will not consider early-time similarity solutions any further in this paper having chosen to leave that aspect for future work, so we focussed instead on late-time travelling wave solutions for which porous media properties over the full range of saturations become pertinent.

We note however that early-time similarity solutions are found in broadly analogous multiphase flow systems (e.g. solid-liquid suspensions). Early on during gravity settling of a suspension, the suspension is mostly uniform, but the bottom of the suspension registers a small localised increase in solids fraction (Buscall and White 1987; Davis and Russel 1989): the amount increases, and the size of the region where it occurs grow over time. Likewise in pressure filtration of a suspension, early on, most of the suspension is uniform, with spatial change in solids fraction being confined to a thin layer, albeit the thickness of that layer grows in extent over time (Landman and White 1994).

7 Conclusion

We have considered solutions for Richards equation using relative hydraulic conductivity and relative diffusivity from Van Genuchten's soil functions (Van Genuchten 1980), and as well as the solution to two foam drainage equation variants. Specifically, we considered travelling wave behaviour which tends to set in at long times for typical infiltration conditions (Broadbridge and White 1988). In general, for Richards equation these solutions (Philip 1957a; Parlange 1971; Broadbridge and White 1988) have been obtained via Simpson's rule, although analytic approximations are available for very low moisture

content ($\Theta \ll 1$), and systems near saturation ($\Theta \rightarrow 1$) (Witelski 1997). Analytical travelling wave solutions are available for the channel- and node-dominated foam drainage cases for general Θ as originally derived by Koehler et al. (2000); Verbist and Weaire (1994); Verbist et al. (1996), with further simplifications in the $\Theta \ll 1$ and $\Theta \rightarrow 1$ limits.

The foam drainage travelling waves have been compared with those for Richards equation. It was found that travelling wave velocities v tend to be lower (see e.g. Fig. 5) in soils compared to foams. The only exceptions are for a soil that is already comparatively wet and then substantially more liquid is added to bring it close to full saturation. This behaviour follows from the shape of the soil relative hydraulic conductivity which is comparatively small for most moisture contents Θ , but which grows substantially near $\Theta = 1$.

Profiles of Θ versus spatial coordinate $\hat{\xi}$ indicate that rise in moisture content Θ with $\hat{\xi}$ is very abrupt (in the limit of small Θ values) in the case of soils (Richards equation). This contrasts with the FDE in which Θ rises much more gradually. As soon as a small Θ is detected at a certain depth, moisture contents much larger than before quickly follow. On the other hand, if Θ at a certain depth is found to be relatively large, the rate at which full saturation is reached in soil moving up in $\hat{\xi}$ is surprisingly slow: much slower than in the case of foams, as indeed follows from the $\Theta \rightarrow 1$ analytical asymptotic formulae that we present. These observations suggest how rapidly an irrigation system might need to be switched off once a predetermined saturation is achieved at a certain depth. Moreover, when one evaluates the total amount of water that has entered the soil behind a travelling wave that has penetrated to a certain depth, it turns out that (in relative terms) more water is added in the case of soil than foam. In other words, the “missing” moisture needed to attain full saturation is less for soil than for foam: this difference between soil and foam results from the abrupt changes in Θ with position in soils in the small Θ limit, notwithstanding the gradual changes seen for higher Θ . More generally, this shows that the solutions to Richards equation based on travelling waves are useful for understanding water transport in soils.

Appendix: Asymptotic Form of Relative Hydraulic Conductivity

The original relative hydraulic conductivity (hereafter RHC) used in this work is given by Eq. (18). It is observed in Sect. 3.2 (see e.g. Fig. 2b for Hygiene Sandstone) that the asymptotic function (20) obtained for $\Theta \approx 1$ overestimates RHC as $m \rightarrow 1$. Retaining an additional term in the asymptotic expansion of Eq. (18), we deduce another expression that also estimates the RHC as $\Theta \rightarrow 1$

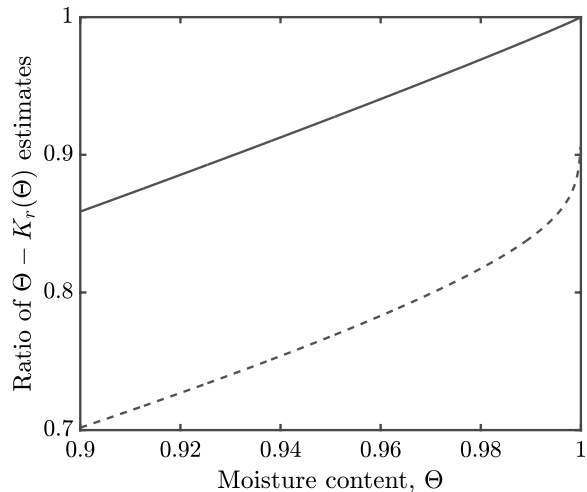
$$K_r(\Theta)|_{\Theta \approx 1} \approx \left(1 - \frac{2}{m^m}(1 - \Theta)^m - \frac{1}{2}(1 - \Theta)\right). \quad (44)$$

Hence,

$$\Theta - K_r(\Theta)|_{\Theta \approx 1} \approx \frac{2}{m^m}(1 - \Theta)^m - \frac{1}{2}(1 - \Theta). \quad (45)$$

For $m = 0.5146$ (silt loam) or $m = 0.6377$ (Guelph loam), the first term on the right hand side of (44) is dominant and the approximation considered in this “Appendix” is not required. However, for $m \rightarrow 1$, e.g. $m = 0.9038$ considered here for Hygiene Sandstone, the term $\frac{1}{2}(1 - \Theta)$ could be around one quarter of the value of $2m^{-m}(1 - \Theta)^m$. Dropping the $\frac{1}{2}(1 - \Theta)$ term, therefore causes $\Theta - K_r(\Theta)$ to be overestimated by a factor of 4/3. If we

Fig. 10 Comparison of the ratio between the true $\Theta - K_r(\Theta)$ and the approximation from Eq. (20), namely $\Theta - K_r(\Theta) \approx 1 - K_r(\Theta) \approx 2m^{-m}(1 - \Theta)^m$ (dashed lines) and also (solid line) the ratio of the true $\Theta - K_r(\Theta)$ to the approximate $\Theta - K_r(\Theta)$ in (45)



look at the ratio of the true $\Theta - K_r(\Theta)$ to an approximation based on just the first term $2m^{-m}(1 - \Theta)^m$, then the ratio could be around $\frac{3}{4}$ which is what we see for $m = 0.9038$ in Fig. 9b, where there is a range of Θ values for which the data stay close to 0.75. On the other hand, if we look at a ratio between the true $\Theta - K_r(\Theta)$ and the approximate formula (45), values much closer to unity result (see Fig. 10). Overestimating $\Theta - K_r(\Theta)$ causes us to underestimate $d\hat{\xi}/d\Theta$ and hence $\hat{\xi}$. Including an extra term in the estimate of $\Theta - K_r(\Theta)$ would improve the estimate of $d\hat{\xi}/d\Theta$ via (30) but would also preclude us from obtaining an analytical formula for $\hat{\xi}$ vs Θ close to $\Theta \approx 1$, so we do not pursue it in this paper.

Acknowledgements We thank Carlos Torres-Ulloa for help with MATLAB codes for this work.

Open Access This article is licensed under a Creative Commons Attribution 4.0 International License, which permits use, sharing, adaptation, distribution and reproduction in any medium or format, as long as you give appropriate credit to the original author(s) and the source, provide a link to the Creative Commons licence, and indicate if changes were made. The images or other third party material in this article are included in the article's Creative Commons licence, unless indicated otherwise in a credit line to the material. If material is not included in the article's Creative Commons licence and your intended use is not permitted by statutory regulation or exceeds the permitted use, you will need to obtain permission directly from the copyright holder. To view a copy of this licence, visit <http://creativecommons.org/licenses/by/4.0/>.

References

- Ahuja, L.R., Swartzendruber, D.: Horizontal soil-water intake through a thin zone of reduced permeability. *J. Hydrol.* **19**(1), 71–89 (1973)
- Anazadehsayed, A., Rezaee, N., Naser, J.: Numerical modelling of flow through foam's node. *J. Colloid Interface Sci.* **504**, 485–491 (2017)
- Anazadehsayed, A., Rezaee, N., Naser, J.: Exterior foam drainage and flow regime switch in the foams. *J. Colloid Interface Sci.* **511**, 440–446 (2018)
- Assouline, S., Tartakovsky, D.M.: Unsaturated hydraulic conductivity function based on a soil fragmentation process. *Water Resour. Res.* **37**(5), 1309–1312 (2001)
- Assouline, S., Tessier, D., Bruand, A.: A conceptual model of the soil water retention curve. *Water Resour. Res.* **34**(2), 223–231 (1998)
- Brito-Parada, P.R., Neethling, S.J., Cilliers, J.J.: Modelling the behaviour of the wetting front in non-standard forced foam drainage scenarios. *Colloids Surf. Physicochem. Eng. Aspects* **438**, 21–27 (2013)
- Broadbridge, P., White, I.: Constant rate rainfall infiltration: a versatile nonlinear model: 1. Analytic solution. *Water Resour. Res.* **24**(1), 145–154 (1988)
- Brooks, R.H., Corey, T.: Hydraulic properties of porous media. Colorado State University, Hydrology Papers (1964)
- Buckingham, E.: Studies on the movement of soil moisture. US Department of Agriculture Bureau of Soils Bulletin **38** (1907)

- Burdine, N.T.: Relative permeability calculations from pore size distribution data. *J. Pet. Technol.* **5**(03), 71–78 (1953)
- Buscall, R., White, L.R.: The consolidation of concentrated suspensions. Part 1. The theory of sedimentation. *J. Chem. Soc. Faraday Trans. Phys. Chem. Condens. Phases* **83**(3), 873–891 (1987)
- Caputo, J.G., Stepanyants, Y.A.: Front solutions of Richards' equation. *Transp. Porous Med.* **74**(1), 1–20 (2008)
- Celia, M.A., Bouloutas, E.T., Zarba, R.L.: A general mass-conservative numerical solution for the unsaturated flow equation. *Water Resour. Res.* **26**(7), 1483–1496 (1990)
- Cox, S.J., Weaire, D., Hutzler, S., Murphy, J., Phelan, R., Verbist, G.: Applications and generalizations of the foam drainage equation. *Proc. R. Soc. Lond. A Math. Phys. Eng. Sci.* **456**, 2441–2464 (2000)
- Davis, K.E., Russel, W.B.: An asymptotic description of transient settling and ultrafiltration of colloidal dispersions. *Phys. Fluids A Fluid Dyn.* **1**(1), 82–100 (1989)
- Gilding, B.H.: Qualitative mathematical analysis of the Richards equation. *Transp. Porous Med.* **6**(5–6), 651–666 (1991)
- Gol'dfarb, I.I., Kann, K.B., Shreiber, I.R.: Liquid flow in foams. *Fluid Dyn.* **23**(2), 244–249 (1988)
- Grassia, P., Cilliers, J.J., Neethling, S.J., Ventura-Medina, E.: Quasi-one-dimensional foam drainage. *Eur. Phys. J. E* **6**(4), 325–348 (2001)
- Kim, M.I., Chae, B.G., Nishigaki, M.: Evaluation of geotechnical properties of saturated soil using dielectric responses. *Geosci. J.* **12**(1), 83–93 (2008)
- Koehler, S.A., Hilgenfeldt, S., Stone, H.A.: Liquid flow through aqueous foams: the node-dominated foam drainage equation. *Phys. Rev. Lett.* **82**(21), 4232–4235 (1999)
- Koehler, S.A., Hilgenfeldt, S., Stone, H.A.: A generalized view of foam drainage: experiment and theory. *Langmuir* **16**(15), 6327–6341 (2000)
- Landman, K., White, L.: Solid/liquid separation of flocculated suspensions. *Adv. Colloid Interface Sci.* **51**, 175–246 (1994)
- Leonard, R.A., Lemlich, R.: A study of interstitial liquid flow in foam. Part I. Theoretical model and application to foam fractionation. *AIChE J.* **11**(1), 18–25 (1965)
- Mualem, Y.: A new model for predicting the hydraulic conductivity of unsaturated porous media. *Water Resour. Res.* **12**(3), 513–522 (1976)
- Neethling, S.J., Cilliers, J.J., Woodburn, E.T.: Prediction of the water distribution in a flowing foam. *Chem. Eng. Sci.* **55**(19), 4021–4028 (2000)
- Neethling, S.J., Lee, H.T., Cilliers, J.J.: A foam drainage equation generalized for all liquid contents. *J. Phys. Condens. Matter* **14**(3), 331–342 (2001)
- Or, D., Assouline, S.: The foam drainage equation for unsaturated flow in porous media. *Water Resour. Res.* **49**(10), 6258–6265 (2013)
- Parlange, J.Y.: Theory of water-movement in soils: 2. One-dimensional infiltration. *Soil Sci.* **111**(3), 170–174 (1971)
- Parlange, J.Y.: Theory of water-movement in soils 8. One-dimensional infiltration with constant flux at the surface. *Soil Sci.* **114**(1), 1–4 (1972)
- Patel, P.M., Pradhan, V.H.: Exact travelling wave solutions of Richards' Equation by modified F-expansion method. *Proc. Eng.* **127**, 759–766 (2015)
- Philip, J.R.: The theory of infiltration 1. The infiltration equation and its solution. *Soil Sci.* **83**(5), 345–358 (1957a)
- Philip, J.R.: The theory of infiltration: 2. The profile of infinity. *Soil Sci.* **83**(6), 435–448 (1957b)
- Philip, J.R.: Fifty years progress in soil physics. *Geoderma* **12**(4), 265–280 (1974)
- Princen, H.M., Kiss, A.D.: Osmotic pressure of foams and highly concentrated emulsions 2. Determination from the variation in volume fraction with height in an equilibrated column. *Langmuir* **3**(1), 36–41 (1987)
- Raats, P.A.C., Van Genuchten, M.T.: Milestones in soil physics. *Soil Sci.* **171**(6), S21–S28 (2006)
- Richards, L.A.: Capillary conduction of liquids through porous mediums. *Physics* **1**(5), 318–333 (1931)
- Stankovich, J.M., Lockington, D.A.: Brooks-Corey and van Genuchten soil–water–retention models. *J. Irrig. Drainage Eng.* **121**(1), 1–7 (1995)
- van Duijn, C.J., Mitra, K., Pop, I.S.: Travelling wave solutions for the Richards equation incorporating non-equilibrium effects in the capillarity pressure. *Nonlinear Anal. Real World Appl.* **41**, 232–268 (2018)
- Van Genuchten, M.T.: A closed-form equation for predicting the hydraulic conductivity of unsaturated soils. *Soil Sci. Soc. Am. J.* **44**(5), 892–898 (1980)
- Van Genuchten, M.T., Nielsen, D.R.: On describing and predicting the hydraulic properties of unsaturated soils. *Ann. Geophys.* **3**, 615–628 (1985)
- Verbist, G., Weaire, D.: A soluble model for foam drainage. *EPL (Europhys. Lett.)* **26**(8), 631 (1994)
- Verbist, G., Weaire, D., Kraynik, A.M.: The foam drainage equation. *J. Phys. Condens. Matter* **8**(21), 3715–3731 (1996)

- Vogel, T., Cislerova, M.: On the reliability of unsaturated hydraulic conductivity calculated from the moisture retention curve. *Transp. Porous Med.* **3**(1), 1–15 (1988)
- Weaire, D., Phelan, R.: The physics of foam. *J. Phys. Condens. Matter* **8**(47), 9519–9524 (1996)
- Weaire, D.L., Hutzler, S.: *The physics of foams*. Clarendon Press, Oxford (2001)
- Witelski, T.P.: Perturbation analysis for wetting fronts in Richard's Equation. *Transp. Porous Med.* **27**(2), 121–134 (1997)
- Zlotnik, V.A., Wang, T., Nieber, J.L., Šimunek, J.: Verification of numerical solutions of the Richards equation using a traveling wave solution. *Adv. Water Resour.* **30**(9), 1973–1980 (2007)

Publisher's Note Springer Nature remains neutral with regard to jurisdictional claims in published maps and institutional affiliations.

Sensitivity of Travelling Wave Solutions to Richards Equation to Soil Material Property Functions

This chapter is prepared in the format of a Transport in Porous Media manuscript but it has not been submitted. The authors are Yaw A. Boakye-Ansah and Paul Grassia. This chapter focuses on the sensitivity of the travelling wave solutions for Richards equation given in Chapter 6 to those soil material property functions that are employed in its solution. Particularly for this study, the van Genuchten capillary suction head is varied in such a manner that it goes smoothly (not abruptly) to zero at full saturation. This was done via constructing a convex hull around the original capillary suction head function using information about the inflection point in this function. This new convex hull head is used with an existing relative hydraulic conductivity function to obtain a new relative diffusivity which was also scaled to be unity at full saturation. Logarithmic travelling profiles are obtained similar to those for the foam drainage equations, but different from the power law behaviour seen in Richards equation without the convex hull variants.

Overview

As previously stated (see Chapter 3), Richards equation which describes transport of water in undersaturated soils requires as input, soil material property functions specifically relative hydraulic conductivity (RHC) and relative diffusivity (RD) which are typically obtained from

the soil-water retention curve (SWRC) function (which is reformulated as a capillary suction-head vs moisture content) in order to solve it. Travelling wave solutions to Richards equation (profiles of height coordinate ξ vs moisture content Θ) using van Genuchten's form of the soil material property functions diverge to arbitrarily large height values close to full saturation. This results from the RD function itself diverging at full saturation, a behaviour imported both from the capillary suction head and the PCM used to obtain RHC: specifically the derivative of the capillary suction head diverging, and the PCM approaching unity lead to divergence of the RD (as Chapter 6 shows).

Analysis of the travelling wave solution to Richards equation highlighted the influence of soil material property functions, particularly relative diffusivity, on the shape and nature of the travelling wave profile as shown in Chapter 6. In determining the relative diffusivity, the first derivative of capillary suction head is used with the relative conductivity function (also obtained via a PCM using the capillary suction head). Therefore, any singular behaviour in the capillary head is magnified in the relative diffusivity function.

In this work, using a newly derived suction head function with the existing Brooks and Corey [56] relative hydraulic conductivity, a new relative diffusivity function is developed to enable us solve the Richards equation. This relative diffusivity function can be scaled to be unity at full saturation $\Theta = 1$ to enable a "fairer" comparison with the foam drainage equations. An RHC is not derived with this new head function since the PCM used does not allow the expression for RHC to converge with the new head function. This is embedded in how these PCMs behave (this is discussed in detail in the appendix section of the manuscript attached in this chapter).

In order to use this newly deduced and rescaled diffusivity function, Richards equation must be rescaled to match it. By definition, the original D_r given by van Genuchten diverges at full saturation. By capping the head which leads to this behaviour by some value, a new relative diffusivity function may be obtained. By choosing different space and time scaling coordinates, a rescaled and new dimensionless form for Richards equation can be obtained. This new equation is equivalent to the foam drainage equations in that both the relative hydraulic conductivity and relative diffusivity functions go to unity at full saturation, equivalent to how the foam drainage equations have been composed in this research. Subsequently, the travelling wave formulation already given and used in Chapter 6 is applied to obtain

solutions.

New numerical travelling wave solutions are derived for Richards equation. Asymptotic behaviour was studied at both dry and wet saturation limits to elucidate behaviours in those regions. Power law behaviour was obtained at very low moisture content which can be shown to be equivalent to the solutions obtained for Richards equation and foam drainage equation in Chapter 6. At full saturation however, a logarithmic relationship was obtained between vertical position $\hat{\xi}$ and moisture content Θ which lead to $\hat{\xi}$ values smaller than those obtained for the FDEs, and much smaller than the Richards equation solutions for $\hat{\xi}$ using the original set of van Genuchten soil parameters [68] (see Chapter 6 in this thesis).

Publication C

Sensitivity of Travelling Wave Solutions to Richards Equation to Soil Material Functions

Sensitivity of Travelling Wave Solution to Richards Equation to Soil Material Property Functions

Y. A. Boakye-Ansah · P. Grassia

Received: date / Accepted: date

Abstract Richards equation describes transport of water in soils, but requires as input soil material property functions specifically relative hydraulic conductivity and relative diffusivity typically obtained from the soil-water retention curve (SWRC) function (expressed in terms of capillary suction head). These properties are often expressed via particular functional forms, with different soil types from sandstones to loams being represented within those functional forms by a free fitting parameter m typically in the domain $m < 1$. Travelling wave solutions (profile of height $\hat{\xi}$ against moisture content Θ) to Richards equation using van Genuchten's form of the soil material property functions diverge to arbitrarily large height close to full saturation. This results from the relative diffusivity function itself diverging at full saturation as a consequence of a weak singularity in the SWRC in that limit. If however soil material property data are sparse near full saturation, evidence for that divergence may be limited. In this work, we rescale the relative diffusivity to approach unity at full saturation. This is achieved by removing a singularity from the original van Genuchten SWRC function by constructing a convex hull around it. We thereby propose a piecewise SWRC function that predicts capillary suction head approaches zero smoothly at full saturation. We use this SWRC function with the Brooks-Corey relative hydraulic conductivity to develop a new relative diffusivity function and proceed to solve Richards equation. We obtain logarithmic relationships between profile of height $\hat{\xi}$ and moisture content Θ close to saturation. Predicted profile $\hat{\xi}$ values are smaller than the heights obtained for the original solution of Richards equation which exhibit power law behaviour.

Y. A. Boakye-Ansah

Present address: Department of Chemical and Process Engineering, University of Strathclyde, James Weir Building, 75 Montrose Street, Glasgow, G1 1XJ, UK

E-mail: yaw.boakye-ansah@strath.ac.uk

Department of Energy and Petroleum Engineering, University of Energy and Natural Resources, Ghana

E-mail: yaw.boakye-ansah@uenr.edu.gh

P. Grassia

Department of Chemical and Process Engineering, University of Strathclyde, James Weir Building, 75 Montrose Street, Glasgow, G1 1XJ, UK

E-mail: paul.grassia@strath.ac.uk

1 Introduction

Modelling flow in porous media is important not only in groundwater flow but in many other areas such as suspension dewatering (Aziz et al., 2000; Buscall and White, 1987) and fluid recovery, e.g. oil recovery (Ahmed, 2006; Grassia et al., 2014). Study of this phenomenon requires detailed and careful formulation of the governing equations which depend not only on the fluid, but also on the properties of the porous media in question. In particular, Richards equation (hereafter RE) is the fundamental equation used to describe groundwater flow (Richards, 1931).

In order to solve RE, we require soil material property (hydraulic) functions, namely, capillary suction head, relative hydraulic conductivity (RHC) and relative diffusivity (RD). Using the soil-water retention curve (SWRC) which gives the relationship between capillary suction head and moisture content present in the soil, the latter two functions can also be derived (van Genuchten, 1980). Usually, an analytical SWRC is used with a predictive conductivity model (hereafter PCM) to determine the RHC (van Genuchten, 1980; Assouline, 2001). This RHC is then used with the derivative of capillary suction head to determine the relative diffusivity. Since the SWRC is used to predict these other hydraulic functions, it is important to have a reasonably accurate representation of the retention curve.

A number of functional forms for SWRC are available in literature (Assouline et al., 1998; Brooks and Corey, 1964; Fredlund and Xing, 1994; van Genuchten, 1980). Among those commonly used are the ones proposed by Brooks-Corey (Brooks and Corey, 1964) and van Genuchten (van Genuchten, 1980). The Brooks-Corey SWRC model is described as accurate at low moisture content but less accurate near full saturation (Assouline et al., 1998; Stankovich and Lockington, 1995). Additionally, it goes to a finite capillary suction-head value at full saturation, whereas zero capillary suction is expected in that limit. The van Genuchten SWRC model is similar to Brooks-Corey at low saturation but matches field data more accurately at higher saturation than the Brooks-Corey SWRC does (Assouline et al., 1998; Stankovich and Lockington, 1995; Vogel and Cislserova, 1988). It goes to zero suction pressure at full saturation, but at the expense, as we will see, of introducing a singularity near full saturation. Specifically, the derivative of the suction pressure is infinite at full saturation. The van Genuchten model achieves this by introducing an inflection point in the SWRC which is absent in the Brooks-Corey model (Stankovich and Lockington, 1995). In van Genuchten's SWRC, the derivative of the SWRC increases moving in either direction away from the inflection point. We shall focus on the van Genuchten SWRC in this paper. The concern addressed here however is that when one is trying to fit van Genuchten SWRC to experimental data, unless a significant amount of experimental data are available in the neighbourhood of full saturation, it is uncertain whether the singular behaviour of the van Genuchten model predicted in that limit really is an accurate reflection of the true SWRC. In view of that, there is scope for exploring variants of the SWRC which do not exhibit such singularities.

As mentioned earlier, a so-called predictive conductivity model (hereafter PCM) can be employed with a SWRC function to obtain the relative hydraulic conductivity (RHC) (Assouline and Tartakovsky, 2001; Burdine, 1953; Mualem, 1976; van Genuchten, 1980). The derivation and application of a PCM is discussed further in Appendix A. By definition, the RHC should approach unity as the system approaches full saturation. It is defined as conductivity relative to the conductivity at full saturation. As we see in Appendix A, the singularity in the SWRC is needed to keep the RHC finite at saturation, at least if a PCM is used. Between the two most commonly used PCM, namely the Burdine (1953) and Mualem (1976) models, the Mualem model is claimed to match field data more accurately and is

thus more commonly used (Assouline and Tartakovsky, 2001; van Genuchten, 1980). Using the Mualem PCM, the singularity in the SWRC predicts a RHC that goes to unity abruptly, again with a derivative that is singular. Similarly, due to this SWRC singularity, the relative diffusivity (which is obtained as a product of the relative hydraulic conductivity and the derivative of the capillary suction head) diverges at full saturation. A consequence of this (as Appendix A explains) is that, if we alter the SWRC to avoid a singularity at full saturation the PCM fails to converge, so we also must alter the conductivity model employed.

As previously deduced (Boakye-Ansah and Grassia, 2021), Richards equation admits travelling wave solutions (profile of height ξ against moisture content Θ) using the hydraulic functions given by van Genuchten (1980). These travelling waves were shown to have known asymptotic analytical forms both in the limit of very low ($\Theta \ll 1$) and large ($\Theta \approx 1$) moisture content. The obtained analytical travelling wave solutions show a power law behaviour in these limits. In particular at $\Theta \approx 1$, the travelling wave solution diverges to infinity as a power law due to the behaviour of relative diffusivity at full saturation. Specifically, height ξ scales as a negative power of $(1 - \Theta)$, the exponent of the power law depending on soil properties. Thus, Θ only approaches full saturation over very large vertical distances, or equivalently at given height ξ , the system can remain surprisingly far away from full saturation.

Previous work (Boakye-Ansah and Grassia, 2021) has shown strong physical and mathematical analogies between foam drainage and Richards equation, foams having a capillary pressure (analogous to the SWRC) and also an analogue of a relative hydraulic conductivity and a relative diffusivity. Unlike the case with Richards equation, these functions do not exhibit singularities in the limit as a foam breaks up into a bubbly liquid (the analogue of what would be considered full saturation in a porous medium). The resulting travelling wave solution for profile of height ξ against moisture content Θ no longer has a power law divergence, but rather diverges less strongly, i.e. logarithmically. Near saturation conditions are thereby attained at far more modest heights. An interesting question is whether, in the case of soils with singularities in the SWRC removed, the behaviour will be similar to the original travelling wave solutions for soils, or whether instead they will be more akin to those results for foam drainage.

To summarise, this work seeks to explore the possibility and consequence of removing the singularity from the SWRC function, and to evaluate the impact of this change on the travelling wave solution to Richards equation. We shall explore numerical and approximate asymptotic travelling wave solutions when the singularities for these soil material properties are relaxed. We find that the travelling wave solutions obtained show a logarithmic law in the region of large moisture content as has been obtained for the two foam drainage equation variants in the same limit.

This paper is laid out as follows: in Section 2, we review the fundamental equations that govern fluid flow in unsaturated soils and in foams. We focus on Richards equation and its dimensionless form, and we give the foam drainage equations and corresponding solutions also. In the next section, namely Section 3, we analyse the equations used to describe the soil material property functions showing how singularities can be removed by suitably modifying the material properties in the governing equation. If SWRC data are sparse near full saturation, there is limited justification for selecting the original singular SWRC over the non-singular variants we derive. We present the results and discussion for profile of heights ξ vs moisture content Θ in Section 4, and then conclude the paper in Section 5. A key result we will find is that close to saturation, the travelling wave solutions from the modified RE behave more similarly to the foam drainage solutions, than to the original RE ones.

2 Governing Equations

We now present the governing equations that we shall use in this work, namely, Richards equation and foam drainage equation. The travelling wave solutions for foam drainage are available (Boakye-Ansah and Grassia, 2021; Cox et al., 2000; Verbist et al., 1996) and shall thus not be rederived. The solutions are merely quoted in this paper. Later on, we also rescale the Richards equation to match the foam drainage equation by rescaling the relative diffusivity to be unity at full saturation since the foam drainage diffusivities already have that property. This will allow for easier comparison of solutions.

2.1 Foam Drainage Equations

We know from literature that there are two main equations that are used to describe drainage in foams. These are the channel-dominated (CD FDE) (Verbist et al., 1996; Weaire and Phelan, 1996) and node-dominated (ND FDE) (Koehler et al., 1999, 2000) foam drainage equations, and they differ according to whether dissipation in the foam is assumed to take place in Plateau border (PB) channels or vertex nodes, respectively. The equations are thus given in dimensionless form as

$$\frac{\partial \Theta}{\partial \hat{\tau}} - \frac{\partial}{\partial \hat{\xi}} \cdot \sqrt{\Theta} \frac{\partial \Theta}{\partial \hat{\xi}} - \frac{\partial \Theta^2}{\partial \hat{\xi}} = 0, \quad (1)$$

and

$$\frac{\partial \Theta}{\partial \hat{\tau}} - \frac{\partial}{\partial \hat{\xi}} \cdot \frac{\partial \Theta}{\partial \hat{\xi}} - \frac{\partial \Theta^{3/2}}{\partial \hat{\xi}} = 0, \quad (2)$$

where equations (1) and (2) are respectively the channel-dominated and node-dominated foam drainage equation. Here, $\hat{\tau}$ is a rescaled dimensionless time and $\hat{\xi}$ is a rescaled dimensionless vertical coordinate measured upward. Details of how to make the equations dimensionless can be found in Boakye-Ansah and Grassia (2021). Also, Θ denotes here not the absolute moisture content in the foam, but rather the relative moisture content, relative to the point at which the foams breaks up into a bubbly liquid. By analogy with Section 2.2 presented later on, we observe that the analogous values to relative hydraulic conductivity (Θ^2 & $\Theta^{3/2}$) and relative diffusivity ($\sqrt{\Theta}$ & 1) are known (for CD and ND FDE respectively), and these go to finite unit values when the system reaches full saturation (i.e. $\Theta = 1$). We examine the travelling wave solution $\Theta(\hat{\xi}, \hat{\tau}) = \Theta(\hat{\xi} + v\hat{\tau})$ for foam drainage. If we consider $\Theta = 1$ upstream and $\Theta = 0$ downstream, then it is possible to show that $v = 1$ (both for CD and ND FDE). After taking the first integral (Boakye-Ansah and Grassia, 2021), we can compute the shape of the travelling wave expressed in the form $\hat{\xi}$ vs. Θ . We deduce for CD FDE,

$$d\hat{\xi}/d\Theta = 1/(\sqrt{\Theta}(1-\Theta)), \quad (3)$$

and for ND FDE,

$$d\hat{\xi}/d\Theta = 1/(\Theta(1-\sqrt{\Theta})). \quad (4)$$

Integrating again, we obtain for CD FDE,

$$\hat{\xi} = 2 \operatorname{arctanh} \sqrt{\Theta}, \quad (5)$$

and for ND FDE,

$$\hat{\xi} = 2 \log(\sqrt{\Theta}/(1-\sqrt{\Theta})). \quad (6)$$

Their asymptotic solutions are for CD FDE,

$$\hat{\xi} \Big|_{\Theta \ll 1} \approx 2\sqrt{\Theta}; \quad \hat{\xi} \Big|_{\Theta \approx 1} \approx \log(1/(1-\Theta)) + \log 4, \quad (7)$$

while for ND FDE, we deduce

$$\hat{\xi} \Big|_{\Theta \ll 1} \approx \log(\Theta); \quad \hat{\xi} \Big|_{\Theta \approx 1} \approx 2 \log(1/(1-\Theta)) + \log 4, \quad (8)$$

where the terms $\log 4$ in (7)–(8) are needed to match with (5)–(6). The behaviour in the $\Theta \rightarrow 0$ limit are clearly very different ($\hat{\xi} \rightarrow 0$ in one case and $\hat{\xi} \rightarrow \infty$ in the other), but we focus here on the $\Theta \approx 1$ behaviour. It is clear that the ND FDE predicts a $\hat{\xi}$ roughly twice the CD FDE value.

2.2 Richards Equations

In solving for the Richards equation, we have previously used (Boakye-Ansah and Grassia, 2021) a diffusivity function that diverges at full saturation. Soil-water diffusivity functions that diverge at full saturation are commonly employed to solve Richards equation (Ahuja and Swartzendruber, 1972). This is certainly the case using the van Genuchten (1980) model and it is unavoidable with that model (see Appendix A). Clearly, if diffusivity diverges at full saturation, there is no scope to rescale it to obtain a relative diffusivity that is unity in that limit. This behaviour does not then allow for an equal comparison with foam drainage, neither with the channel-dominated case nor with the node-dominated FDE since their relative diffusivity functions ($\sqrt{\Theta}$ and 1 respectively) go to unity at full saturation. In what follows, we depart from the van Genuchten model in order to formulate a variant of Richards equation with a finite relative diffusivity in the $\Theta \rightarrow 1$ limit that allows for a rescaled relative diffusivity (given in Section 3.3) which is equal to 1 when moisture content is unity ($\Theta = 1$). For the moment however, we consider Richards equation as originally formulated.

2.2.1 Rescaling Richards Equation

The moisture-based Richards equation is given as (Philip, 1957; Celia et al., 1990),

$$\partial \theta / \partial t - \nabla \cdot D(\theta) \nabla \theta - \partial K(\theta) / \partial z = 0. \quad (9)$$

Here, θ is volumetric moisture content, t is time, $D(\theta)$ is diffusivity, $K(\theta)$ is hydraulic conductivity and z is depth of infiltration (measured positive upward). The relative/rescaled moisture content which describes the volumetric moisture content θ , is given as

$$\Theta = (\theta - \theta_r) / (\theta_s - \theta_r), \quad (10)$$

where θ_r and θ_s are residual and saturated moisture content respectively.

After suitable nondimensionalization of equation (9), we deduce (Boakye-Ansah and Grassia, 2021)

$$\frac{\partial \Theta}{\partial \tau} - \frac{\partial}{\partial \xi} \cdot D_r(\Theta) \frac{\partial \Theta}{\partial \xi} - \frac{\partial K_r(\Theta)}{\partial \xi} = 0, \quad (11)$$

which is the dimensionless Richards equation. Here τ is dimensionless time, ξ is dimensionless spatial coordinate (measured upwards), $K_r(\Theta)$ is relative hydraulic conductivity and $D_r(\Theta)$ is relative diffusivity. Note that

$$D_r(\Theta) = K_r(\Theta) |dH_+ / d\Theta|, \quad (12)$$

where $H_+(\Theta)$ is dimensionless capillary suction-head. More discussion of the functional form of H_+ will be given in Section 3. Strictly speaking, capillary suction-head H is negative, but we define $H_+ = -H$ to obtain a positive quantity. However, H_+ decreases as Θ increases, so $dH_+/d\Theta$ is negative but its absolute value $|dH_+/d\Theta|$ is positive. Here $\lim_{\Theta \rightarrow 1} K_r = 1$ by definition but $\lim_{\Theta \rightarrow 1} D_r = \lim_{\Theta \rightarrow 1} |dH_+/d\Theta|$.

Even though $\lim_{\Theta \rightarrow 1} K_r = 1$ as we have said, making (11) directly comparable with the foam drainage equations (3)–(4) is problematic as was alluded to previously, since according to the van Genuchten formula for suction head H_+ , it turns out $\lim_{\Theta \rightarrow 1} |dH_+/d\Theta| \rightarrow \infty$. Thus, $\lim_{\Theta \rightarrow 1} D_r(\Theta) \rightarrow \infty$. We can however resolve this by capping the value of $dH_+/d\Theta$ at some value β rather than letting it diverge as van Genuchten would (more details of this in Section 3.3). We then take $D_r = \beta \hat{D}_r$ with \hat{D}_r being a rescaled relative diffusivity. This helps to achieve our aim of making the Richards equation relative diffusivity comparable to the foam drainage relative diffusivity (see Section 3.3). We now choose $\hat{\tau} = \beta^{-1}\tau$ and $\hat{\xi} = \beta^{-1}\xi$. From these definitions and equation (11), we obtain a new dimensionless form for Richards equation,

$$\frac{\partial \Theta}{\partial \hat{\tau}} - \frac{\partial}{\partial \hat{\xi}} \cdot \hat{D}_r(\Theta) \frac{\partial \Theta}{\partial \hat{\xi}} - \frac{\partial K_r(\Theta)}{\partial \hat{\xi}} = 0. \quad (13)$$

This form of Richards equation is scaled to be equivalent to the foam drainage equations (1)–(2) since both relative hydraulic conductivity and relative diffusivity are scaled to become unity at full saturation.

Following from previous derivations, we look for travelling wave solution to Richards equation of the form $\Theta = \Theta(\hat{\xi} + v\hat{\tau})$. If we impose conditions $\Theta = 1$ upstream, and $\Theta = 0$ downstream, then again $v = 1$ and the equation for $\hat{\xi}$ turns out to be,

$$\frac{d\hat{\xi}}{d\Theta} = \frac{\hat{D}_r(\Theta)}{\Theta - K_r(\Theta)}, \quad (14)$$

upon which we shall base all our solutions (and then compare with equations (5)–(6)).

The solutions to Richards equation will be studied in further detail in Section 4. Before that however, we need to supply the soil material property functions $K_r(\Theta)$ and $\hat{D}_r(\Theta)$.

3 Soil Material Property Functions

In this section, we consider the equations that we shall employ in this paper to model the properties of the porous media. We first study the capillary suction head by formulating a new equation based on the existing van Genuchten one. The new equation goes smoothly to zero suction at full saturation and is realised by constructing a convex hull around the original van Genuchten capillary suction-head. We subsequently focus on the relative hydraulic conductivity model we shall use, and thence develop the relative diffusivity function.

Throughout, we work in terms of dimensionless variables as was done by [Boakye-Ansah and Grassia \(2021\)](#); the conversions between dimensional and dimensionless variables are again detailed by [Boakye-Ansah and Grassia \(2021\)](#).

3.1 Capillary Suction Head

[Brooks and Corey \(1964\)](#) proposed an SWRC (head) function given as

$$H_+ = \Theta^{-1/\lambda}, \quad (15)$$

where λ is the pore-size distribution parameter. This SWRC is reported to be very accurate for dry systems ($\Theta \ll 1$) but less so as $\Theta \rightarrow 1$ (Assouline et al., 1998; Stankovich and Lockington, 1995; Vogel and Cislserova, 1988). Note in particular that this function does not go to zero ($H_+ \neq 0$) as $\Theta \rightarrow 1$. van Genuchten (1980) modified equation (15) by choosing a formula that agrees with it in the dry ($\Theta \ll 1$) limit but which has $H_+ \rightarrow 0$ when $\Theta \rightarrow 1$ albeit with an abrupt approach to $H_+ \rightarrow 0$. The van Genuchten (1980) SWRC function has been described as performing better than the Brooks-Corey SWRC function near full saturation (Assouline et al., 1998). The van Genuchten SWRC function is given as

$$\Theta = [1/(1 + H_+^n)]^m; \quad H_+ = (\Theta^{-1/m} - 1)^{1/n}; \quad H_+ = (\Theta^{-1/m} - 1)^{1-m}, \quad (16)$$

where in the first instance m and n are independent parameters but for the Mualem predictive conductivity model (PCM) (van Genuchten, 1980), $m = 1 - 1/n$ (and the Brooks-Corey λ can be identified with $\lambda = m/(1 - m)$). The parameter m can be considered to determine the type of soils, with $m \rightarrow 1$ corresponding to sandstone and significantly smaller m (down to about $m \approx 1/2$) corresponding to clayey loams. Appendix A discusses how m influences pore size distribution, particularly in the limit of large pores. The Mualem choice of $m = 1 - 1/n$ by van Genuchten (1980) fits experimental data less well than keeping m & n general, but since a general form leads to more complicated expressions for material property functions (van Genuchten and Nielsen, 1985), we choose to retain $m = 1 - 1/n$ as given by van Genuchten (1980).

Note that, the derivative of (16) diverges as $\Theta \rightarrow 1$. In this limit (16) can be written as

$$H_+ \approx ((1 - \Theta)/m)^{1-m}, \quad (17)$$

so that

$$\left| \frac{dH_+}{d\Theta} \right| \approx \frac{(1-m)}{m^{1-m}} (1-\Theta)^{-m}. \quad (18)$$

If the data that one is using to fit the H_+ vs Θ profile comes primarily from the dry region ($\Theta \ll 1$), it may be difficult to distinguish Brooks-Corey head function from van Genuchten head. Under these circumstances, it may also be difficult to decide whether the details of how van Genuchten head approaches zero in the $\Theta \rightarrow 1$ are correct. Particularly, it may be difficult to decide whether the SWRC/head function really exhibits a singular behaviour approaching full saturation. Alternatives to equation (16) are therefore worth exploring.

3.1.1 Developing New Head Function

We can identify a point at which (16) definitely differs from (17), namely an inflection point at which (16) admits $d^2H_+/d\Theta^2 = 0$, whereas (17) never has an inflection point. We identify the inflection point of equation (16) by setting a double differential to zero as

$$\frac{d^2H_+}{d\Theta^2} = \frac{(1+m)(1-m)}{m^2} \frac{(\Theta^{-1/m} - 1)^{-m}}{\Theta^{1/m+2}} - \frac{(1-m)}{m} \frac{(\Theta^{-1/m} - 1)^{-1-m}}{\Theta^{2/m+2}} = 0, \quad (19)$$

for which we obtain

$$\Theta_{\text{infl}} = (1+m)^{-m}, \quad (20)$$

the value of which is given for different soils in Table 1.

As alluded to above, this inflection point in the van Genuchten SWRC equation (16) indicates a clear departure from the Brooks-Corey SWRC equation (15). It marks a point

where $|dH_+/d\Theta|$ in the SWRC stops decreasing and starts increasing again. The Brooks-Corey SWRC by contrast has a $|dH_+/d\Theta|$ that decreases monotonically. If the parameter m in the van Genuchten SWRC has been estimated based on fitting to data with $\Theta < \Theta_{\text{inf}}$ it becomes very difficult to distinguish van Genuchten SWRC from Brooks-Corey SWRC. In a situation like that, we can modify the van Genuchten SWRC by constructing a convex hull around it. The convex hull will agree with the van Genuchten SWRC for $\Theta \ll 1$ but with $H_+ \rightarrow 0$ as $\Theta \rightarrow 1$, albeit now having $|dH_+/d\Theta|$ being a monotonically decreasing function as Θ increases (hence, no inflection point). If available data for constructing the SWRC tend to be weighted towards small Θ , there is little evidence to support choosing the original van Genuchten SWRC over the convex hull variant.

The convex hull can be constructed by finding a so-called point of tangency Θ_t , and drawing a straight line from $(\Theta_t, H_+(\Theta_t))$ to $(1, 0)$. The value of Θ_t is less than Θ_{inf} and satisfies

$$1 - \Theta_t = \frac{H_+(\Theta_t)}{|dH_+/d\Theta|_{\Theta=\Theta_t}}, \quad (21)$$

where Θ_t is the value of Θ at tangency for each profile with different m (different soil type). We obtain

$$1 - \Theta_t = \frac{m}{(1-m)} \frac{(\Theta_t^{-1/m} - 1)}{\Theta_t^{-(1+1/m)}}; \quad \Theta_t = \frac{1-m}{1-m\Theta_t^{1/m}}, \quad (22)$$

after some algebra. The exact value for Θ_t for each m is obtained via Newton-Raphson method, and it markedly decreases as $m \rightarrow 1$. Table 1 gives the Θ_t values for three different soil types. Note that $\Theta_t < \Theta_{\text{inf}}$ always. Having identified Θ_t , we define the new (piecewise) head function as

$$H_{+(\text{new})}(\Theta, m) = \begin{cases} H_+(\Theta), & \text{if } \Theta \leq \Theta_t \\ H_+(\Theta)_{\Theta=\Theta_t} - |H'_+(\Theta)|_{\Theta=\Theta_t}(\Theta - \Theta_t), & \text{if } \Theta > \Theta_t. \end{cases} \quad (23)$$

Substituting equation (16) in (23), we obtain

$$H_{+(\text{new})}(\Theta, m) = \begin{cases} (\Theta^{-1/m} - 1)^{1-m}, & \text{if } \Theta \leq \Theta_t \\ (\Theta_t^{-1/m} - 1)^{1-m} - \left| \frac{(1-m)}{m} \cdot \frac{(\Theta_t^{-1/m} - 1)^{-m}}{\Theta_t^{1+1/m}} \right| (\Theta - \Theta_t), & \text{if } \Theta > \Theta_t, \end{cases} \quad (24)$$

which can also be presented as

$$H_{+(\text{new})}(\Theta, m) = \begin{cases} (\Theta^{-1/m} - 1)^{1-m}, & \text{if } \Theta < \Theta_t \\ \left| \frac{(1-m)}{m} \frac{(\Theta_t^{-1/m} - 1)^{-m}}{\Theta_t^{1+1/m}} \right| (1 - \Theta), & \text{if } \Theta > \Theta_t. \end{cases} \quad (25)$$

Fig. 1 shows a profile of equations (16) and (24). In contrast with equation (16), by construction (24) goes smoothly to zero at full saturation. Additionally, there is no inflection point in this latter equation. Instead, $|dH_+/d\Theta|$ decreases monotonically until Θ_t after which it remains fixed. Note that although equations (23)–(24) clearly give a different function from (16) by introducing a convex hull, we have not introduced any additional free-fitting parameters in (23)–(24). The parameter Θ_t is a well defined function of m , not a free parameter. Thus (23)–(24) can be viewed as a variant of equation (16) that approaches $H_+ \rightarrow 0$ smoothly

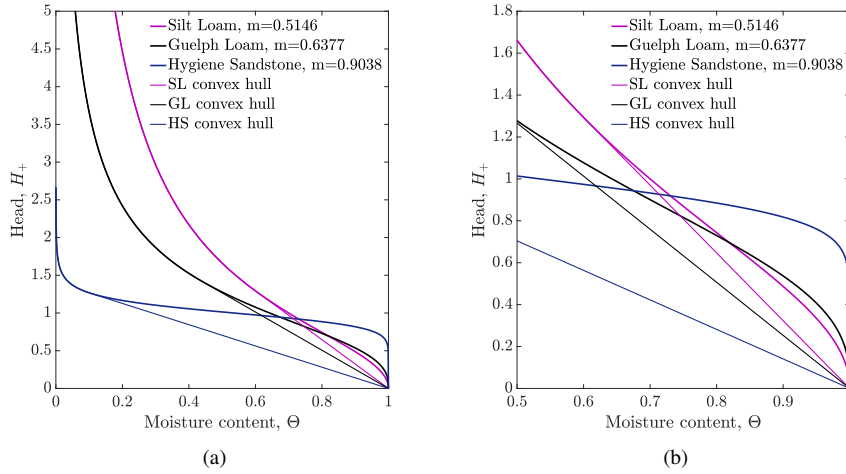


Fig. 1 Capillary suction head (24) profile for three soil samples. The thick lines are plotted using (16) whereas the thin lines represent those from (25). The profile in (a) covers the entire moisture content range while (b) is a zoomed in view near $\Theta \rightarrow 1$.

as $\Theta \rightarrow 1$ but which does not contain any additional fitting parameters. Not introducing new parameters was the rationale for using a convex hull rather than some other variant of the original van Genuchten SWRC.

In what follows, we use the function $H_{+(new)}$ exclusively instead of the original H_+ . For compactness of notation, we now start to denote this simply by H_+ .

$$\left| \frac{dH_+}{d\Theta} \right| = \begin{cases} \frac{(1-m)}{m} \frac{(\Theta^{-1/m} - 1)^{-m}}{\Theta^{1+1/m}}, & \text{if } \Theta \leq \Theta_t \\ \frac{(1-m)}{m} \frac{(\Theta_t^{-1/m} - 1)^{-m}}{\Theta_t^{1+1/m}}, & \text{if } \Theta > \Theta_t, \end{cases} \quad (26)$$

Table 1 Soil-specific properties of the three example soils. Values of m are reported in van Genuchten (1980).

Soil	m	Θ_{infl}	Θ_t	$ dH_+/d\Theta _{\Theta=\Theta_t}$	c_m	\hat{c}_m
Silt Loam	0.5146	0.8076	0.5996	3.2330	0.2918	0.1194
Guelph Loam	0.6377	0.7301	0.4395	2.5327	0.2243	0.1085
Hygiene Sandstone	0.9038	0.5588	0.1039	1.4085	0.0759	0.0471

3.2 Relative Hydraulic Conductivity

The relative hydraulic conductivity (RHC) of porous media describes the relationship between unsaturated hydraulic conductivity and water content (Assouline and Or, 2013; Or

and Assouline, 2013). It is required for formulation of Richards equation (RE) describing unsaturated flow in soils. RHC may be obtained experimentally but this is tedious, time consuming and expensive (Assouline, 2001; Assouline et al., 1998; Or and Assouline, 2011). Thus, a model or mathematical function that can predict RHC is usually employed (Assouline, 2001). One such model is the predictive conductivity model (PCM). The way in which a PCM converts a H_+ vs Θ profile into a K_r vs Θ is detailed in Appendix A. A specific RHC is obtained by inserting a particular soil-water retention curve SWRC function in this PCM. The theory underlying these PCMs involves a number of assumptions which are never perfectly accurate, so whilst the PCM is often useful, it does not provide an exact representation of K_r vs Θ (Or and Assouline, 2013; van Genuchten and Nielsen, 1985; Vogel and Cislerova, 1988). Thus, even deploying a PCM it is not always possible to obtain RHC which closely match field data (Or and Assouline, 2011; Stankovich and Lockington, 1995; van Genuchten and Nielsen, 1985) making it problematic to rely on the PCM formulation (Vogel and Cislerova, 1988) to give values for RHC in any soil study.

Since K_r is a *relative* hydraulic conductivity (i.e. relative to saturation), we expect that $K_r \rightarrow 1$ as $\Theta \rightarrow 1$. For a H_+ vs Θ model that fails to fall to zero at full saturation, it turns out that $K_r \rightarrow 1$ in a non-singular fashion. By contrast, for a H_+ vs Θ model that falls to zero at full saturation but does so abruptly (i.e. $|dH_+/d\Theta| \rightarrow \infty$ at $\Theta \rightarrow 1$), K_r still manages to reach unity at full saturation but has a singularity $dK_r/d\Theta \rightarrow \infty$ as $\Theta \rightarrow 1$ (van Genuchten, 1980). However, for a H_+ vs Θ model, such as we study here, that approaches zero smoothly (with finite $dH_+/d\Theta$ as $\Theta \rightarrow 1$ and $H_+ \rightarrow 0$), it turns out that the PCM does not converge. The issue (as explained in the appendix) is that almost all the flow at saturation is through the largest pores, meaning that slightly below saturation, where these largest pores are no longer filled with liquid, the flow is in relative terms much smaller than at saturation. The PCM then predicts negligible flow except at saturation.

In other words, the hydraulic conductivity is so strongly weighted to the largest pores that the computation is sensitive to the largest pore size in a given sample. Convergence in the PCM is obtained when one has hardly any pore space in the largest pores, or equivalently hardly any pore space in the pores with the smallest capillary suction i.e. $|d\Theta/dH_+| \rightarrow 0$ as $1/H_+ \rightarrow \infty$, or $|dH_+/d\Theta| \rightarrow \infty$ as $H_+ \rightarrow 0$. This is however not the case when (24) is used.

To summarise, given the convex hull SWRC in equation (24), we find that using the Mualem PCM yields equations for RHC which do not converge. Thus, we are unable to use the PCM to obtain an RHC expression using the head function we have derived via the convex hull. To avoid these issues, we abandon the PCM for our convex hull head function and employ instead a RHC equation that does not exhibit singular behaviour near full saturation. Specifically, we use the Brooks and Corey RHC (Brooks and Corey, 1964). We use this RHC function in the interest of simplicity (van Genuchten and Nielsen, 1985; Vogel and Cislerova, 1988) and also because it follows a similar pattern to what is seen in the FDE, namely a power law function of saturation albeit with different exponents in the power law between the FDE and RE. It is given as

$$K_r(\Theta) = \Theta^{5/2+2/\lambda} = \Theta^{1/2+2/m}, \quad (27)$$

where $\lambda = m/(1-m)$. This profile is shown in Fig. 2. The RHC for the two foam drainage variants (Koehler et al., 1999, 2000; Verbist and Weaire, 1994; Verbist et al., 1996; Weaire and Phelan, 1996) are also plotted (Θ^2 and $\Theta^{3/2}$ for channel- and node-dominated FDE respectively). What we notice is that RHC for soils tends to be less than that for foam.

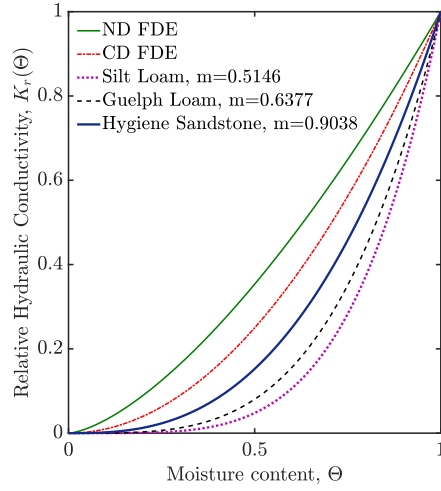


Fig. 2 Plot of RHC profile for three soil samples based on (27) and the two FDE variants. The analogous RHC values for channel-dominated FDE (1) and node-dominated FDE (2) are Θ^2 and $\Theta^{3/2}$ respectively.

3.3 Relative Diffusivity

In what follows, we develop a rescaled relative diffusivity (RD) function that goes to unity when moisture content approaches unity at full saturation, which matches the behaviour within the two foam drainage equations (FDEs), thereby allowing for a “fairer” comparison between soils and foams. Once the SWRC and RHC are defined, these two soil material functions are used to determine relative diffusivity (RD) (van Genuchten, 1980). This can be accomplished using equation (12). We therefore first define the RD using our newly defined head function (24) and the Brooks and Corey (1964) RHC functions (27) as

$$D_r(\Theta) = \begin{cases} \frac{(1-m)}{m} \cdot \frac{\Theta^{1/m-1/2}}{(\Theta^{-1/m}-1)^m}, & \text{if } \Theta \leq \Theta_t \\ \left[\frac{(1-m)}{m} \cdot \frac{(\Theta_t^{-1/m}-1)^{-m}}{\Theta_t^{1+1/m}} \right] \Theta^{1/2+2/m}, & \text{if } \Theta > \Theta_t. \end{cases} \quad (28)$$

We then obtain a rescaled $\hat{D}_r(\Theta)$ by dividing both parts of the equation (28) by β defined as the (fixed) value of $|dH_+/d\Theta|$ for $\Theta > \Theta_t$ according to equation (26). That this is the $\Theta \rightarrow 1$ limit of D_r follows from equation (12) remembering from (27) that $K_r \rightarrow 1$ as $\Theta \rightarrow 1$. Hence, $\hat{D}_r(\Theta)$ is given below as,

$$\hat{D}_r(\Theta) = \begin{cases} \Theta_t^{1+1/m} \cdot (\Theta_t^{-1/m}-1)^m \frac{\Theta^{1/m-1/2}}{(\Theta^{-1/m}-1)^m}, & \text{if } \Theta \leq \Theta_t \\ \Theta^{1/2+2/m}, & \text{if } \Theta > \Theta_t. \end{cases} \quad (29)$$

The prefactor in second part of equation (28) has been scaled out when $\Theta > \Theta_t$ in this new formula for the relative diffusivity. Meanwhile, the prefactor of the first part of equation

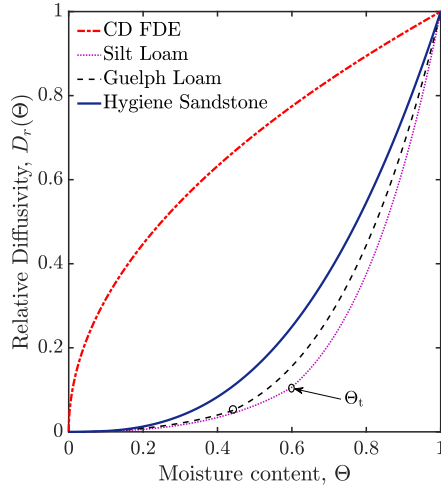


Fig. 3 Relative diffusivity profiles for three soil samples based on (27) and channel-dominated foam drainage. The solution for node-dominated foam drainage is identically unity for all values of Θ and is thus not displayed. In the case of soils, the slope of \hat{D}_r is discontinuous at Θ_t although \hat{D}_r is continuous.

(29) which hereafter we denote c_m decreases as $m \rightarrow 1$ as shown in Table 1. Equation (29) is shown in Fig. 3.

From Fig. 3, we observe that by design when $\Theta = 1$, $\hat{D}_r(\Theta) = 1$. We compare the profile of relative diffusivity for three soil samples, and the channel-dominated foam drainage in this plot. The node-dominated profile is not shown as it is identically unity at all values of Θ . The soils (especially Silt Loam, $\Theta_t = 0.5996$) show an observable kink in \hat{D}_r when $\Theta = \Theta_t$. Even though $dH_+/d\Theta$ and hence \hat{D}_r are continuous at Θ_t , $d^2H_+/d\Theta^2$ and hence $d\hat{D}_r/d\Theta$ are not.

This new format rescaled relative diffusivity $\hat{D}_r(\Theta)$ will be used in Section 4 to obtain the travelling wave solution for Richards equation (30).

4 Results: Solution to Richards Equation

We solve for the travelling wave solution to Richards equation for different soil types using the known Brooks-Corey RHC function (27) and the modified relative diffusivity function (29). From equation (14), we obtain the following expressions,

$$\hat{\xi} = \begin{cases} \Theta_t^{1+1/m} \cdot (\Theta_t^{-1/m} - 1)^m \int_0^\Theta \frac{\Theta^{1/m-1/2}}{(\Theta^{-1/m} - 1)^m (\Theta - \Theta^{1/2+2/m})} d\Theta, & \text{if } \Theta \leq \Theta_t \\ \int_{\Theta_t}^\Theta \frac{\Theta^{1/2+2/m}}{\Theta - \Theta^{1/2+2/m}} d\Theta + \hat{\xi}(\Theta_t), & \text{if } \Theta > \Theta_t. \end{cases} \quad (30)$$

These integrals cannot be solved analytically, hence, we employ Simpson's rule to obtain numerical solutions, similar to what was done in Boakye-Ansah and Grassia (2021). The solution for different soil types are shown in a profile in Fig. 4 for each soil type. Additionally, the profiles of channel- and node-dominated foam drainage are also shown.

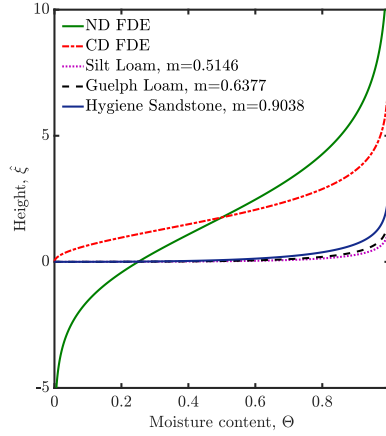


Fig. 4 Profile of numerical travelling wave solution (using Simpson's rule) to equation (30) for three soil samples.

We see that the behaviours both as $\Theta \rightarrow 0$ and $\Theta \approx 1$ are very different between foams and soils. The $\hat{\xi}$ values in soils are very slow to increase when $\Theta \ll 1$, and the increase at $\Theta \rightarrow 1$ is also slow compared to foam. These limiting cases are discussed next.

4.1 Asymptotic Behaviour of Solutions

Although analytic solutions to equation (30) are not available in general, it is possible to study analytically how the solution to Richards equation behaves in the limit of small or large Θ . We deduce that the Richards equation travelling wave (14) goes to,

$$\frac{d\hat{\xi}}{d\Theta} \approx \begin{cases} \hat{D}_r(\Theta)/\Theta, & \text{if } \Theta \ll 1, \\ \frac{\hat{D}_r(1)}{(1-\Theta)(K'_r(1)-1)}, & \text{if } \Theta \approx 1. \end{cases} \quad (31)$$

For $\Theta \ll 1$, from (29), we obtain for $\hat{D}_r(\Theta)/\Theta \approx c_m \Theta^{1/m-1/2}$ where as was mentioned earlier $c_m = \Theta_t^{1+1/m} \cdot (\Theta_t^{-1/m} - 1)^m$. Meanwhile, the relative diffusivity $\hat{D}_r(1) \equiv \lim_{\Theta \rightarrow 1} \hat{D}_r(\Theta)$ equals unity, whereas the denominator of the second part of equation (31) has been obtained via Taylor series expansion in the $\Theta \approx 1$ limit. Note that $K'_r(1)$ equals $(4+m)/(2m)$ and decreases monotonically as $m \rightarrow 1$. Hence,

$$\frac{d\hat{\xi}}{d\Theta} \approx \begin{cases} c_m \Theta^{1/m-1/2}, & \text{if } \Theta \ll 1 \\ 2m/((4-m)(1-\Theta)), & \text{if } \Theta \approx 1. \end{cases} \quad (32)$$

Integrating equation (32), we obtain

$$\hat{\xi}(\Theta) \approx \begin{cases} \hat{c}_m \cdot \Theta^{1/2+1/m}, & \text{if } \Theta \ll 1 \\ (2m/(4-m)) \cdot \log(1/(1-\Theta)) + \tilde{c}_2, & \text{if } \Theta \approx 1. \end{cases} \quad (33)$$

where $\hat{c}_m = c_m \cdot 2m/(2+m)$, this value being reported in Table 1 and \tilde{c}_2 is a value that can be obtained by matching to the solution of equation (30) via Simpson's rule to an arbitrary Θ value ($\Theta = 0.9$, say) in that limit.

In the dry limit ($\Theta \ll 1$), we observe that the asymptotic approximation exhibits a power law behaviour. This power law behaviour is no different from what was observed in Boakye-Ansah and Grassia (2021) except for having a different prefactor owing to replacing D_r by \hat{D}_r . On the contrary, the large Θ behaviour is very different from Boakye-Ansah and Grassia (2021) being not a power law but rather a logarithmic law behaviour in the limit where $\Theta \rightarrow 1$. Specifically, $\hat{\xi}$ exhibits a logarithmic law behaviour in the limit where $\Theta \rightarrow 1$.

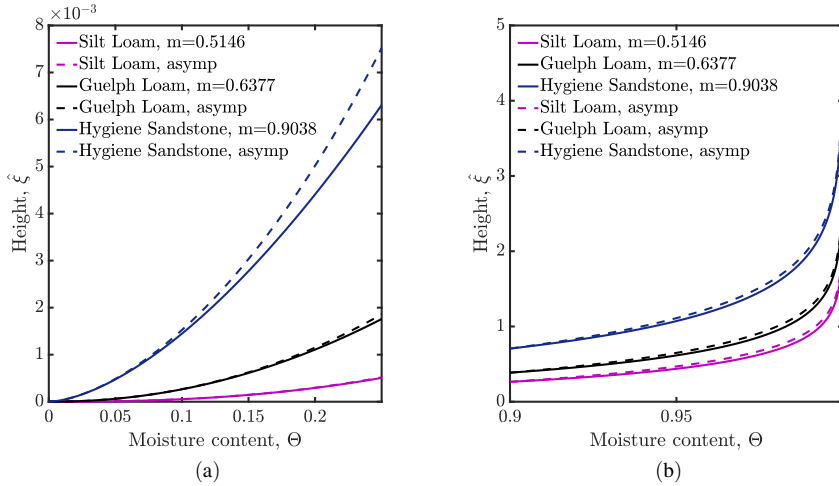


Fig. 5 Profiles of numerical and asymptotic travelling wave solutions to Richards equation in the limit (a) $\Theta \ll 1$ (b) $\Theta \approx 1$. The numerical solutions are the solid lines while the approximate analytical ones are the dashed lines.

On the contrary, the large Θ behaviour is very different, being not a power law but rather a logarithmic law behaviour in the limit where $\Theta \rightarrow 1$. The foam drainage equations also exhibit logarithmic behaviour in these limits, but with a different prefactor multiplying the logarithm, 2 for the ND FDE (equation (4)), 1 for the CD FDE (equation (3)), and $2m/(4-m)$ for soils with $m < 1$ here. Clearly, the $\hat{\xi}$ values predicted for soils are less than those for the FDE.

Fig. 5 shows a comparison of the numerical solution to equation (30) and its analytical (33) solutions. We observe from these profiles that the analytical solutions in Fig. 5(a) are slight overestimates as $m \rightarrow 1$ although it must be stated that the scale of the graph is very small (on the order of 10^{-3}) indicating that $\hat{\xi}$ increases only very slowly with Θ . The approximation for Silt Loam ($m = 0.5146$) is very accurate. Note also that increasing m increases $\hat{\xi}$ monotonically in Fig. 5(a). This monotonicity was not seen uniformly in Boakye-Ansah and Grassia (2021) because of the different way in which prefactors depended on m in the scaling used there.

Likewise in Fig. 5(b), the profiles for $\hat{\xi}$ are overestimated by the $\Theta \approx 1$ asymptotic formulae for all m values, but these overestimations are small in relative terms for each m . The difference between numerical and asymptotic analytical solutions is far less significant

than the difference between soils samples and foam drainage in Fig. 4. The solutions show a slower growth in soil than foam as shown in Fig. 4 (whereas with the original SWRC, RHC and RD, the growth was like a power law, not a logarithm and hence was much more rapid: see Boakye-Ansah and Grassia (2021) and see also Appendix B). This then indicates an important qualitative change in the travelling wave solution as our original SWRC is replaced by a convex hull SWRC. With the original SWRC, Boakye-Ansah and Grassia (2021) found heights for soils to be much larger than for foam. Here however, the foams attain greater heights than the soils.

The logarithmic law (equation (33)) obtained here for the shape of the travelling wave profile close to saturation is actually unsurprising. We are using Brooks-Corey type RHC $K_r = \Theta^{1/2+2/m}$ (defined here without applying any PCM) but a monotonically decreasing $|dH_+/d\Theta|$ (obtained here via applying convex hull to the van Genuchten-Mualem SWRC). Qualitatively however this is similar to using a Brooks-Corey RHC along with a Brooks-Corey SWRC $H_+ = \Theta^{-(1-m)/m}$ (the latter also gives a monotonically decreasing $|dH_+/d\Theta|$, and leads to $\hat{D}_r = \Theta^{1/2+1/m}$). Although the Brooks-Corey SWRC clearly does not give vanishing head at full saturation, modifying it to $H_+ = -1 + \Theta^{-(1-m)/m}$ (whilst keeping the RHC unchanged) does give vanishing head in that limit and moreover (like the aforementioned convex hull SWRC) still captures the correct power law SWRC behaviour for dry soils such that $\Theta \ll 1$. The above mentioned change in H_+ (introducing an additive constant) has no effect whatsoever on $|dH_+/d\Theta|$, hence no effect whatsoever on $\hat{D}_r(\Theta)$, nor on $\hat{\xi}^*$ vs Θ , which remains unchanged from the Brooks-Corey case. However these Brooks-Corey type formulae (i.e. power laws for $K_r(\Theta)$ and $\hat{D}_r(\Theta)$ in terms of Θ) qualitatively are the same as what is found for channel- or node-dominated foam drainage (again $K_r(\Theta)$ and $\hat{D}_r(\Theta)$ are power laws, just with different powers). Since the foam drainage cases lead to logarithmic $\hat{\xi}^*$ vs Θ behaviour near saturation (see equations (7)–(8)), it is unsurprising that the Brooks-Corey predictions for soils do so also. Moreover since $\hat{D}_r(1) = 1$ regardless of whether we use a Brooks-Corey SWRC or a convex hull constructed around a van Genuchten SWRC, and since the $K_r(\Theta)$ we use is the same in either case, it follows that equation (31) remains unchanged near $\Theta \approx 1$. The $\Theta \rightarrow 1$ prediction of equation (33) is therefore exactly the same as what a Brooks-Corey model would predict.

5 Conclusion

We have considered the travelling wave solution for Richards equation using a modified relative diffusivity function that goes to unity smoothly at full saturation, and a relative hydraulic conductivity function that goes to unity smoothly in the same limit. Here we achieved this by employing a new capillary suction head expression for unsaturated soils constructing a convex hull around the existing van Genuchten SWRC. Our head expression goes to zero smoothly at full saturation for all soil types. This is in contrast to the Brooks-Corey SWRC which does not go to zero, and the van Genuchten SWRC which goes to zero but does so abruptly in a singular fashion. If data used to estimate the SWRC are weighted towards the dry limit, it may be difficult to distinguish these different SWRC, but the predictions they make in the wet limit are very different. We also note that with our chosen convex hull SWRC, we used a Brooks-Corey RHC rather than a PCM, which would not have converged. Employing a Brooks-Corey RHC is compatible in any case with the approach in the foam drainage equation. The solutions of Richards equation were obtained via Simpson's rule, while asymptotic analytical solutions were also derived for very low moisture content ($\Theta \ll 1$), and systems near full saturation ($\Theta \approx 1$).

We found that for the soils, using these modified material properties, we obtain travelling wave solutions ξ vs Θ that follow a logarithmic law as in foam drainage as $\Theta \rightarrow 1$. The foam heights ξ for a given saturation Θ are however larger than those for the soil solutions. Moreover, clayey soils (smaller values of parameter m) attain even lower heights than porous sandstones (m close to unity). The previous Richards equation solutions obtained without rescaling the relative diffusivity to unity at full saturation went to even larger heights as $\Theta \rightarrow 1$. These diverged as a power law rather than logarithmically and were therefore even larger than the foam drainage solutions. We infer then that generally, depending on the scaling of relative diffusivity near full saturation, we may obtain either power law or logarithmic law travelling wave solutions to Richards equation.

References

- Ahmed T (2006) *Reservoir Engineering Handbook*, 2nd edn. Elsevier
- Ahuja LR, Swartzendruber D (1972) An improved form of soil-water diffusivity function 1. *Soil Science Society of America Journal* 36(1):9–14
- Assouline S (2001) A model for soil relative hydraulic conductivity based on the water retention characteristic curve. *Water Resources Research* 37(2):265–271
- Assouline S, Or D (2013) Conceptual and parametric representation of soil hydraulic properties: A review. *Vadose Zone Journal* 12(4)
- Assouline S, Tartakovsky DM (2001) Unsaturated hydraulic conductivity function based on a soil fragmentation process. *Water Resources Research* 37(5):1309–1312
- Assouline S, Tessier D, Bruand A (1998) A conceptual model of the soil water retention curve. *Water Resources Research* 34(2):223–231
- Aziz AA, De Kretser RG, Dixon DR, Scales PJ (2000) The characterisation of slurry dewatering. *Water Science and technology* 41(8):9–16
- Boakye-Ansah YA, Grassia P (2021) Comparing and contrasting travelling wave behaviour for groundwater flow and foam drainage. *Transport in Porous Media* 137(1):255–280
- Brooks RH, Corey AT (1966) Properties of porous media affecting fluid flow. *Journal of the Irrigation and Drainage Division* 92(2):61–90
- Brooks RH, Corey T (1964) Hydraulic properties of porous media. *Hydrology Papers*, Colorado State University 24
- Burdine NT (1953) Relative permeability calculations from pore size distribution data. *Journal of Petroleum Technology* 5(03):71–78
- Buscall R, White LR (1987) The consolidation of concentrated suspensions. part 1. — The theory of sedimentation. *Journal of the Chemical Society, Faraday Transactions 1: Physical Chemistry in Condensed Phases* 83(3):873–891
- Celia MA, Bouloutas ET, Zarba RL (1990) A general mass-conservative numerical solution for the unsaturated flow equation. *Water Resources Research* 26(7):1483–1496
- Cox SJ, Weaire D, Hutzler S, Murphy J, Phelan R, Verbist G (2000) Applications and generalizations of the foam drainage equation. *Proceedings of the Royal Society of London A: Mathematical, Physical and Engineering Sciences* 456:2441–2464
- Fredlund DG, Xing A (1994) Equations for the soil-water characteristic curve. *Canadian Geotechnical Journal* 31(4):521–532
- van Genuchten MT (1980) A closed-form equation for predicting the hydraulic conductivity of unsaturated soils. *Soil Science Society of America Journal* 44(5):892–898
- van Genuchten MT, Nielsen DR (1985) On describing and predicting the hydraulic properties of unsaturated soils. In: *Annales Geophysicae*, vol 3, pp 615–628

- Grassia P, Mas-Hernández E, Shokri N, Cox SJ, Mishuris G, Rossen WR (2014) Analysis of a model for foam improved oil recovery. *Journal of Fluid Mechanics* 751:346–405
- Koehler SA, Hilgenfeldt S, Stone HA (1999) Liquid flow through aqueous foams: The node-dominated foam drainage equation. *Physical Review Letters* 82(21):4232–4235
- Koehler SA, Hilgenfeldt S, Stone HA (2000) A generalized view of foam drainage: Experiment and theory. *Langmuir* 16(15):6327–6341
- Mualem Y (1976) A new model for predicting the hydraulic conductivity of unsaturated porous media. *Water Resources Research* 12(3):513–522
- Or D, Assouline S (2011) The Drainage Foam Equation: An alternative to the Richards Equation for transient unsaturated flows. In: AGU Fall Meeting Abstracts
- Or D, Assouline S (2013) The foam drainage equation for unsaturated flow in porous media. *Water Resources Research* 49(10):6258–6265
- Philip JR (1957) The theory of Infiltration: 1. The Infiltration Equation and its solution. *Soil Science* 83(5):345–358
- Richards LA (1931) Capillary conduction of liquids through porous mediums. *Physics* 1(5):318–333
- Stankovich JM, Lockington DA (1995) Brooks-Corey and van Genuchten soil-water-retention models. *Journal of Irrigation and Drainage Engineering* 121(1):1–7
- Verbist G, Weaire D (1994) A soluble model for foam drainage. *EPL (Europhysics Letters)* 26(8):631–634
- Verbist G, Weaire D, Kraynik AM (1996) The foam drainage equation. *Journal of Physics: Condensed Matter* 8(21):3715–3731
- Vogel T, Cislerova M (1988) On the reliability of unsaturated hydraulic conductivity calculated from the moisture retention curve. *Transport in Porous Media* 3(1):1–15
- Weaire D, Phelan R (1996) The physics of foam. *Journal of Physics: Condensed Matter* 8(47):9519–9524

A Theoretical Basis for the Predictive Conductivity Models

This appendix outlines the basis for predictive conductivity models (PCM). Although we do not ultimately apply a PCM in our analysis, we include this appendix to demonstrate why a soil-water retention curve (SWRC) that goes to zero smoothly at high saturation is incompatible with convergence of a PCM hence the reason a PCM was not employed in our analysis. Conversely, we show why the SWRC (if it goes to zero at all at full saturation) must do so abruptly in order for the PCM to converge, and moreover why the PCM approaches unity abruptly at full saturation in that case. Full details of the theory presented in this section are given in [Burdine \(1953\)](#); [Brooks and Corey \(1964, 1966\)](#); [Mualem \(1976\)](#).

The reason why PCM have been developed in the first place is that the experimental determination of relative hydraulic conductivity (RHC) is often considered complicated and expensive ([Or and Assouline, 2011](#)). Thus, for many practical applications, it can be advantageous to attempt to determine RHC mathematically from SWRC data which are based on soil pore-size distribution. The more commonly used PCM ([Burdine, 1953](#); [Mualem, 1976](#)) that link SWRC to RHC functions assume a simple pore geometry and link capillary properties of pores to RHC. However, as we will see, they also impose a constraint on the SWRC if the RHC is to converge.

A typical PCM leads to a general expression given as

$$K_r(\Theta) = \Theta^\kappa \left[\frac{\int_0^\Theta \frac{1}{H_+^\delta} d\Theta}{\int_0^1 \frac{1}{H_+^\delta} d\Theta} \right]^\eta. \quad (\text{A. 1})$$

where κ , δ , η are model parameters. It is found that $\kappa = 2$, $\delta = 2$, and $\eta = 1$ for the Burdine model ([Burdine, 1953](#)), and $\kappa = 1/2$, $\delta = 1$, and $\eta = 2$ for the Mualem model ([Mualem, 1976](#)). We focus on the derivation of the Mualem model.

A.1 Mualem's Predictive Conductivity Model

Mualem (1976) considers a homogeneous porous medium with a set of interconnected pores defined by their radius r , and a pore-water distribution function $f(r)dr$. The contribution of filled pores of radii between r and $r + dr$ to the volumetric water content θ (rescaled here as Θ) is

$$f(r)dr = d\Theta(r). \quad (\text{A. 2})$$

Considering a porous slab of thickness Δx , the pore area distribution at the two slab sides is assumed to be identical. The probability $a(r, \rho)$ of a pore moving from r to $r + dr$ at x encountering a pore of radius ρ to $\rho + d\rho$ at $x + \Delta x$ is

$$a(r, \rho) = f(r)f(\rho) dr d\rho. \quad (\text{A. 3})$$

More generally, the probability of connection for a pore of radius between r and $r + dr$ to a pore of radius between ρ and $\rho + d\rho$ may be given as

$$a(r, \rho) = G(r, \rho)f(r)f(\rho) dr d\rho, \quad (\text{A. 4})$$

where the function $G(r, \rho)$ accounts for partial correlation between the pores r and ρ at a given moisture content Θ . In what follows, two pores in series with radius r and ρ respectively are replaced by a single equivalent pore radius R and it is assumed that $G(r, \rho)$ can be expressed as a function $G(R)$. To determine conductivity, this connection probability needs to be weighted by a local hydraulic conductivity for each equivalent pore.

Mualem (1976) considers a pair of capillary elements whose lengths are proportional to their radii to replace the pore configuration, and estimates the local hydraulic conductivity as proportional to $r\rho$ or more specifically as $T(r, \rho)r\rho$ where $T(r, \rho)$ is a correction due to tortuosity. Again, it is assumed that $T(r, \rho)$ can be expressed as $T(R)$ where R is a single equivalent radius. The term in $r\rho$ comes about as follows. Two pores in series (length l_r and l_ρ respectively) are replaced by a single equivalent pore (length L). The pressure drop across the equivalent pore is assumed to be the same as the total pressure drop along the two original pores in series. Since Poiseuille pressure drops scale as $(8/\pi)\mu QL/R^4$ (and μ is viscosity and Q is flow rate, which is the same in all cases), it follows

$$L/R^4 = l_r/r^4 + l_\rho/\rho^4. \quad (\text{A. 5})$$

Moreover, since the volume of the equivalent pore is assumed to be the same as total volume of the two original pores, it follows that

$$LR^2 = l_r r^2 + l_\rho \rho^2. \quad (\text{A. 6})$$

Significantly, the length of the equivalent pore need not be the same as the total length of the two original ones. Finally the aspect ratio of the pores is assumed fixed, hence

$$l_r/r = l_\rho/\rho. \quad (\text{A. 7})$$

The above constitute 3 homogeneous linear equations (A. 5)–(A. 7) in 3 unknowns L , l_r and l_ρ . Non-trivial solutions only result if the determinant of the system of equations is zero. This provides a condition linking R to r and ρ , specifically

$$R = \sqrt{r\rho}. \quad (\text{A. 8})$$

Taking the local hydraulic conductivity proportional to $r\rho$ as was suggested above is equivalent to taking the conductivity of equivalent pore properties to R^2 which is what is expected for a single pore. Solutions can now be obtained for l_r and l_ρ assuming L is given. (It is necessary to fix the value of L since when the determinant vanishes, the equations are not all linearly independent).

$$l_r = Lr^2\rho/(r^3 + \rho^3), \quad l_\rho = Lr\rho^2/(r^3 + \rho^3). \quad (\text{A. 9})$$

Note that:

$$l_r + l_\rho = Lr\rho(r + \rho)/(r^3 + \rho^3) \quad (\text{A. 10})$$

which is always smaller than L . Note however that the volume of the equivalent pore is the same as the sum of the volumes of the two original ones by construction. Once we have established the size of a single equivalent pore, we have also established the liquid saturation, since we consider that the medium is filled up to pores of a given size but no further. Supposing we can re-write the tortuosity and connectivity factors as functions of Θ (not in terms of r and ρ , or in terms of R), it follows that the hydraulic conductivity K is

$$K \propto T(\Theta)G(\Theta) \int_{r_{min}}^r r f(r) dr \int_{\rho_{min}}^\rho \rho f(\rho) d\rho, \quad (\text{A. 11})$$

and relative hydraulic conductivity is

$$K_r(\Theta) = T(\Theta)G(\Theta) \left[\frac{\int_{R_{min}}^R r f(r) dr}{\int_{R_{min}}^{R_{max}} r f(r) dr} \right]^2. \quad (\text{A. 12})$$

Here we have exploited the fact that the integrals over r and ρ are the same, the denominator of (A. 12) is a normalisation condition. The important point here is that unless $f(r)$ decays quite rapidly as r becomes large (decaying faster than $1/r^2$), K does not converge, or equivalently the denominator of K_r diverges, making K_r itself tend to zero.

If too much volume is associated with the large pores, which only fill near saturation, effectively all the flow at saturation is dominated by transport through those large pores, and in relative terms, below saturation flow is negligible. In situations like that, we can expect to see large variations in conductivity between rock samples, since the presence of slightly different numbers of large pores in different samples may influence hydraulic conduction.

The tortuosity correction factor $T(\Theta)$ that is applied, and the connectivity correlation factor $G(\Theta)$ are assumed to be power-law functions of Θ , and are replaced by a single factor Θ^κ . Substituting $\kappa = 1/2$ (fit by Mualem (Mualem, 1976; Assouline, 2001) to 45 soil samples) within the correction term, applying the capillary law relating pore radius to capillary head $r = C/H_+$ where C is a constant (independent of geometry), and using equation (A. 2), we obtain for equation (A. 12)

$$K_r(\Theta) = \Theta^{1/2} \left[\frac{\int_0^\Theta \frac{d\Theta}{H_+}}{\int_0^1 \frac{d\Theta}{H_+}} \right]^2. \quad (\text{A. 13})$$

As noted in the main text, there are convergence issues here if H_+ is too small for too large a fraction of the volume in the limit as $H_+ \rightarrow 0$. If, for example, $H_+ \approx |dH_+/d\Theta|_{\Theta=1} (1 - \Theta)$ for some finite $|dH_+/d\Theta|_{\Theta=1}$, $\int_0^1 d\Theta/H_+$ diverges. As mentioned earlier, the issue is that there is now so much volume in large radius (small H_+) pores ($d\Theta \approx dH_+/|dH_+/d\Theta|$) that almost all conduction occurs through large pores. A larger (i.e. singular) $|dH_+/d\Theta|$ resolves the issue by having less volume in such small H_+ pores. The SWRC selected by Van Genuchten typically has,

$$H_+ \approx ((1 - \Theta)/m)^{1-m}; \quad \Theta \approx (1 - mH_+^{1/(1-m)}), \quad (\text{A. 14})$$

for some value $m < 1$ (typically with m close to 1 for sandstones, and m significantly less than 1 for loams). Recognising via (A. 2),

$$f(r) = \frac{d\Theta}{dr} = \frac{d\Theta}{dH_+} \cdot \frac{dH_+}{dr}, \quad (\text{A. 15})$$

and recognising that (as alluded to earlier),

$$H_+ = \frac{C}{r}. \quad (\text{A. 16})$$

It follows then that in the limit of large r (i.e. small H_+)

$$\begin{aligned} f(r) &\approx \frac{m}{(1-m)} H_+^{m/(1-m)} \cdot \frac{C}{r^2} \\ &\approx \frac{m}{(1-m)} \frac{C^{m/(1-m)} C}{r^{m/(1-m)} r^2} \\ &\approx \frac{m}{(1-m)} \frac{C^{1/(1-m)}}{r^{(2-m)/(1-m)}} \end{aligned} \quad (\text{A. 17})$$

Notice how this function decays in the large r limit. If m is close to 1 (e.g. sandstone), $f(r)$ decays very rapidly at large r , so there are comparatively few pores that are much larger than the sample average. If m is rather smaller than unity (e.g. loam), the population of pores that are significantly larger than the sample average increases. Certainly, the average pore size in loam tends to be much smaller than in sandstone but that effect is already accounted for in our dimensionless system. What we are considering here is not the average pore size, but rather the pore size distribution relative to that average. Note that in the limit as $m \rightarrow 0$, hence with a non-singular $H_+ \propto (1 - \Theta)$, it follows via (A. 17) that $f(r)$ becomes proportional to r^{-2} , and (as noted earlier) the denominator of (A. 12) then fails to converge as $R_{max} \rightarrow \infty$. Yet again this demonstrates that there are now, in relative terms, so many large pores that almost all the flow is passing through them, so the (total)

conductivity we compute is sensitive to what exactly the largest pore size R_{max} is. As $R_{max} \rightarrow \infty$, the hydraulic conductivity up to any finite pore size $R < R_{max}$ is then negligibly small compared to the conductivity through the very largest pores, so that relative conductivity K_r (considered only up to that finite pore size) tends to zero.

Assuming on the other hand that $0 < m < 1$ so that equation (A. 13) does indeed converge, notice however

$$\frac{dK_r}{d\Theta} \approx \frac{1}{2\Theta} K_r + \frac{2\Theta^{1/2}}{H_+} \int_0^\Theta \frac{d\Theta}{H_+} / \left(\int_0^1 \frac{d\Theta}{H_+} \right)^2. \quad (\text{A. 18})$$

The consequence of having $H_+ \rightarrow 0$ abruptly as $\Theta \rightarrow 1$, e.g. H_+ scaling as proportional to $(1 - \Theta)^\alpha$ for some $0 < \alpha < 1$ with $\alpha = 1 - m$ here (see equation (A. 14)), is that $dK_r/d\Theta$ also diverges as $(1 - \Theta)^{-\alpha}$ in that same limit. A singular H_+ vs Θ relation leads to a convergent K_r vs Θ but *not* a convergent $dK_r/d\Theta$ vs Θ , at least in the PCM adopted here. The only way to keep $dK_r/d\Theta$ from diverging is to take $\alpha \rightarrow 0$, i.e. $m \rightarrow 1$. However that means according to (A. 14) H_+ must stay non-zero as full saturation is approached. Returning to the case $0 < m < 1$ however, the value of $D_r(\Theta)$ predicted by the PCM meanwhile is divergent, since $D_r = K_r |dH_+/d\Theta|$ (van Genuchten, 1980), and since we require $dH_+/d\Theta$ to diverge in order to have a convergent K_r , it necessarily follows that D_r diverges.

In conclusion, using the predictive conductivity model PCM we have a choice between a system in which H_+ remains non-zero at full saturation (in which case K_r converges to unity at $\Theta \rightarrow 1$ with finite $dK_r/d\Theta$ there), or a system in which H_+ approaches zero smoothly at full saturation (in which case K_r is not well defined in the PCM, since conduction is dominated by the flow through the largest pores in the sample, hence is extremely sensitive to the particular sample), or else a system in which $H_+ \rightarrow 0$ and $K_r \rightarrow 1$ at full saturation, but necessarily with mild singularities in that limit (both $|dH_+/d\Theta|$ and $|dK_r/d\Theta|$ diverge at full saturation). In the main text, we have avoided with issue by abandoning the PCM.

B Appendix B

This appendix summarises some of the findings from Boakye-Ansah and Grassia (2021) regarding how travelling wave solutions of Richards equation behave when using the original van Genuchten (1980) soil material property functions. The relevant solutions are presented here for ease of comparison with those presented in the main text that use modified soil material property functions.

The profile of the travelling wave to Richards equation previously obtained within the limit of the special case we consider is

$$\frac{d\xi}{d\Theta} = \frac{D_r(\Theta)}{\Theta - K_r(\Theta)}, \quad (\text{B. 1})$$

which is analogous to equation (14). In the case of (B. 1) above, the original D_r and K_r functions given by van Genuchten are used in its solution.

Near $\Theta \approx 1$,

$$D_r(\Theta) \approx \left| \frac{dH_+}{d\Theta} \right| \approx \frac{(1-m)}{m^{(1-m)}} (1-\Theta)^{-m}, \quad (\text{B. 2})$$

is the approximation used which is the derivative of the original van Genuchten SWRC in the same limit (Boakye-Ansah and Grassia, 2021). The denominator of equation (B. 1) is also scaled as

$$\Theta - K_r \approx (1 - K_r) - (1 - \Theta). \quad (\text{B. 3})$$

If $K_r \rightarrow 1$ abruptly as $\Theta \rightarrow 1$, then typically, $1 - \Theta \ll 1 - K_r$, and also as explained in Boakye-Ansah and Grassia (2021),

$$1 - K_r \approx \frac{2}{m^m} (1 - \Theta)^m. \quad (\text{B. 4})$$

Hence,

$$\frac{d\xi}{d\Theta} \approx \frac{|dH_+/d\Theta|}{1 - K_r(\Theta)}; \quad \frac{d\xi}{d\Theta} \approx \frac{(1-m)}{2m^{1-2m}} (1-\Theta)^{-2m}, \quad (\text{B. 5})$$

for which we obtain

$$\xi = c_0 + \frac{(1-m)m^{2m-1}}{2(2m-1)} (1-\Theta)^{1-2m}, \quad (\text{B. 6})$$

where c_0 is an integration constant. Here we are primarily interested in m values $0.5 < m < 1$ so that $-1 < 1 - 2m < 0$. Note that this is a power law for ξ , hence it grows more rapidly than the logarithmic law discussed in the main text. We have expressed this in terms of a variable ξ rather than a rescaled variable $\hat{\xi}$ which was not used in Boakye-Ansah and Grassia (2021) owing to (B. 2) diverging in the $\Theta \rightarrow 1$ limit. However, for comparison we can convert from ξ to $\hat{\xi}$ by dividing through by the capped maximum value of $|dH_+/d\Theta|$ given in Table 1.

Conclusions and Future Work

8.1 Conclusions

Richards equation, a nonlinear partial differential equation that describes flow of water in unsaturated soils, has been studied alongside the two variants of equations that describe foam drainage. Specifically, early-time and late-time solutions have been obtained for these equations using varying underlying conditions and set-ups. Analogies in their solutions are studied (all these equations are ultimately convection-diffusion equations) as well as marked differences (soils and foams behave differently both in the dry and wet limit, due to differences in material property functions). In soils, the key material property function that was identified to capture the aforementioned differences is the capillary head function or soil-water retention curve. The head function is subsequently used with a conductivity model to predict a relative hydraulic conductivity function, and hence a relative diffusivity function for soils. The fact that relative hydraulic conductivity and relative diffusivity tend to zero very rapidly in dry soils explains differences between soils and foams in the dry limit. Meanwhile the fact that (the derivative of) the soil water retention curve and hence the relative diffusivity exhibit singularities in a fully saturated soils explains differences between soils and foams in the wet limit.

From their structure, soils have very large local variations in their pore sizes unlike the typical situation within foams where capillary suction limits the local variation of the Plateau border cross-sectional area. Despite these structural differences, foams and soils have many

other similarities. Capillary suction effects are strongest when both porous systems are dry but falls to zero at full saturation. Such similarities were exploited to compare drainage in foams and soils throughout this thesis. For instance, the law governing flow in soils and foams is the same, namely Darcy's law. Other similarities are detailed in the Chapters 5 and 6. Nonetheless, a few subtle differences were discovered in the literature for flow in foams and flow in soils. Particularly, the terminology for describing flow in these soils and foams differ even when they refer to similar processes.

This thesis set out to bridge the terminology between the flow in foams and flow in soils research fields. For instance, drainage in foams represent movement of liquid through the foam but in soils, drainage usually refers to expulsion of water out of the soil. Infiltration is used in soil literature as the equivalent term for drainage in foams. However, both foams and soils may be equivalently described with imbibition at early times. Early-time imbibition is dependent on capillary diffusivity whereas late time drainage is a mixture between capillary forces and gravity (hydraulic conductivity). Gravity is the term used in foams whereas hydraulic conductivity is the equivalent term in soils.

Data was presented for solutions of early-time nonlinear diffusion in soils and foams (see Chapter 5). Here, a constant boundary flux imbibition in foams and soils was studied. Using the diffusivity functions for foams, and the limiting early-time function for soils via van Genuchten equations, solutions were sought. This work examined what evolving moisture content at the boundary of a system develops as a known imbibition flux is delivered into the system. In foams, it was found that this required value is greater in channel-dominated foams than in node-dominated foams. In soils, the top boundary moisture content depends on a soil specific parameter m which is close to unity for sandstones, but smaller than that for loams. The moisture content required at the boundary to deliver a known flux increases as the value of m decreases. Overall, this required value is greater in soils than in foams. Singular solutions were observed in soils where moisture content falls to zero whereas the profile for channel-dominated foam drainage via the same boundary conditions occurred at a finite distance but less abruptly compared with soils. For node-dominated foam drainage, the solution goes to infinity and thus does not terminate at a finite distance. It was however observed for node-dominated foam drainage that after a certain finite distance, there was a marginal contribution since the moisture profile from there till infinity was negligible. The

solutions obtained for imbibition in soils and foam drainage were then used to estimate the moisture content at the top boundaries that produced these observed profiles. Additionally, the maximum depth or distance for the imbibition process were presented, being greater in channel-dominated foam than in node-dominated foam. In soils, the observed behaviour is dependent on the parameter m .

This work also examined how moisture content on the top boundary $\Theta(0, t)$ evolves. Profiles that have faster growing $\Theta(0, t)$ at the top terminate at much lower x_{\max} values (i.e. at lesser depth). Both $\Theta(0, t)$ and x_{\max} evolve with t as power laws, but the exponents depend on the soil specific parameter m . The exponents of the various power laws indicate $\Theta(0, t)$ is faster growing for loams than for sandstones (or indeed for foam drainage) whereas x_{\max} is slower growing for loams. The solution developed for this study also develops a benchmark for other systems (channel-dominated foams and imbibition into soils) where the diffusivity functions are variable.

The results from the travelling wave solutions presented in Chapter 6 indicate that there are subtle differences in the shapes of travelling wave solutions between foam drainage and Richards equation. Using soil material property functions via van Genuchten [38] models for Richards equation and the equivalent functions from both channel-dominated and node-dominated foam drainage equation, these solutions were obtained. Asymptotic behaviour was studied in both dry and wet saturation limits to elucidate behaviours in those regions. Power-law behaviour was obtained in both of these saturation limits. For Richards equation, it was concluded that (owing to the behaviour of relative diffusivity D_r), (a) as the porous medium system becomes very dry, the slope of the profile of height vs. moisture content becomes significantly less than unity, and (b) near full saturation, the profile of height vs moisture content increases abruptly to values significantly larger than unity. This is in contrast to the FDE, where (a) at low moisture content, the slope of the profile of height against moisture content is much greater than unity, and (b) in the nearly fully saturated limit, the height against moisture content relation is very large, but not so large as in Richards equation.

During an irrigation process in soils, these findings presented in Chapter 6 suggest how long an irrigation system may need to remain switched on once a predetermined saturation can be achieved at a certain depth. A procedure was presented on how to estimate the

volume of water that needs to be injected or pumped to achieve such a desired saturation. From the data presented in the same chapter, it was estimated that loams, or soils with smaller m flooded more readily than sandstones (with higher m), indicating that the latter may require more water to be pumped to reach a desired saturation.

In Chapter 7, the van Genuchten [38] material property functions that were used to derive travelling solutions for Richards equation in Chapter 6 were modified and used to derive new numerical travelling wave solutions comparable to the foam drainage equation. Here also, asymptotic behaviour was studied in both the dry and wet saturation limits to elucidate behaviours in those regions. Power-law behaviour was obtained at very low moisture content which can be shown to be equivalent to the solutions obtained for Richards equation and foam drainage equation in Chapter 6. At full saturation however, a logarithmic relationship was obtained between vertical position $\hat{\xi}$ and moisture content Θ which led to $\hat{\xi}$ values smaller than those obtained for the FDEs, and much smaller than the Richards equation solutions for $\hat{\xi}$ using the original set of van Genuchten soil parameters which yield a power-law. This behaviour in the wet limit is however not surprising. It is shown in Appendix A that for long-time behaviour, power-law functions predict logarithmic behaviour in soils. Since either set of material property functions presented in Chapter 7 or Appendix A require a numerical procedure to obtain these travelling wave solutions, there is no incentive to use these modified van Genuchten property functions.

From the data presented for the late-time solutions of Richards equation in Chapters 6 & 7, the solutions in the limit of lower moisture content show power law behaviour of moisture content against position irrespective of the exact soil type being considered for Richards equation. This leads to an abrupt approach to the dry state. This is comparable to the early-time solutions which are presented for behaviour at the onset of infiltration. Here, diffusive transfer in porous media dominates gravity effects as described in Chapter 5, but diffusivity itself going to zero in the dry limit requires abrupt spatial changes in moisture content. On the other hand, the large diffusivity seen in soils near the wet limit (chapter 6) leads to very gradual changes in moisture content. If singularities near the fully saturated limit are relaxed (as was done in chapter 7), the behaviour of soils then becomes more akin to the behaviour of foams.

To the best of this author's knowledge, this work is the first that seeks to compare and

contrast systematically the similarities and differences between foam drainage and flow in unsaturated soils. Some previously published works [41, 91] compared some functions describing hydraulic conductivity within foams and soils, and in an effort to develop a foam drainage-like equation that describes flow in soils. However focus was not given on either the very dry or very wet limits where differences between foams and soils can be seen.

The work here presented thereby offers steps towards a systematic comparison of drainage in foams and soils which can drive future applications and easier communication between the two research communities.

8.2 Future Work

Whereas chapters 6 and 7 focussed on individual travelling waves, Appendix B introduces the interaction between such travelling waves. This appendix seeks to explain the process of setting up a solution for when one travelling wave merges with an already existing travelling wave. Solving a problem like this is worthwhile since it can be used to predict behaviour of irrigation patterns and soil remediation problems, e.g. when an infiltration rate is suddenly increased. The same mathematics can be extended to other porous media applications (e.g., improved oil recovery and flow in porous media in general). Particularly, this solution can be used to analyse a recovery process where there is continuous injection of different streams of water at different rates (or more generally, injection of any fluids used in a recovery process).

Although this work has not yet implemented the Crank-Nicolson algorithm for the time evolution of two interacting travelling waves, some progress have been made towards this. Specifically, an initial condition for studying two interacting travelling waves has been set up capturing various different initial conditions. The solution procedure can be extended to other sets of initial and/or boundary conditions.

Of particular interest for instance is the transition during infiltration between the early-time solutions of chapter 5 and the late-time solutions of chapters 6 & 7. What was found in chapter 5 (in the scaled dimensionless system) is that moisture content starts off growing at early times inherently more slowly in sandstones than in loams. On the other hand, for a given low moisture content, relative hydraulic conduction tends to be larger (again in the scaled

dimensionless system) in sandstones compared to loams. The net effect turns out to be that relative hydraulic conduction grows more slowly with time in sandstones, the remainder of any specified infiltration then being delivered by capillary diffusivity. Since the transition between early-time and late-time infiltration behaviour is associated with diffusion-dominated infiltration giving way to convection-dominated infiltration (i.e. hydraulic conduction), it is possible to estimate when such a transition occurs for different soil types. Examining this transition in detail is however a task for a numerical algorithm (e.g. Crank-Nicolson).

Bibliography

- [1] A. J. Ward-Smith. *Internal Fluid Flow: The fluid dynamics of flow in pipes and ducts*. Clarendon Press, Oxford, 1980.
- [2] A. E. Green, P. M. Naghdi, and M. J. Stallard. A direct theory of viscous fluid flow in pipes II. Flow of incompressible viscous fluid in curved pipes. *Philosophical Transactions of the Royal Society of London. Series A: Physical and Engineering Sciences*, 342(1666):543–572, 1993.
- [3] J. R. Calvert. Pressure drop for foam flow through pipes. *International Journal of Heat and Fluid Flow*, 11(3):236–241, 1990.
- [4] D. Weaire and R. Phelan. The physics of foam. *Journal of Physics: Condensed Matter*, 8(47):9519–9524, 1996.
- [5] S. J. Cox, D. Weaire, S. Hutzler, J. Murphy, R. Phelan, and G. Verbist. Applications and generalizations of the foam drainage equation. In *Proceedings of the Royal Society of London A: Mathematical, Physical and Engineering Sciences*, volume 456, pages 2441–2464. The Royal Society, 2000.
- [6] P. Grassia, J. J. Cilliers, S. J. Neethling, and E. Ventura-Medina. Quasi-one-dimensional foam drainage. *The European Physical Journal E*, 6(4):325–348, 2001.
- [7] D. L. Weaire and S. Hutzler. *The Physics of Foams*. Clarendon Press, 2001. ISBN 9780198510970.
- [8] D. Weaire, S. Hutzler, S. Cox, N. Kern, M. D. Alonso, and W. Drenckhan. The fluid dynamics of foams. *Journal of Physics: Condensed Matter*, 15(1):S65–S73, 2002.
- [9] S. Hutzler, D. Weaire, A. Saugey, S. Cox, and N. Peron. The physics of foam drainage. In *Proceedings of MIT European Detergents Conference, Wurzburg*, pages 191–206. Citeseer, 2005.
- [10] E. Buckingham. Studies on the movement of soil moisture. *U. S. Dept. of Agric. Bureau of Soils Bulletin*, 38, 1907.
- [11] W. B. Haines. Studies in the physical properties of soil. V. The hysteresis effect in capillary properties, and the modes of moisture distribution associated therewith. *The Journal of Agricultural Science*, 20(1):97–116, 1930.

- [12] L. A. Richards. Capillary conduction of liquids through porous mediums. *Physics*, 1(5):318–333, 1931.
- [13] H. P. G. Darcy. *Les Fontaines publiques de la ville de Dijon. Exposition et application des principes à suivre et des formules à employer dans les questions de distribution d'eau*. Victor Dalmont, 1856.
- [14] S. A. Koehler, S. Hilgenfeldt, and H. A. Stone. Liquid flow through aqueous foams: the node-dominated foam drainage equation. *Physical Review Letters*, 82(21):4232–4235, 1999.
- [15] T. Ahmed. *Reservoir Engineering Handbook*. Elsevier, 2nd edition, 2006.
- [16] R. H. Brooks and A. T. Corey. Properties of porous media affecting fluid flow. *Journal of the Irrigation and Drainage Division*, 92(2):61–90, 1966.
- [17] J. R. Philip. The theory of infiltration: 1. The Infiltration Equation and its Solution. *Soil Science*, 83(5):345–358, 1957.
- [18] Y. Mualem. A new model for predicting the hydraulic conductivity of unsaturated porous media. *Water Resources Research*, 12(3):513–522, 1976.
- [19] S. Whitaker. Flow in porous media II: The governing equations for immiscible, two-phase flow. *Transport in Porous Media*, 1(2):105–125, 1986.
- [20] M. A. Celia, E. T. Bouloutas, and R. L. Zarba. A general mass-conservative numerical solution for the unsaturated flow equation. *Water Resources Research*, 26(7):1483–1496, 1990.
- [21] B. H. Gilding. Qualitative mathematical analysis of the Richards Equation. *Transport in Porous Media*, 6(5):651–666, 1991.
- [22] T. P. Witelski. Perturbation analysis for wetting fronts in Richards Equation. *Transport in Porous Media*, 27(2):121–134, 1997.
- [23] F. T. Tracy. Clean two- and three-dimensional analytical solutions of Richards' Equation for testing numerical solvers. *Water Resources Research*, 42(8):W08503, 2006.
- [24] D. Or and S. Assouline. The drainage foam equation-an alternative to the Richards Equation for transient unsaturated flows. In *AGU Fall Meeting Abstracts*, 2011.

- [25] P. M. Patel and V. H. Pradhan. Exact travelling wave solutions of Richards' Equation by modified f-expansion method. *Procedia Engineering*, 127:759–766, 2015.
- [26] C. J. van Duijn, K. Mitra, and I. S. Pop. Travelling wave solutions for the Richards Equation incorporating non-equilibrium effects in the capillarity pressure. *Nonlinear Analysis: Real World Applications*, 41:232–268, 2018.
- [27] J. R. Philip. Fifty years progress in soil physics. *Geoderma*, 12(4):265–280, 1974.
- [28] P. A. C. Raats and M. Th. van Genuchten. Milestones in soil physics. *Soil Science*, 171(6):S21–S28, 2006.
- [29] J. A. F. Plateau. *Statique expérimentale et théorique des liquides soumis aux seules forces moléculaires*, volume 2. Gauthier-Villars, 1873.
- [30] H. M. Princen and A. D. Kiss. Osmotic pressure of foams and highly concentrated emulsions. 2. Determination from the variation in volume fraction with height in an equilibrated column. *Langmuir*, 3(1):36–41, 1987.
- [31] I. I. Gol'dfarb, K. B. Kann, and I. R. Shreiber. Liquid flow in foams. *Fluid Dynamics*, 23(2):244–249, 1988.
- [32] G. Verbist, D. Weaire, and A. M. Kraynik. The foam drainage equation. *Journal of Physics: Condensed Matter*, 8(21):3715–3736, 1996.
- [33] S. A. Koehler, S. Hilgenfeldt, and H. A. Stone. A generalized view of foam drainage: Experiment and theory. *Langmuir*, 16(15):6327–6341, 2000.
- [34] S. J. Neethling, J. J. Cilliers, and E. T. Woodburn. Prediction of the water distribution in a flowing foam. *Chemical Engineering Science*, 55(19):4021–4028, 2000.
- [35] R. A. Leonard and R. Lemlich. A study of interstitial liquid flow in foam. part i. theoretical model and application to foam fractionation. *AIChE journal*, 11(1):18–25, 1965.
- [36] G. Verbist and D. Weaire. A soluble model for foam drainage. *EPL (Europhysics Letters)*, 26(8):631–634, 1994.
- [37] S. Hilgenfeldt, S. Arif, and J.-C. Tsai. Foam: A multiphase system with many facets. *Philosophical Transactions of the Royal Society of London A: Mathematical, Physical and Engineering Sciences*, 366(1873):2145–2159, 2008.

- [38] M. Th. van Genuchten. A closed-form equation for predicting the hydraulic conductivity of unsaturated soils. *Soil Science Society of America Journal*, 44(5):892–898, 1980.
- [39] BP p.l.c. BP Statistical Review of World Energy 2019, 2020. URL <http://gourl.gr/ckbe>. Accessed: 2020-04-24.
- [40] S. J. Neethling, H. T. Lee, and J. J. Cilliers. A foam drainage equation generalized for all liquid contents. *Journal of Physics: Condensed Matter*, 14(3):331–342, 2001.
- [41] P. L. J. Zitha. Foam drainage in porous media. *Transport in Porous Media*, 52(1):1–16, 2003.
- [42] P. Grassia, E. Mas-Hernández, N. Shokri, S. J. Cox, G. Mishuris, and W. R. Rossen. Analysis of a model for foam improved oil recovery. *Journal of Fluid Mechanics*, 751:346–405, 2014.
- [43] J. R. Cannon and F. Browder. *The one-dimensional heat equation*. Encyclopedia of Mathematics and its Applications. Cambridge University Press, 1984.
- [44] V. A. Zlotnik, T. Wang, J. L. Nieber, and J. Šimunek. Verification of numerical solutions of the Richards Equation using a traveling wave solution. *Advances in Water Resources*, 30(9):1973–1980, 2007.
- [45] J.-G. Caputo and Y. A. Stepanyants. Front solutions of Richards' equation. *Transport in Porous Media*, 74(1):1–20, 2008.
- [46] P. Broadbridge and I. White. Constant rate rainfall infiltration: A versatile nonlinear model: 1. Analytic solution. *Water Resources Research*, 24(1):145–154, 1988.
- [47] J. R. Philip. The theory of infiltration: 2. the profile of infinity. *Soil Science*, 83(6):435–448, 1957.
- [48] J. R. Philip. The theory of infiltration: 3. Moisture profiles and relation to experiment. *Soil Science*, 84(2):163–178, 1957.
- [49] J. R. Philip. The theory of infiltration: 4. Sorptivity and algebraic infiltration equations. *Soil Science*, 84(3):257–264, 1957.
- [50] J. R. Philip. The theory of infiltration: 5. The influence of the initial moisture content. *Soil Science*, 84(4):329–340, 1957.

- [51] J. R. Philip. The theory of infiltration: 6. Effect of water depth over soil. *Soil Science*, 85(5):278–286, 1958.
- [52] J. R. Philip. The theory of infiltration: 7. *Soil Science*, 85(6):333–337, 1958.
- [53] P. Broadbridge, R. Srivastava, and T-C. J. Yeh. Burgers' equation and layered media: Exact solutions and applications to soil-water flow. *Mathematical and Computer Modelling*, 16(11):163–169, 1992.
- [54] C. J. van Duijn, K. Mitra, and I. S. Pop. Travelling wave solutions for the Richards Equation incorporating non-equilibrium effects in the capillarity pressure. *Nonlinear Analysis: Real World Applications*, 41:232–268, 2018. ISSN 1468-1218.
- [55] J. R. Philip. Theory of infiltration. 5:215–296, 1969.
- [56] R. H. Brooks and T. Corey. Hydraulic properties of porous media. *Hydrology Papers, Colorado State University*, 24:37, 1964.
- [57] Foams@Aber. Foam, October 2011. URL http://users.aber.ac.uk/sxc/FOYER/IMG_1238.JPG. [Online; accessed May 14, 2018].
- [58] L. F. Richardson. *Weather prediction by numerical process*. Cambridge university press, 2007.
- [59] J. M. Stankovich and D. A. Lockington. Brooks-Corey and van Genuchten soil-water-retention models. *Journal of Irrigation and Drainage Engineering*, 121(1):1–7, 1995.
- [60] D. G. Fredlund and A. Xing. Equations for the soil-water characteristic curve. *Canadian Geotechnical Journal*, 31(4):521–532, 1994.
- [61] S. Assouline and D. M. Tartakovsky. Unsaturated hydraulic conductivity function based on a soil fragmentation process. *Water resources research*, 37(5):1309–1312, 2001.
- [62] A. Peters and W. Durner. A simple model for describing hydraulic conductivity in unsaturated porous media accounting for film and capillary flow. *Water Resources Research*, 44(11), 2008.
- [63] J. M. Hill. Similarity solutions for nonlinear diffusion — a new integration procedure. *Journal of Engineering Mathematics*, 23(2):141–155, 1989.

- [64] D. L. Hill and J. M. Hill. Similarity solutions for nonlinear diffusion — further exact solutions. *Journal of Engineering Mathematics*, 24(2):109–124, 1990.
- [65] P. L. J. Zitha and F. J. Vermolen. Self-similar solutions for the foam drainage equation. *Transport in Porous Media*, 63(1):195–200, 2006.
- [66] Y. A. Boakye-Ansah and P. Grassia. Similarity solutions for early-time constant boundary flux imbibition in foams and soils. *Transport in Porous Media*, XX(XX): AA–BB, 2020. Submitted.
- [67] W. H. Press, S. A. Teukolsky, W. T. Vetterling, and B. P. Flannery. *Numerical recipes: The art of scientific computing*. Cambridge University Press, 2007.
- [68] Y. A. Boakye-Ansah and P. Grassia. Comparing and contrasting travelling wave behaviour for groundwater Flow and Foam Drainage. *Transport in Porous Media*, 137(1):255–280, 2021.
- [69] Y. A. Boakye-Ansah and P. Grassia. Sensitivity of Travelling Wave Solution to Richards equation to Soil Material Property Functions. *Transport in Porous Media*, XX(XX): AA–BB, 2020. In preparation.
- [70] C. N. Mulligan and F. Eftekhari. Remediation with surfactant foam of PCP-contaminated soil. *Engineering Geology*, 70(3–4):269–279, 2003.
- [71] S. Wang and C. N. Mulligan. An evaluation of surfactant foam technology in remediation of contaminated soil. *Chemosphere*, 57(9):1079–1089, 2004.
- [72] D. Weaire, S. Hutzler, G. Verbist, and E. A. J. F. Peters. A review of foam drainage. *Advances in Chemical Physics*, 102:315–374, 1997.
- [73] J. E. Taylor. The structure of singularities in soap-bubble-like and soap-film-like minimal surfaces. *Annals of Mathematics*, pages 489–539, 1976.
- [74] D. Weaire, N. Pittet, S. Hutzler, and D. Paldal. Steady-state drainage of an aqueous foam. *Physical Review Letters*, 71(16):2670–2673, 1993.
- [75] H. A. Stone, S. A. Koehler, S. Hilgenfeldt, and M. Durand. Perspectives on foam drainage and the influence of interfacial rheology. *Journal of Physics: Condensed Matter*, 15(1):S283–S290, 2002.

- [76] A. M. Kraynik. Foam drainage. Technical report, Sandia National Labs., Albuquerque, NM (USA), 1983.
- [77] A. Anazadehsayed, N. Rezaee, and J. Naser. Numerical modelling of flow through foam's node. *Journal of Colloid and Interface Science*, 504:485–491, 2017.
- [78] A. Anazadehsayed, N. Rezaee, and J. Naser. Exterior foam drainage and flow regime switch in the foams. *Journal of Colloid and Interface Science*, 511:440–446, 2018.
- [79] N. T. Burdine. Relative permeability calculations from pore size distribution data. *Journal of Petroleum Technology*, 5(03):71–78, 1953.
- [80] M. A. Celia and P. Binning. A mass conservative numerical solution for two-phase flow in porous media with application to unsaturated flow. *Water Resources Research*, 28: 2819–2828, October 1992.
- [81] M. Kutílek and D. R. Nielsen. *Soil hydrology: textbook for students of soil science, agriculture, forestry, geoecology, hydrology, geomorphology and other related disciplines*. Catena Verlag, 1994.
- [82] L. P. Dake. *The Practice of Reservoir Engineering (Revised Edition)*. Elsevier, 2001.
- [83] S. Assouline, D. Tessier, and A. Bruand. A conceptual model of the soil water retention curve. *Water Resources Research*, 34(2):223–231, 1998.
- [84] S. Assouline. A model for soil relative hydraulic conductivity based on the water retention characteristic curve. *Water Resources Research*, 37(2):265–271, 2001.
- [85] V. K. Too, C. T. Omuto, E. K. Biamah, and J. P. Obiero. Review of Soil Water Retention Characteristic (SWRC) models between saturation and oven dryness. *Open Journal of Modern Hydrology*, 4:173–182, Oct 2014.
- [86] M. Tani. The properties of a water-table rise produced by a one-dimensional, vertical, unsaturated flow. *Journal of the Japanese Forestry Society*, 64(11):409–418, 1982.
- [87] W. R. Gardner. Some steady-state solutions of the unsaturated moisture flow equation with application to evaporation from a water table. *Soil Science*, 85(4):228–232, 1958.
- [88] A. Peters. Simple consistent models for water retention and hydraulic conductivity in the complete moisture range. *Water Resources Research*, 49(10):6765–6780, 2013.

- [89] M. Th. van Genuchten and D. R. Nielsen. On describing and predicting the hydraulic properties. 3:615–628, 1985.
- [90] J. Williams, R. E. Prebble, W. T. Williams, and C. T. Hignett. The influence of texture, structure and clay mineralogy on the soil moisture characteristic. *Soil Research*, 21(1):15–32, 1983.
- [91] S. Assouline and D. Or. Conceptual and parametric representation of soil hydraulic properties: A review. *Vadose Zone Journal*, 12(4), 2013.
- [92] S. Irmay. On the hydraulic conductivity of unsaturated soils. *Transactions, American Geophysical Union*, 35(3):463–467, 1954.
- [93] Y. Mualem. Hydraulic conductivity of unsaturated porous media: generalized macroscopic approach. *Water Resources Research*, 14(2):325–334, 1978.
- [94] T. Vogel and M. Cislérova. On the reliability of unsaturated hydraulic conductivity calculated from the moisture retention curve. *Transport in Porous Media*, 3(1):1–15, 1988.
- [95] J. Kozeny. Über kapillare leitung der wasser in boden. *Royal Academy of Science, Vienna, Proc. Class I*, 136:271–306, 1927.
- [96] E. C. Childs and N. Collis-George. The permeability of porous materials. *Proceedings of the Royal Society of London. Series A. Mathematical and Physical Sciences*, 201(1066):392–405, 1950.
- [97] R. J. Millington and J. P. Quirk. Permeability of porous solids. *Transactions of the Faraday Society*, 57:1200–1207, 1961.
- [98] R. J. Kunze, G. Uehara, and K. Graham. Factors important in the calculation of hydraulic conductivity. *Soil Science Society of America Journal*, 32(6):760–765, 1968.
- [99] D. Hillel. *Introduction to Environmental Soil Physics*. Elsevier, 2003.
- [100] T. J. Marshall, J. W. Holmes, and C. W. Rose. *Soil Physics*. Cambridge University Press, 1996.
- [101] D. Or and S. Assouline. The foam drainage equation for unsaturated flow in porous media. *Water Resources Research*, 49(10):6258–6265, 2013.

- [102] M. I. Kim, B.-G. Chae, and M. Nishigaki. Evaluation of geotechnical properties of saturated soil using dielectric responses. *Geosciences Journal*, 12(1):83–93, 2008.
- [103] K. Huang, B. P. Mohanty, and M. Th. van Genuchten. A new convergence criterion for the modified picard iteration method to solve the variably saturated flow equation. *Journal of Hydrology*, 178(1-4):69–91, 1996.
- [104] K. Rathfelder and L. M. Abriola. Mass conservative numerical solutions of the head-based richards equation. *Water Resources Research*, 30(9):2579–2586, 1994.
- [105] L. Pan and P. J. Wierenga. A transformed pressure head-based approach to solve richards' equation for variably saturated soils. *Water Resources Research*, 31(4): 925–931, 1995.
- [106] E. L. Cussler. *Diffusion: mass transfer in fluid systems*. Cambridge University Press, 2009.
- [107] P. G. Debenedetti and R. C. Reid. Diffusion and mass transfer in supercritical fluids. *AIChE Journal*, 32(12):2034–2046, 1986.
- [108] J. Y. Parlange, D. A. Barry, M. B Parlange, W. L. Hogarth, R. Haverkamp, P. J. Ross, L. Ling, and T. S. Steenhuis. New approximate analytical technique to solve Richards equation for arbitrary surface boundary conditions. *Water Resources Research*, 33(4): 903–906, 1997.
- [109] J. M. Burgers. *The nonlinear diffusion equation: asymptotic solutions and statistical problems*. Springer Science & Business Media, 2013.
- [110] C. F. Kennel, R. D. Blandford, and P. Coppi. MHD intermediate shock discontinuities. Part 1. Rankine-Hugoniot conditions. *J. Plasma Physics*, 42(2):299–319, 1989.
- [111] I. S. Gradshteyn and I. M. Ryzhik. *Table of integrals, series, and products*. Academic Press, 2014.
- [112] E. C. Leong and H. Rahardjo. Review of soil-water characteristic curve equations. *Journal of Geotechnical and Geoenvironmental engineering*, 123(12):1106–1117, 1997.

- [113] J. Crank and P. Nicolson. A practical method for numerical evaluation of solutions of partial differential equations of the heat-conduction type. *Mathematical Proceedings of the Cambridge Philosophical Society*, 43(1):50–67, 1947.
- [114] J. W. Thomas. *Numerical partial differential equations: finite difference methods*. 22. Springer Science & Business Media, 2013.

Travelling Wave Solutions: Brooks-Corey Models

A.1 Overview

Travelling wave solution obtained for the two variants of the foam drainage equation [32, 33] and Richards equation [12] have been presented in Chapter 6. The similarities and contrasts between solutions obtained for these two governing equations were presented and discussed in detail. Solutions for Richards equation were obtained using van Genuchten [38] soil material property functions. The observed similarities and contrasts are therefore dependent upon those soil functions used. In this appendix, travelling wave solutions to Richards equation are presented for another commonly used soil material property model given by Brooks and Corey [56], which are power-law functions just as those for the foam drainage equation variants. Similarities and differences of this model within Richards equation compared to foam drainage and van Genuchten property models solutions to Richards equation are also presented and discussed.

A.2 Richards Equation

In order to obtain solutions for Richards equation [12], the rescaled moisture-based form of this equation is employed. It is here given as

$$\frac{\partial \theta}{\partial \tau} - \frac{\partial}{\partial \xi} \cdot D_r^*(\theta) \frac{\partial \theta}{\partial \xi} - \frac{\partial K_r}{\partial \xi} = 0, \quad (\text{A.1})$$

where θ is moisture content, τ is time ξ is spatial coordinate measured upwards, K_r is relative hydraulic conductivity, and D_r^* is relative hydraulic diffusivity. Relative diffusivity D_r^* is rescaled as $D_r = K_r |dH_w/d\theta|$ where $D_r = (\theta_s - \theta_r) D_r^*$. Using the following rescaled distance and time $\hat{\xi} = \xi$ and $\hat{\tau} = (\theta_s - \theta_r)^{-1} \tau$ respectively, and rescaled moisture content $\Theta = (\theta - \theta_r)/(\theta_s - \theta_r)$, a dimensionless form of equation (A.1) is obtained as

$$\frac{\partial \Theta}{\partial \hat{\tau}} - \frac{\partial}{\partial \hat{\xi}} \left(D_r(\Theta) \frac{\partial \Theta}{\partial \hat{\xi}} \right) - \frac{\partial}{\partial \hat{\xi}} K_r(\Theta) = 0 \quad (\text{A.2})$$

Travelling wave profiles (see Section 3.5.2) are obtained for (A.2) using,

$$\frac{d\hat{\xi}}{d\Theta} = \frac{D_r(\Theta)}{\Theta - K_r(\Theta)}. \quad (\text{A.3})$$

Equation (A.3) has been used to present travelling wave solutions to foams and soils in Chapter 6 & 7. It is again employed to elucidate travelling wave behaviour in Section A.4 using Brooks and Corey [56] soil material property functions.

A.3 Soil Material Property Functions

In this section, the Brooks and Corey [56] soil material property functions that are required to solve Richards equation, namely relative hydraulic conductivity and relative diffusivity, are given. As previously mentioned, usually, the capillary suction head function is used to obtain the relative hydraulic conductivity via a predictive conductivity model. The relative hydraulic conductivity obtained is then used with the derivative of capillary head to obtain the relative diffusivity. These material property functions are discussed below.

A.3.1 Capillary Suction Head

The Brooks and Corey [56] capillary suction head functions are given in terms of m defined by Mualem [18] ($m = 1 - 1/n$) and Burdine [79] ($m = 1 - 2/n$) respectively as

$$H_{+BCM} = \Theta^{-(1-m)/m}, \quad (\text{A.4a})$$

$$H_{+BCB} = \Theta^{-(1-m)/2m}. \quad (\text{A.4b})$$

The profiles for three soils samples based on the above equations are plotted in Figure A.1a and A.1b for Mualem [18] and Burdine [79] models respectively. As has been previously pointed out, the capillary head values do not go to zero at full saturation, but rather unity for the Brooks-Corey set of functions and the way they behave away from full saturation depends on the soil type (or equivalently the parameter m). Hygiene sandstone (and generally $m \rightarrow 1$) shows H_+ increasing from unity gradually at Θ decreases, but soils with $m \ll 1$ have very large H_+ values in the dry region. The closer m is to zero, the larger the initial H_+ values. This gives some insight into the behaviour of these two models. This behaviour has previously been discussed (see Section 4.2). Note that the suction head expressions here given are equivalent to a limiting case of van Genuchten [38] suction head equation in a very low moisture content limit (see Section 4.3). Note here also that these expressions are used to predict behaviour in the whole saturation limit.

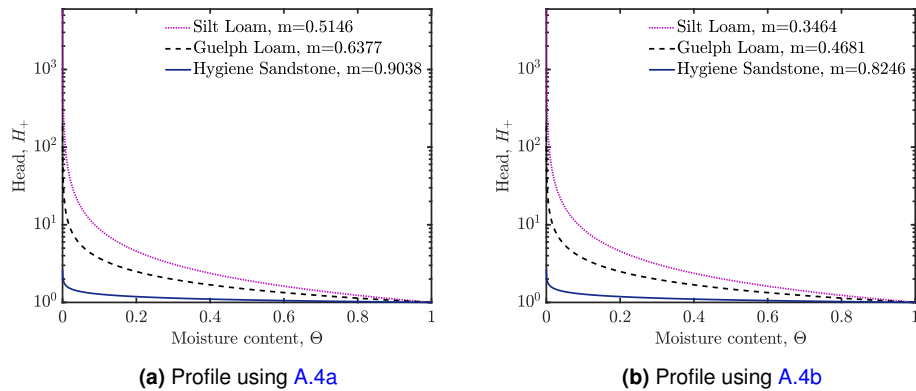


Figure A.1: Semi-log profile of capillary suction head for three soil samples. The data is largely comparable for each soil over the entire range of moisture content.

A.3.2 Relative Hydraulic Conductivity

The Brooks-Corey SWRC [56] are easy to manipulate using the predictive models given by Mualem [18], Burdine [79]. These are obtained using basic laws of integration as opposed to those obtained by van Genuchten [38], Assouline and Tartakovsky [61] which require the use of *integral definitions*. The relative hydraulic conductivity for Brooks and Corey [56] using the predictive model proposed by Mualem [18] and Burdine [79] respectively are given, again in terms of m as

$$K_{rBCM}(\Theta) = \Theta^{1/2} \left(\frac{\int_0^\Theta d\Theta/H_+}{\int_0^1 d\Theta/H_+} \right)^2 = \Theta^{1/2+2/m} \quad (\text{A.5a})$$

$$K_{rBCB}(\Theta) = \Theta^2 \frac{\int_0^\Theta d\Theta/H_+^2}{\int_0^1 d\Theta/H_+^2} = \Theta^{(1+2m)/m}. \quad (\text{A.5b})$$

These functions are shown as profiles in Figure A.2. Observe in Figure A.2a that for $m \rightarrow 1$ (e.g. sandstones), the profiles obtained using (A.5a) are higher at any given Θ than those for $m \ll 1$ (e.g. loams). Qualitatively the profiles obtained using (A.5b) are similar to those obtained using (A.5a). Both sets of profiles cover the domain $0 \leq K_r \leq 1$ as Θ varies over the domain $0 \leq \Theta \leq 1$.

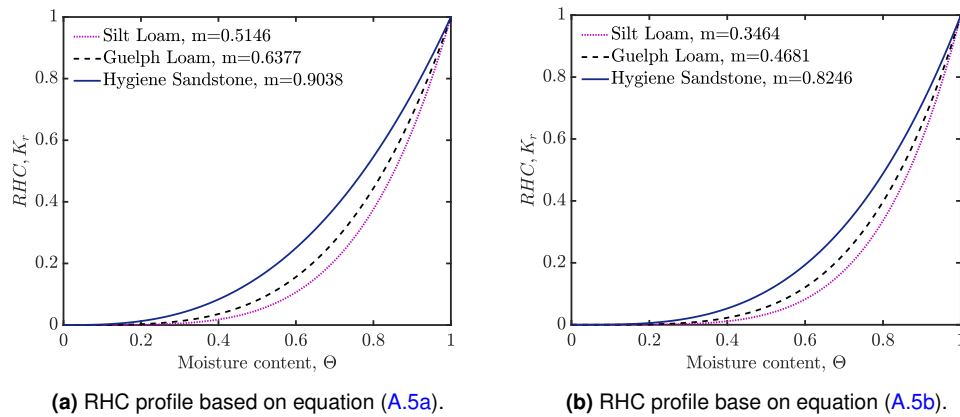


Figure A.2: RHC profile for three soil samples using Brooks-Corey models

Note that equation (A.5a) has the same form as the $\Theta \ll 1$ limit of the van Genuchten model, equation (4.7a) apart from a prefactor m^2 in the van Genuchten case. This prefactor arises from the fact that (compared to Brooks-Corey) a significant amount of the total hydraulic conductivity in the van Genuchten case comes from large pores with small H_+ . In relative terms then, less of the conductivity comes from small pores with suction head greater than or equal to any given H_+ .

A.3.3 Relative Diffusivity

From literature [17, 38], relative diffusivity is mathematically defined as

$$D_r(\Theta) = K_r(\Theta) \left| \frac{dH_+}{d\Theta} \right|. \quad (\text{A.6})$$

Using the head and RHC functions given in equations (A.4) and (A.5), the following relative diffusivity functions are obtained for the Mualem and Burdine definitions as,

$$D_r(\Theta) = \frac{(1-m)}{m} \Theta^{1/2+1/m}, \quad (\text{A.7a})$$

$$D_r(\Theta) = \frac{(1-m)}{2m} \Theta^{3/2+1/2m}, \quad (\text{A.7b})$$

from which travelling wave solution for Richards equation will be derived. Profiles for these equations are given in Figure A.3.

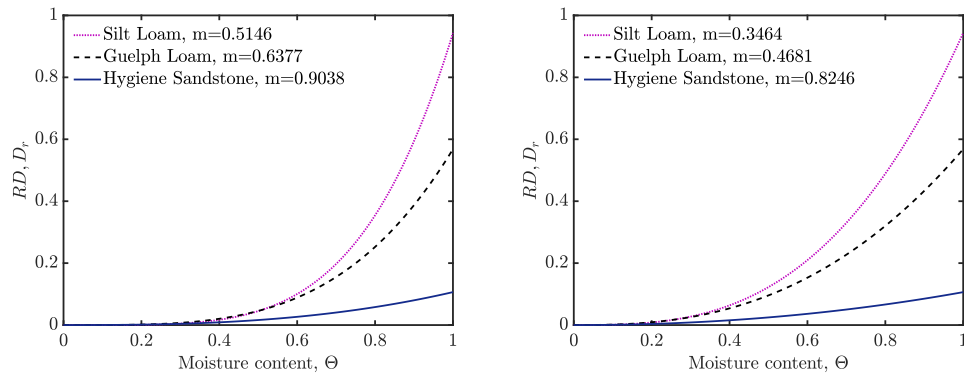


Figure A.3: Relative diffusivity profile for three soil samples using (A.7).

In the neighbourhood of $\Theta \rightarrow 1$ relative diffusivity values for $m \rightarrow 1$ tend to be surprisingly small, a result which can be attributed to the prefactor in the expressions. This prefactor arises from H_+ being relatively insensitive to Θ when $m \rightarrow 1$. Note that unlike what was seen for the van Genuchten case in chapter 6, D_r does not diverge to infinity in the $\Theta \rightarrow 1$ limit. Instead D_r remains finite. It is possible to rescale these equations such that D_r scales to unity at full saturation (as was already done in chapter 7, albeit using a different soil water retention curve, i.e. a convex hull of a van Genuchten SWRC rather than a Brooks-Corey SWRC as is used here). However (for consistency with chapter 6) the practice of rescaling D_r is not followed here.

Moving away from the neighbourhood of $\Theta \approx 1$ towards much smaller Θ , it is the small

m case (not the large m case) that gives smaller D_r . This is due to the m dependence of the exponent in equations (A.7a) & (A.7b).

A.4 Richards Equation: Travelling Wave Solution

A travelling wave solution to the rescaled mixed-form Richards equation (A.2) is obtained using RD equations (A.7a) & (A.7b) and RHC functions (A.5a) & (A.5b) for three different soil types. From (A.4), the following is obtained,

$$\hat{\xi}_{BCM} = \frac{(1 - m)}{m} \int \frac{\Theta^{1/m-1/2}}{(1 - \Theta^{1/m-1/2})} d\Theta, \tag{A.8a}$$

$$\hat{\xi}_{BCB} = \frac{(1 - m)}{2m} \int \frac{\Theta^{1/2m+1/2}}{(1 - \Theta^{1/m+1})} d\Theta, \tag{A.8b}$$

where the subscripts BCM and BCB represent solutions using the Mualem [18] and Burdine [79] formulation of Brooks-Corey [56] soil material property functions respectively.

These integrals cannot be determined analytically, so instead, using Simpson’s rule, a numerical solution is obtained analogous to what was done in [68] (also shown in Chapter 6). The solution using soil material property functions here presented is shown as a profile in Figure A.4 for three different soil types below.

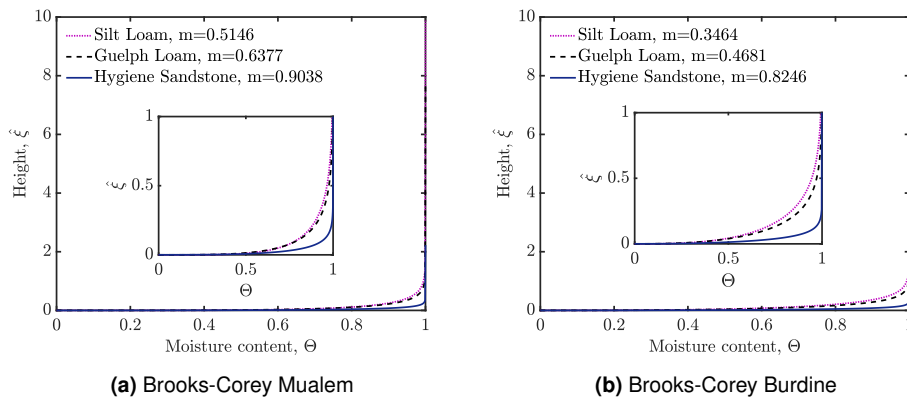


Figure A.4: Numerical solution to Richards Equation using (A.8a) & (A.8b).

For each soil type, both sets of solutions show $\hat{\xi}$ starts off growing slowly with Θ and then $\hat{\xi}$ increases much more abruptly near full saturation. Another way of saying this is that for small Θ , the value $\Theta \rightarrow 0$ is approached abruptly (over a small $\hat{\xi}$ range) whereas for large Θ , the value $\Theta \rightarrow 1$ is approached more gradually (over a large $\hat{\xi}$ range)

Moreover, for moderate to large Θ , Hygiene Sandstone ($m = 0.9038$, hence m reasonably close to 1) leads to noticeably smaller $\hat{\xi}$ for the *BCM* solutions. For soils with $m \rightarrow 1$, the diffusivity has a very small prefactor (respectively $(1 - m)/m$ or $(1 - m)/(2m)$), and hence the prefactors of the integrals in equations (A.8a) and (A.8b) are small compared with soils with lower m (e.g. $m \approx 0.5$ give a prefactor of approximately unity and a power-law of approximately 5/2). This is what contributes to the behaviour of the profiles as shown.

A.4.1 Asymptotic Behaviour of Solutions

While analytic solutions to (A.3) are not generally available using these soil functions proposed by Brooks and Corey [56], the travelling waves can be studied analytically within the limits where moisture content is either very small or near full saturation. The expressions in these limits are obtained via Taylor expansion. The travelling wave solutions to Richards equation in these limits are therefore given as,

$$\frac{d\hat{\xi}}{d\Theta} = \begin{cases} \frac{D_r(\Theta)}{\Theta}, & \text{if } \Theta \ll 1 \\ \frac{D_r(\Theta)}{(1 - \Theta)(K_r'(1) - 1)}, & \text{if } \Theta \approx 1 \end{cases} \quad (\text{A.9})$$

The equations that must be solved using the expressions above and the relative diffusivity and hydraulic conductivity functions in those limits are given as

$$\hat{\xi}_{BCMs}(\Theta) \approx \int \frac{(1 - m)}{m} \Theta^{1/m-1/2}, \quad (\text{A.10a})$$

$$\hat{\xi}_{BCBs}(\Theta) \approx \int \frac{(1 - m)}{2m} \Theta^{1/2+1/2m}. \quad (\text{A.10b})$$

Integrating these above equations, the following are obtained

$$\hat{\xi}_{BCMs}(\Theta) \approx \frac{2(1 - m)}{(2 + m)} \Theta^{1/2+1/m}, \quad (\text{A.11a})$$

$$\hat{\xi}_{BCBs}(\Theta) \approx \frac{(1 - m)}{(1 + 3m)} \Theta^{3/2+1/2m}. \quad (\text{A.11b})$$

Equation (A.11a) has the same form as the $\Theta \ll 1$ limit of the van Genuchten solution, (already obtained in chapter 6) apart from an additional prefactor m^2 present in the van Genuchten solution, but absent here. We have already discussed (in section A.3.2) why this prefactor appears in the van Genuchten case. The profile of this solution is presented

as short-dashed lines in Figure A.5 for three soil types. Observe that analytical solutions obtained for Burdine [79] scaling of material property functions more closely match numerical solutions obtained with same than those obtained using the Mualem [18] scaling of functions. Observe also that the solutions for the Burdine [79] occur in a smaller domain than those for Mualem [18], with the latter reaching larger height values in this low moisture content limit than the former.

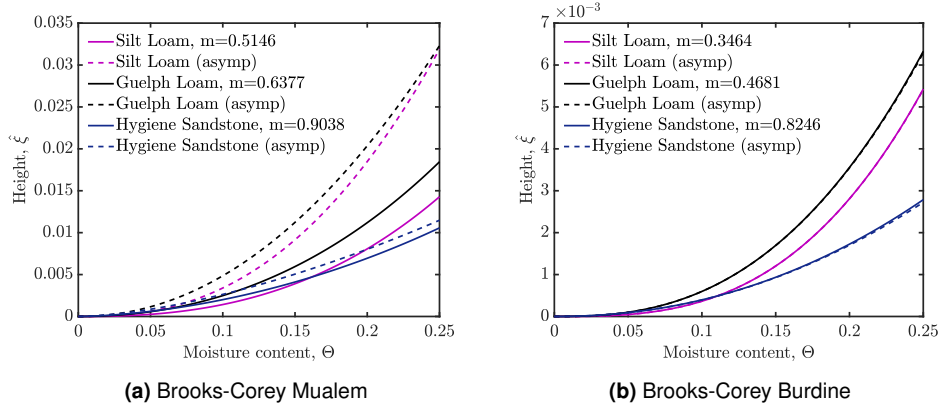


Figure A.5: Profile of asymptotic analytical and numerical solution in the limit as $\Theta \rightarrow 0$.

Asymptotic solutions are also obtained in the limit $\Theta \approx 1$ as follows. Taking equation (A.9) in the $\Theta \approx 1$ limit,

$$\hat{\xi}_{aBCM}(\Theta) \approx \int \frac{(1-m)}{m(1-\Theta)}, \quad (\text{A.12a})$$

$$\hat{\xi}_{aBCB}(\Theta) \approx \int \frac{(1-m)}{2m(1-\Theta)}. \quad (\text{A.12b})$$

These equations can be solved analytically. They are integrated to obtain the following

$$\hat{\xi}_{BCM}(\Theta) \approx \frac{(1-m)}{m} \log \frac{1}{(1-\Theta)} + c_{BCM}, \quad (\text{A.13a})$$

$$\hat{\xi}_{BCB}(\Theta) \approx \frac{(1-m)}{2m} \log \frac{1}{(1-\Theta)} + c_{BCB} \quad (\text{A.13b})$$

where c_{BCM} and c_{BCB} are integration constants. Hence solutions are obtained for the limit $\Theta \approx 1$. From Figure A.6, the Mualem [18] scaling produced analytical expressions which are more exact approximations to the numerical solutions obtained than the Burdine [79] scaling of the material property functions. The latter Burdine [79] scaling overestimates the analytical solutions especially as $m \rightarrow 0$, but less so as $m \rightarrow 1$. For the Mualem [18] scaling, $m \rightarrow 1$ is underestimated in this wet limit, a similar situation observed using the van

Genuchten [38] model defined with Mualem [18] scaling.

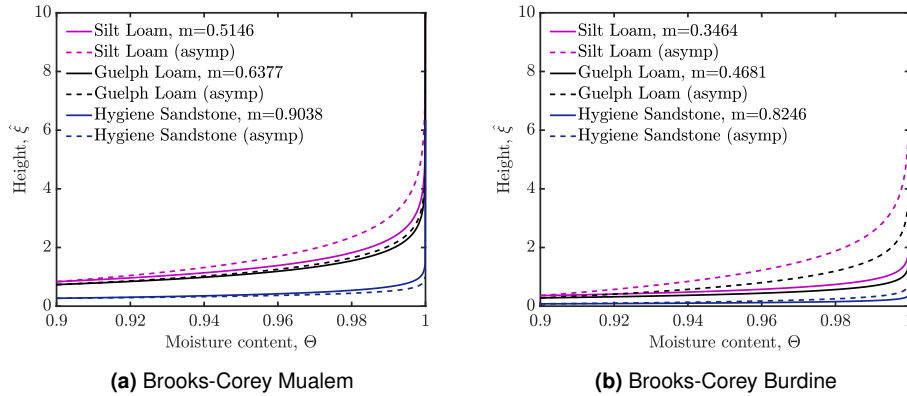


Figure A.6: Profile of asymptotic analytical and numerical solution in the limit as $\Theta \approx 1$.

Observe here that power law behaviour in Θ for RHC and RD yields a logarithmic law for $\hat{\xi}$ in the $\Theta \approx 1$ limit just as observed for foam drainage (shown in Chapter 6). Analogous logarithmic behaviour is observed in Chapter 7 for the modified soil material property functions for which power-law functions are also used for relative hydraulic conductivity and relative diffusivity. The more general RHC and RD of van Genuchten [38] in the case of soils were not simply power laws in Θ , and in chapter 6 this led to a different asymptotic behaviour in $\hat{\xi}$ (not logarithmic, but instead a faster growing power law).

A.5 Conclusion

The conclusion from the current appendix is that even though Brooks-Corey type functions for head H_+ , relative hydraulic conductivity K_r and relative diffusivity D_r in soils are very simple (i.e. power laws of Θ , as in the case of foam drainage), it is still not possible to attain the same level of simplification for $\hat{\xi}$ vs Θ as in foam drainage. Analytical solutions are obtained in foam drainage, but numerical expressions are obtained for soil thereby requiring Simpson's rule in the solution of those solutions, despite using simple Brooks-Corey material property functions.

The reason for the difference is that the powers of Θ which are encountered in foam drainage are relatively easy ones to deal with, e.g. $\Theta^{-1/2}$ or Θ^2 for relative diffusivity and $\Theta^{1/2}$ or 1 for relative hydraulic conductivity. This means it is possible to find analytic solutions for $\hat{\xi}$ vs Θ in foam drainage, but not in soils.

Near $\Theta = 1$, the Brooks-Corey type functions for soils give logarithmic behaviour ($\hat{\xi}$ proportional to $\log(1/(1 - \Theta))$). Qualitatively speaking, this is the same behaviour as in the “convex hull modified” versions of van Genuchten’s formula for soils (see Chapter 7). This is despite the fact that the Brooks-Corey formulae give finite H_+ at $\Theta = 1$, but the “convex hull” van Genuchten gives zero H_+ in that limit. The reason is that the $\hat{\xi}$ vs Θ curve is not directly sensitive to the value of H_+ itself, only to the value of $dH_+/d\Theta$. Specifically $D_r = K_r|dH_+/d\Theta|$.

Indeed any material properties that give finite $dH_+/d\Theta$ and finite $dK_r/d\Theta$ near $\Theta = 1$ produce logarithmic behaviour. Interestingly, a function:

$$H_+(\Theta) = H_{+BC}(\Theta) - H_{+BC}(1), \quad (\text{A.14})$$

has (by construction) $H_+ = 0$ when $\Theta = 1$, but has exactly the same $\hat{\xi}$ vs Θ as Brooks-Corey for all Θ , provided the original Brooks-Corey K_r is retained, instead of using the predictive conductivity models (which would not even converge with the above H_+). Indeed mathematically the above H_+ vs Θ function is even easier to construct than the convex hull used in chapter 7, but still exhibits similar mathematical behaviour, i.e. $H_+ \rightarrow 0$ but finite $dH_+/d\Theta$ as $\Theta \rightarrow 1$ and $\hat{\xi}$ proportional to $\log(1/(1 - \Theta))$ in that limit.

Setting Up an Initial Condition for Use in a Crank-Nicolson Solution to Richards Equation

B.1 Overview

Wetting fronts which produce travelling waves which propagate at different elevations of the same porous medium and which later interact are considered. The interaction of these fronts may occur in the case of pulsed drainage or irrigation with a sudden increase in infiltration rate. A mathematical procedure which can be used to predict an initial state for these two travelling waves is outlined based on models from Richards equation. The formulation of suitable boundary conditions for the various configurations assumed is also presented. Although full solutions are not given for this outlined problem, due to time constraints for this research, the set-up that is presented here may be used to obtain the solutions in questions presented.

B.2 Introduction

The problem here presented is based on Richards' equation [12] which is employed in modelling one-dimensional vertical infiltration of water in unsaturated soil. Richards equation

as used in this thesis is

$$\frac{\partial \Theta}{\partial \hat{\tau}} - \frac{\partial}{\partial \hat{\xi}} D_r \frac{\partial \Theta}{\partial \hat{\xi}} - \frac{\partial K_r}{\partial \hat{\xi}} = 0. \quad (\text{B.1})$$

where Θ is moisture content (relative to full saturation), $\hat{\tau}$ is time, $\hat{\xi}$ is distance measured upwards, D_r is relative diffusivity and K_r is relative hydraulic conductivity of the soil.

As previously mentioned (see chapter 3), this equation neglects the presence of air, evaporation, and any hysteresis that may occur in the soil. This has been done to obtain a simple and ideal form of Richards equation, which is nevertheless very useful and has been extensively studied [27, 28].

Previous chapters (6 & 7) of this thesis have presented travelling wave solutions for a single wetting front. This chapter however considers the solution for two separate travelling waves that interact from two different regions, an upper and a lower region, as a result of vertical infiltration. Here, the two travelling waves are considered to move at different velocities. Since one wave with higher moisture content is above another with lower moisture content, it follows from the results of Chapter 6 (see also Section 3.5.2) the wave above travels at a higher velocity and thus it catches up with the wave below at some point in time. It is of interest to predict the time it takes for these waves to interact, the subsequent motion of the newly developed wave, and the time for a new travelling wave to be obtained.

Generally speaking an interaction problem like this can only be solved numerically, e.g. via a Crank-Nicolson numerical scheme [113, 114]. Even before obtaining solutions however, initial conditions to be used within the Crank-Nicolson scheme must be defined. That is what is considered here.

Consider two travelling waves covering the domain $\Theta_{2l} \leq \Theta \leq \Theta_{1u}$ where one wave covers the zone $\Theta_{2l} \leq \Theta \leq \Theta_m$, and the other one covers the zone $\Theta_m \leq \Theta \leq \Theta_{1u}$ which shall be referred to as the lower and upper travelling wave respectively. Here Θ_m is a point somewhere in the middle between the two travelling waves which can also be denoted Θ_{1l} and Θ_{2u} for the lower and upper domains respectively. In what follows Θ_{2l} and Θ_{1u} are selected to be respectively 0 and 1.

B.3 Lower Travelling Wave

Consider a travelling wave covering the domain $\Theta_{2l} \leq \Theta \leq \Theta_m$. From the general travelling wave profile given in equation (3.36), it can be deduced that

$$d\hat{\xi} = \frac{\Theta_m D_r(\Theta)}{\Theta K_r(\Theta_m) - \Theta_m K_r(\Theta)} d\Theta, \quad (\text{B.2})$$

where $K_r(\Theta_m)$ is a constant for any soil type. Values of $K_r(\Theta_m)$ for different Θ_m are given in Table B.1. Note that the value of $K_r(\Theta_m)$ increases with both increasing m and Θ_m . The profile of this solution in the case $\Theta_m = 0.5$ is shown as the solid line in Figure B.1a.

Table B.1: Table showing the midpoint relative hydraulic conductivity values for three soil types.

Soil	m	$K_r(\Theta_m)$		
		$\Theta_m = 0.25$	$\Theta_m = 0.5$	$\Theta_m = 0.75$
Silt Loam	0.5146	0.0006	0.0146	0.1083
Guelph Loam	0.6377	0.0027	0.0376	0.1961
Hygiene Sandstone	0.9038	0.0194	0.1315	0.4136

B.3.1 Asymptotic Behaviour in Lower Travelling Wave

Considering $\Theta \ll 1$, the expression for determining the travelling wave may be given as

$$d\hat{\xi} \approx \frac{\Theta_m}{K_r(\Theta_m)} \frac{D_r(\Theta)}{\Theta} d\Theta. \quad (\text{B.3})$$

From equations (4.5a) and (4.7a) (behaviour of van Genuchten [38] functions as $\Theta \rightarrow 0$), the solution to the equation above is deduced as

$$d\hat{\xi} \approx \frac{\Theta_m}{K_r(\Theta_m)} m(1-m) \Theta^{1/m-1/2} d\Theta, \quad (\text{B.4})$$

which when integrated gives

$$\hat{\xi} \approx \frac{2\Theta_m m^2(1-m)}{(2+m)K_r(\Theta_m)} \Theta^{1/m+1/2} + c_{2l}, \quad (\text{B.5})$$

and (supposing $\Theta_m = 0.5$) can again be expressed as

$$\hat{\xi} \approx \frac{m^2(1-m)}{(2+m)K_r(\Theta_m)} \Theta^{1/m+1/2} + c_{2l}. \quad (\text{B.6})$$

The constant c_{2l} in this limit is set to zero. The profile of this solution is shown as short dashes in Figure B.1a for three soil types. This asymptotic profile matches the numerical solution profile more closely as $m \rightarrow 0$ over the entire domain shown.

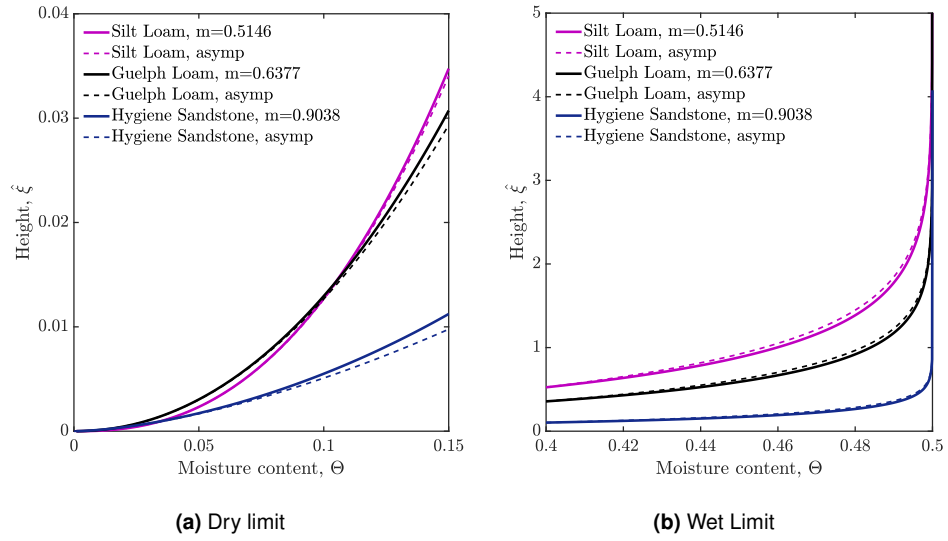


Figure B.1: Asymptotic approximation profiles for lower travelling waves

For $\Theta \approx \Theta_m = 0.5$, the following approximate solution is obtained

$$d\hat{\xi} \approx \frac{0.5D_r(\Theta_m)}{(-K_r(\Theta_m) + 0.5K'_r(\Theta_m))} \frac{1}{(-\Theta + 0.5)} d\Theta, \quad (\text{B.7})$$

where the soil material functions are defined in the limit $\Theta \rightarrow \Theta_m = 0.5$. This equation is integrated to obtain

$$\hat{\xi} \approx \frac{0.5D_r(\Theta_m)}{(-K_r(\Theta_m) + 0.5K'_r(\Theta_m))} \log \frac{1}{(1 - 2\Theta)} + c_{1l} \quad (\text{B.8})$$

where c_{2l} is an integration constant, that can be determined by matching with the full solution at some specified location slightly smaller than $\Theta_m = 0.5$ e.g. at $\Theta = 0.4$.

The above equation can also be written in the form

$$\hat{\xi} \approx \frac{0.5D_r(\Theta_m)}{(-K_r(\Theta_m) + 0.5K'_r(\Theta_m))} \log \frac{1}{(\Theta_m - \Theta)} + c'_{1l} \quad (\text{B.9})$$

just with a value of integration constant c'_{1l} that differs from the original integration constant c_{1l} . This is shown as short dashes for three soil types in Figure B.1b.

B.4 Upper travelling wave

Using equation (3.36), a special case is considered for when a travelling wave moves from $\Theta_{1u} = 1 \rightarrow \Theta_{2u} = \Theta_m = 0.5$. It can be observed via equation (3.36) that,

$$d\hat{\xi} = \frac{(1 - \Theta_m)D_r(\Theta)}{(\Theta - \Theta_m)K_r(1) - (\Theta - 1)K_r(\Theta_m) - (1 - \Theta_m)K_r(\Theta)} d\Theta, \quad (\text{B.10})$$

where since $K_r(1) = 1$, this reduces to

$$d\hat{\xi} = \frac{(1 - \Theta_m)D_r(\Theta)}{(\Theta - \Theta_m) - (\Theta - 1)K_r(\Theta_m) - (1 - \Theta_m)K_r(\Theta)} d\Theta, \quad (\text{B.11})$$

As earlier noted, $K_r(\Theta_m)$ is known for each soil type. For $\Theta_m = 0.5$ it is estimated as 0.0146 for Silt Loam ($m = 0.5146$), 0.0376 for Guelph Loam ($m = 0.6377$), and 0.1315 for Hygiene Sandstone ($m = 0.9038$). These values are previously given in Table B.1. Equation B.11 can only be solved numerically. Its profile in the upper and lower regions of this upper travelling wave are presented in Figure B.2.

B.4.1 Asymptotic Analysis in Upper Travelling Wave

Using approximate asymptotic definitions, an expression for the approximations at the various limits (low moisture and near full saturation) using RHC and RD is found.

For $\Theta \approx \Theta_m = 0.5$ (the lower limit for this upper travelling wave), the following is obtained

$$d\hat{\xi}_{1u} \approx \frac{(1 - \Theta_m)D_r(\Theta_m)}{(1 - K_r(\Theta_m) - (1 - \Theta_m)K'_r(\Theta_m))} \frac{1}{(\Theta - \Theta_m)} d\Theta. \quad (\text{B.12})$$

The above equation is integrated to obtain

$$\hat{\xi}_{1u} \approx -\frac{(1 - \Theta_m)D_r(\Theta_m)}{(1 - K_r(\Theta_m) - (1 - \Theta_m)K'_r(\Theta_m))} \log \frac{1}{(\Theta - \Theta_m)} + c_{2u}, \quad (\text{B.13})$$

where this constant c_{2u} is a constant that can be fixed by knowing the value of $\hat{\xi}$ at some Θ value slightly greater than $\Theta_m = 0.5$ e.g. at $\Theta = 0.6$.

Note that as Θ decreases towards Θ_m , $\hat{\xi}$ decreases whilst $d\hat{\xi}/d\Theta$ becomes arbitrarily large and positive; in other words, in the upper travelling wave, Θ only approaches Θ_m gradually as $\hat{\xi}$ decreases. The behaviour of the upper travelling wave as $\Theta \rightarrow \Theta_{2u} \equiv \Theta_m$

therefore contrasts with that of the lower travelling wave as $\Theta \rightarrow \Theta_{2l} \equiv 0$: that approach is abrupt as previously seen in Chapter 6.

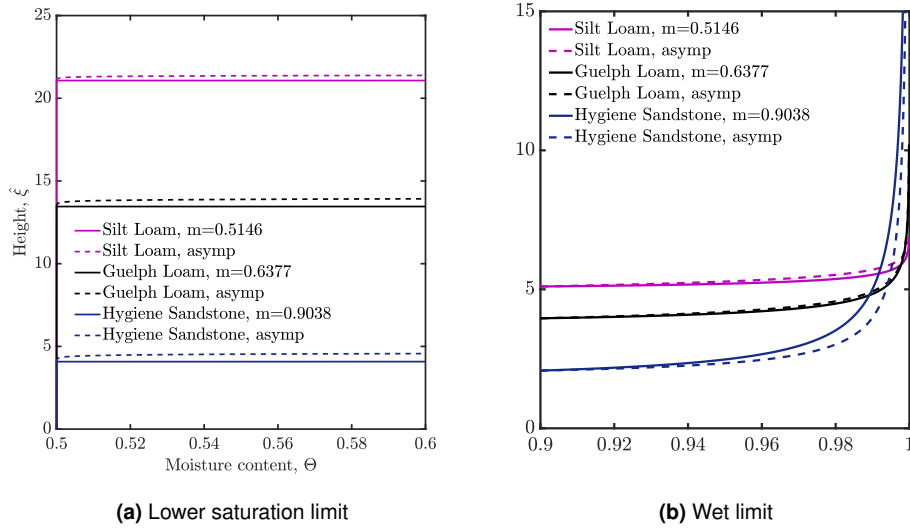


Figure B.2: Asymptotic approximation profiles for upper travelling waves. Note that although the figure in (b) starts from lower values than those in (a), the solution is qualitatively the same since Θ_m can be moved upward or downward.

For $\Theta \approx 1$ (the upper limit of the upper travelling wave) also, the solution is given as

$$d\hat{\xi}_{1u} \approx \frac{D_r(\Theta)}{1 - K_r(\Theta)} d\Theta \quad (\text{B.14})$$

where the soil properties $D_r(\Theta)$ and $K_r(\Theta)$ have known asymptotic forms in this limit, and where $1 - K_r(\Theta)$ is much greater than $1 - \Theta$ because $dK_r/d\Theta$ diverges in the limit $\Theta \rightarrow 1$. Note that the asymptotic equation is independent of Θ_m in this limit ($\Theta \rightarrow 1$).

Using asymptotic formulae presented in Chapter 6 (see also Section 4.3), equation (B.14) is integrated to obtain

$$\hat{\xi}_{1u} \approx \frac{(1 - m)m^{2m-1}}{2(2m - 1)} (1 - \Theta)^{1-2m} + c_{1u}. \quad (\text{B.15})$$

The constant c_{1u} here is matched to the numerical solution from (B.10) (or equivalently (B.11)) at $\Theta = 0.9$.

B.5 Interaction of Travelling Waves

Considering the lower and upper travelling wave solutions, the following profile (Figure B.3 below) is obtained. The “middle” point or meeting point of the waves is given as either $\Theta_m = 0.25$, $\Theta_m = 0.5$ or $\Theta_m = 0.75$. In both (b) and (c) of these figures, note that Θ_m is the same value, but the profiles differ only because the upper travelling wave is shifted either downwards or upwards.

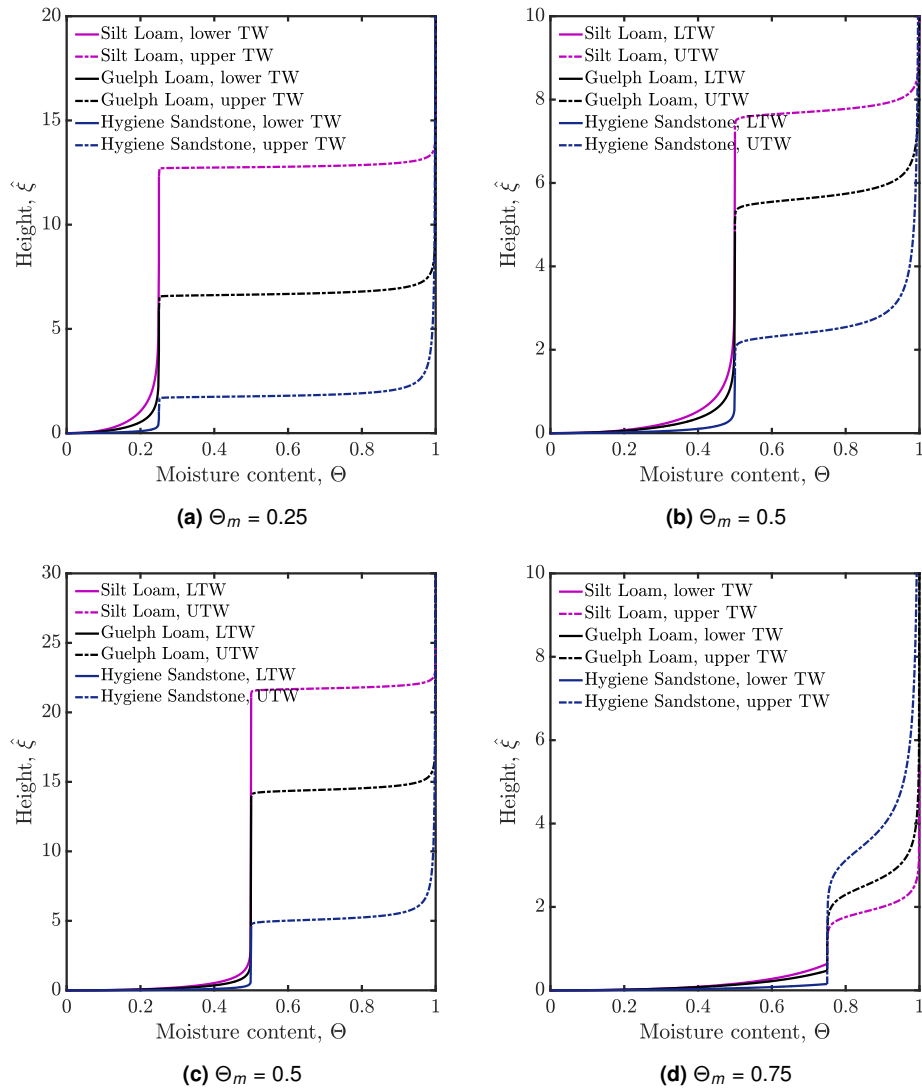


Figure B.3: Profile of two interacting travelling waves using (B.2) (solid lines) and (B.10) (or equivalently (B.11)) (dash-dot lines) for the lower and upper travelling waves respectively for various choices of Θ_m . Note that (b) and (c) are for the same $\Theta_m = 0.5$ just with the upper travelling wave shifted further upwards in (c).

B.6 Setting Up the Crank-Nicolson Scheme

In Section B.3 and B.4 above, initial conditions have been proposed for studying the subsequent interaction of travelling waves. Such a travelling wave in the range $0 \leq \Theta \leq \Theta_m$ satisfies

$$\frac{d\hat{\xi}}{d\Theta} = \frac{\Theta_m D_r(\Theta)}{\Theta K_r(\Theta_m) - \Theta_m K_r(\Theta)}, \quad (\text{B.16})$$

whilst a travelling wave in the range $\Theta_m \leq \Theta \leq 1$ satisfies

$$\frac{d\hat{\xi}}{d\Theta} = \frac{(1 - \Theta_m) D_r(\Theta)}{(\Theta - \Theta_m) - (\Theta - 1) K_r(\Theta_m) - (1 - \Theta_m) K_r(\Theta)}. \quad (\text{B.17})$$

Note that close to Θ_m the denominator here becomes,

$$\begin{aligned} (\Theta - \Theta_m) - (\Theta - \Theta_m)(K_r(\Theta_m) + (1 - \Theta_m)K_r'(\Theta_m)) = \\ (\Theta - \Theta_m)(1 - K_r(\Theta_m) - (1 - \Theta_m)K_r'(\Theta_m)) \end{aligned} \quad (\text{B.18})$$

and hence equation (B.17) reduces to

$$\frac{d\hat{\xi}}{d\Theta} = \frac{(1 - \Theta_m) D_r(\Theta_m)}{(\Theta - \Theta_m)(1 - K_r(\Theta_m) - (1 - \Theta_m)K_r'(\Theta_m))}. \quad (\text{B.19})$$

Note the geometric interpretation of $(1 - K_r(\Theta_m) - (1 - \Theta_m)K_r'(\Theta_m))$. It is not simply the amount that $K_r(\Theta_m)$ falls below unity, but rather the amount that a tangent line to the K_r vs Θ curve extrapolated from $\Theta = \Theta_m$ to $\Theta = 1$ falls below unity.

It is interesting to examine what happens to this value when Θ_m is itself relatively close to unity (as e.g. in Figure B.3(d)). Since $K_r \approx 1 - O((1 - \Theta)^m)$ close to $\Theta = 1$ (see Chapter 6), it turns out that this extrapolated value is less than the amount that K_r falls below unity, but of a similar order of magnitude. Meanwhile (again see Chapter 6) D_r for $\Theta \approx 1$ is order $(1 - \Theta)^{-m}$. Therefore, $d\hat{\xi}/d\Theta$ close to $\Theta = \Theta_m$ is of order $(1 - \Theta_m)^{(1-2m)}/(\Theta - \Theta_m)$. Note that (since for the soils considered, i.e. Silt Loam, Guelph Loam and Hygiene Sandstone, all the m values exceed 0.5), the prefactor here $(1 - \Theta_m)^{(1-2m)}$ is largest when Θ_m is larger, and this is reflected in the shape of $\hat{\xi}$ vs Θ curves near $\Theta = \Theta_m$ (again see e.g. Figure B.3(d)).

In the next section, a way to generalise the above mentioned profiles is presented to account for varying distance between the interacting travelling waves.

B.6.1 Generalising Interacting Travelling Wave Profiles

In what follows, not only values close to $\Theta = \Theta_m$ are considered but rather the full range of Θ values. Hence, equations (B.16) and (B.17) are employed (rather than (B.19)) and the solution proceeds as follows.

A value Θ_{m+} which is very slightly larger than the original Θ_m is chosen. Equation (B.16) is solved for $\hat{\xi}$ vs Θ but with Θ_{m+} replacing the original Θ_m . The vertical separation between the lower and upper travelling wave can be controlled by moving Θ_{m-} and Θ_{m+} closer to Θ_m . Here, Θ_{m-} is only slightly smaller than the original Θ_m . The closer Θ_{m-} and Θ_{m+} move to Θ_m , the larger the initial vertical separation between the two waves and the less they interact initially.

The upper travelling wave profile up to a Θ value equal to the original Θ_m is solved. There will be a well defined large but finite $d\hat{\xi}/d\Theta$ value at this point. Having obtained the $\hat{\xi}$ vs Θ travelling wave profile for the lower travelling wave, it can now be shifted vertically so that the point with Θ equal to the original Θ_m is at $\hat{\xi} = 0$, and the remainder of the profile is at $\hat{\xi} < 0$. A value Θ_{m-} is selected which is very slightly smaller than the original Θ_m . Equation (B.17) is solved from the original Θ_m up to some sufficiently large $\hat{\xi}$ that Θ is very close to unity there. For sufficiently large Θ (i.e. sufficiently close to 1), it turns out

$$\frac{d\hat{\xi}}{d\Theta} \approx \frac{D_r(\Theta)}{(1 - K_r(\Theta))}, \quad (\text{B.20})$$

regardless of the value of Θ_m , and the asymptotic behaviour close to $\Theta = 1$ is known [68].

Thus, it is already known how the height ($\hat{\xi}_{top}$ say) of the solution domain must vary in order to have some well-defined value of Θ close to unity at the top ($\Theta = \Theta_{top}$ say). Specifically (see Chapter 6), $\hat{\xi}_{top}$ must be proportional to $(1 - \Theta_{top})^{-(2m-1)}$, so the closer Θ_{top} is to 1, the larger $\hat{\xi}_{top}$ must be, and hence the larger the solution domain.

The Θ vs $\hat{\xi}$ (or equivalently $\hat{\xi}$ vs Θ) initial condition is now fully defined. Importantly, it has been defined in such a way that Θ vs $\hat{\xi}$ is continuous at $\Theta = \Theta_m$. It is also possible incidentally to define the initial condition in such a way that $d\Theta/d\hat{\xi}$ is continuous there. This can be done by judicious selection of Θ_{m-} for a given Θ_m and Θ_{m+} .

Equation (B.16) (but with Θ_{m+} replacing Θ_m and with Θ_m replacing Θ) defines the value

of $d\hat{\xi}/d\Theta$ at the point where the two travelling waves match. (As mentioned, first Θ_m is replaced by Θ_{m+} in that equation, then Θ is also replaced by the original Θ_m). Equation (B.19) (which is a local approximation to equation (B.17)) can then be used to estimate the Θ_{m-} value required to keep $d\hat{\xi}/d\Theta$ continuous.

First, the equation is rearranged into the form

$$(\Theta - \Theta_m) = \frac{(1 - \Theta_m)D_r(\Theta_m)}{\frac{d\hat{\xi}}{d\Theta} \left(1 - K_r(\Theta_m) - (1 - \Theta_m)K_r'(\Theta_m) \right)}, \quad (\text{B.21})$$

where the value of $d\hat{\xi}/d\Theta$ on the right hand side is known at $\Theta = \Theta_m$ and all other terms on the right are only weakly affected if Θ_m is shifted to a nearby value Θ_{m-} . Then on the left hand side, Θ_m is replaced by Θ_{m-} . Subsequently, Θ on the left hand side is substituted by the original Θ_m . This supplies a leading order estimate for Θ_{m-} which keeps $d\Theta/d\hat{\xi}$ continuous for any Θ_{m+} and Θ_m .

This chapter to date has defined an initial condition for Θ vs $\hat{\xi}$ that can subsequently be used to study travelling wave interactions via a Crank-Nicolson numerical scheme. To proceed with a Crank-Nicolson solution it is also necessary however to define boundary conditions at the top $\hat{\xi}_{top}$ and at the bottom $\hat{\xi}_{bottom}$. Ideally, the conditions would be $\Theta = 1$ at the top (ideally $\hat{\xi}_{top} \rightarrow \infty$) and $\Theta = 0$ at $\hat{\xi}_{bottom}$ (ideally $\hat{\xi}_{bottom} \rightarrow -\infty$). Maintaining $\Theta = 0$ at the bottom is unlikely to be problematic, since most of the travelling wave solutions that have been considered (apart from the node dominated foam drainage equation case) do seem to attain $\Theta = 0$ at a finite $\hat{\xi}$ location.

Setting $\Theta = 1$ at the top is more problematic, since Θ might only approach unity quite slowly and, in a numerical study, computation is done on a finite domain. One option is to impose a boundary condition holding Θ at the top at the same value as it had initially.

Another option is to figure out what the final state of the system is, in theory (on an infinite domain) since the two interacting travelling waves should eventually merge into a single travelling wave spanning (in principle at least on an infinite domain) the full range $\Theta = 0$ to $\Theta = 1$, and then at the top of our finite domain $\hat{\xi} = \hat{\xi}_{top}$, set whatever Θ value that travelling wave would have. The reason that two interacting travelling waves should eventually merge is discussed in Chapter 6: a travelling wave covering the domain $\Theta = 0 \rightarrow \Theta = \Theta_m$ is always

slower than a wave covering the domain $\Theta = \Theta_m \rightarrow \Theta = 1$.

B.6.2 Travelling Wave Solution

In order to solve the interaction of two travelling waves via Richards equation it is useful to re-formulate the coordinate system as explained below. Specifically what is done is to switch into a coordinate system that convects with the speed of the single merged travelling wave. In that coordinate system, the upper travelling wave appears to move downwards towards the region where the waves merge, whilst the lower travelling wave appears to move upwards. The final merged solution should be a steady state in that convecting coordinate system.

Richards equation can be written in the form,

$$\frac{d\Theta}{d\hat{\tau}} - \frac{d}{d\hat{\xi}} \left(D_r \frac{d\Theta}{d\hat{\xi}} \right) - \frac{dK_r}{d\hat{\xi}} = 0, \quad (\text{B.22})$$

where $\hat{\xi}$ is measured upwards. Suppose two new variables are defined

$$\Xi = \hat{\xi} + v\hat{\tau}; \quad T = \hat{\tau}, \quad (\text{B.23})$$

where v is a velocity that will be specified later. Then Θ can be written in the form $\Theta = \Theta(\Xi, T)$ instead of $\Theta = \Theta(\hat{\xi}, \hat{\tau})$. Richards equation can be written in terms of Ξ and T remembering that

$$\frac{d}{d\hat{\tau}} = \frac{dT}{d\hat{\tau}} \frac{d}{dT} + \frac{d\Xi}{d\hat{\tau}} \frac{d}{d\Xi}, \quad (\text{B.24a})$$

$$\frac{d}{d\hat{\xi}} = \frac{dT}{d\hat{\xi}} \frac{d}{dT} + \frac{d\Xi}{d\hat{\xi}} \frac{d}{d\Xi}, \quad (\text{B.24b})$$

where $dT/d\hat{\tau} = 1$, $d\Xi/d\hat{\tau} = v$, $dT/d\hat{\xi} = 0$ and $d\Xi/d\hat{\xi} = 1$.

Hence,

$$\frac{d}{d\hat{\tau}} = \frac{d}{dT} + v \frac{d}{d\Xi}; \quad (\text{B.25a})$$

$$\frac{d}{d\hat{\xi}} = \frac{d}{d\Xi}, \quad (\text{B.25b})$$

giving Richards equation as

$$\frac{d\Theta}{dT} + v \frac{d\Theta}{d\Xi} - \frac{d}{d\Xi} \left(D_r \frac{d\Theta}{d\Xi} \right) - \frac{dK_r}{d\Xi} = 0. \quad (\text{B.26})$$

Note that the solution of this equation $\Theta = \Theta(\Xi, T)$ is not generally a travelling wave solution. It would only become a travelling wave solution if Θ ceased to depend on T (but depended only on Ξ). As alluded to earlier, when two travelling waves interact, it is expected eventually that at large times T , the solution $\Theta(\Xi, T)$ for the system tends towards a solution denoted $\Theta_\infty(\Xi)$ say, that is independent of T . The final state is therefore a travelling wave, even though the state at finite times is not.

Specifically, if there were one travelling wave spanning the range from $\Theta = 0$ to $\Theta = \Theta_m$ (travelling downwards at speed v_{lower}) and another travelling wave spanning the range from $\Theta = \Theta_m$ to $\Theta = 1$ (travelling downwards at speed v_{upper}), then it is expected that the final state of the system would be a travelling wave spanning the full range from $\Theta = 0$ to $\Theta = 1$.

This is known to move downwards at unit speed, so it is natural to choose $v = 1$. The coordinate $\Xi = \hat{\xi} + v\hat{t}$ now convects downwards at this speed. In the original coordinate system, the lower travelling wave ($0 \leq \Theta \leq \Theta_m$) moves down with a speed v_{lower} , which is less than unity. In the new coordinate system, the wave appears to move upwards with a speed equal to $1 - v_{lower}$. Likewise in the original coordinate system, the upper travelling wave ($\Theta_m \leq \Theta \leq 1$) moves down with a speed v_{upper} , which is greater than unity. In the new coordinate system it moves down with a speed $v_{upper} - 1$.

The advantage of using the Ξ coordinate system then is that the two travelling waves move closer together over time, so it is not necessary to look at an arbitrarily large domain of Ξ values. (In the original $\hat{\xi}$ coordinate system, the waves are continually exploring new $\hat{\xi}$ values as time evolves, so the domain could need to be very large indeed). Since (as mentioned earlier) the two travelling waves move at different speeds, the solution as a whole is not a travelling wave in general. In other words the shape of the Θ vs Ξ profile necessarily depends on T , because the vertical offset between the two travelling waves is T dependent.

Moreover, since the shape of a travelling wave spanning the range from $\Theta = 0$ to $\Theta = 1$ is known, it is actually known what the final limiting value $\Theta_\infty(\Xi)$ will be. It is easy then to know at which time T a numerical computation of $\Theta(\Xi, T)$ can safely stop. Specifically, this can stop as soon as the computed $\Theta(\Xi, T)$ is close to the known $\Theta_\infty(\Xi)$.

B.7 Summary

Set-up of the initial state with which to solve for the interacting travelling wave forms have been considered in this chapter. The ideas here presented can be used to study the time evolution of the behaviour of the travelling waves. Additionally, the solutions obtained can be used to interpret the behaviour when two existing travelling waves at different velocities interact. This section has been proposed as the framework for future (numerical) work on this problem.

Of course, interaction of two travelling waves is not the only situation in Richards equation which is of interest to explore numerically (using e.g. a Crank-Nicolson scheme). It is also of interest for instance to examine a constant infiltration rate problem, and examine how the early-time similarity solution of Chapter 5 gives way to the late-time travelling wave solution of Chapter 6. That is again left for future work.